Fate and importance of respired CO_2 transport in trees

ir. Jasper Bloemen

UNIVERSITEIT GENT

FACULTEIT **BIO-INGENIEURSWETENSCHAPPEN**

What could possibly go wrong?

- Robert O. Teskey

Promotor

Prof. dr. ir. Kathy Steppe

Department of Applied Ecology and Environmental Biology

Laboratory of Plant Ecology

Universiteit Gent

Members of the examination board

Prof. dr. ir. Pascal Boeckx (Secretary)

Department of Applied Analytical and Physical Chemistry

Isotope Bioscience Laboratory – ISOFYS

Universiteit Gent

Prof. dr. Ivan Janssens

Department of Biology

Plant & Vegetation ecology

Universiteit Antwerpen

Prof. dr. ir. Steven Sleutel

Department of Soil Management

Soil fertility and nutrient management

Universiteit Gent

Prof. dr. ir. Filip Tack (Chairman)

Department of Applied Analytical and Physical Chemistry

Laboratory of Analytical Chemistry and Applied Ecochemistry

Universiteit Gent

Prof. dr. Susan E. Trumbore

Department of Biogeochemical processes

Max-Planck Institute for Biogeochemistry

Dean

Prof. dr. ir. Guido Van Huylenbroeck

Rector

Prof. dr. Anne De Paepe

ir. Jasper Bloemen

Fate and importance of respired CO_2 transport in trees

Thesis submitted in fulfillment of the requirements
for the degree of Doctor (PhD) in Applied Biological Sciences

Dutch translation of the title:
LOT EN BELANG VAN GERESPIREERD CO_2 TRANSPORT IN BOMEN

Illustration on the cover:
Swiss Stone pine (*Pinus cembra*) at 2000 m asl, Obergurgl, Tyrol, Austria

Citation of this thesis:
Bloemen, J. (2013). Fate and importance of respired CO_2 transport in trees. PhD thesis, Ghent University, Belgium.

ISBN-number: 978-90-5989-673-4

Dankwoord

Beste lezer, waarom bestaan dankwoorden?

Ondertussen zou het namelijk al zeer duidelijk moeten zijn hoe dankbaar ik je ben voor de hulp en steun bij dit doctoraat de afgelopen vier jaar. Ik denk dat ik vrij duidelijk ben geweest in het 'bedanken' gedurende de voorbije vier jaar. Echter mensen vergeten snel (of worden gewoon wat ouder) of luisteren soms niet goed. Daarom een korte recapitulatie van mijn bedankingen zodat iedereen een neergeschreven bewijs heeft van mijn dankbaarheid.

Voor het wetenschappelijke gedeelte zou ik vooreerst mijn promotor Kathy Steppe willen bedanken. Kathy, sinds ik in het onderzoek ben gestapt heb ik nog niemand ontmoet die kan tippen aan jouw hyper aanstekelijk enthousiasme. De eerste lessen bij jou zullen me als één van de weinige in mijn studies bio-ingenieur altijd bijblijven. Het was dan ook een uitstekende keuze om mijn thesis en later doctoraat bij jou te doen. Ik was dan ook ontzettend gelukkig toen het BOF starterskrediet goedgekeurd werd (maar 7 van de 31!), waarvoor zoals al gezegd, ik je altijd dankbaar blijf. Je goede en creatieve ideeën die in je hoofd opkwamen over dit super interessant onderwerp resulteerden in interessante discussies en ideeën en in een goede samenwerking tussen ons twee. Daarnaast gaf je me ook het vertrouwen om mijn eigen ding te doen of liet je me toe om naar elk congres te gaan dat ik aanstipte als interessant of om in het buitenland onderzoek te voeren. Dus bedankt voor dit alles en ik ben zeker dat het labo onder jou op zijn zelfde fantastisch wetenschappelijk elan zal verder gaan.

Besides Kathy's creative and enthousiastic help, I received advice from someone a tiny bit older, with lots of experience and who challenged me in my quest for good science. Bob Teskey was this experienced mentor, whose contribution to this PhD should not be underestimated (at least already the first sentence of this PhD…). Together with THE master correctors, Mary Anne and Doug, he gave my good additional advice on most of my experiments. I always waited soft-hearted for your revisions of my drafts (>50 comments or not?), but for sure they improved the quality of the articles. Mary Anne, I would like to thank you for all the work on the isotope experiments and for sending

numerous e-mails to obtain the isotope data for me. Doug, thanks for helping me with the statistics and your help on the isotope experiments. Once I'll be living in the Alps you can pass by, so you can take a break from the Georgia flatlands.

Now I could try to write the next paragraph in Tyrolean, but I still need to decipher their vocabulary and work on my Schuhplattler skills. Nonetheless, I want to thank prof. dr. Michael Bahn and the members of his lab for my stay in Innsbruck last summer and for the great advice on my hiking trip to the stunning Rinnenspitze. I really enjoyed our discussions, while sitting in the office or walking up- and downhill in the mountains. I'm looking forward to working together in the future, eating some more Strudel and tour skiing in the winter and hiking in the summer.

Daarnaast wil ik Lynn Vanhaeck en Lieven Van Meulebroek van de Vakgroep Veterinaire Volksgezondheid bedanken voor de hulp bij de suikeranalyses, Katja Van Nieuland van het ISOFYS lab voor de isotopen analyses en de thesisstudenten die ik begeleid heb (Sim, Laura en Yentl) voor het goede werk en de leuke momenten samen. Een deel van dit doctoraat is dankzij jullie tot stand gekomen. I would also like to thank Michael Thorpe for his help and his knack in creating labeling systems from bits and pieces during our small ^{11}C project at INFINITY lab.

I would like to thank the members of the examination board, prof. dr. Susan E. Trumbore, prof. dr. Ivan Janssens, prof. dr. ir. Steven Sleutel, prof. dr. ir Pascal Boeckx, and prof. dr. ir. Filip Tack for their thoughtful review of my PhD thesis.

Sinds 'Het Eiland' in 2004-2005 werd uitgezonden weten we allemaal hoe het bij een gemiddeld Belgisch bedrijf er echt aan toe gaat… . Echter, in het labo voor Plantecologie, was het toch veel beter toeven en dat dankzij de vele leuke en aangename collega's. Philip en Geert (toch wel de technische wonderboys van het labo) van de toekomstig Spin-off PH&G: bedankt voor het leggen van kilometers kabel en leiding in Zwijnaarde, voor de bouw van 'het frietkot' van Sim en mijn aquarium en voor de hulp bij de overige experimenten. Eigenlijk was het gewoon altijd plezierig met jullie. We zullen nog eens naar de Lekkerbek moeten gaan met mijn busje voor mijn vertrek naar het buitenland. Ann, bedankt voor de toffe gesprekken en ik ben vooral blij dat je terug bent. Pui Yi, bedankt voor het maken van de creatieve cadeaus en het deskundig advies voor mijn

trouwkostuum. En Margot, spijtig dat je weg bent, maar toch bedankt voor de administratieve hulp. Ik hoop dat we elkaar nog eens tegen het lijf lopen.

Naast deze vaste waarden, waren ook de 'nieuwelingen' zeer aangename collega's. Hannes, Jackie, Michiel, Niels, Erik, Thomas, Elizabeth, Bart en Ingvar bedankt voor het samenwerken en voor de leuke momenten aan de koffietafel. Wouter en ex-collega's Maja, Tom en Bruno, bedankt voor alles wat ik opgestoken heb van jullie en de heren voetballers voor de talloze gloriemomenten. Hans, bedankt voor het nalezen van mijn master thesis en voor de tips die je me gaf. Lidewei, merci voor de toffe verhalen over fietsen in Wit-Rusland en rond het Bajkal meer (het geeft me zin om er nog eens op uit te gaan met de fiets!) en voor de toffe discussies rond cavitatie. Maurits, ex-eiland genoot en beroemd bomenklimmer, je weet dat je welkom zal zijn éénmaal ik in de Alpen woon, waar er bomen genoeg staan om al je sap flow en dendro meetfantasiën op los te laten. Tot slot, dé derde verdiepers. Veerle en Marjolein, bijna bureau genoten, bedankt voor de zeer leuke babbels, voor het etentje zojuist in de Walrus en voor de talrijke tips en tricks. En finaal mijn bureau genoten Jochen en Annelies, bedankt voor de mopjes, gedeelde frustraties bij wijlen, maar vooral de leuke momenten. Het was mij een waar genoegen om bij jullie op bureau te zitten en hopelijk kijken jullie later ook met evenveel plezier terug naar deze periode als ik.

Naast werk is er nog zoveel meer in het leven, en daarvoor moet ik zeer veel mensen bedanken om mij dat te helpen herinneren! Hier dus de niet-wetenschappelijke bedankingen:

Vooreerst mijn vrienden, waarmee ik al vele leuke momenten en avonturen mee beleefd heb en/of mee heb samengewoond. Een dikke bedankt voor de afgelopen jaren (tot zelfs de afgelopen 15 jaar…)! We hebben ons toch wel al geamuseerd en leuke momenten beleefd wat ideale ontspanning was voor het werk in mijn doctoraat. Jullie zijn allemaal welkom (en dus verplicht) om langs te komen eens Katrien en ik in het buitenland wonen. Geen excuses.

Daarnaast heeft mijn familie mij altijd gesteund in wat ik doe, zodat ik al alles heb kunnen doen wat ik wou. Dus bedankt aan mijn ouders voor de steun en de hulp de afgelopen jaren, hetzij financieel, hetzij door te behangen of te verhuizen, hetzij… . Daarnaast mijn broer Wieter en mijn zus Siets. Ik heb al veel aan jullie gehad en ik heb

het geluk om jullie kleinere broer te zijn (ondanks onze vele ruzies als kind die ik als underdog stelselmatig verloor). Ik hoop dat ik jullie toch een beetje gelukkig maak en zal dat ook blijven proberen voor de rest van mijn leven. Daarnaast wil ik mijn schoonfamilie, Els en Luc, Karolien en Harold (en Julien), en Nathalie en Sebastien (en Mila) bedanken voor de gezellige momenten samen en voor de interesse in mijn doctoraat. Ik heb geluk met zo een schoonfamilie.

Tot slot wil ik mijn fantastische vrouw Katrien bedanken. We hadden onze eerste date in de Hot Club de Gand een week voor het begin van mijn doctoraat en ondertussen ben je al enkele maanden mevrouw Bloemen. Jij bent de persoon die ik het meest van al moet bedanken voor je steun (zelfs bij het gras knippen!), voor je begrip (als ik weer langer dan beloofd op mijn werk bleef of als ik naar het buitenland moest) en om me op te beuren als het wat moeilijker ging. Mijn Haeckje, je weet maar half hoe graag ik je zie en hoe dankbaar ik je hiervoor ben. Ik heb al zoveel mooie herinneringen aan wat we al samen beleefd hebben, maar ik kijk nog meer uit naar al onze toekomstplannen!

Gent, december 2013

Jasper

Contents

CHAPTER 6

ROLE OF WOODY TISSUE PHOTOSYNTHESIS IN TREE DROUGHT STRESS RESILIENCE 137

CHAPTER 7

TREE GIRDLING CONFIRMS THAT ROOT RESPIRATION CONTRIBUTES TO XYLEM CO_2 TRANSPORT 155

List of abbreviations and symbols

Abbreviations

AE	Acoustic emission
AIC_c	Akaike information criterion corrected for small sample sizes
ANOVA	Analysis of variance
ATP	Adenosine-triphosphate
C	Carbon content
CO_2	Carbon dioxide
DBH	Diameter at breast height
DIC	dissolved inorganic carbon
DM	Dry mass
DOY	Day of the year
DG	Stem daily growth rate
EA	Elemental Analyzer
EC	Electron capture
FACE	Free-air CO_2 enrichment
HB	Heat balance
HL	High label
IPCC	Intergovernmental panel climate change
IR	Infrared
IRGA	Infrared gas analyzer
IRMS	Isotope ratio mass spectrometer
LA	Leaf area
LL	Low label
LVDT	Linear variable displacement transducer
NDIR	Non dispersive infrared
PAR	Photosynthetic active radiation
PEPc	Phosphoenolpyruvate carboxylase

PET	Positron emission tomography
RH	Relative humidity
Rubisco	Ribulose-1,5-biphosphate carboxylase oxygenase
ROI	Region of interest
SFD	Sap flux density
TDP	Thermal dissipation probe
VPD	Vapor pressure deficit
VPDB	Vienna pee dee belemnite

Latin symbols

Symbol	Description	Unit
A_s	Surface area of the stem enclosed in a stem cuvette	m^2
A	Atom%	%
A_t	Atom% of the labeled tissue	%
A(C)	Atomic weight of carbon	g mol^{-1}
A_{atm}	total amount of atmospheric carbon assimilated	g
A_{net}	Net photosynthesis	µmol CO_2 m^{-2} s^{-1}
A_{max}	Maximum photosynthesis	µmol CO_2 m^{-2} s^{-1}
A_{root}	Soil area occupied by the root system	m^2
$[CO_2]$	Gaseous CO_2 concentration	% or µmol mol^{-1}
$[CO_2^*]$	Dissolved CO_2 concentration	mM
$^{13}C_t$	^{13}C tissue content	mg
$^{13}C_{assim}$	Amount of ^{13}C assimilated	mg
$^{13}C_{uptake}$	Amount of ^{13}C label taken up	mg
$^{13}C_{efflux}$	Amount of ^{13}C label lost to the atmosphere by efflux	mg
ΔT	Temperature difference between heated and reference needle	°C
ΔT_0	Temperature difference between heated and reference needle when there is no sap flow	°C
ΔCO_2	Gasous CO_2 concentration difference between measurement and reference air	µmol mol^{-1}
D	Stem diameter	mm

E	Transpiration	mmol H_2O m^{-2} s^{-1}
E_{soil}	Soil CO_2 efflux	mg C m^{-2} h^{-1}
E_{stem}	Stem CO_2 efflux	µmol CO_2 m^{-2} s^{-1}
$E_{stem}(ref)$	Stem CO_2 efflux at reference stem temperature	µmol CO_2 $m^{-2}s^{-1}$
f_a	Flow rate through stem cuvette	l s^{-1}
F_s	Sap flow rate	l h^{-1}
F_t	Xylem transport of CO_2 derived from belowground respiration	mmol h^{-1}
$F_{t,scaled}$	Xylem transport of CO_2 derived from belowground respiration scaled with the soil area occupied by the roots	mg C m^{-2} h^{-1}
$F_{t,scaled-g}$	Xylem transport of CO_2 derived from belowground respiration scaled with the soil area occupied by the roots in the girdled plot	mg C m^{-2} h^{-1}
$F_{t,scaled-c}$	Xylem transport of CO_2 derived from belowground respiration scaled with the soil area occupied by the roots in the girdled plot	mg C m^{-2} h^{-1}
g_S	Stomatal conductance	mol H_2O m^{-2} s^{-1}
k	site and species specific correction factor for sap flow rate	-
K	Acidity constant	-
K_H	Henry's constant	-
m/z	Mass to charge ratio	kg/C
n	amount of gas	mol
$[O_2]$	Gaseous O_2 concentration	%
P	Atmospheric pressure	Pa
pCO_2	Partial pressure of CO_2 over the xylem sap	Pa
Q_{10}	Change in rate for a 10°C change in temperature	-
r	Radius of the soil area occupied by the root system	cm
R	Universal gas constant	J mol^{-1} K^{-1}
R_a	Autotrophic component of respiration	mg C m^{-2} h^{-1}
$R_{a,b}$	Autotrophic component of belowground respiration	mg C m^{-2} h^{-1}

$R_{a,b\text{-}conv}$	Conventional estimate of the autotrophic component of belowground respiration	mg C m^{-2} h^{-1}
$R_{a,b\text{-}new}$	New estimate of the autotrophic component of belowground respiration	mg C m^{-2} h^{-1}
R_h	Heterotrophic component of respiration	mg C m^{-2} h^{-1}
$R_{h,b}$	Heterotrophic component of belowground respiration	mg C m^{-2} h^{-1}
R_{sample}	Abundance ratio of the heavier to lighter isotope in sample	-
$R_{standard}$	Abundance ratio of the heavier to lighter isotope in standard	-
S_i	Illuminated stem section number i	-
t	Time	s
T	Temperature	°C or K
T_{air}	Air temperature	°C
T_{stem}	Stem temperature	°C
$T_{1/2}$	Half life	yr or min
V	Gas volume	m^3
$X_{^{13}C}$	Number of ^{13}C atoms present in the sample	-
$X_{^{12}C}$	Number of ^{12}C atoms present in the sample	-

Greek symbols

β^-	Electron	-
β^+	Positron, i.e. an anti-electron	-
$\delta^{13}C$	Carbon isotopic composition ($^{13}C/^{12}C$)	‰
$\delta^{13}C_a$	Carbon isotopic composition ($^{13}C/^{12}C$) related to enrichment of the air inside the cuvette	‰
$\delta^{13}C_b$	Carbon isotopic composition ($^{13}C/^{12}C$) in baseline samples	‰
$\delta^{13}C_s$	Carbon isotopic composition ($^{13}C/^{12}C$) in ^{13}C enriched samples	‰
$\delta^{13}C_t$	Difference in carbon isotopic composition ($^{13}C/^{12}C$) related to tissue enrichment	‰

Introduction and outline of the thesis

Since the foundation of the intergovernmental panel on climate change (IPCC) in 1988, substantial progress has been made in understanding greenhouse gas induced changes in the earth's climate. The fourth assessment report of working group three of the IPCC states that global greenhouse gas emissions due to human activities have increased with 70% between 1970 and 2004, with carbon dioxide (CO_2) considered as the primary source, having grown by approximately 80% (Rogner *et al.*, 2007). However, we still lack detailed information on what the future holds for climate-mediated changes in the CO_2 emission by plant respiration and its role in the biosphere's response to climate change. While providing the energy and respiratory products necessary for biosynthesis and cellular maintenance (e.g. adenosine-triphosphate (ATP), reducing equivalents, and carbon skeletons (Atkin *et al.,* 2010)), plant respiration releases eighteen times as much CO_2 into the atmosphere than does the burning of fossil fuels in the 1990s (Prentice *et al.*, 2001; Trumbore, 2006). For instance in forests, ecosystem respiration is of particular importance for the local carbon balance with an estimated >50% release of the annual amount of carbon fixed by photosynthesis (Janssens *et al.*, 2001; Luyssaert *et al.*, 2007; Baldocchi, 2008; Schulze *et al.*, 2010). Forests in general act as a sink for CO_2, but there is a delicate balance between the amount of carbon imported into ecosystems and the fraction released back into the atmosphere. Only a detailed understanding of how both processes respond to climate change, from the cellular to the ecosystem level, will enable us to predict whether forests will act as sources or sinks in the future.

Compared with the relatively comprehensive understanding of photosynthesis, we lack basic information on the key determinants of respiration rates in plant organs (Atkin *et*

al., 2010). Moreover, our ability to match predictions of process-based models with upscaled bulk CO_2 flux respiration estimates remains limited (Trumbore, 2006). The main bottleneck to accurately predict and measure ecosystem respiration is its complex nature. Where photosynthesis is a single well-known process, respiration at ecosystem level integrates the variety of plant and microbial processes both above- and belowground by which CO_2 is released back into the atmosphere (Fig. 1, Trumbore, 2006).

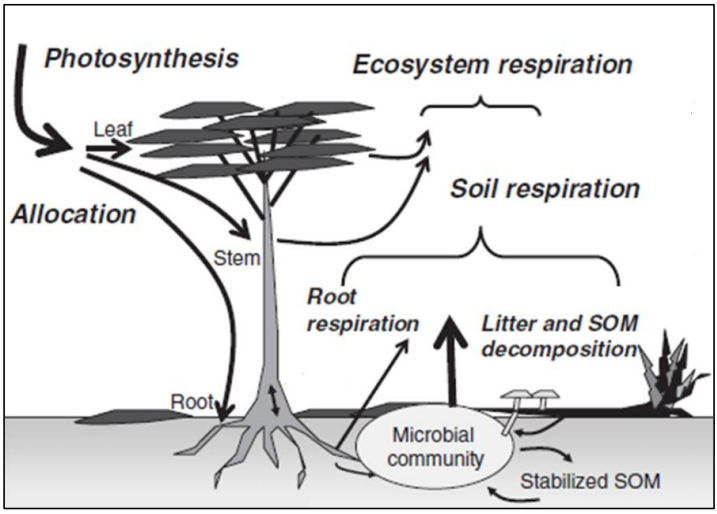

Fig. 1 Release of carbon by respiration into the atmosphere after carbon is imported into the forest ecosystem by photosynthesis (adapted from Trumbore *et al.*, 2006).

In the literature, these processes are functionally divided in an autotrophic (R_a) and heterotrophic (R_h) component according to the substrate that living organisms use to sustain their metabolism. R_h involves the decomposition of organic material in the soil by micro-organisms and is generally considered as being part of a slow cycling process (in the order of months to centuries; Epron, 2009). On the other hand, R_a occurs both above- (in foliar and woody tissues) and belowground (in roots, their mycorrhizal fungal symbionts, and rhizosphere micro-organisms) and relies on carbohydrates that are allocated from the canopy to the other plant tissues, referred to as sinks (Litton *et al.*, 2007).

Adding to the complex nature of ecosystem respiration, a fraction of CO_2 derived from R_a remains within trees and diffuses remote from the site of respiration (Teskey &

McGuire, 2002) or is assimilated by chlorophyll containing tissues (Zelawski *et al.*, 1970; Stringer & Kimmerer, 1993; McGuire *et al.*, 2009), which reminds us to be careful about invoking respiration when we are actually measuring the CO_2 flux from a tissue surface (Trumbore *et al.*, 2013). Since the first observation by Bushong in 1907 on the occurrence of high CO_2 concentrations ($[CO_2]$) in tree stems, scientists have been wondering about the different physiological processes that produce the CO_2 present inside trees. Local respiration of living cells has been described as an important source of CO_2 in tree stems, because of the high resistance to radial diffusion exerted by stem tissues (Boysen-Jensen, 1933; Teskey & McGuire, 2002; McGuire & Teskey, 2004; Teskey *et al.*, 2008). A fraction of respired CO_2 has been found to originate lower down the stem (McGuire & Teskey, 2004; Teskey & McGuire, 2007), or even in the root system from belowground R_a ($R_{a,b}$), because a fraction of the respired CO_2 dissolves in the transpiration stream and is transported upwards throughout the tree (Teskey *et al.*, 2008). A substantial amount might move with the transpiration stream into foliage (Teskey & McGuire, 2002), but the relative proportions of respired CO_2 that diffuse into the atmosphere or that are re-assimilated in chlorophyll containing tissues during this transport, is yet unknown (Hanson & Gunderson, 2009). Therefore **the main objectives of this PhD study** were to elucidate sources and fate of internal CO_2 and to assess the mechanistic significance of internal CO_2 for understanding tree functioning under varying conditions. To this end, a series of experimental studies on different tree species under controlled or field conditions was conducted using carbon isotopes and detailed plant measurements.

Since the first continuous *in situ* measurements of stem CO_2 by McGuire & Teskey (2002), an increasing number of studies have been reporting on the significance of internal CO_2 in trees (e.g. Teskey & McGuire, 2002; McGuire & Teskey, 2004; Maier & Clinton, 2006; Teskey & McGuire, 2007; Aubrey & Teskey, 2009; Grossiord *et al.,* 2012). Therefore, research on internal CO_2 is of topical interest in plant sciences and further pushes the boundaries of our understanding of plant functioning. In **Chapter 1** of this thesis, current knowledge about the sources and fate of internal CO_2 is summarized. In particular the contribution of root-respired CO_2 to internal CO_2 and transport of internal CO_2 with the transpiration stream is assessed in detail. In addition, the second part of

Chapter 1 describes the different techniques used in this thesis to quantify xylem CO_2 transport and to trace the fate of xylem-transported CO_2.

In the past years stable isotopes have been recognized as a powerful tool to trace carbon fluxes and to disentangle soil and plant processes at an unprecedented resolution and scale (Bahn *et al.*, 2012). In particular ^{13}C pulse-labeling has been previously used to trace the fast transfer of recently assimilated carbon from leaves to sink tissues via the phloem (e.g. Epron *et al.*, 2011; 2012 and references therein). Based on the utility of ^{13}C to understand carbon cycling in trees, results from pulse labeling studies are described in **Chapters 2, 3, and 4**, which used ^{13}C to trace xylem CO_2 transport. As described in **Chapter 2** and **Chapter 3**, dissolved ^{13}C-labeled CO_2 (referred to in the text as $^{13}CO_2$) was introduced in detached leaves and branches under controlled conditions, respectively and analyzed for ^{13}C tissue enrichment, as outlined in **Chapter 1**. Moreover, in **Chapter 2** ^{11}C labeling was used to obtain a more accurate tracer distribution at leaf level based on positron autoradiography. In **Chapter 3**, measurements of xylem CO_2 assimilation were compared relative to atmospheric CO_2 assimilation in the leaves. In **Chapter 4**, an experiment on 7-year old field-grown *Populus deltoides* Bartr. ex Marsh. trees was performed, where the ^{13}C label was infused at the stem base to simulate belowground respired CO_2 entering the stem. It was hypothesized that as the label was transported throughout the tree, a portion would be assimilated by chlorophyll containing woody and leaf tissues and a portion would diffuse into the atmosphere. To this end, the isotopic composition of branch and stem CO_2 efflux (E_{stem}) was measured in order to validate the radial diffusion of the ^{13}C label into the atmosphere.

In the past years, several researchers have pondered over the nature and physiological significance of internal CO_2 assimilation by woody tissue photosynthesis (e.g. Bossard & Rejmanek, 1992; Nilsen, 1995; Eyles *et al.*, 2009; Saveyn *et al.*, 2010). Overall, woody tissue photosynthesis contributes to the tree carbon income by recycling respired CO_2 that would otherwise be lost from the plant to the atmosphere (Wittmann *et al.*, 2001; Pfanz *et al.*, 2002; Cernusak & Hutley, 2011). Under specific environmental or physiological conditions woody tissue photosynthesis might gain more significant importance for plant metabolism. In dormant trees, Saveyn *et al.* (2008a) hypothesized that woody tissue photosynthesis induced non-temperature related depressions in

efflux-based stem respiration measurements. In **Chapter 5**, this hypothesis was tested on dormant *Quercus robur* L. trees during a light-manipulation experiment under temperature controlled conditions. Woody tissue photosynthesis is assumed to be less drought-sensitive compared to leaf photosynthesis (Pfanz *et al.*, 2002), but its physiological significance in tree resilience to drought stress remains unclear. To this end, the impact of woody tissue photosynthesis on tree physiology under drought stress was experimentally tested in **Chapter 6**. Detailed stem diameter and leaf gas exchange measurements were compared for control and light-excluded *Populus deltoides x nigra* 'Monviso' trees under well-watered and dry conditions. Moreover, it was tested whether woody tissue photosynthesis plays a role in light-dependent repair of cavitated vessels, as hypothesized by Schmitz *et al.* (2012), which links plant hydraulics to the local plant carbon status.

Observations on the internal transport of belowground respired CO_2 with the transpiration stream (F_t, Aubrey & Teskey, 2009; Grossiord *et al.*, 2012) have raised important questions about our understanding of the tree carbon cycling and root metabolism (Hanson & Gunderson, 2009). Generally, studies exclusively measure soil CO_2 efflux (E_{soil}) when estimating belowground respiration and therefore neglect a fraction of $R_{a,b}$ that is transported with the transpiration stream inside the tree. In **Chapter 7**, F_t and E_{soil} were simultaneously measured according to the techniques outlined in **Chapter 1,** and compared for non-girdled and girdled *Quercus robur* L. trees. The girdling technique, which is based on the removal of a circumferential band of bark and phloem from the tree stem to interrupt belowground carbon transfer (De Schepper *et al.*, 2010), is frequently applied to estimate $R_{a,b}$ (Högberg *et al.*, 2001; 2009; Subke *et al.*, 2011). The girdling approach used in this PhD study allowed a reevaluation of $R_{a,b}$ which is important for understanding belowground respiration, from a mechanistic perspective. Moreover, manipulation of $R_{a,b}$ by tree girdling enabled assessment of the root-respired nature of xylem CO_2 imported into the stem.

In conclusion, the main findings and main contributions of this study to the fields of internal CO_2 and plant respiration research are summarized in **Chapter 8**. Based on this summary, implications and unanswered research questions for ongoing and current research are formulated. Finally, promising future avenues of research which will

improve our current knowledge on the role of internal CO_2 in trees are identified and discussed.

- Chapter 1 -

Sources, fate, and transport of internal CO_2 within the soil plant continuum

1.1 Introduction

Understanding and characterizing variation in plant respiration is of paramount importance for global change science, as well as fundamental to plant ecology and physiology, because the efflux of CO_2 from plant respiratory processes is a critical and uncertain component of plant, ecosystem, and global carbon budgets (King *et al.*, 2006; Houghton, 2007; Reich *et al.*, 2008). To this end, above- and belowground respiration measurements are performed according to the long standing approach that CO_2 efflux reflects underlying local respiration rates because all respired CO_2 diffuses locally into the atmosphere (Teskey *et al.*, 2008; Atkin, 2011; Trumbore *et al.*, 2013).

However, the observation that respired CO_2 can accumulate in tree stems challenges this generally accepted measurement practice to estimate respiration. Transport of internal CO_2 in plants can lead to respiration rates being underestimated at source level, while overestimated in remote organs (Teskey *et al.*, 2008; Atkin, 2011). The discovery that in plants, and in particular trees, high gaseous CO_2 concentrations ($[CO_2]$) are present relative to the atmospheric one (c. 0.04% at 2013) is not new. Based on extraction of gases from stems, Bushong (1907), MacDougal *et al.* (1927), MacDougal & Working (1933), and Chase (1934) discovered early 20th century that CO_2 can build up in stems because the different woody tissues (xylem, vascular cambium and bark layers) exert a

resistance to radial diffusion of CO_2 into the atmosphere (Eklund & Lavigne, 1995; Steppe *et al.*, 2007; Teskey *et al.*, 2008). [CO_2] in tree stems is reported within the range of <1 to over 26% for various tree species (see Table 1 in Teskey *et al.*, 2008). Due to the high solubility of CO_2 in water, a substantial amount of this respired CO_2 can dissolve in the xylem sap and is transported upwards with the transpiration stream. In the liquid phase, dissolved CO_2 is present in different forms ($[CO_2]_{aq}$, $[HCO_3^-]$, and $[CO_3^{2-}]$) which are collectively referred to as dissolved inorganic carbon (DIC) and indicated in the text as [CO_2*].

Recognition of this internal CO_2 flux has lead to novel insights on the role of respired CO_2 recycling in tree physiology and a new proposed methodology for estimating aboveground woody tissue respiration (see review by Teskey *et al.,* 2008). Recent studies have indicated that even belowground respired CO_2 might remain inside the root system and dissolve in the transpiration stream. Aubrey & Teskey (2009) observed for *Populus deltoides* Bartr. ex Marsh trees that the amount of xylem-transported root-respired CO_2 rivaled the amount of belowground respired CO_2 that diffused into the soil environment and contributed to soil CO_2 efflux (E_{soil}). Once transported aboveground, this respired CO_2 can diffuse into the atmosphere or is assimilated in chlorophyll containing tissues in stems and branches, as previously observed for locally respired CO_2 (Teskey *et al.*, 2008). However, the actual impact of the internal transport of root-respired CO_2 on aboveground tree physiology remains unclear.

In this chapter the different sources, fate, and transport of internal CO_2 are reviewed. In particular the fate of root-respired CO_2 and the characteristic of high internal [CO_2] in roots will be highlighted in this review, because to date detailed knowledge on the belowground contribution to internal CO_2 is lacking. Finally in the second part of this chapter an overview of different non-isotopic and isotopic methods used to quantify and trace xylem transport of internal CO_2 in trees is given. The use of isotopes to trace internal CO_2 is new and therefore methods based on carbon isotope labelling of the transpiration stream are highlighted.

1.2 Sources of internal CO_2 in stems

The different sources of internal CO_2 can be functionally and spatially divided in different groups. Aboveground the different sources (i.e. stem and branch respiration) that contribute to internal CO_2 are part of the autotrophic component of respiration (R_a), while belowground both R_a (referred to in the text as $R_{a,b}$ for belowground R_a) and to a lesser extent the heterotrophic component of respiration (referred to in the text as $R_{h,b}$ for belowground R_h) will contribute to respired CO_2 imported into the stem. Although information on the contribution of both above- and belowground sources to stem [CO_2] is scanty, most recent reports indicate that a substantial fraction of belowground respired CO_2 might contribute to stem [CO_2] (Aubrey & Teskey, 2009; Grossiord *et al.,* 2012). These belowground sources of internal CO_2 have not been described in detail previously and will therefore be highlighted.

1.2.1 Belowground respiration

1.2.1.1 Uptake of soil dissolved inorganic carbon

In forests soils, the [CO_2] ranges through the rooting zone from less than 0.1% to more than 1% and generally increases with depth (Pumpanen *et al.*, 2003). A part of this respired CO_2 is dissolved in the soil solution as DIC. It is hypothesized that this soil DIC might influence plant growth, either by affecting the [CO_2] gradient from the roots to the soil, or by supplying substrate for aboveground plant fixation after uptake by the roots (Enoch & Olesen, 1993; Ford *et al.*, 2007). Vuorinen *et al.* (1989) supplied ^{14}C-labeled $NaHCO_3$ as a proxy for soil DIC to roots of hydroponically grown willow plants and detected the radiocarbon tracer within 24 h in the shoot. In a similar hydroponics experiment with *Nicotiana tabacum*, Hibberd & Quick (2002) proposed that assimilation of ^{14}C supplied to the roots in cells around the vascular tissue supports the existence of a C_4-like mechanism in C_3 plants. However, under natural conditions the [CO_2] within tree tissues is generally reported higher than observed for the soil (Teskey *et al.*, 2008), indicating that a decreasing [CO_2] gradient exist from the root tissues towards the soil. Teskey & McGuire (2007) measured simultaneously soil [CO_2] at 15 cm depth and stem [CO_2] at 0.1 m height and observed that mean [CO_2] at stem level (7.6%) was

significantly higher than reported at soil level (mean 1.2%). Similarly, Ubierna *et al.* (2009) observed higher [CO_2] at the base of the stem than in the soil. Moreover, based on [CO_2] measurements in the stem and in the soil, Aubrey & Teskey (2009) estimated that for *Populus deltoides* only up to 8% of belowground respired CO_2 transported with the transpiration stream in the stem is derived from the uptake of soil DIC.

Moreover, there is little evidence that the uptake of soil DIC by roots has a substantial impact on plant physiology. By irrigating crops with a CO_2 enriched solution, it was believed that yield could be increased. While theoretically, aboveground assimilation of CO_2 dissolved in the soil solution by chlorophyll containing tissues could contribute up to 5% of plant carbon assimilation, results indicated that it usually contributed less than 1% (see review by Enoch & Olesen, 1993). More recently, Ford *et al.* (2007) and Ubierna *et al.* (2009) applied a ^{13}C labeled solution isotope to soil around the stem of conifer seedlings in pot and field-grown conifer trees, respectively, which served as a proxy of the uptake of soil DIC via the roots. Ford *et al.* (2007) concluded that assimilation of soil DIC will only contribute to a very limited extent to the tree carbon income. Ubierna *et al.* (2009) observed no ^{13}C enrichment of stem CO_2 efflux (E_{stem}) after application of the label to the soil. Therefore it is unlikely that uptake of soil DIC will contribute substantially to internal CO_2 in stems.

1.2.1.2 Root respiration

Similar as for aboveground organs, CO_2 in roots is derived from respiration in living cells. These are found in the vascular cambium and the parenchyma cells of the phloem and the xylem rays (Fig. 1.1A,B). However substantial parts of the xylem are composed of non living cells. The overall structure of the root is similar as described for tree stems (compare Fig 1.1 with Fig 1.4). In roots, xylem and phloem strands originate which extend throughout the plant body. The periderm, which is composed of cork cambium, cork, and the phelloderm forms a protective exodermis in tree roots after secondary growth of woody plants and is mainly constructed of suberin (Taiz & Zeiger, 2006). Lenticels in the periderm allow gas exchange of O_2 and CO_2 between the root and soil environment. The suberized periderm makes more mature regions of the root system relatively impermeable to water. Therefore, water uptake in the root system mainly occurs by the less suberized root tips (Kramer & Boyer, 1995; Zwieniecki *et al.*, 2002).

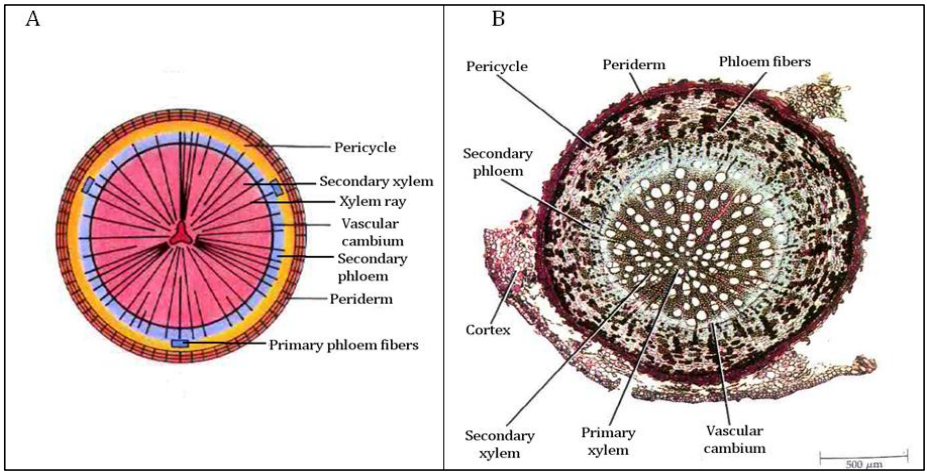

Fig. 1.1 Anatomical structure of a tree root (A) after secondary growth and (B) at the end of first years's growth. Primary phloem and xylem tissues originate from the procambium while secondary phloem and xylem are formed from the vascular cambium (adapted from Raven *et al.*, 1999).

Many plant and environmental factors determine short- and long-term dynamics in root respiration rate. These factors might contribute to variations in internal [CO_2] observed at stem level.

Temperature

Among the environmental factors, temperature is most commonly correlated with respiration. From a theoretical point of view, respiration is partitioned in growth and maintenance respiration and the latter is considered to be highly temperature-sensitive (Amthor, 1989). Variations in soil temperature are often dampened relative to air temperature (T_{air}) dynamics, because the soil takes much longer to warm and cool down. Nonetheless, substantial short- and long-term variation in soil temperature might occur, inducing varying root respiration rates at daily to seasonal scale (Atkin *et al.*, 2000).

Respiration is assumed to increase exponentially with an increase in temperature and a Q_{10} factor (the proportional change in respiration rate with a 10°C increase in temperature) is commonly used to describe this relationship. For roots, Q_{10} values in the range from 1.1 to 2.9 are reported (see Table 1 in Atkin *et al.*, 2000). Boone *et al.* (1998) reported substantially higher Q_{10} values for root respiration and rhizosphere decomposition (4.6) than for respiration in soils lacking roots (2.5) or in bulk soil (3.5).

Therefore, they hypothesized that within the context of climate change, roots will exert a strong influence on the sensitivity of belowground respiration to increasing temperatures. However, Q_{10} values that are significantly above 2.5 may indicate that substrate supply confounds an observed temperature effect, because diffusion of substrates used for respiration might covary with temperature (Davidson *et al.*, 2006a). Moreover, recent studies consider soil temperature to only directly affect the decomposition rate of substances in soil, i.e. $R_{h,b}$, while $R_{a,b}$ is directly related to belowground transport of photosynthates (see review by Kuzyakov & Gavrichkova, 2010). Finally, Q_{10} values of respiration are found to vary among a temperature range and thermal acclimation of respiration might occur (Atkin *et al.*, 2005) and therefore results from temperature-based models of root respiration are often incorrect.

Soil moisture

Soil moisture is considered as another important abiotic factor determining soil and root respiration rates. Overall, soil moisture will reduce the contribution of root respiration to E_{soil} under drought conditions (Bryla *et al.*, 1997; Burton *et al.*, 1998; Moyano *et al.*, 2009). During drought events, a reduction in root cell turgor will lead to a reduced growth and consequently to reduced growth respiration rates. Therefore, observed summer drought induced reductions in E_{soil} (e.g. Davidson *et al.*, 1998; Epron *et al.*, 1999; Curiel Yuste *et al.*, 2004) are partially explained by the reduction in root growth respiration. On the other hand, excess soil water will reduce root metabolism, mainly because oxygen availability in the soil becomes sub-optimal (Moyano *et al.*, 2009).

Carbohydrate supply

Within the soil, root respiration is strongly tied to the consumption of carbon allocated belowground (Hanson *et al.*, 2000). On average nearly half of the carbon assimilated at leaf level is allocated to the root system via the phloem where between one-quarter and two-thirds of this carbon is used for respiration (Lambers, 1987; Farrar & Williams, 1990; Lambers *et al.*, 2002; Moyano *et al.*, 2009). The remainder of the carbon allocated belowground is used to sustain root growth, is stored or is released from roots as root exudates into the rhizosphere.

The strong coupling of tree canopy photosynthesis with $R_{a,b}$ has been overlooked in the past because temperature variations are highly correlated with solar radiation and therefore mask the effect of carbohydrate supply on belowground metabolism (see review by Kuzyakov & Gavrichkova, 2010). Results from recent studies that measured the reduction in E_{soil} after girdling (e.g. Högberg *et al.*, 2001; Högberg *et al.*, 2009; Subke *et al.*, 2011) or traced ^{14}C and ^{13}C in E_{soil} after pulse labeling the canopy with $^{14}CO_2$ (Carbone *et al.*, 2007) or $^{13}CO_2$ (e.g. Högberg *et al.*, 2008; Epron *et al.*, 2011; Epron *et al.*, 2012) (Fig. 1.2), respectively, found that current photosynthesis drives belowground respiration in the order of days or less. Observed lag times in assimilate allocation depended on tree height (Fig. 1.2), and are found to correlate well with results predicted on estimated phloem rates, which typical range from 0.5 to 1 m h^{-1} (Kuzyakov & Gavrichkova, 2010 and references therein). Moreover, the higher lag times observed for coniferous species relative to deciduous species most likely reflect a difference in phloem anatomy (Epron *et al.*, 2012; Jensen *et al.*, 2012) (Fig. 1.2). A rapid coupling of above- and belowground processes by pressure-concentration waves through the phloem is theoretically possible (Thompson & Holbrook, 2004) but its role in trees remains yet unclear.

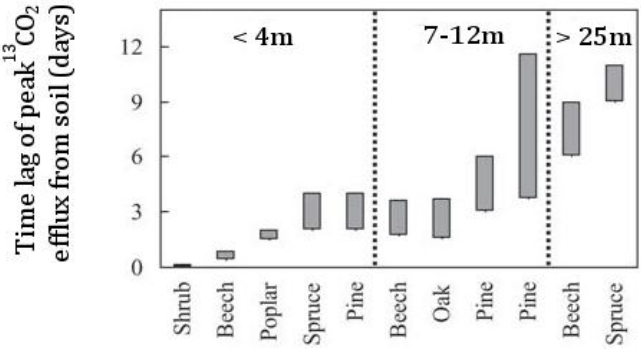

Fig. 1.2 Time lag of peak $^{13}CO_2$ in soil CO_2 efflux or coarse roots after pulse labeling the canopy with $^{13}CO_2$ for varying species with a varying height (after Epron *et al.*, 2012).

The impact of belowground carbohydrate supply on root respiration is assumed to vary on a seasonal scale, in particular for deciduous trees. While during the dormant season root reserves are used to fulfill maintenance root respiration, growing season root respiration and root growth will mainly be fueled by the belowground supply of fresh

assimilates (Moyano *et al.*, 2008 and references therein). However, presence of large carbohydrate reserves in roots in the growing season might explain observed decoupling of belowground carbon allocation and root respiration in some species (Farrar, 1999). Regardless whether belowground respired CO_2 is derived from stored carbohydrates or recent photosynthates, a fraction is transported within the tree with the transpiration stream (Aubrey & Teskey, 2009). However, the coupling of xylem CO_2 transport with belowground metabolism remains unclear.

Soil nitrogen

Supplying plants with inorganic nutrients is one of the major functions of the roots (Jungk, 2002) and therefore a change in soil nutrient concentration will importantly affect root metabolism. In this section we highlight the effect of soil nitrogen on root respiration. Overall, nitrogen content is believed to be a key determinant of (root) maintenance respiration (Comas & Eissenstat, 2004; Atkinson *et al.*, 2007; Wang *et al.*, 2010), because nitrogen plays an important role in metabolic processes in the form of enzymes or co-factors (Reich *et al.*, 2008) of which the replacement and repair are tightly linked with cellular activity (Ryan *et al.*, 1996). Therefore, root respiration is expected to increase with greater soil nitrogen availability (Wang *et al.*, 2010). Ryan *et al.* (1996) found a strong correlation of fine root nitrogen content with root respiration for *Pinus radiata* trees either subjected to a control or fertilization treatment. Moreover, Reich *et al.* (2008) reported based on an extensive dataset that root respiration rates per unit of nitrogen are generally higher than what is measured for leaves, presumably because nitrogen in roots are involved in high demanding metabolic functions, while in leaves a large fraction of the nitrogen is used in photosynthetic machinery. Hence, an important fraction of the nutrients absorbed at root level like nitrogen might be used to sustain aboveground plant functioning for instance at leaf level. In addition, this transport of nutrients provides a means for achieving root-shoot signalling of whole-plant nutrients status, leading to a proper integration of root nutrient uptake in response to whole plant demand (Glass, 2002).

Morphology and age

The root system is composed of roots with different diameters (Fig 1.3A,B), which possess different morphological traits and have a wide range of different physiological

functions (Eissenstat *et al.*, 2000; Chen *et al.*, 2010). As a result, metabolic root tissue demands are highly variable and therefore a large range in respiration rates is observed among the different roots of the root system. Fine roots (diameter <2 mm or <5mm, depending on the definition by the author) are assumed to be more metabolically active, with higher reported respiration rates (Fig. 1.3A), and sustain physiological functions such as water and nutrient uptake of trees (Gill & Jackson, 2000; George *et al.*, 2003). The larger roots, which are often suberized and whose primary function is support and transport of nutrients and water from the very fine roots to other portions of the tree, are not as active in nutrient uptake and are expected to have lower respiration rates than the very fine roots (Fig. 1.3a, Pregitzer *et al.*, 1998). This decrease in specific root respiration (i.e. respiration per unit dry mass) with increasing diameter is found to correlate with decreasing nitrogen content (Ryan *et al.*, 1996; Pregitzer *et al.*, 1998; Bahn *et al.*, 2006), an increase in tissue and plant age (George *et al.*, 2003; Volder *et al.*, 2005; Moyano *et al.*, 2009), and with differences in growth respiration (Lambers *et al.*, 2002).

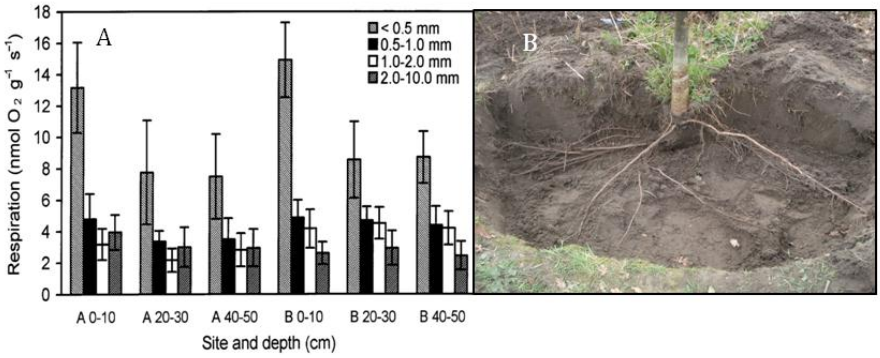

Fig. 1.3 (A) Specific respiration rate (measured as O_2 uptake) of *Acer sacharum* Marsh roots of different diameters measured for two sites and at different depths (after Pregitzer *et al.*, 1998). (B) View of the excavated root system of a 9-y old *Quercus robur* tree.

CO_2 and O_2 concentration

Overall, roots thrive in substantially higher [CO_2] as compared to aboveground tissues (see Section 1.2.1.1). Soil [CO_2] is found to vary strongly across the growing season (Sands *et al.*, 2000) and even during the day (Bouma & Bryla, 2000) and there are conflicting views regarding the sensitivity of root CO_2 efflux to varying soil [CO_2] (Subke

et al., 2006). Ryan *et al.* (1996) observed an exponential increase in root CO_2 efflux of *Pinus radiata* roots with an artificial decrease in surrounding [CO_2] from 1500 to 400 µmol mol^{-1}. Similarly, Qi *et al.* (1994) and McDowell *et al.* (1999) observed a decrease in root CO_2 efflux with increasing [CO_2] for *Pseudotsuga menziesii* and *Tsuga heterophylla*, respectively, while other authors reported little or no sensitivity of root CO_2 efflux to soil [CO_2] for temperate (Burton & Pregitzer, 2002) and Mediterranean (Bouma *et al.*, 1997) species, tested in a range of 100-2000 µmol mol^{-1} and 400-25000 µmol mol^{-1}, respectively. The exact mechanism responsible for the [CO_2] sensitivity of root CO_2 efflux remains unclear and to date the respiratory inhibition of root respiration by increase [CO_2] is assumed to be taxon-specific (Subke *et al.*, 2006). In spite of the conflicting views regarding the sensitivity of root respiration to soil [CO_2], efflux-based measurements of root respiration should preferably be made at concentrations closest to those present in the soil (Hanson *et al.*, 2000; Subke *et al.*, 2006).

Less controversial seems the inhibitory effect of the low soil O_2 concentrations ([O_2]) on root respiration. Limited soil [O_2] in soils prone to flooding is an important constraint for plant metabolism because gas diffusivity is 10^4 fold slower in water than in air (Nobel, 1999; Abiko *et al.*, 2012). Therefore, internal transport of O_2 from the aerial shoot to the root is crucial for these plants, which is enhanced by tissues high in porosity and the formation of aerenchyma in corticular root and stem tissues (Armstrong, 1979; Colmer, 2003). On the other hand, root-respired CO_2 might be transported via the aerenchyma towards the shoot, where it is used as substrate in photosynthesis (Wetzel & Grace, 1983). Moreover, many of these wetland species possess roots with strongly suberized cells walls and/or a thickened exodermis (De Simone *et al.*, 2003), which form an important barrier to radial oxygen loss (Colmer, 2003). At the same time, these barriers will also limited radial CO_2 diffusion of root-respired CO_2 and sediment-derived CO_2, leading to an accumulation of CO_2 in the roots of these wetland and aquatic species (Brix, 1990; Li & Jones, 1995; Colmer, 2003; Aubrey & Teskey, 2009).

1.2.2 Stem and branch respiration

Within forest ecosystems stem and branch respiration is considered as an important component of the ecosystem respiration, with an estimated 30-70% of Gross primary

productivity released back to the atmosphere via aboveground woody tissue respiration (Ryan *et al.*, 1996; Damesin, 2003). While results from these studies were based on the generally accepted assumption that stem and branch respired CO_2 diffused immediately into the atmosphere (Hölttä & Kolari, 2009), it is now generally accepted that a substantial quantity of locally respired CO_2 is retained in the xylem and contributes to internal CO_2 (Steppe *et al.*, 2007; Teskey *et al.*, 2008) beside belowground respired CO_2.

Within trees, gaseous CO_2 can accumulate to concentrations (range <1 to over 26%) substantially higher than the atmospheric one (C. 0.04% in 2013), implying that woody tissues like the xylem (Sorz & Hietz, 2006), cambium (Hook *et al.*, 1972) and bark (Lendzian, 2006) exert an important resistance for radial diffusion of locally respired CO_2. Moreover, variation in these resistances to radial CO_2 diffusion might contribute to intra-species variation in CO_2 efflux (Steppe *et al.*, 2007) (see Section 1.3.3).

Local respiration in stem and branches is performed by mitochondria in living phloem parenchyma, cambium, and parenchyma cells in the xylem rays of heart and sapwood (Fig 1.4). The dead xylem vessels in the sapwood are used for water transport. In particular the cells in the inner bark (part of the stem from vascular cambium till the last formed periderm, which includes the phloem, Pfanz & Aschan, 2001) are considered to have a higher respiratory acitivity as compared to xylem ray cells (Teskey *et al.*, 2008; Araki *et al.*, 2010), in particular during periods of high metabolic activity like during springtime (Maier & Clinton, 2006). Goodwin & Goddard (1940) measured oxygen consumption rate as a proxy for respiration rate in black ash stems and observed that uptake rates were several magnitudes higher near the inner bark compared to the xylem. Pruyn *et al.* (2002a; 2002b; 2003) measured CO_2 efflux and observed that respiration of the inner bark of different conifer species was between 2-15 times greater than that of the sapwood. Therefore in smaller woody organs (<~0.10 m diameter) inner bark respiration will be the largest respiratory component. However, when the number of living cells is scaled with tissue volume for stems and larger branches, generally more living cells are found in the xylem than in the inner bark. For instance, Ryan (1990) determined for *Pinus contorta* and *Picea engelmanni* trees that the xylem contained more than 80% of the total live-cell volume in their stems. Similarly, Ceschia *et al.* (2002) found that sapwood in *Fagus sylvatica* stems contained an important

fraction of total number of living cells in the stem. Therefore, in stem and larger branches, CO_2 derived from living xylem parenchyma cells will be the paramount local respiratory source that contributes to internal CO_2 at stem level.

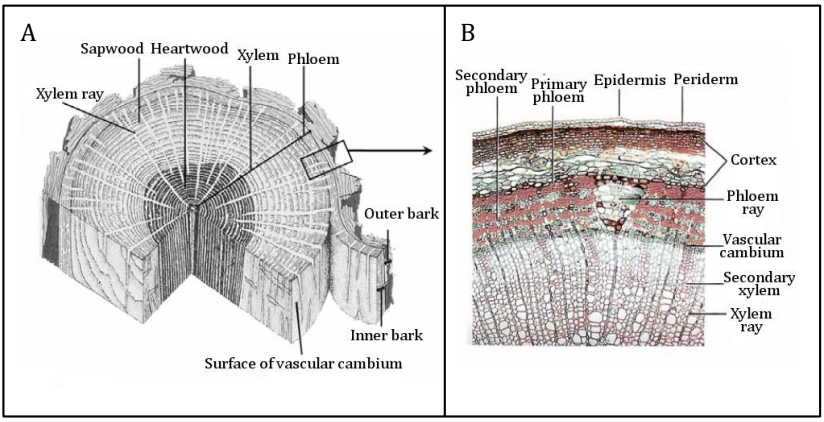

Fig. 1.4 Anatomical structure of a tree stem (adapted from Raven *et al.*, 1999)

Besides distribution and the amount of living cells, other factors that affect woody tissue respiratory activity will influence internal CO_2 at stem level. Overall, these are similar as the factors that influence respiratory activity at root level, discussed in Section 1.2.1.2.

1.3 Fate of internal CO_2

Depending on the site of respiration discussed in the previous sections and on plant physiological factors like sap flow rate (F_s) and xylem sap pH, internal CO_2 is transported within the tree towards the canopy, assimilated by chlorophyll containing tissues or diffuses through stems and branches towards the atmosphere (Fig. 1.5). In particular, the aboveground transport of (belowground) respired CO_2 either by axial diffusion or by bulk flow with the transpiration stream is an important new aspect of internal CO_2 research.

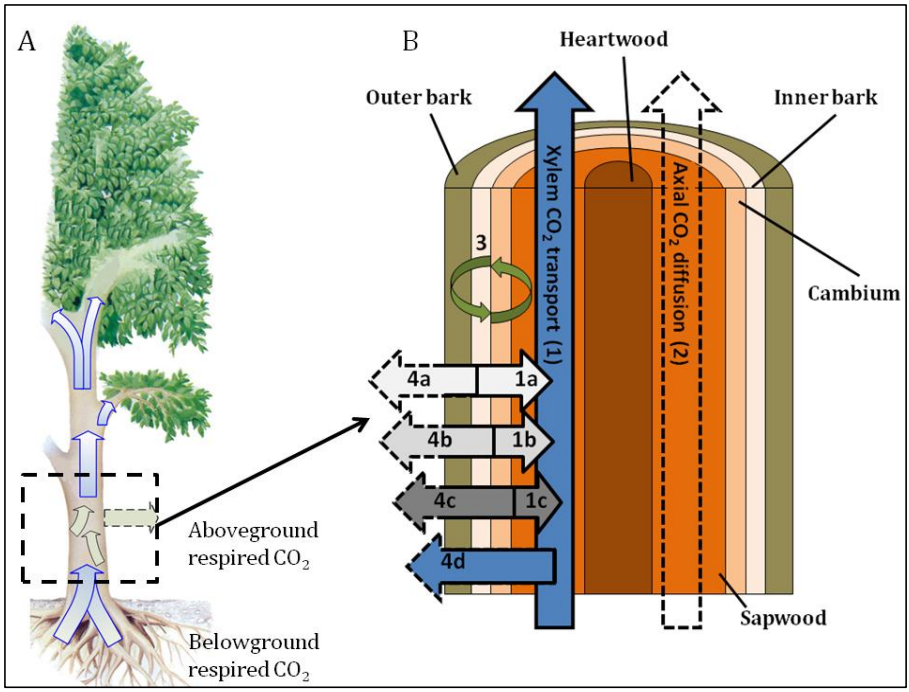

Fig. 1.5 (A) Overview of the fate of internal CO_2 within trees either derived from below- or aboveground respiration (adapted from Cruiziat & Tyree, 1990). (B) Schematic of the fate of internal CO_2 inside a tree segment. Number 1 indicates transport of respired CO_2 with the transpiration stream, number 2 axial diffusion of respired CO_2 (potentially significant in dormant trees), number 3 CO_2 assimilation by woody tissue photosynthesis, number 4 radial diffusion of respired CO_2 to the atmosphere. Letter a indicates fluxes from inner bark tissues, letter b fluxes from cambium tissues, letter c fluxes from xylem tissues and letter d flux from the transpiration stream. In both (A) and (B), solid lines represent combined dissolved and gaseous CO_2 transport (determined by the equilibrium between $[CO_2]$ and $[CO_2^*]$), dashed lines gaseous CO_2 transport (adapted from Teskey *et al.*, 2008).

1.3.1 Transport of respired CO_2 in trees

1.3.1.1 Transport with the transpiration stream

While most studies report on gaseous CO_2 present in trees, a large quantity of respired CO_2 in stems and branches is dissolved in the xylem sap (Teskey *et al.*, 2008) and is transported away from the site of respiration (number 1 in Fig. 1.5B). The gaseous phase in intercellular spaces, pore spaces within the cell walls, and the lumen of cells is in contact with this liquid phase (Hari *et al.*, 1991), and an equilibrium exists between both gaseous and the different forms of dissolved CO_2. $[CO_2^*]$ can be calculated according to the law of Henry based on measurements of gaseous $[CO_2]$. Therefore measurements of

gaseous [CO_2] in holes drilled in the stem are commonly used to estimate the amount of CO_2 dissolved in the xylem sap and the total quantity of CO_2 transported internally (see Section 1.4.1.1).

High F_s can substantially dilute xylem [CO_2*] and therefore diurnal variation in [CO_2*] are inversely correlated to transpiration and F_s dynamics. Based on laboratory and field experiments Teskey & McGuire (2002) reported xylem sap [CO_2*] in the range of 0.9 to 8.3 mM at seasonal scale for *Quercus alba* L. and *Liriodendron tulipifera* L., which differ in xylem anatomy, and observed that diurnal dynamics were negatively correlated with F_s. Similarly, McGuire *et al.* (2007) artificially manipulated F_s in branch segments of *Platanus occidentalis* L. and found that xylem [CO_2*] strongly decreased from around 1.5 to 0.2 mM when increasing sap flux density (SFD) from around 0.008 $cm^3\ cm^{-2}\ h^{-1}$ to 0.2 $cm^3\ cm^{-2}\ h^{-1}$. Maier & Clinton (2006) progressively removed the canopy of *Pinus taeda* L. and observed that xylem [CO_2] and therefore [CO_2*] gradually increased over time. However, when expressed as the total quantity of CO_2 transported with the transpiration stream (as calculated in Section 1.4.1.4), the largest amount of xylem-dissolved CO_2 will be transported at high F_s (McGuire *et al.*, 2007), because the increase in F_s compensates for the decrease in xylem sap [CO_2*] due to dilution.

While previous studies focused on internal transport of respired CO_2 to account for observed midday depressions in E_{stem} (see Section 1.3.3 and references therein) or to provide additional substrate for photosynthesis in leaves (see Section 1.3.2 and references therein), results from recent studies highlight the transport of belowground respired CO_2 within trees. In the root system, respired CO_2 may dissolve in water taken up by the roots, instead of contributing to E_{soil}, thereby representing an internal flux that rivals the autotrophic contribution to E_{soil} (Fig. 1.6). Teskey & McGuire related high internal [CO_2] measured at the stem base to the transport of root-respired CO_2 with the transpiration stream. Aubrey & Teskey (2009) were the first that quantified the internal flux of root-respired CO_2 versus the contribution of $R_{a,b}$ to E_{soil}. With simultaneous measurements of F_s and [CO_2] in stems and soil [CO_2] profiles, they estimated that for eastern cottonwood (*Populus deltoides* Bartr. ex Marsh), twice the amount of CO_2 derived from $R_{a,b}$ was transported with the transpiration stream compared with that which diffused into the soil environment and contributed to E_{soil} (Aubrey & Teskey,

2009). Similarly, transport of root-respired CO_2 with the transpiration stream was observed for *Eucalyptus* (Grossiord *et al.,* 2012). However, in their study only 24% of root-respired CO_2 was found to be diverted from E_{soil} to transport with the transpiration stream.

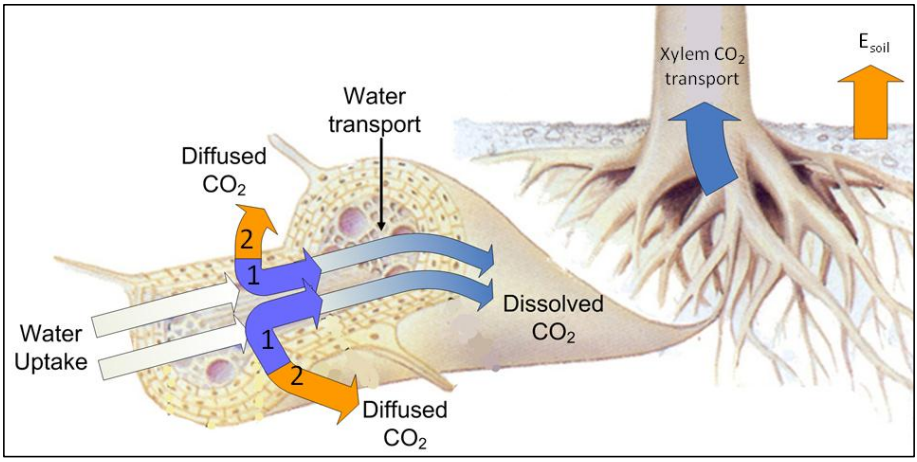

Fig. 1.6 Schematic of the fate of CO_2 respired within living cells of the roots. Number 1 indicate transport of root-respired CO_2 with the transpiration stream, number 2 diffusion of respired CO_2 into the soil environment which contributes to soil CO_2 efflux (E_{soil}) (adapted from Cruiziat & Tyree, 1990).

Nevertheless, the transport of root-respired CO_2 raises important questions about our understanding of belowground respiration because efflux-based measurements of belowground respiration routinely underestimate the carbon needed to sustain belowground tissues (Aubrey & Teskey, 2009; Hanson & Gunderson, 2009). Moreover, increased [CO_2*] in the xylem at night suggests that roots might possess substantial barriers to radial diffusion of respired CO_2 into the soil environment (Aubrey & Teskey, 2009), resulting in high [CO_2] in the roots relative to the soil (Box 1.1). Nevertheles, most studies on belowground respiration neglect the transport of root-respired CO_2 with the transpiration stream or the possible occurrence of high internal [CO_2] in roots.

Box 1.1 Occurrence of high internal [CO_2] in roots?

Occurrence of high [CO_2] in tree roots might be related to an oxygen concentrating trait in roots of wetland species (Aubrey & Teskey, 2009). As a result a substantial fraction of respired CO_2 might accumulate in roots, in particular in the older sections of the root system where root tissue is more suberized.

Different observations underpin the possible existence of high internal [CO_2] in roots. Root respiration is frequently estimated in the field based on excised root measurements (see review by Kuzyakov, 2006). By excising the roots, barriers to radial diffusion are removed, and a large amount of root-respired CO_2 concentrated in the roots might flush into the incubation chamber, accounting for the high increase and subsequent rapid decline in respiration rate estimates observed within one hour after root excision (Rakonczay *et al.*, 1997; Kuzyakov, 2006; Marsden *et al.*, 2008) and the significantly higher respiration rates measured for excised roots compared to those for living ones (Makita *et al.*, 2012). In addition, variation in the resistance to radial diffusion among roots of different species might account for the taxon-specific sensitivity of root CO_2 efflux to increased [CO_2] levels in the soil (see Section 1.2.1.2). Upward transport of root-respired CO_2 which partially accumulates in the roots may interfere with efflux-based estimates of root and belowground respiration. Subke *et al.* (2009) observed unexpected decreases in daytime E_{soil}, related to daytime depressions in the autotrophic component of E_{soil}. At root level, similar depressions in CO_2 efflux related to varying transpiration rates were observed (Bekku *et al.*, 2009; 2011), presumably because a fraction of respired CO_2 will be retained in the root and transported away with the transpiration stream instead of diffusing into the soil environment.

1.3.1.2 Axial diffusion of respired CO_2

During the dormant season, when trees are leafless, no xylem transport of respired CO_2 occurs due to the lack of sap flow. As a result, dormant season E_{stem} is assumed to be a good estimator of stem respiration (McGuire *et al.*, 2007) which equals maintenance respiration as radial stem growth does not occur during dormancy (Maier, 2001).

However, when sap flow is absent, respired CO_2 in gaseous form may be transported by axial diffusion along a [CO_2] gradient in the stem (number 2 in Fig. 1.5B), according to the law of Fick (Jones, 1992; Sorz & Hietz, 2006). While the formation of aerenchyma tissue is mainly constrained to plants growing on waterlogged soils (see Section 1.2.1.2),

trees contain large gas volumes (range 18-50%, Gartner *et al.* (2004)) allowing considerable gas movements in trunks along axial and radial axis (MacDougal & Working, 1933; Hook & Brown, 1972; Armstrong & Armstrong, 2005). Saveyn *et al.* (2008a) reported non-temperature related depressions in E_{stem} and $[CO_2]$ for dormant *Quercus robur* and *Fagus sylvatica* trees concomitant with a 12h light period under a controlled light-regime. They hypothesized that during the light period, vertical internal CO_2 gradients arose due to local decreases in internal CO_2 by woody tissue photosynthesis in uncovered stem sections relative to internal $[CO_2]$ in the stem section covered with an opaque cuvette for efflux-based stem respiration measurements. As a consequence, CO_2 molecules were transported away from the site of respiration along this CO_2 gradient, detected as a reduction in E_{stem} and local internal $[CO_2]$.

Similarly, illumination triggered stem photosynthesis in young *Alnus glutinosa* trees which increased local $[O_2]$ in the cortex and enabled O_2 transport from the shoot to the roots (Armstrong & Armstrong, 2005). Therefore, axial diffusion of respired CO_2 might account for dormant season E_{stem} and $[CO_2]$ dynamics, even in large field-grown trees (Etzold *et al.*, 2013), however we currently lack detailed information on the significance of axial CO_2 diffusion for efflux-based estimates of stem respiration.

1.3.2 Re-fixation of respired CO_2

Within trees, chlorophyll containing stem and branch tissues are capable of assimilating respired CO_2 in addition to atmospheric CO_2 assimilation by green leaves (Pfanz *et al.*, 2002; Berveiller *et al.*, 2007a). Despite the fact that the photosynhetic biochemistry is similar, both processes show distinctly different characteristics (Table 1.1). Within stems and branches, most chlorophyll containing woody tissue can be found in the inner bark (Fig. 1.7) where woody tissue photosynthesis occurs (number 3 in Fig. 1.5B). However a fraction of the chlorophyll is present in the ray cells of the wood (Rentzou & Psaras, 2008) and even in the pith (Van Cleve *et al.*, 1993), justifying the use of woody tissue photosynthesis instead of corticular or bark photosynthesis when referring to stem CO_2 assimilation (Saveyn *et al.*, 2010).

Fig. 1.7 (A) Chlorophyll present in segments of young *Platanus occidentalis* stems. In the current year stem segment (far right) chlorophyll is found throughout the stem. With increasing size, age, and bark thickness, chlorophyll is mostly present in the inner bark (after Teskey *et al.*, 2008). (B) Bark chlorophyll in a branch of a young *Populus canadensis* tree.

Table 1.1 Features of woody tissue photosynthesis and leaf photosynthesis. Modified according to Aschan & Pfanz (2003). WUE: Water Use Efficiency; PAR: Photosynthetic Active Radiation; Diff. conduct.: Diffusive conductance

Type of photosynthesis	Carbon source	Longevity	WUE	Limiting factor	Diff. conduct.	Significance?
Woody tissue photosynthesis	Respired CO_2	< than sufficient to pay for construction and maintenance	High	PAR	Low	In leafless trees or when leaf photosynthesis is limited (e.g. stress)
Leaf photosynthesis	Atmospheric CO_2	> than required for construction and maintenance	Low	CO_2	High	Main carbon income of plants

Woody tissue photosynthesis is generally widespread among plants and trees (see Table 3 in Teskey *et al.*, 2008) and it is believed to positively contribute to the overall plant carbon economy (Pfanz *et al.*, 2002), by recapturing respired CO_2 that otherwise would have been lost from the plant to the atmosphere (Cernusak & Hutley, 2011). Within illuminated branches of *Betula pendula* Roth. woody tissue photosynthesis was able to refix up to 97% of respired CO_2 (Wittmann *et al.*, 2006). According to Aschan *et al.* (2001) chlorophyll in current year *Populus tremula* L. twigs refixed around 80% of internal CO_2. However, the efficiency of refixation decreased with increasing plant age

(Pfanz *et al.*, 2002) and it is well accepted that rates of woody tissue photosynthesis are relatively low compared to atmospheric assimilation rates and stem CO_2 assimilation very rarely leads to a net carbon gain, but merely entails a recycling of respired CO_2 (Pfanz *et al.*, 2002).

Overall, woody tissue photosynthesis is important for the tree carbon income but it might gain even more importance when trees are leafless (Eyles *et al.*, 2009; Saveyn *et al.*, 2010) or when atmospheric CO_2 uptake by leaves is reduced under limited water conditions (Wittmann & Pfanz, 2008). During a light exclusion experiment, Saveyn *et al.* (2010) observed that young *Prunus ilicifoila, Umbellularia californica*, and *Arctostaphylos Manzanita* plants rely on sugars from woody tissue photosynthesis for bud development at the end of the dormant season. Moreover, Eyles *et al.* (2009) performed a defoliation experiment on young *Eucalyptus globulus* seedlings and observed that defoliated seedlings had an increased capacity to refix respired CO_2 (up to 96%). One of the fundamental advantage of woody tissue photosynthesis over leaf photosynthesis is that in order to take up CO_2, leaves have to open their stomata, hence exposing the drought-sensitive mesophyll tissue to the drying power of the air, whereas woody tissue chlorophyll is supplied with endogenously respired CO_2 (Pfanz *et al.*, 2002). Moreover, there is very limited water loss via the stem (Cernusak & Marshall, 2000; Wittmann & Pfanz, 2008). Therefore, woody tissue photosynthesis is expected to increase the plants resilience to drought, since partial closure of stomata has only a limited effect on the xylem [CO_2] (Teskey *et al.*, 2008; Angert *et al.*, 2012). Moreover, xylary chloroplasts potentially play an important role in providing sugars needed for the refilling and sensing of cavitated xylem vessels (Box 1.2).

Finally, recent studies indicate that xylem-transported CO_2 can be assimilated in photosynthetic cells in woody tissues and leaves. McGuire *et al.* (2009) supplied a dissolved ^{13}C isotope to detached *Platanus occidentalis* L. branches and observed that on average 35% of the label was assimilated. The majority of the label was assimilated by the woody tissue, where at leaf level the petiole assimilated most of the label. These results corroborate with previous findings on the role of xylem-transported CO_2 as substrate for photosynthesis in detached leaves (Stringer & Kimmerer, 1993) and herbaceous plants (Hibberd & Quick, 2002). Moreover, assimilation of xylem-

transported CO_2 fits seamlessly with the possible existence of a C_4-like mechanism in C_3 plants (Hibberd & Quick, 2002). However, to date we lack knowledge on the extent of assimilation of xylem-transported CO_2 in field-grown trees and its significance in maintaining the carbon and water status of plants under varying environmental conditions.

Box 1.2 Role of woody tissue photosynthesis in xylem cavitation repair

Embolism results in a dramatic loss of the xylem hydraulic function (Zwieniecki & Holbrook, 2009). Therefore cavitation repair, by refilling embolized vessels, is crucial for plant survival. Schmitz *et al.* (2012) observed that for a diverse range of mangrove species stem hydraulic conductivity was lower in branches where woody tissue photosynthesis was excluded relative to control branches. They suggested that xylary chloroplasts in particular could play an important role in light-dependent repair of embolized xylem vessels, because of their proximity to the xylem vasculature. Sugars synthesized by these chloroplasts potentially supply the necessary energy for vessel refilling (Zwieniecki & Holbrook, 2009) or are used for xylem embolism sensing which is crucial within the context of a refilling mechanism (Secchi & Zwieniecki, 2011).

1.3.3 Diffusion of respired CO_2 into the atmosphere

Internal CO_2 derived from local respiration or imported by the transpiration stream with the xylem sap can diffuse radially to the atmosphere (number 4 in Fig. 1.5), thereby confounding efflux-based estimates of local stem respiration rates (Teskey *et al.*, 2008). Moreover, when the transpiration stream acts as a sink, a large fraction of respired CO_2 can be transported upwards to the canopy and diffuse remote from the site of respiration, leading to an underestimation of local stem respiration.

Based on measurements of F_s, internal $[CO_2]$, and E_{stem} (see Section 1.4.1), McGuire & Teskey (2004) and Teskey & McGuire (2007) have quantified the contribution of different sources to E_{stem}. When F_s are low, E_{stem} is primarily derived from local tissue respiration by living cells and CO_2 stored temporarily in the stem. The amount of respired CO_2 diffusing into the atmosphere is dependent on the $[CO_2]$ gradient and on the diffusion resistance (Steppe *et al.*, 2007; Hölttä & Kolari, 2009), as characterized by a

modified version of Fick's law of diffusion (Pfanz & Aschan, 2001; Teskey *et al.*, 2008), where resistance in trees is highly variable among individual trees (Steppe *et al.*, 2007) and diffusion changes at least according to tissue type (Teskey *et al.*, 2008) and stem gas and water content (Sorz & Hietz, 2006). Within the bark, resistance is determined by the cortex, periderm (consisting of phelloderm, cork cambium and cork) and the rhytidome (dead outer tissue of the bark) (Ziegler, 1957; Teskey *et al.*, 2008) (Fig. 1.4). Additionally, the vascular cambium limits radial diffusion of respired CO_2 from the xylem towards the atmosphere (Hook *et al.*, 1972; Kramer & Kozlowski, 1979). Therefore the stem of some species could contain two disconnected CO_2 pools (Ubierna *et al.*, 2009), one inside the part of the stem enclosed by the cambium, with high xylem [CO_2] (see Section 1.1) and one in the stem outside of the cambium, containing lower [CO_2] (Cernusak & Marshall, 2000; Wittmann *et al.*, 2006; Teskey *et al.*, 2008).

At high F_s, a large fraction of locally respired CO_2 might be transported away from the site of respiration leading to an underestimation when using efflux-based measurements to quantify stem respiration (McGuire *et al.*, 2007). First studies reported daytime E_{stem} rates lower than those modeled from bark or sapwood temperature, due to transport of respired CO_2 with the transpiration stream (e.g. Edwards & Mclaughlin, 1978; Negisi, 1979; Kaipiainen *et al.*, 1998; Gansert & Burgdorf, 2005). McGuire & Teskey (2004) proposed a new mass balance approach for quantifying stem respiration and estimated that up to 55% of locally respired CO_2 could be transported away from the site of respiration in the transpiration stream of *Platanus occidentalis* L. stems. Angert *et al.* (2012) measured the ratio of E_{stem} to O_2 influx for different Amazonian species and observed that on average around 35% of locally respired CO_2 was transported away with the transpiration stream.

At the same time that respired CO_2 is transported away from the site of respiration, at high xylem sap [CO_2*] or high F_s a large amount of xylem-transported CO_2 is imported into the stem section, from lower stem segments or the root system, which partially contributes to E_{stem}. By manipulating sap [CO_2*], Teskey & McGuire (2002) and Steppe *et al.* (2007) showed that CO_2 efflux was strongly dependent on xylem sap [CO_2*]. However, a decoupling between E_{stem} and xylem [CO_2*] has been observed in other studies, due to the large barriers for radial diffusion (Saveyn *et al.*, 2008b) or due to the

high activity of cambial and phloem cells during spring (Maier & Clinton, 2006; Gruber *et al.*, 2009). All previous studies mainly focused on the radial diffusion of xylem-transported CO_2 derived from aboveground sources. The recent discovery of an internal xylem-transported flux of belowground respired CO_2 of large magnitude by Aubrey & Teskey (2009) might imply that a fraction of E_{stem} is derived from belowground sources. Therefore, the interpretation of efflux-based estimates of respiration are potentially even more complex than previously assumed (Box 1.3), and the fraction of belowground respired CO_2 released via the stem is as yet unknown (Hanson & Gunderson, 2009).

Box 1.3 Is belowground respired CO_2 released into the atmosphere from stems?

An important consequence of the internal transport of CO_2 within the soil plant continuum is that a substantial fraction of belowground respired CO_2 might be released through stems (Aubrey & Teskey, 2009; Hanson & Gunderson, 2009). Levy *et al.* (1999) was the first to hypothesize that a fraction of E_{stem} was derived from belowground sources. They observed for *Betula pendula* Roth. and varying tropical species a positive correlation between sap flow and E_{stem}, which they attributed to the import of xylem sap at high [CO_2*] from the roots. During a free-air CO_2 enrichment (FACE) experiment on *Pinus taeda* L., Moore *et al.* (2008) estimated that 19% of the average E_{stem} was contributed by CO_2 taken up from the soil instead of local respiration. Recently, Yang *et al.* (2012) observed a correlation between root-respired CO_2 efflux with E_{stem} in a temperate forest in China. However, during a ^{13}C soil labeling experiment near the stem of various conifer species, used as a proxy of DIC uptake, Ubierna *et al.* (2009) found no ^{13}C enrichment in E_{stem} after label application. Moreover Ubierna *et al.* (2009) did not observe a reduction in E_{stem} after artificially reducing sap flow by crown removal. They hypothesized that their conifer species had lower F_s and a more impermeable cambium, thereby reducing the potential diffusion of belowground respired CO_2 through the stem.

To date, information on the extent of aboveground diffusion of belowground respired CO_2 among trees is scanty. This characteristic is potentially species specific. First, stem anatomy will affect radial diffusion and xylem transport rates of belowground respired CO_2. Second, trees with larger root systems potentially transport more belowground respired CO_2 upwards into the stem, as hypothesized by Teskey & McGuire (2007) .

1.4 Measuring and tracing internal CO_2 in trees

Different methods are used to study the fate of internal CO_2 in trees or to measure related ecophysiological variables. These methods can be divided in two groups: non-isotopic measurements and isotopic measurements. The first non-isotopic measurements of internal CO_2 date from early 20th century (Bushong, 1907; MacDougal, 1927; MacDougal & Working, 1933). Since then studies on internal [CO_2] have been using different techniques, ranging from non-continuous gas extraction combined with gas chromatography to continuous solid state non dispersive infrared (NDIR) sensor-based measurements (see Table 1 in Teskey *et al.*, 2008). Moreover, with the discovery of xylem CO_2 transport in trees, assimilation of internal CO_2, and the diffusion of xylem-transported CO_2 to the atmosphere in the past years, the entire gamut of different non-isotopic techniques applied in internal CO_2 research have been extended tremendously. In particular, combined F_s and xylem sap [CO_2*] measurements are now being used to estimate the magnitude of xylem CO_2 transport in trees.

The use of carbon isotopes, either stable or unstable, have only recently received attention as a tool for gaining insight into the fate of internal CO_2 in trees. Isotopes are introduced in the xylem as a tracer of xylem CO_2 transport, and either diffuse into the atmosphere or are assimilated in plant tissue (McGuire *et al.*, 2009). To our knowledge, the first who introduced isotopes directly in the xylem to trace respired CO_2 transport in trees were Stringer & Kimmerer (1993). In their experiment, excised *Populus deltoides* leaves were allowed to transpire a 1 mM [^{14}C]$NaHCO_3$ solution and analysis revealed that 99.6% of the label was assimilated by the leaf and this mainly in the xylem vasculature. Recently, McGuire *et al.* (2009) introduced ^{13}C in the xylem of excised *Platanus occidentalis* L. branches and observed that the label was transported with the transpiration stream from the branch base to the leaves.

In the next sections, the most common (non)-isotopic techniques used in internal CO_2 research will be reviewed. In particular, we will highlight the methods used in this thesis and discuss their benefits and shortcomings and their applicability within the context of internal CO_2 and plant respiration research.

1.4.1 Non-isotopic techniques

1.4.1.1 Measuring xylem CO_2 concentration

In this thesis, xylem [CO_2] was measured using a solid state NDIR sensor (Model GMM 221, Vaisala inc., Helsinki, Finland). After drilling a hole of 20 mm wide and approximately 5 cm deep, sensors are installed in the stem base and soft rubber foam or a flexible putty adhesive is used to seal off the space between sensor housing and stem, allowing CO_2 to build up at the site of sensor insertion (Fig. 1.8) (e.g. Teskey & McGuire, 2007; Saveyn *et al.*, 2008b; Etzold *et al.*, 2013). In this thesis, sensors were installed at stem base, because xylem CO_2 measurements were used to estimate the flux of xylem-transported CO_2 derived from belowground respiration (F_t) entering the stem (see Section 1.4.1.4).

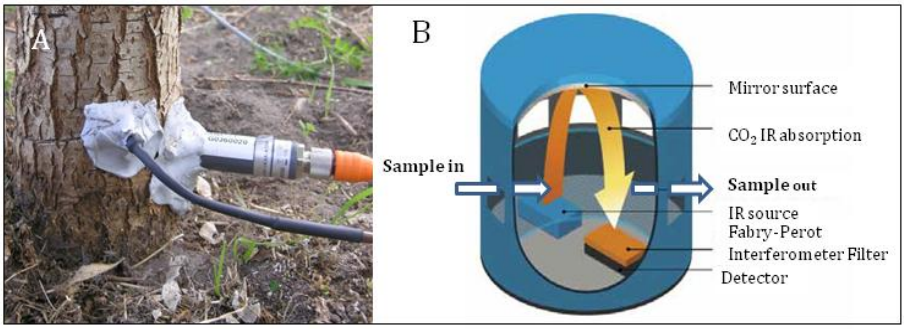

Fig. 1.8 (A) NDIR sensor installed in the stem base of a 9-y old *Quercus robur* L. tree. An additional thermocouple is installed to measure stem temperature (T_{stem}). (B) Structure of the sensor head of the Vaisala NDIR sensor (adapted from Vaisala application note B211228EN) IR: infrared.

The NDIR measurement of [CO_2] is based on Vaisala's Carbocap technology, which uses infrared sensing to measure the volumetric concentration of CO_2 within a range of 0-20%. The sensor consists of an infrared (IR) source, measurement chamber, interference filter and IR detector (Fig. 1.8B). When gas samples pass through the measurement chamber, CO_2 molecules absorb a fraction of the IR light at a specific wavelength. The filter in front of the detector prevents wavelengths other than the specific one to pass to the detector. This filter is an electrically tunable interferometer

filter, allowing an additional compensation for any changes in the light source intensity by dirt accumulation and contamination. Finally, the IR light reaches the detector, where the light intensity is converted into a gas concentration value.

Because most gas produce a signal proportional to molecular density of gases according to the ideal gas law (Equation 1.1), a twofold correction of the sensor signal is needed when measuring internal [CO_2] (%) (Equation 1.2) at different conditions than the standard one (25°C, 1013 hPa).

$$\mathbf{P\,V = n\,R\,T} \tag{1.1}$$

$$\mathbf{[CO_2](T,P) = [CO_2](25°C, 1013\ hPa)\frac{P}{1013}\frac{298.15}{T}} \tag{1.2}$$

where P is the atmospheric pressure (Pa), V is the gas volume (m^3), n the amount of gas (mol), R is the universal gas constant (8.3145 J mol^{-1} K^{-1}), and T the temperature (K).

First of all a gas pressure correction is needed because the IR-detector will detect less CO_2 molecules for the same [CO_2] at lower atmospheric pressures. Secondly, continuous stem temperature (T_{stem}) data is needed to correct for a temperature effect, because under increasing temperature less CO_2 molecules will be detected at a constant [CO_2]. Correcting for the sensitivity of the NDIR sensor for temperature can also be performed while calibrating the NDIR sensors with different reference gases with a known [CO_2] in range of 0 to 20%. The experimental setup for this calibration and additional temperature correction is described in Saveyn (2007).

During their long-term internal [CO_2] measurements, Etzold *et al.* (2013) have raised concerns about the formation of wound tissue around the sensor head, thereby limiting diffusion of respired CO_2 to the sensor head. Therefore, re-installation of sensors in neighboring bottom stem sections is potentially needed in long-term studies. Overall, Vaisala sensors are very stable over time, in particular compared to previously used micro-electrodes (McGuire & Teskey, 2002). However an important shortcoming of the NDIR sensors is that the IR-based technology is very sensitive to water present in the stem tissue, which might eventually lead to sensor breakdown at high stem water content. Therefore, sensors can be wrapped in porous tubing, allowing diffusion of CO_2 to the sensor head, while protecting the sensor to moisture.

1.4.1.2 Conversion of xylem [CO_2] to [CO_2]*

Although measurements of xylem-dissolved CO_2 in woody tissue cannot currently be made in situ (Aubrey *et al.*, 2011), the amount of all products of CO_2 dissolved in the xylem sap can be calculated based on measurements of xylem [CO_2], T_{stem}, and pH. Because both the gaseous and aqueous phase are in contact, an equilibrium exists between the [CO_2] present in both phases. According to Henry's law, the partial pressure of a gas over a solution is proportional to the concentration of that gas in the solution (mM) (Stumm & Morgan, 1996; McGuire & Teskey, 2002):

$$[\mathbf{CO_2^*}] = \left(\mathbf{1} + \frac{\boldsymbol{K_1}}{\mathbf{10^{-pH}}} + \frac{\boldsymbol{K_2 K_1}}{\mathbf{(10^{-pH})^2}}\right) \boldsymbol{K_H}\, \boldsymbol{p}\mathbf{CO_2} \qquad (1.3)$$

with K_1 and K_2, the first and second acidity constant, respectively, K_H, Henry's constant, and pCO_2 the partial pressure of CO_2 over the xylem sap (= gaseous [CO_2] expressed in atm). Gaseous [CO_2] and T_{stem} can be measured continuously with a NDIR sensor and thermocouple, respectively (Fig. 1.8A). The constants K_1, K_2, and K_H are temperature-dependent (see Butler, 1991) and the solubility of CO_2 decreases with increasing temperature (Stumm & Morgan, 1996; Teskey *et al.*, 2008). Xylem sap pH has a pronounced effect on the solubility of [CO_2] within the xylem sap (Fig 1.9) and on the distribution of dissolved CO_2 among its different forms (Erda *et al.*, 2013). Within the xylem sap pH range reported for trees, 4.5 to 7.4 among different species (see Table 2 in Teskey *et al.*, 2008), most dissolved CO_2 is present in the carbonic acid (H_2CO_3) or bicarbonate (HCO_3^-) form. In spite of recent developments in online measuring of pH in liquids (e.g. Presens microsensor©), xylem sap is still being measured non-continuously and destructively (Aubrey *et al.*, 2011). The major problem with sampling xylem sap is the negative pressure in the xylem of transpiring plants (Schneider *et al.*, 1997). Therefore xylem sampling in the field is based on taking detached parts of a plant, putting them under pressure and collecting the sap that is squeezed out of the cut end. Xylem sap can be extracted from stems, branches, and twigs and this sap is then applied on a pH electrode. In this PhD thesis we expelled xylem sap from twigs with a Scholander pressure bomb and used xylem sap twig pH to convert xylem [CO_2] to [CO_2*] measured at stem base. Previously, Aubrey *et al.* (2011) observed that for *Populus*

deltoides Bartr. ex. Marsh xylem sap pH derived from twigs is a good proxy for stem xylem sap pH.

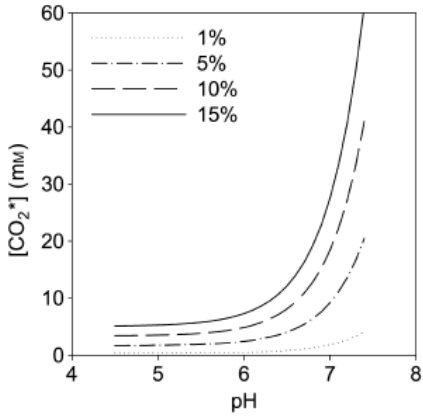

Fig. 1.9 Effect of xylem sap pH on the concentration of all products of CO_2 dissolved in water ($[CO_2^*]$, after Erda *et al.*, 2013).

A point of discussion regarding xylem sap pH measurements is the sampling frequency required to account for potential variation. Recent studies indicate that at diurnal scale variations in xylem sap pH are limited (Aubrey *et al.*, 2011; Erda *et al.*, 2013). At seasonal scale, variation in xylem sap pH might occur and might cause substantial errors in $[CO_2^*]$ estimates, in particular when xylem sap pH is more in the upper range reported within trees (pH > 6.5) (Erda *et al.*, 2013). Additionally, pH can be influenced by environmental factors that affect transpiration rates (Stoll *et al.*, 2000; Beis *et al.*, 2009; Aubrey *et al.*, 2011), such as vapor pressure deficit (VPD) or solar radiation. Increases in xylem sap pH have been observed under reduced transpiration rates (Campbell & Strother, 1996) or when the soil dries out (Wilkinson, 1999). In this PhD thesis we sampled xylem sap biweekly to account for potential variation in xylem sap pH at the seasonal scale.

1.4.1.3 Measuring sap flow

Accurate determination of F_s within tree stems is a another key issue when estimating xylem CO_2 transport in trees or for understanding diurnal dynamics in stem $[CO_2]$ and E_{stem}. Commonly, sap flow measurements for woody species and some herbaceous plants are based on heat transport within the stem (Smith & Allen, 1996; Vandegehuchte

& Steppe, 2013) but utilized methods are fundamentally different in their operating principles (Smith & Allen, 1996).

In this thesis, two types of sap flow sensors were used to measure sap flow, the heat balance (HB) and the thermal dissipation probes (TDP) (Fig. 1.10). The heat balance sensor is used to determine sap flow rate in the stem or in a specific stem segment. The sensor itself consists of a heater element, a few centimeters in width, and thermocouple pairs both embedded in a cork shielding. The shielding is wrapped around the stem to ensure good contact of both the heater and thermocouples with the stem surface. Heat is applied to the entire circumference of the stem and the balance of the heat fluxes into and out of the stem section registered with the thermocouple pairs is used to quantify sap flow (Sakuratani & Abe, 1985; Baker & Van Bavel, 1987). These sensors are used to estimate whole plant water use, however limited to small herbaceous species and small trees (Smith & Allen, 1996).

Sap flow measurements with TDP sensors are based on a temperature differences between a heated and reference needle and is the most widely applied SFD method, because of its simplicity and low cost (Vandegehuchte & Steppe, 2013). Constant power is applied to the upper heater needle and as sap flow increases, heat is more rapidly dissipated with the transpiration stream, which decreases the temperature difference between heated and reference needle. The empirical basis for measuring sap flow with TDP sensors was developed by Granier (1985). He found experimentally for *Pseudotsuga menziessii* (Mirb.) Franco, *Pinus nigra* Arnold, and *Quercus pedunculata* Ehrh. that SFD (cm^3 cm^{-2} h^{-1}) was related to measured temperature difference by the following equation

$$\mathbf{SFD} = \mathbf{0.000119}\frac{(\Delta \boldsymbol{T_0} - \Delta \boldsymbol{T})}{\Delta \boldsymbol{T}}^{\mathbf{1.231}} \quad (1.4)$$

where ΔT is the temperature difference between heated and reference needle, and ΔT_0 is the value of ΔT when there is no sap flow. SFD multiplied with the cross sectional area of the sapwood is used to obtain F_s (l h^{-1}).

Fig. 1.10 (A) Heat balance sensor installed on a *Populus deltoides* x *nigra* 'Monivso' stem. (B) Thermal dissipation probe (TDP) installed on a 9-y old *Quercus robur* tree. After installation, the sensor is wrapped in aluminum foil and sheet of reflectix foil, as in (A), to ensure thermal insulation.

While Granier (1985) assumed that this experimentally determined regression TDP-based measurements is species independent, results from recent studies indicate that SFD is underestimated between 6 and 90% for a wide variety of species compared to other SFD methods or when compared to results from mass-based calibration experiments on excised stem and branch segments or cut trees (Vandegehuchte & Steppe, 2013 and references therein). Therefore species specific correction factors should be used to obtain accurate F_S estimates (Steppe *et al.*, 2010). In this PhD thesis, we obtained site and species specific correction factors for SFD measurements on *Quercus robur* L. by comparing TDP measurements on excised *Quercus robur* L. stem segments with mass-based estimates of sap flow, using the Mariotte based verification system of Steppe *et al.* (2010). We observed that on average TDP sensors underestimated actual F_s by 66.4% in these *Quercus robur* trees.

1.4.1.4 Estimating xylem transport of root-respired CO_2

As described by Aubrey & Teskey (2009), measurements of $[CO_2^*]$ and F_s are used to estimate F_t (mmol h^{-1}) according to the following formula:

$$\mathbf{F_t = F_s\,[CO_2^*]\,k} \qquad (1.5)$$

where k is a site and species specific correction factor for F_s based on sap flow calibration experiments. In this PhD thesis, NDIR and TDP sensors (model TDP-10, Dynamax inc., Houston, Texas, USA) were installed at stem base on 5 and 35 cm above the soil, respectively. The diel pattern in F_t will mimick that of F_s, but its magnitude will additionally depend on $[CO_2^*]$ dynamics. Aubrey & Teskey (2009) observed large day-

night variations in F_t for *Populus deltoides* with maxima during the day and zero flux at night, when no sap flow occurred (Fig. 1.11).

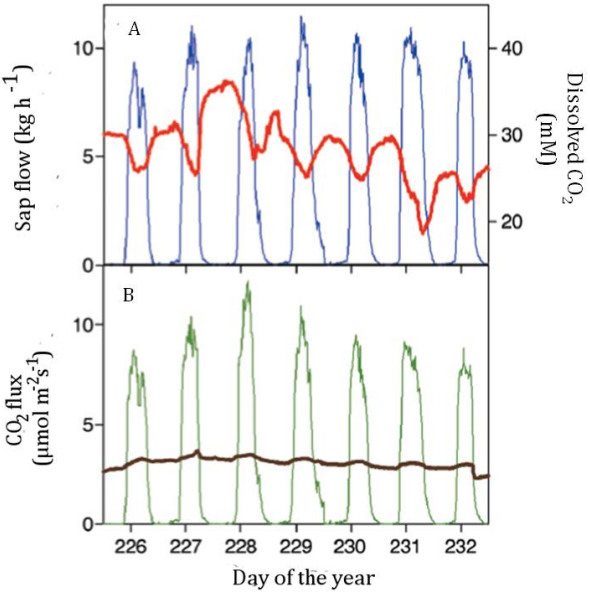

Fig. 1.11 (A) Sap flow rate (F_s, blue) and xylem-dissolved CO_2 ([CO_2*], red) measured in 9-year old *Populus deltoides* trees. (B) Comparison of the scaled flux of root-respired CO_2 transported via the xylem (F_t, green) calculated from data in (A) and soil CO_2 efflux (E_{soil}, black) (adapted from Aubrey & Teskey, 2009).

1.4.1.5 Comparing xylem transport of root-respired CO_2 with soil CO_2 efflux

F_t and E_{soil} measurements were compared, to quantify the total belowground $R_{a,}$. One of the main issues when comparing F_t with the flux of root-respired CO_2 contributing to E_{soil} is that both fluxes are expressed on a different unit scale. Therefore, in this PhD thesis F_t was scaled ($F_{t,scaled}$, mg C m^{-2} h^{-1}) based on the soil area occupied by the root system:

$$\mathbf{F_{t,scaled}} = {\mathbf{F_t\, A(C)}}/{\mathbf{A_{root}}} \qquad (1.6)$$

with A_{root} the soil area occupied by the root system (m^2), A(C) the atomic mass of carbon (12 g mol^{-1}). Data from root excavation measurements on additional trees with similar dimensions was used to estimate A_{root}. For older trees, root excavation is an elaborate task and therefore general rule of thumbs regarding the extension of roots relative to an imaginary downward projection of the branch tips can be applied (Lyford & Wilson,

1964; Perry, 1982). Nonetheless, this A_{root} factor is potentially a large source of uncertainty for $F_{t,scaled}$ estimates. Therefore other, more precise approaches are needed to estimate this parameter.

Within A_{root}, roots will contribute both to F_t and E_{soil} (Fig. 1.12A) and therefore it is important that measurements of the latter are representative for efflux rates within this zone, given the potential large spatial variability for E_{soil} observed within forests (e.g. Soe & Buchmann, 2005; Katayama *et al.*, 2009). Aubrey & Teskey (2009) performed E_{soil} measurements at a distance of 0.75 m of the stem of 9-y old *Populus deltoides* trees. In this PhD thesis we measured E_{soil} at 0.40 m and 0.70 m from the stem of 9-y old smaller *Quercus robur* trees, within a circular shaped A_{root} of 3.14 m^2 (Fig. 1.12B). Measurements of E_{soil} should be performed at the same high temporal resolution as for F_t measurements, either using the CO_2 gradient method along a vertical soil profile (Aubrey & Teskey, 2009), described in detail in Tang *et al.* (2003), or by using automatic efflux chambers, as performed in this thesis, based either on an open or closed dynamic system (Pumpanen *et al.*, 2009).

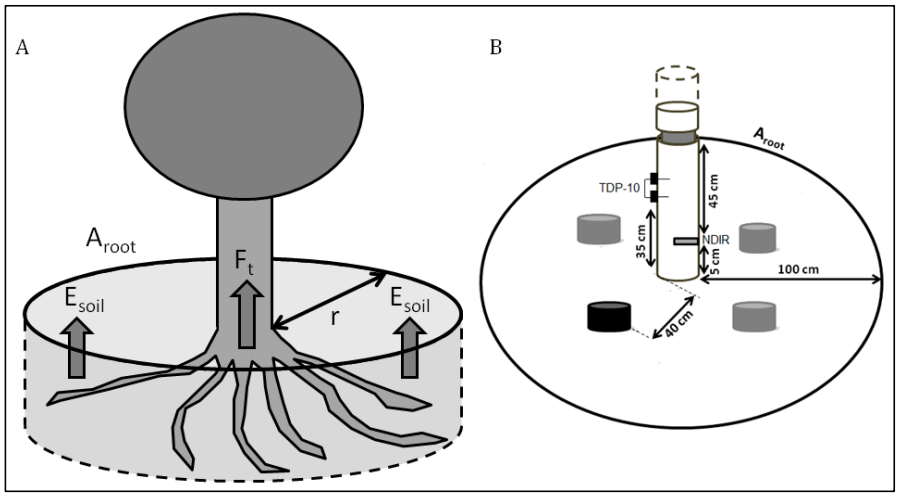

Fig 1.12 (A) Schematic of the fluxes of root-respired CO_2, both transported internally in trees with the transpiration stream (F_t) and contributing to soil CO_2 efflux (E_{soil}) within the soil area occupied by the root system (A_{root}) with radius r. (B) Set up used in this PhD study to estimate F_t and the contribution of root respiration to E_{soil}. F_t estimates are derived from stem [CO_2] and sap flow measurements with a non dispersive infrared (NDIR) and a thermal dissipation probe (TDP) sensor, respectively. E_{soil} is measured in A_{root} with automatic (black chamber) (see Fig 1.13A,B) and manual chambers (grey chambers) (see Fig. 1.13C). Manual chamber measurements performed at 70 cm are not presented. Measurements of F_t are scaled with A_{root} ($F_{t,scaled}$) for comparison with the fraction of E_{soil} derived from root respiration (see Equation 1.6).

In this PhD study automated dynamic PVC chambers (20 cm diameter, 15 cm height, design adapted from Suleau *et al.*, 2009) were used to measure E_{soil} (Fig 1.13A,B). The chambers were connected to an infrared gas analyzer (IRGA) (model GMP 343, Vaisala inc., Helsinki, Finland) in a closed loop, to estimate the slope of the increase in $[CO_2]$ within the chamber headspace. In addition, manual E_{soil} measurements were performed at varying positions and distances from the stem to complement these automated measurements (Fig. 1.13C) and to account for spatial heterogeneity within the soil area occupied by the roots. These measurements were performed using a CO_2 analyzer (EGM-4, PP systems, Amesbury, MA, USA) connected to a soil chamber (SRC-1, PP systems, Amesbury, Massachusetts, USA) which was installed on PVC chambers (20 cm diameter, 12 cm height).

Fig 1.13 (A,B) Automated soil CO_2 efflux (E_{soil}) chamber installed near the stem of 9-y old *Quercus robur* trees (design adapted from Suleau *et al.* (2009)). (C) Manual E_{soil} measurements were performed on PVC chambers using a CO_2 analyzer. Additionally, a soil temperature probe is displayed to measure soil temperature simultaneously with E_{soil} measurements.

The benefit of estimating E_{soil} with chambers is that measurements and calculations are more straightforward compared to the CO_2 gradient method, for which site-specific estimates of soil diffusion and tortuosity are needed, as described by Tang *et al.* (2003). On the other hand with the CO_2 gradient method, the fraction of xylem-transported CO_2 derived from the uptake of soil solution can be estimated, based on soil $[CO_2]$ and F_s measurements (Aubrey & Teskey, 2009). Regardless of the technique, additional manual measurements of E_{soil} - at lower temporal frequency - should be performed to account for spatial variation of E_{soil} in A_{root} and to validate the automatic measurements.

Finally, to quantify the total $R_{a,b}$ accounting both for xylem CO_2 transport and the autotrophic contribution to E_{soil}, the latter needs to be estimated. In their study, Aubrey

& Teskey (2009) assumed that 50% of E_{soil} was derived from autotrophic sources, based on the average of the reported range of 10-90% among different studies and different ecosystems (Hanson *et al.*, 2000). However different isotopic as well as non-isotopic methods can be applied to estimate this autotrophic fraction, of which the discussion on their advantages and limitations lies out of the scope of this thesis but is available in reviews by Hanson *et al.* (2000) and Kuzyakov (2006). Grossiord *et al.* (2012) estimated the fraction of E_{soil} derived from $R_{a,b}$ based on the isotopic signature of E_{soil} after conversion of C_4-type vegetation into C_3-type vegetation. In this thesis, we used the girdling method to quantify $R_{a,b}$. By removing a circumferential band of bark and phloem from a tree stem during girdling (Högberg *et al.*, 2001; De Schepper *et al.*, 2010), the belowground transport of recent photosynthates is interrupted, decreasing the amount of substrate available for $R_{a,b}$.

1.4.1.6 Measuring stem CO_2 efflux

E_{stem} measurements used to estimate stem respiration during the growing season are considered to be biased by xylem CO_2 transport, because a substantial fraction of respired CO_2 is potentially transported away from the site of respiration with the transpiration stream or a fraction of xylem-transported CO_2 diffuses radially to the atmosphere (see Section 1.3.3). Therefore, E_{stem} measurements have been used in combination with $[CO_2^*]$ and F_s measurements to quantify stem respiration, according to the mass balance approach proposed by McGuire *et al.* (2004) and Teskey & McGuire (2007). In this PhD thesis, we measured E_{stem} on intact stems of dormant *Quercus robur* trees and non-dormant *Populus deltoides* trees. In the study on dormant *Quercus robur* trees, sap flow and xylem CO_2 transport were absent and E_{stem} can be assumed to represent local stem respiration rates (McGuire *et al.*, 2007). However, we performed E_{stem} measurements in combination with artificial illumination of remote stem sections at varying distances from the stem cuvette, to elucidate the impact of axial diffusion of respired CO_2 on dormant season E_{stem} measurements (Fig 1.14).

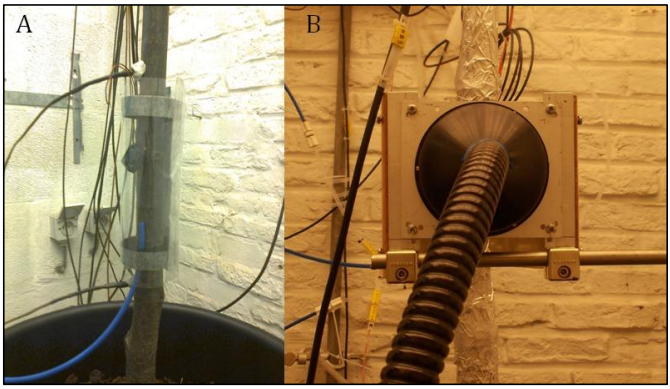

Fig. 1.14 (A) Cuvette installed on a stem of a 4-y old *Quercus robur* tree to measure stem CO_2 efflux (E_{stem}). After installation, the cuvette is covered with aluminum foil to exclude woody tissue photosynthesis. Thermocouples installed in the stem are used to measure the stem temperature (T_{stem}) above and below the cuvette. (B) Movable fiber optic light source used to induce axial diffusion of respired CO_2 in a dormant tree stem.

We enclosed the stem segments with a flexible fan-stirred stem cuvette constructed of Polycarbonate film and sealed to the stem with adhesive closed-cell foam gasket material and silicone sealer. Previous studies mainly used solid acrylic or Lexan tubes cut in two and clamped around the stem to form a cylindrical cuvette and made leak tight with flexible putty adhesive. However, based on the experience during previous studies, these were more prone to gas leaks compared to the flexible cuvettes. Stem cuvettes were covered with aluminium foil to exclude local woody tissue photosynthesis. The [CO_2] of the air leaving the cuvette that enclosed a stem segment was measured with an IRGA (IRGA, LI-7000, Li-COR, Lincoln, TE, USA) and was compared with the [CO_2] of the air leaving a reference cuvette, which enclosed a PVC tube with approximately the same dimensions as the average stem diameter of the stem sections enclosed for E_{stem} measurements. E_{stem} (µmol CO_2 m^{-2} s^{-1}) was calculated according to Long & Hallgren (1985) and was expressed per unit of surface area:

$$\mathbf{E_{stem}} = \left(\frac{\mathbf{f_a}}{\mathbf{A_s}}\right) * \mathbf{\Delta CO_2} * \mathbf{22.4\ mol\ l^{-1}} \qquad (1.7)$$

where f_a is the flow rate through the cuvette (l s^{-1}), A_s is the surface area of the stem segment (m^2) and ΔCO_2 is the difference in [CO_2] of measurement and reference air (µmol mol^{-1}).

1.4.2 Isotopic techniques

Approaches for studying the fate of xylem-transported CO_2 is based on the use of isotopes, which are atoms of an element with the same atomic number, but with different atomic masses (Dawson & Brooks, 2001). These isotopes can be applied for tracing fluxes in the soil plant atmosphere continuum (Brüggemann *et al.*, 2011), because they have identical physicochemical properties to the substance of interest and are detectable at low concentrations (Schurr, 1998). Overall, the commonly used carbon isotopes can be divided in three groups (Table 1.2; Shirley & Lederer, 1980), one containing stable isotopes (^{12}C and ^{13}C) and two groups of unstable isotopes which decay either by emission of a β^+ (a positron, i.e. an anti-electron) like ^{11}C or by emission of a β^- (an electron) which includes ^{14}C (Minchin & Thorpe, 2003). In this thesis we used ^{11}C and ^{13}C to trace xylem CO_2 transport and therefore use of these carbon isotopes will be further discussed in detail.

Table 1.2 The different carbon isotopes commonly used to study carbon pools and fluxes in plants. Plant applications indicate the main application, but this list is extensive. $T_{1/2}$: half-life. EC: electron capture (adapted from Shirley & Lederer, 1980).

Nuclide	% Abundance or $T_{1/2}$	Decay mode	Plant applications
^{11}C	20.38 min	β^+, 99.76%, EC 0.24%, no γ	Short term photosynthate tracing studies
^{12}C	98.89%	-	CO_2 flux studies
^{13}C	1.11%	-	Photosynthate tracing
^{14}C	5730 y	β^-, no γ	Long term photosynthate allocation studies

1.4.2.1 ^{13}C concepts, use and measurements

Since the first report on ^{13}C isotopic values of plant materials (commonly expressed as $\delta^{13}C$) by Craig (1953; 1954) ^{13}C has seen an increased use as an important tool for understanding and quantifying C pools and fluxes in terrestrial ecosystems (Norby, 2009). Overall, studies on stable isotopes can be categorized in those working at naturally occurring levels (called 'natural abundance'), reported around -27‰ and -12‰ for C_3 and C_4 plants (Farquhar *et al.*, 1989), respectively, and others that work

outside the natural range of values (called "enriched" levels) with isotopically labeled substances (Dawson *et al.*, 2002). Because working at natural abundance requires repeatable and distinct δ values and no significant fractionation of tracers or mixing of sources (Dawson *et al.*, 2002), many stable isotope studies rely on the enriched isotope approach. Hence the addition of an enriched substance acts as a powerful tracer for following the flow of a specific element (Nadelhoffer & Fry, 1994).

At lower tracer enrichment levels, $\delta^{13}C$ (‰) can be expressed relative to an internationally accepted standard:

$$\boldsymbol{\delta^{13}C = 1000 * \left(\frac{R_{sample}}{R_{standard}} - 1\right)} \quad (1.8)$$

Where R_{sample} and $R_{standard}$ are the abundance ratios of the heavier to the lighter isotope (i.e. $^{13}C/^{12}C$) of the sample and standard, respectively. Vienna Pee Dee Belemnite (VPDB) is used as standard for ^{13}C with an $R_{standard}$ of 0.0112372. In this thesis, $\delta^{13}C$ of enriched samples was expressed relative to $\delta^{13}C$ values of baseline samples to obtain the enrichment of the labeled tissues.

At high tracer enrichment levels, commonly at $\delta^{13}C$ levels > 500‰, the isotopic composition of labeled substance should be expressed in atom% (A, %), which is defined as:

$$\boldsymbol{A = \frac{X_{13_C}}{X_{13_C} + X_{12_C}} = 100 * \left(\frac{R_{sample}}{R_{sample} + 1}\right)} \quad (1.9)$$

where X_{13_C} and X_{12_C} are the numbers of ^{13}C and ^{12}C atoms, respectively, present in the sample.

Tracing xylem-transported CO_2 with ^{13}C

To date, ^{13}C tracers have mainly been used to trace the fate of photosynthates allocated within plants and to the soil, stored within ecosystems and lost by respiration to the atmosphere (Brüggemann *et al.*, 2011; Epron *et al.*, 2012). Epron *et al.* (2012) synthesized data from short term labeling studies (called pulse labeling), in which the tracer was applied at canopy level by enclosing one or several trees in chambers or using free air carbon isotope enrichment systems. They observed that the time lag between peak $^{13}CO_2$ efflux from the soil and label application at leaf level, varied with

tree height, and was longer for coniferous trees compared to deciduous trees (Fig. 1.2, Epron *et al.*, 2012). Hence, results from ^{13}C tracer studies have provided substantial information on the fate of labeled carbon after assimilation within the leaves (Fig. 1.15).

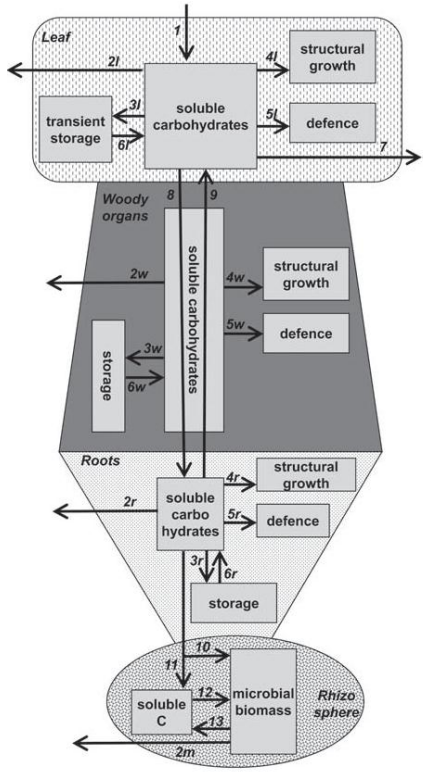

Fig. 1.15 Fate of labelled carbon in a tree. The isotopically labeled carbon is applied at the leaves (1) and fills a soluble carbohydrates pool that is further allocated to respiration (2), storage (3), structural growth (4) and defense compounds (5). The soluble carbohydrate pools are also filled by remobilization from transient storage (6) or are potentially used for emission of organic compounds (7). Soluble carbohydrates are transferred both basipetally via the phloem (8) or acropetally from storage in perennial organs to new shoots (9). A fraction of the labelled carbon is also transferred to the rhizosphere, either indirectly via hyphae of mycorrhiza (10) or directly via exudation (11). There it can be transferred into microbial biomass (12) and further recycled due to the high turnover rate of microbes (13). Letters, l, w, r, and m indicate the compartment (leaf, woody organs, roots, and microbes, respectively) (after Epron *et al*., 2012).

In this PhD thesis, ^{13}C was used to trace the flow of xylem CO_2 transport within field-grown trees, detached branches, and leaves (Fig. 1.16). Previously, xylem pulse labeling studies were limited to detached branches (McGuire *et al.*, 2009) or leaves (Stringer & Kimmerer, 1993; Hibberd & Quick, 2002). To our knowledge one study has used ^{13}C to

trace the fate of xylem-transported CO_2 in field grown trees. Powers & Marshall (2011) dissolved ^{13}C-Na_2CO_3 into a small volume of water and injected it into the xylem of a 4 m tall *Thuja occidentalis* tree at breast height. They observed five days after label injection isotopic enrichment of 6.1‰ and 7.7‰ in E_{stem} and phloem tissues, respectively, however bulk foliage samples were not enriched. In this thesis, the transpiration stream of field-grown *Populus deltoides* trees was pulse labeled using an infusion technique (Fig 1.16 A, B). Holes were drilled in the stem base and containers containing $^{13}CO_2$-labeled solutions were connected to the stem with CO_2 impermeable tubing. The $^{13}CO_2$-labeled solutions were prepared by dissolving compressed 100% CO_2 gas at 99A^{13}C in an aqueous solution, as described by McGuire *et al.* (2009).

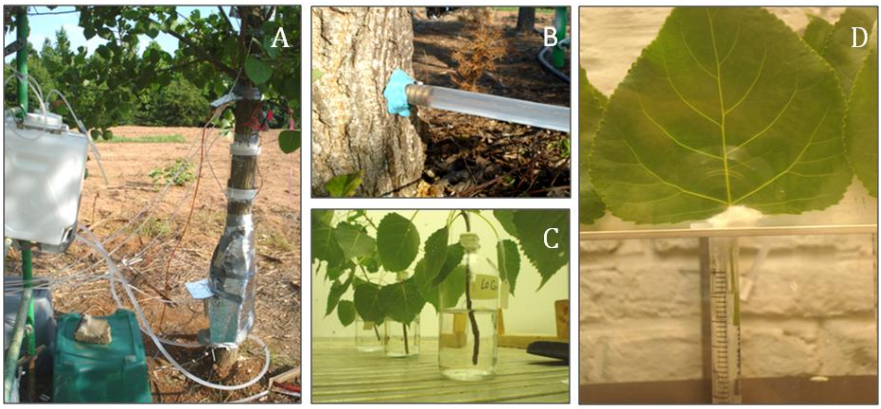

Fig. 1.16 Experiments performed in this PhD thesis based on the introduction of a ^{13}C label in the xylem at tree (A, B), branch (C), and leaf (D) level.

Moreover in two other experiments, we used a similar dissolved ^{13}C label to determine the impact of sap flow rate dynamics on the assimilation of xylem-transported CO_2 in detached *Populus deltoides* branches (Fig 1.16C) and detached *Populus deltoides x canadensis* 'Robusta' leaves (Fig. 1.16D).

Measuring the fate of xylem-transported $^{13}CO_2$

In this thesis $\delta^{13}C$ of woody and leaf tissue samples and the isotope composition of stem and branch CO_2 efflux was measured, to determine the fate of xylem-transported CO_2. Solid woody and leaf tissue samples collected during the ^{13}C infusion experiments were oven-dried, grinded, weighed in tin capsules, and flash-combusted before being

analyzed. Gas samples were collected from the efflux cuvettes installed on the field-grown *Populus deltoides* trees using syringes and injected in evacuated vials for storage before analysis. Both tissue and gas samples were analyzed by an Element Analyzer (EA) coupled to an Isotope Ratio Mass Spectrometry (IRMS).

1.4.2.2 ^{11}C concepts, use and measurements

While ^{11}C was used in photosynthesis research before ^{14}C became available (Benson, 2002), it has seen only limited use (Minchin & Thorpe, 2003), because of its very short-half-life (20.4 min) and the specialized facility its use requires (Norby, 2009). Because of its short half-life, ^{11}C has been used in most plant applications exclusively to trace short term processes, for instance the carbon partitioning within leaves of *Glycine max* (L.) Merr. (Dirks *et al.*, 2012) or carbon import within root systems of *Hordeum vulgare* L. (Beer *et al.*, 2010) or *Zea mays* L. (Jahnke *et al.*, 2009) after pulse-labeling the leaves with $^{11}CO_2$. On the other hand, the fast decay of ^{11}C allows the application of a sequences of independent pulses, as there is no build up of tracer from previous pulses (Minchin & Thorpe, 2003).

In vivo observation of ^{11}C tracer movement in plants is based on the detection of γ-rays, due to the annihilation of β^+ particles emitted by ^{11}C with an electron in plant tissue, or on the direct detection of β^+ particles during ^{11}C decay. Commonly, γ-ray detection is used for imaging tracers in humans, animals, and in the bulk of plants, while β^+ imaging is usually performed for thinner tissues, like leaves (Dirks *et al.*, 2012). In this PhD thesis direct detection of the β^+ particles with autoradiography was used to image xylem CO_2 transport in leaves.

Tracing xylem CO_2 transport with ^{11}C

We used ^{11}C as proxy for xylem-transported CO_2 entering the leaf to obtain a more detailed spatial analysis of its distribution among leaf tissue components than obtained with ^{13}C. Similar as for the ^{13}C experiment on excised leaves, we infused ^{11}C in detached *Populus deltoides x canadensis* 'Robusta' leaves via the petiole. We dissolved gaseous CO_2 containing a small amount of $^{11}CO_2$ produced on site with a cyclotron into a TRIS buffer solution. Leaves were allowed to take up the labeled solution with a specially designed label application system.

To our knowledge, none have yet used ^{11}C to track xylem CO_2 transport. One study has observed movement of ^{11}C labeled methyl jasmonate in the xylem in *Nicotiana tabacum* L. (Thorpe *et al.*, 2007). However, Thorpe *et al.* (2007) administered the ^{11}C label to the leaf blade, instead of to the petiole, and observed that after export from the labeled region, ^{11}C methyl jasmonate moved in the xylem vasculature.

Measuring the fate of xylem-transported $^{11}CO_2$

For autoradiographic analysis, we exposed the leaf to an imaging phosphor plate for approximately 5 min. We used these high-efficient phosphor screens instead of the classic autoradiographic films because these capture signals more efficiently and are re-usable. Subsequently, we scanned the latent image on the film with a plate reader to visualize the distribution of the ^{11}C tracer in the leaf.

1.5 Conclusions

Recognition that tree stems can contain substantial amounts of respired CO_2 has led to new insights regarding the use of efflux-based measurements to estimate respiration and the role of a recycling mechanism in trees. While previous research almost exclusively attributed internal CO_2 in tree stems to aboveground respiration, recent studies expand these observations to the soil, because a fraction of belowground respired CO_2 dissolves in the xylem and is transported aboveground towards the canopy.

In the first part of this chapter we combined today's literature on internal CO_2 research to obtain a clearer picture on the significance of internal CO_2 in plant physiology. We discussed the different sources of internal CO_2 and focused primarily on the belowground ones. In particular, root respiration is recently acknowledged as an important source for internal CO_2 in stems. Therefore, further research on the fraction of respired CO_2 remaining inside the root system and thereby contributing to high internal $[CO_2]$ is crucial to elucidate the contribution of root-respired CO_2 to stem internal CO_2.

Aboveground, respired CO_2 within trees diffuses radially into the atmosphere, is assimilated in chlorophyll containing woody tissues, or is transported upwards to the canopy, where it might serve as additional substrate in photosynthetic reactions.

However, we still lack a clear picture of the fate of xylem-transported CO_2 under field conditions. The relation between internal CO_2 and E_{stem} has been established previously, but results on excised branches, leaves or stem segments under controlled conditions should be translated to field experiments. New field observations will lead to a better understanding of the tree carbon economy and might provide new visions on the coupling between the carbon and water cycle in trees, given the potential role of xylary chloroplasts in xylem cavitation repair. In particular, aboveground diffusion of belowground respired CO_2 from the tree stem into the atmosphere might incur a revolution in the way scientist will partition and measure above- and belowground respiration in the near future.

In the second part of this chapter, we discussed the different techniques available for tracing and measuring the fate of xylem-transported CO_2. Previous studies mainly applied non-isotopic methods to quantify the amount of internal CO_2 that is transported via the xylem or that diffused radially into the atmosphere. However, the use of stable or unstable isotopes might give us new insights in the fate of xylem-transported CO_2, similar as currently obtained for the fate of labelled carbon applied at leaf or canopy level. By pulse-labeling the xylem and tracking the fate of the label, scientists will be able to quantify upward below- and aboveground xylem CO_2 transport and estimate radial diffusion of xylem-transported CO_2 into the atmosphere and assimilation rates in woody and leaf tissues.

- Chapter 2 -

^{13}C and ^{11}C-based detection of xylem CO_2 transport in leaves of poplar

After: Bloemen J. , Bauweraerts I., De Vos F., Vanhove C., Vandenberghe S., Boeckx P., and Steppe K. (2013) Fate of xylem-transported ^{11}C- and ^{13}C-labeled CO_2 in leaves of poplar. *Physiologia Plantarum* (submitted).

Abstract

In recent studies, assimilation of xylem-transported CO_2 has gained considerable attention as a means of recycling respired CO_2 in trees. However, we still lack a clear and detailed picture on the magnitude of xylem-transported CO_2 assimilation, in particular within leaf tissues. To this end, detached poplar leaves (*Populus x canadensis* Moench 'Robusta') were allowed to take up dissolved $^{13}CO_2$ serving as a proxy of xylem-transported CO_2 entering the leaf from the branch. The uptake rate of the ^{13}C was manipulated by altering the vapor pressure deficit (VPD) (0.84, 1.29, and 1.83 kPa). Highest tissue enrichments were observed under the highest VPD. Among tissues, highest enrichment was observed in the petiole and the veins, regardless of the VPD treatment. However, results derived from ^{13}C leaf tissue enrichment were limited in spatial resolution. Therefore, $^{11}CO_2$ was used and its detection by positron autoradiography showed a more detailed spatial distribution in particular in secondary veins. There ^{11}C is presumably assimilated in chlorophyll containing bundle sheath tissues, positioned in between the phloem and the xylem vasculature. Therefore, in addition to ^{13}C, ^{11}C based autoradiography can be used to study the fate of xylem-transported CO_2 at leaf level, allowing the acquisition of data at a yet unprecedented resolution. Results from these labeling studies at leaf level might help us to better

understand the role of xylem CO_2 assimilation within bundle sheath cells in plant functioning.

2.1 Introduction

In plants, carbon assimilation is a relatively straightforward process with a well-established theoretical background (Trumbore, 2006). Atmospheric CO_2 enters the leaf via the stomates and diffuses to the parenchyma tissue where chlorophyll containing cells use light to reduce this CO_2, thereby synthesizing a wide range of carbon compounds, primarily sugars (Taiz & Zeiger, 2006). These sugars are the basis of plant growth via the catabolic and anabolic reactions of metabolism (Amthor, 1989). Therefore, assimilation of atmospheric CO_2 is generally considered as the sole pathway by which plants sustain their carbon economy.

However over the past decade, observations of assimilation of respired CO_2 in trees have led to newly emerging views on tree carbon budgets. While since the early 20th century stem-respired CO_2 was generally believed to entirely diffuse into the atmosphere (Johansson, 1933) it is now acknowledged that a substantial amount of respired CO_2 remains inside the tree, contributing to internal CO_2 concentrations ($[CO_2]$) substantially higher than the atmospheric one (Teskey *et al.*, 2008) (**Chapter 1**). This internal CO_2 is partially transported through the transpiration stream towards the canopy, where it either diffuses into the atmosphere (McGuire & Teskey, 2004; McGuire *et al.*, 2007) or is assimilated by chlorophyll containing woody and leaf tissues (McGuire *et al.*, 2009; Bloemen *et al.*, 2013b; 2013a) (**Chapter 1**). Recycling of respired CO_2 in woody and leaf tissues is assumed to partially pay for local carbon demands and to positively contribute to the carbon income of plants (Aschan & Pfanz, 2003).

Previous studies traced the fate of xylem-transported CO_2 by using ^{13}C-labeled CO_2 (referred to as $^{13}CO_2$ in the text) added to the transpiration stream and by analyzing ^{13}C tissue enrichment in field-grown trees (Powers & Marshall, 2011; Bloemen *et al.*, 2013b) and detached branches (McGuire *et al.*, 2009; Bloemen *et al.*, 2013a). Powers & Marshall (2012) observed no substantial leaf enrichment after injecting a dissolved ^{13}C-carbonate label into a *Thuja occentalis* tree at breast height. Bloemen *et al.* (2013b) observed for *Populus deltoides* Bartr. ex. Marsh trees that the ^{13}C label infused at the base of the stem

was transported with the transpiration stream throughout the tree and that at leaf level the label was mainly assimilated by the petioles. McGuire *et al.* (2009) and Bloemen *et al.* (2013a) introduced a dissolved $^{13}CO_2$ label into detached branches and observed a similar enrichment of the petioles relative to the other leaf tissue components. However, leaf tissue enrichment was observed to be strongly dependent on the transpiration rate, with increased enrichment levels at higher transpiration rates (Bloemen *et al.*, 2013a). Nonetheless, branch and stem ^{13}C infusion as a proxy of xylem CO_2 transport underestimates the actual amount of xylem CO_2 that is transported to the leaves, because this method does not account for CO_2 derived from local respiration between the point of infusion and the leaf. Moreover, we lack detailed results on the extent of xylem-transported CO_2 assimilation within the leaf tissues under varying transpiration rates.

To grasp the full picture, isotopic proxies of xylem CO_2 transport can be used at leaf level. While ^{13}C based techniques require destructive tissue analysis to estimate assimilation of xylem-transported CO_2 within a specific tissue, the use of radiocarbon tracers is non-destructive and might be a promising tool in xylem-transported CO_2 research. As explained in **Chapter 1**, these unstable carbon isotopes, which decay by emission of a charged particle, can be subdivided in heavy isotopes, including ^{14}C, and in light isotopes, which include ^{11}C (Minchin & Thorpe, 2003; Matsuhashi *et al.*, 2006). In the past decades, most experiments have used ^{14}C as radiocarbon tracer, given its longer half-life (5730 years) and lower experimental cost compared to the use of ^{11}C (half-life of 20.4 min) (Minchin & Thorpe, 2003). Previously, ^{14}C autoradiography has been applied to detached leaves (Stringer & Kimmerer, 1993; Hibberd & Quick, 2002), hydroponically grown tree seedlings and cuttings (Zelawski *et al.*, 1970; Vapaavuori & Pelkonen, 1985; Vuorinen *et al.*, 1989) and herbaceous plants (Amiro & Ewing, 1992; Hibberd & Quick, 2002) for studying xylem CO_2 fixation at a detailed spatial resolution. On the other hand, ^{11}C-based studies have exclusively traced the carbon export from labeled leaves, by applying ^{11}C as gaseous ^{11}C-labeled CO_2 (referred to in the text as $^{11}CO_2$) (Minchin & Thorpe, 2003; Thorpe *et al.*, 2007; Dirks *et al.*, 2012). The higher energy of the positron emitted during ^{11}C decay than that from electron emission during ^{14}C decay allows a more efficient *in vivo* detection of ^{11}C decay relative to ^{14}C decay

(Minchin & Thorpe, 2003). Therefore, ^{11}C labeling could provide us detailed information on a whole array of short-term plant processes, amongst which xylem-transport of CO_2 in leaves might be of particular importance.

The aim of this study was to investigate in detail where xylem-transported CO_2 assimilation occurred at leaf level. Detached poplar leaves (*Populus x canadensis* Moench 'Robusta') were allowed to take up an aqueous solution enriched with dissolved $^{13}CO_2$. We manipulated the uptake rates of xylem CO_2 by altering the vapor pressure deficit (VPD) of the atmosphere under controlled conditions and analyzed the enrichment of the different leaf tissue components. We hypothesized that a larger enrichment would be observed under high VPD. However, the spatial resolution of the results derived from the ^{13}C labeling was too limited. Therefore, an additional detached leaf of the same species was allowed to take up an aqueous solution enriched with dissolved $^{11}CO_2$ to obtain a detailed picture of xylem CO_2 assimilation in leaves using autoradiography.

2.2 Materials and methods

2.2.1 Plant material

For this study, 20 cm long poplar cuttings (*Populus x canadensis* Moench 'Robusta') were planted early April 2012 in 4 l pots containing a commercial potting mixture (DCM, Grobbendonk, Belgium) and slow-releasing fertilizer (Basacote Plus 6M, Compo Benelux nv, Deinze, Belgium), and were grown within a growth chamber. Air temperature (T_{air}) was controlled day and night at 25°C and photosynthetic active radiation (PAR) was provided with densely packed fluorescent lamps (TLD 80, Philips Lighting NV, Eindhoven) from 8:00 h until 22:00 h. The cuttings were watered every two days.

2.2.2 Baseline sampling

Prior to ^{13}C labeling, leaf baseline samples of the same cuttings were used to determine the natural abundance carbon isotopic composition ($\delta^{13}C$, ‰) to which $\delta^{13}C$ values of treated tissues would be compared. Baseline samples were collected on all treatment days and were immediately frozen in liquid nitrogen and then stored in a freezer at -18°C before further processing.

2.2.3 Experimental setup ^{13}C labeling

The control and $^{13}CO_2$ treatment solutions were prepared as described by McGuire *et al.* (2009). Solutions were either enriched with 99 atom% (A) $^{13}CO_2$ (treatment) or with $^{13}CO_2$ at natural abundance and atmospheric concentration (control). To prepare the solutions, 2 l bottles were completely filled with deionized water, which was amended with KCl to 40 mM concentration to facilitate solution uptake (Zwieniecki *et al.*, 2001) and with 1 mM sodium bicarbonate to control pH at a level of around 7. One of these bottles was set aside and used for providing the KCl solution that treatment and control leaves were allowed to transpire before and after the labeling treatment. For another bottle, 160 ml of the solution was displaced with 99 A $^{13}CO_2$ gas from a compressed gas cylinder (Buchem BV, Minden, The Netherlands). Subsequently, the gas was then circulated with a pump through water in a closed loop for at least 3 h. For the control bottle, gas with $^{13}CO_2$ at natural abundance and atmospheric concentration was circulated through the control solution for the same amount of time. After bubbling, pH dropped by 0.5 units, slightly affecting the final dissolved inorganic carbon concentration ([CO_2*]) (Erda *et al.*, 2013). [CO_2] measured with a microelectrode (Model Mi-720, Microelectrodes, Bedford, NH, USA) and dissolved CO_2 concentration ([$^{13}CO_2$*], mM) of the enriched solutions were 15.07 % and 10.51 mM, respectively.

Leaves were excised under water right before the start of the experiment to avoid xylem embolism formation. The cut end of the petiole was sealed with a closed-cell foam gasket in a 3 ml syringe (BD, Franklin Lakes, NJ, USA) filled with KCl solution and connected to a syringe and valve system enabling the supply of either KCl solution or treatment or control CO_2 solutions. Syringes were placed in a plexiglas box (0.56 x 0.45 x 1.6 m, H x W x L), which was specifically designed for this experiment. This box allowed the control of temperature, PAR and relative humidity (RH). RH inside the box was altered during three treatment days by controlling the water vapor content of the air entering the box. To this end, a gas cooling unit (Van der Heyden, Brussels, Belgium) was used to dehumidify the incoming air. Subsequently, the incoming air was bubbled in a beaker containing deionized water placed in a temperature controlled water bath (Colora Messtechnik GmbH, Frankenthal, Germany) to alter the water vapor content of the air to a set level. RH was varied from day to day and RH levels of 42.4 , 59.5, and 73.6% were

imposed, corresponding with a high (1.83 kPa), mid (1.29 kPa) and low (0.84 kPa) vapour pressure deficit (VPD) treatment, respectively, hereafter referred to as high, mid, and low VPD. Box temperature was maintained at 25°C for the different days, while three SON-T lights (type 400 W/2220 E40 1SL, Philips, Eindhoven, The Netherlands) installed at approximately 35 cm above the box provided PAR of 530 µmol m^{-2} s^{-1} measured at the top of the box. Per day, a set of 22 syringes containing 16 treatment and six control leaves in total were randomly installed in the box. The control leaves were used to determine whether any of the $^{13}CO_2$ diffused from the treatment leaves to the atmosphere and was subsequently assimilated by the control leaves during the course of the experiment.

Pre-labeling, each leaf initially transpired the KCl solution for 1 h. The solution was then switched for 2 h to the treatment and control solutions. The time of labeling was determined by a preliminary experiment in which leaves from additional *Populus x canadensis* cuttings were placed in a dye solution. The dye was clearly visible in the veins after 15 min, indicating that 2 h was sufficient for xylem-transported CO_2 to be distributed in the leaves. After 2 h labeling, solutions for the control and treatment leaves were switched back to KCl solution for another 30 min, to allow complete assimilation of the xylem-transported label in leaf tissues.

2.2.3.1 Tissue sampling

After the 2 h labeling, the uptake of ^{13}C (mg) was recorded and calculated as described in McGuire et al. (2009):

$$\mathbf{^{13}C_{uptake} = [CO_2^*]\ A\ w} \qquad (2.1)$$

where $[CO_2^*]$ was calculated using Henry's coefficients (Butler, 1991; McGuire & Teskey, 2002) and w is water uptake of the leaf (ml).

After the final 30 min uptake of KCl solution, leaves were removed from the syringes and immediately frozen in liquid nitrogen and transferred to a freezer at -18°C to stop all metabolic activity.

Each leaf was thawed individually and the portion of the petiole below the foam gasket was removed. All leaves were separated into subsamples of petiole, primary vein, secondary veins and mesophyll. Baselines samples were processed similarly. All leaf subsamples were dried to a constant weight in an oven at 65°C and the dry weight was recorded for scaling the data from stable isotope analysis samples to leaf level. Finally all samples were ground to powder in a ball mill (Mixer Mill MM 200, Retsch, Haan, Germany) for ^{13}C analysis.

2.2.3.2 Isotopic analysis

Ground tissue samples of four leaves per treatment were weighed to µg precision in tin capsules and analyzed by Element Analyzer (ANCA-SL, SerCon, Crew, UK) coupled to an Isotope Ratio Mass Spectrometry (20-20, SerCon, Crew, UK) (EA-IRMA). Baking flour with a $\delta^{13}C$ value of -27.01 ‰ (certified by IsoAnalytical, UK) was used as a laboratory reference and all $\delta^{13}C$ are expressed relative to VPDB.

Enrichment of the labeled tissues ($\delta^{13}C_t$, ‰) was calculated as the difference between the $\delta^{13}C$ value of the labeled sample ($\delta^{13}C_s$, ‰) and the $\delta^{13}C$ value of the baseline sample ($\delta^{13}C_b$, ‰) of similar tissue (Bloemen *et al.*, 2013b):

$$\boldsymbol{\delta^{13}C_t = \delta^{13}C_s - \delta^{13}C_b} \qquad (2.2)$$

A of the labeled tissues (A_t, %) was calculated as:

$$\boldsymbol{A_t = \frac{\left(\delta^{13}C_t/1000\right)*0.0112372}{\left(1+\left(\delta^{13}C_t/1000\right)*0.0112372\right)}} \qquad (2.3)$$

Where 0.0112372 is the ratio of $^{13}C/^{12}C$ of the VPDB standard.

Dry mass of the leaf tissue component subsamples was used to determine the mass proportions of the different leaf components. These mass proportions were used to calculate the amount of ^{13}C assimilated in each leaf tissue component ($^{13}C_t$, mg) based on A_t:

$$\boldsymbol{^{13}C_t = A_t\ DM\ C} \qquad (2.4)$$

where DM is the dry mass of the leaf tissue component (mg) and C is the carbon content of the tissue component (%). The calculated $^{13}C_t$ was corrected for potential assimilation by the leaves of ^{13}C present in the air in the box, based on observed differences in baseline and control leaf tissue enrichment.

2.2.4 Experimental setup ^{11}C labeling

We used positron autoradiography on leaves from the same *Populus x canadensis* cuttings to provide a greater detail on the spatial distribution of tracer assimilation in leaves. Because ^{11}C is a short living isotope, this part of the experiment was performed close to the cyclotron (18/9 Mev, IBA, Belgium). The close distance allowed fast transport of the produced ^{11}C to the INFINITY imaging lab of Ghent University, Gent, Belgium. There, $^{11}CH_4$ produced from the (p, α) nuclear reaction in the cyclotron on a nitrogen target was oxidized in a synthetic train to yield $^{11}CO_2$ as described by Landais & Finn (1989). The captured $^{11}CO_2$ gas was immediately bubbled in 500 mM TRIS buffer containing 0.05 M KOH at a set pH of 7.2 to obtain $^{11}CO_2$ solution and the leaf was allowed to transpire this solution during the experiment.

Labeling was performed in a cylindrical airtight labeling chamber (135 mm inner diameter and 68 mm height), which was kept just below atmospheric pressure to avoid potential diffusion of $^{11}CO_2$ out of the chamber. RH and T_{air} measured inside the labeling chamber and averaged (±SD) over the entire labeling period were 28.4 ± 0.8% and 30.2 ± 0.6°C, respectively. A light source provided a PAR of 926 μmol CO_2 m^{-2} s^{-1} at the leaf surface. After leaf excision under water, the leaf was installed in the labeling chamber and the cut end of the petiole was fixed with polysiloxan material (Xantopren, Heraeus Kulzer, GmbH, Hanau, Germany) in a plastic pipette tip filled with non-labeled aqueous TRIS buffer solution and connected to two 3 ml syringes with 0.6 mm tubing. The labeling chamber was closed and one syringe was used to supply the $^{11}CO_2$ solution at the start of the experiment, while the other syringe was used to replace the non-labeled solution with the labeled solution and to reduce the transfer time of $^{11}CO_2$ label from the other syringe to the pipette tip, given the short half-life of ^{11}C. Two ml of $^{11}CO_2$ solution was supplied to the leaf with an activity at labeling of 7.42 MBq. The leaf was labeled for 1 h, after which autoradiogaphy was performed.

2.2.4.1 Autoradiography

Distribution of the radioactivity was imaged by positron autoradiography, exposing the leaf by direct contact with an imaging phosphor plate for 5 min, after which the plate was scanned digitally (Cyclone Plus Phosphor imager, Perkin Elmer, Waltham, MA, USA). The autoradiographic image was quantified using OptiQuant (Perkin Elmer, Waltham, MA, USA). Different regions of interest (ROI) were selected in the autoradiogram corresponding with the petiole, primary vein and single secondary veins. A background ROI outside the leaf was used to subtract background scatter from the leaf data. Digital lighting units, which are used to express the ^{11}C decay rate based on autoradiogram analysis, were summed per ROI and divided by the surface area of the ROI.

2.2.5 Statistical analysis

For the ^{13}C experiment, we analyzed $\delta^{13}C_t$ of the treatment leaves, as well as $^{13}C_t$, using multi-factorial analysis of variance (ANOVA). VPD treatment (n=3) and tissue component (n=4, petiole, primary vein, secondary veins, and leaf mesophyll) were treated as fixed factors and individual leaf (n=4 per VPD treatment) was treated as a random factor. We also used a similar ANOVA model to compare $\delta^{13}C_t$ in the treatment versus control leaves with leaf type (n=2; control and treatment), VPD treatment (n=3), and tissue component (n=4) treated as fixed factors and individual leaf (n=4) treated as random factor. Solution uptake was analyzed using a similar ANOVA model with only leaf type (n=2) and VPD treatment (n=3) considered as fixed factors and individual leaf as random factor. Treatment means were compared using Fisher's Least Significance Difference test. ANOVA analyses were performed using the mixed model procedure (PROC MIXED) of SAS (Version 9.1.3, SAS inc., Cary, NC, USA) with α=0.05.

2.3 Results

2.3.1 $^{13}CO_2$ uptake

VPD had a significant effect on solution uptake in both treatment (P=0.003) and control (P=0.010) leaves. Therefore in treatment leaves, mean ^{13}C uptake (± SE) during the 2 h $^{13}CO_2$ label uptake period under high (0.93 ± 0.09 mg ^{13}C) and mid (0.81 ± 0.09 mg ^{13}C)

VPD was significantly higher than under low VPD (0.54 ± 0.05 mg ^{13}C). In control leaves, the mean uptake of non-labeled solution under high VPD (1.08 ± 0.17 ml) was significantly higher than under mid (0.64 ± 0.22 ml) and low (0.50 ± 0.08 ml) VPD.

2.3.2 ^{13}C tissue enrichment

Due to differences in ^{13}C uptake, significant differences in tissue ^{13}C enrichment ($\delta^{13}C_t$) were observed among VPD treatments (P<0.0001, Fig. 2.1). The $\delta^{13}C_t$ values were significantly higher under high VPD than under mid and low VPD in the petiole, the primary and secondary vein tissues. In contrast, VPD had no significant effect on $\delta^{13}C_t$ (P=0.60) in leaf mesophyll, which is more distal from the ^{13}C source than the other tissues. Among leaf tissue components, significant differences in $\delta^{13}C_t$ were observed (Fig. 2.1). Petioles were most enriched, regardless of the VPD treatment. For the most distal tissues (secondary veins and leaf mesophyll) no significant differences in $\delta^{13}C_t$ were observed. In control leaves, $\delta^{13}C_t$ ranged from -0.19 to 2.65‰ across the different VPD treatments, indicating that the isotope composition of control leaves was similar as for baseline leaves. Petiole and primary vein enrichment of control leaves were significantly lower than corresponding tissues of treatment leaves, for all VPD treatments. For leaf mesophyll no significant differences were observed between treatment and control leaves (P=0.2779) due to the low tissue enrichment in treatment leaves, regardless of the VPD treatment.

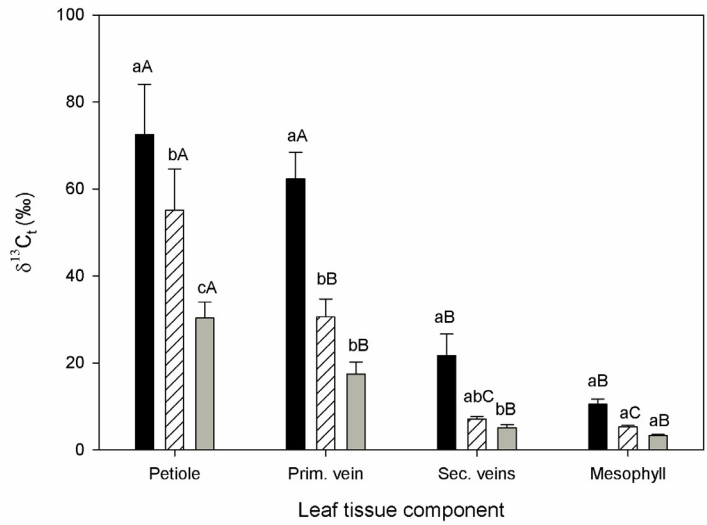

Fig. 2.1 Tissue enrichment ($\delta^{13}C_t$) of petiole, primary (prim.) vein, secondary (sec.) veins and leaf mesophyll of leaves under high (black), mid (hatched) and low (grey) vapor pressure deficit (VPD) treatment. Data are averaged for four leaves per VPD treatment. Different lower case letters indicate significant differences (P<0.05) in $\delta^{13}C_t$ among VPD treatments within a leaf tissue component. Different upper case letters indicate significant differences among leaf tissue components within VPD treatment. Bars indicate standard error.

2.3.3 ^{13}C assimilation

Significant differences in the amount of label assimilated per leaf tissue component ($^{13}C_t$) were observed among VPD treatments for leaf mesophyll (P<0.0001), primary vein (P=0.0002) and secondary veins (P=0.0001), with highest $^{13}C_t$ observed under high VPD (Fig. 2.2). For the petiole, $^{13}C_t$ was highest under high VPD, but only significantly higher as compared to $^{13}C_t$ under low VPD treatment. Because leaf mesophyll constitutes on average 73.20 ± 1.09% of the dry mass of the leaves used in the ^{13}C experiment, highest $^{13}C_t$ was observed for this leaf tissue component, regardless of VPD treatment (Fig. 2.2). Under both high and mid VPD treatment, assimilation levels were significantly different among leaf tissue components, whereas under low VPD treatment, $^{13}C_t$ was approximately equal for the different leaf tissue components. The potential amount of $^{13}C_t$ derived from the uptake of ^{13}C of the atmosphere ranged between -0.0002 to 0.0028 mg ^{13}C. In contrast to $^{13}C_t$ of treatment leaves, VPD treatment or tissue component had no effect on $^{13}C_t$ of control leaf tissues.

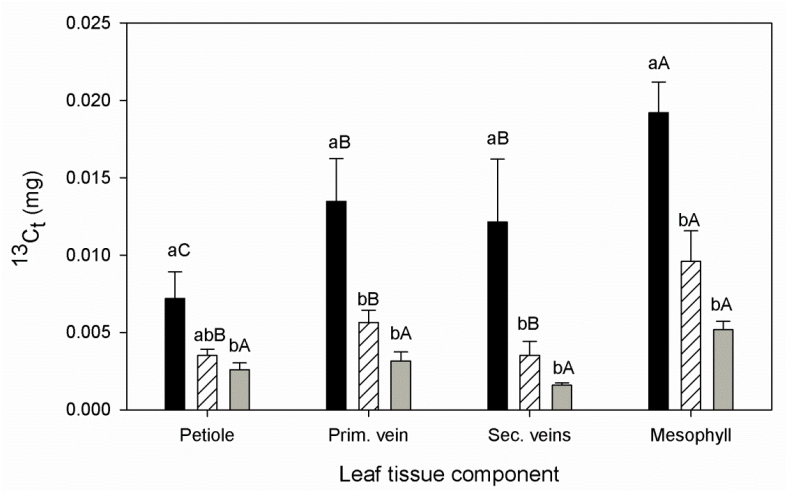

Fig. 2.2 Label assimilation ($^{13}C_t$) of petiole, primary (prim.) vein, secondary (sec.) veins and leaf mesophyll of leaves under high (black), mid (hatched) and low (grey) vapor pressure deficit (VPD) treatment. Data are averaged for four leaves per VPD treatment. Different lower case letters indicate significant differences (P<0.05) in $^{13}C_t$ among VPD treatments within a leaf tissue component. Different upper case letters indicate significant differences among leaf tissue components within a VPD treatment. Bars indicate standard error.

2.3.3 ^{11}C autoradiography: detailed analysis of xylem CO_2 assimilation

Positron autoradiography was used to assess the spatial distribution of xylem-transported $^{11}CO_2$ assimilation (Fig. 2.3). Clear differences are observed between the leaf vasculature, including the petiole, and the leaf mesophyll tissue: most $^{11}CO_2$ accumulated in the vasculature, while only a limited amount of $^{11}CO_2$ reached the mesophyll. Summation of the digital lighting units for the petiole, primary vein and the secondary veins recorded in the autoradiogram (Fig. 2.4A) indicate that $^{11}CO_2$ accumulated mainly in the petiole and in the major vein, and to a lesser extent in the secondary veins (Fig. 2.4B). Additionally, among secondary veins, there was an important distance-to-source effect on the $^{11}CO_2$ distribution, with highest ^{11}C activity observed for the secondary veins closest to the petiole.

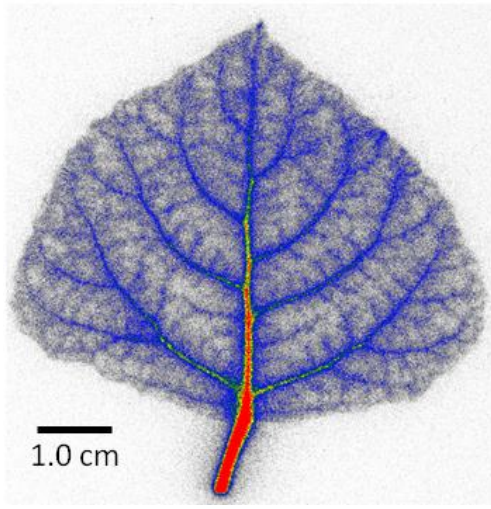

Fig. 2.3 Positron autoradiogram showing the distribution of xylem-transported $^{11}CO_2$ in an excised poplar leaf (*Populus x canadensis* Moench 'Robusta'), 1 h after the $^{11}CO_2$ label was administered to the leaf via the petiole.

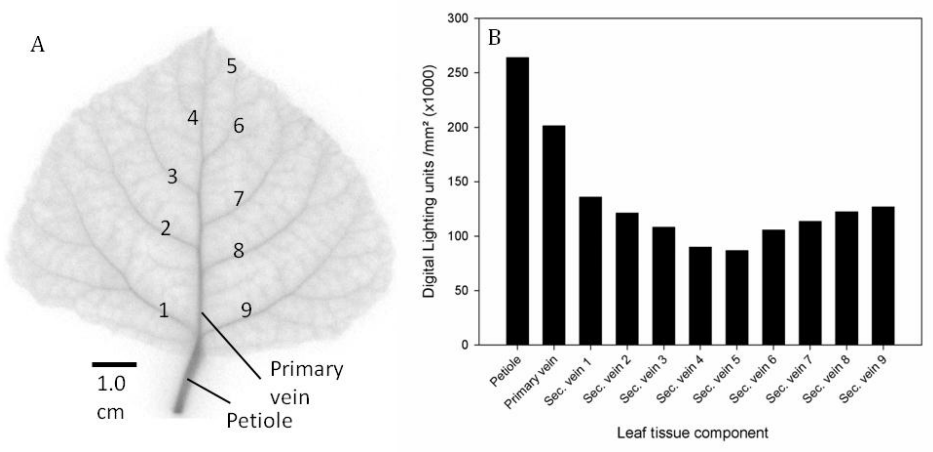

Fig. 2.4 Distribution of xylem-transported ^{11}C among petiole, primary vein and secondary veins in an excised poplar leaf (*Populus x canadensis* Moench 'Robusta'), 1 h after the $^{11}CO_2$ label was administered to the leaf via the petiole. The numbers indicated in the autoradiogram (A) are used to rank the secondary veins in (B). The digital lighting units were summed for the petiole, primary, and the different secondary veins, background subtracted and divided by the area corresponding with the surface area of the different tissue components and single secondary veins considered in (A).

2.4 Discussion

Leaves absorbed both $^{11}CO_2$ or $^{13}CO_2$ enriched solution which were both detected in all leaf tissues, but mainly in the petiole and primary and secondary veins. Results from our ^{13}C labeling experiment are in line with previous studies which traced xylem CO_2 transport at tree (Bloemen *et al.*, 2013b) and branch (McGuire *et al.*, 2009; Bloemen *et al.*, 2013a) level. We observed that under high vapor pressure deficit (VPD) solution uptake was higher, resulting in a higher label uptake (0.126 ± 0.012 mg ^{13}C) than under mid (0.110 ± 0.012 mg ^{13}C) and low (0.073 ± 0.006 mg ^{13}C) VPD. Similarly, Bloemen *et al.* (2013a) manipulated, in their study on *P. deltoides* branches, $^{13}CO_2$ uptake rates by altering the VPD under controlled conditions and found a similar effect of VPD on the transpiration rate and leaf tissue enrichment, both depending on the applied $^{13}CO_2$ label concentration. Among leaf tissue components, highest tissue enrichment was observed in the petiole and to a lesser extent in primary and secondary veins. Petiole enrichment was also highest among different leaf tissue components after label infusion in the stem base of field-grown *Populus deltoides* trees Moreover, Stringer & Kimmerer (1993) observed that most of a ^{14}C label introduced via the petiole of *P. deltoides* leaves was assimilated in the petiole. Once scaled with leaf tissue dry mass, we found that most ^{13}C was assimilated in leaf mesophyll because almost three-quarter of the dry mass of the *P. x canadensis* leaves used in this study consisted of mesophyll tissue. Also Bloemen *et al.* (2013a) found that most ^{13}C was assimilated in the leaf mesophyll as compared to other leaf tissue components, regardless of the applied $^{13}CO_2$ label concentration or VPD treatment.

However, the destructive nature of ^{13}C analysis limits its applicability for detailed detection of xylem CO_2 assimilation in leaves. Leaf tissue component samples need to be separated, dried, and milled before $\delta^{13}C$ determination by isotope ratio mass spectrometry. Moreover, single secondary leaf veins are pooled to obtain enough sample material for ^{13}C analysis. Therefore, the spatial resolution of a ^{13}C-based analysis is constrained to the leaf tissue component level. To circumvent this limitation in spatial resolution, we additionally used autoradiographic tracing of ^{11}C to study xylem CO_2 assimilation in leaves. In the case of radiocarbon tracing of xylem CO_2, previous studies have solely used ^{14}C in combination with autoradiography (Zelawski *et al.*, 1970;

Vapaavuori & Pelkonen, 1985; Vuorinen *et al.*, 1989; Amiro & Ewing, 1992; Stringer & Kimmerer, 1993; Hibberd & Quick, 2002). To date, ^{11}C has been used almost exclusively for *in vivo* studies on short-term transfer of photosynthates from leaves to sinks via the phloem (Minchin & Thorpe, 2003; Kawachi *et al.*, 2011b). One study yet observed ^{11}C movement in the xylem by applying a gaseous ^{11}C labeled phytohormone to *Nicotiana tabacum* leaves (Thorpe *et al.*, 2007). We fed a dissolved $^{11}CO_2$ label to the petiole and autoradiography showed that the infused ^{11}C label was transported throughout the leaf and mainly confined to petiole and leaf vein tissue (Fig. 2.3), which confirmed the results obtained with our ^{13}C leaf labeling. However, in the positron autoradiogram, ^{11}C distribution in smaller tertiary or even quaternary leaf veins could be detected, while in the ^{13}C analysis these smaller veins were included in leaf mesophyll due to practical reasons. Moreover, ^{11}C autoradiography allows a detailed analysis of label distribution, even within a single leaf tissue component. For instance, we observed among secondary veins differences in radioactivity, with highest label activity in the veins closest to the petiole, implying a variation in the assimilation of xylem-transported CO_2 (Fig. 2.4). In addition, positron autoradiography showed that xylem-transported $^{11}CO_2$ was able to reach the leaf mesophyll. This was unclear from the data derived from the ^{13}C tissue analysis from a statistical standpoint, because of the lack of significant enrichment in the leaf mesophyll of the treatment leaves compared to the control ones, regardless of VPD treatment. Therefore, we believe that ^{11}C tracing in plants might help us to better understand plant processes in the context of future studies on xylem CO_2 assimilation, by allowing a more detailed visualization of the fate of xylem-transported CO_2 in plants. However, the isotopes' radioactive nature, its short-half life and the experimental cost related to its production limit the wide scale application of ^{11}C.

The role of xylem-transported CO_2 as carbon source for photosynthetically active cells surrounding the xylem vasculature in petiole and leaf veins is intriguing. One of the main functions of leaf venation is to efficiently distribute water and solutes among the entire leaf surface (Roth-Nebelsick *et al.*, 2001; Brodribb *et al.*, 2010). From the leaf veins, xylem-transported CO_2 enters the bundle sheath cells (Sack & Holbrook, 2006) where chloroplasts use this respiratory CO_2 as substrate (Leegood, 2008). Photosynthetic activity in these bundle sheath cells has long been related to the origins of the C_4

pathway. However, Hibberd & Quick (2002) suggested that in C_3 plants a C_4-like carbon concentrating mechanism might exist in which these chlorophyll containing cells are supplied with respiratory carbon from the vascular system and not with atmospheric carbon from stomata (**Chapter 1**). They found that a ^{14}C label supplied to the roots and stems of tobacco and celery was assimilated in photosynthetic cells adjacent to the xylem tissue (Hibberd & Quick, 2002). Similarly, Stringer & Kimmerer (1993) performed a labeling experiment on *P. deltoides* leaves and observed assimilation of xylem-transported CO_2 in the veins, mainly by Ribulose-1,5-biphosphate carboxylase oxygenase (Rubisco) and in a lesser extent by Phosphoenolpyruvate carboxylase (PEPc). Janacek *et al.* (2009) found for Arabidopsis that respired CO_2 is the sole substrate source for cells adjacent to the leaf veins and that sugars and carbon skeletons synthesized in these cells are important for phloem transport and the Shikimate pathway, which is described as the biosynthetic route to aromatic amino acids (Herrmann & Weaver, 1999 and references therein). Moreover, the location of the bundle sheath cells, adjacent to the phloem strands, facilitates a direct loading of synthesized sugars into the phloem tissue. Therefore, assimilation of respired CO_2 in bundle sheath cells of leaves might have important implications for the physiology of the entire plant.

In particular for plants with heterobaric leaves, which is the case for poplar, dissolved CO_2 transport via the dense vein network might be an important means for redistributing substrate for photosynthetic reactions (Bloemen *et al.*, 2013a). In these leaves, lateral diffusion of gaseous CO_2 is restricted due to the strong compartmentalization of the leaf by bundle sheath extensions (McClendon, 1992; Pieruschka *et al.*, 2005). Lynch *et al.* (2012) observed that CO_2 refixation in heterobaric leaves might contribute to the difference in isotopic composition of different leaf sections, because isotopic signatures of respired CO_2 are either depleted or enriched relative to the substrate (Ghashghaie *et al.*, 2003) or the tissues (Bowling *et al.*, 2008), respectively. They observed an isotopic depletion in leaf tissue $\delta^{13}C$ near the main vein as compared to tissue near the leaf margin (Lynch *et al.*, 2012) which they related to a potential assimilation of respired CO_2. However, the role of assimilation of respired CO_2 in cells surrounding the vasculature in leaves might extend beyond maintaining the plant carbon status at leaf level. Griffiths *et al.* (2013) hypothesized that bundle sheaths

might play a central role in cavitation repair in leaves, by contributing to the considerable energetic demand for cavitation repair (Zwieniecki & Holbrook, 2009; Secchi & Zwieniecki, 2011). Refilling of embolized vessels requires a source of water and the release of energy stored in parenchymatous cells (Secchi & Zwieniecki, 2011). Given its close proximity to the xylem vasculature, bundle sheath cells might provide the sugars respired by living cells which are used to meet the energetic requirements to refill vessels under tension (Zwieniecki & Holbrook, 2009). This is consistent with their previously observed role in protecting the leaf mesophyll against water deficit (Terashima, 1992; Leegood, 2008). At branch and stem level, assimilation of xylem-transported CO_2 in xylary chloroplasts has been found to maintain hydraulic conductivity by repairing embolized xylem vessels (Schmitz *et al.*, 2012) (**Box 1.2**). However, the hypothesis that CO_2 assimilation in the bundle sheath might play a crucial role in the local plant water status still needs to be tested experimentally.

In conclusion, stable and unstable isotope carbon tracing of xylem CO_2 transport reveals a wealth of information on the quantification and imaging of xylem CO_2 assimilation and might serve as useful tool to unravel its role in plant functioning. While in ^{14}C tracing studies radiation safety is of important concern in particular regarding the disposal of radioactive waste, our results show that the short-living ^{11}C tracer can be used to visualize xylem CO_2 transport in plants. Moreover, *in vivo* real-time imaging of xylem CO_2 transport in entire plants is potentially possible, given the recent advances in positron emission tomography (PET) ^{11}C detection (e.g. Beer *et al.*, 2010; Kawachi *et al.*, 2011b). Therefore, a ^{11}C labeling approach, recently used to trace carbon partitioning in leaves (Dirks *et al.*, 2012), might be a next step in studying xylem CO_2 transport in plants. This will broaden our current knowledge on plant physiology and deepen our understanding on the significance of xylem CO_2 transport in maintaining the carbon and water status of plants.

- Chapter 3 -

Xylem [CO_2] and transpiration rate affect xylem-transported CO_2 assimilation

After: Bloemen J., McGuire M.A., Aubrey D.P., Teskey R.O. and Steppe K. (2013) Assimilation of xylem-transported CO_2 is dependent on transpiration rate, but small relative to atmospheric fixation. *Journal of Experimental Botany* **64:** 2129-2138.

Abstract

The effect of transpiration rate on internal assimilation of CO_2 released from respiring cells has not previously been quantified. In this study, detached branches of *Populus deltoides* were allowed to take up $^{13}CO_2$-labeled solution at either high (high label, HL) or low (low label, LL) $^{13}CO_2$ concentrations. The uptake of the $^{13}CO_2$ label served as a proxy for the internal transport of respired CO_2, while the transpiration rate was manipulated at the leaf level by altering the vapor pressure deficit (VPD) of the air. Simultaneously, leaf gas exchange was measured, allowing comparison of internal CO_2 assimilation to that assimilated from the atmosphere. Subsequent ^{13}C analysis of branch and leaf tissues revealed that woody tissues assimilated more label under high VPD, corresponding with higher transpiration, than under low VPD. More ^{13}C was assimilated in leaf tissue than in woody tissue under the HL treatment, whereas more ^{13}C was assimilated in woody tissue than in leaf tissue under the LL treatment. The ratio of $^{13}CO_2$ assimilated from the internal source to CO_2 assimilated from the atmosphere was highest for the branches under the HL and high VPD treatment, but was relatively small regardless of VPD x label treatment combination (up to 1.9%). Our results show that assimilation of internal CO_2 is highly dependent on the rate of transpiration and xylem sap [CO_2]. Therefore, it can be

expected that the relative contribution of internal CO_2 recycling to tree carbon gain is strongly dependent on factors controlling transpiration, respiration, and photosynthesis.

3.1 Introduction

A portion of CO_2 released by mitochondrial respiration of living cells in tree stems and branches diffuses to the atmosphere through woody tissues (Saveyn *et al.*, 2010). However, branch and stem tissues impede gaseous diffusion (Kramer & Kozlowski, 1979; Lendzian, 2006; Sorz & Hietz, 2006; Steppe *et al.*, 2007), resulting in internal CO_2 concentrations ($[CO_2]$) that substantially exceed atmospheric $[CO_2]$ (Teskey *et al.*, 2008; McGuire *et al.*, 2009) (**Chapter 1**).

The importance of accounting for internal transport of CO_2 to accurately assess estimates of respiration based on measurements of CO_2 efflux has been previously described (e.g. Levy *et al.*, 1999; Teskey & McGuire, 2007; Saveyn *et al.*, 2008b). CO_2 originating from respiration both below- (Aubrey & Teskey, 2009; Grossiord *et al.*, 2012; Bloemen *et al.*, 2013b) and aboveground (Teskey & McGuire, 2007) can dissolve in xylem sap and be transported upward via the transpiration stream from the stem base to the top of the canopy (Bloemen *et al*., 2013b), and can diffuse into the atmosphere via aboveground tissues remote from the site of respiration (Teskey & McGuire, 2007) (**Chapter 1**).

Along the transport pathway, this internal CO_2 can be assimilated by active chloroplasts within the stem, branches and leaves (McGuire *et al.*, 2009; Saveyn *et al.*, 2010), thereby contributing to the whole-plant carbon gain. In woody tissues, chloroplasts occur both in the xylem and inner bark which justifies the use of the term woody tissue photosynthesis instead of bark or corticular photosynthesis when referring to stem CO_2 assimilation (Saveyn *et al.*, 2010). In the leaves, it is believed that xylem-transported CO_2 is mainly fixed in the cells surrounding the xylem vasculature in the petioles and near the veins (Stringer & Kimmerer, 1993; McGuire *et al.*, 2009). McGuire *et al.* (2009) found that assimilation of xylem-transported ^{13}C-labeled CO_2 (referred to as $^{13}CO_2$ in the text), supplied in high concentrations as a tracer, averaged 6% of the assimilation of atmospheric CO_2 by the leaves in detached sycamore branches. Given that respired CO_2 is re-distributed by the transpiration stream (**Chapter 1**), it might be expected that at a

high transpiration rate and/or at high xylem sap [CO_2] a larger amount of CO_2 could be transported in the xylem towards photosynthetically active tissues in woody organs and leaves. Therefore, transpiration rate and xylem sap [CO_2] might be critical factors to consider when assessing assimilation of internally transported CO_2 in the context of whole-plant carbon cycling.

However, to our knowledge, the combined effect of transpiration and xylem sap [CO_2] on the assimilation of xylem-transported CO_2 has not been investigated. In this study, detached branches of *Populus deltoides* Bartr. Ex. Marsh trees were allowed to take up an aqueous solution enriched with either a low or a high concentration of $^{13}CO_2$ while the transpiration rate was manipulated by varying the atmospheric vapor pressure deficit (VPD). Simultaneous leaf gas exchange measurements allowed us to compare the contributions of assimilation of internally transported CO_2 and atmospheric CO_2. We hypothesized that more ^{13}C label would be assimilated in chlorophyll-containing woody and leaf tissues under the high [$^{13}CO_2$] solution treatment and at high transpiration because a greater quantity of ^{13}C-labeled substrate would be transported in those conditions.

3.2 Material and methods

3.2.1 Plant material

Branches were cut from *P. deltoides* trees that were part of a 7-y-old plantation in Whitehall Forest, a research facility of the University of Georgia near Athens, Georgia, USA. Branches (length >2m) were collected around 06:30 h on 16 and 17 July 2010 and their cut ends were placed immediately in water to prevent wilting. In the lab, lateral segments of these branches that were between 20-50 cm long and <1 cm in diameter were cut under water to prevent embolism formation in the xylem. The experiment was conducted on these lateral segments; hereafter referred to as branches.

3.2.2 Baseline sampling

Prior to the start of the labeling experiment, baseline samples were taken from the same trees to determine the natural abundance carbon isotopic composition ($\delta^{13}C$) to which

$\delta^{13}C$ values of treated tissues would be compared. For baseline sampling, branches of similar dimensions and at approximately the same canopy position were cut from the trees and separated into woody and leaf tissues. Baseline samples were immediately frozen in liquid nitrogen and then moved to a freezer at -9°C for storage before processing.

3.2.3 Experimental setup

The control solution (10 l in total) enriched with $^{13}CO_2$ at natural abundance and atmospheric concentration was prepared as described in **Chapter 2**. The $^{13}CO_2$ treatment solutions were enriched with 99 atom% (A) $^{13}CO_2$ either at a high (high label, hereafter referred to as HL) or a low (low label, hereafter referred to as LL) concentration to account for the variation in internal [CO_2] generally observed within trees. 10 l bottles were completely filled with deionized water, which was amended with KCl to 40 mM concentration to facilitate solution uptake (Zwieniecki *et al.,* 2001). Depending on the desired concentration, 1 or 3 l of the solution was displaced with 99 A $^{13}CO_2$ gas from a compressed gas cylinder (ICON Services, Summit, NJ, USA). The gas was then circulated with a pump through the water in a closed loop for at least 3 h. Solutions were amended with sodium bicarbonate to control pH and achieve and dissolved CO_2 concentration ([$^{13}CO_2$*]) target according to modeled [CO_2*] at a set pH (Erda *et al.*, 2013). [CO_2] and [$^{13}CO_2$*] concentration were 8.9%, and 3 mM for the LL solution and 18.5%, and 13 mM for the HL solution. Based on preliminary measurements, we assumed that the [CO_2] of the HL and LL solutions represented high and low xylem sap [CO_2], respectively. The pH of the HL and LL solutions were 6.4 and 4.8, respectively, which is within the range measured previously in *P. deltoides* (Aubrey & Teskey, 2009; Aubrey *et al.*, 2011). On the first day (16 July), the experiment was performed with ten branches using the LL solution, while on the following day (17 July) the experiment was repeated with the HL solution on another set of ten branches collected that morning.

The cut end of each branch was placed in a 500 ml glass bottle containing 300 ml of solution enriched with CO_2. Immediately after placing a branch into a solution, the top of the bottle was sealed with a closed-cell foam gasket to minimize diffusion of CO_2 to the atmosphere. Bottles were placed in two growth chambers (Model GC36, Environmental Growth Chambers, Chagrin Falls, OH, USA) where different vapor pressure deficit (VPD)

treatments were imposed to manipulate transpiration rate and thus, uptake of the treatment solutions. Five treatment branches were placed in each chamber. In addition, two control branches with non-labeled solution were placed in each chamber to determine if any of the $^{13}CO_2$ label diffused from the treatment bottles to the atmosphere and was subsequently assimilated by leaf photosynthesis during the course of the experiment. Control and treatment branches were randomly placed 20 cm apart on the floor of the growth chambers. Air temperature (25°C) and photosynthetic active radiation (500 µmol m^{-2} s^{-1}) were similar in both chambers. In the first chamber, low atmospheric relative humidity was imposed (30%) producing the high VPD treatment (2.23 kPa). In the second chamber, higher atmospheric relative humidity was imposed (60%), producing the low VPD treatment (1.27 kPa).

Branches were allowed to transpire for 1 h prior to the start of measurements to ensure that the labeled solution had reached the leaves. Similar as in **Chapter 2**, this time period was determined through a preliminary dye experiment. For the P. *deltoides* branches, the dye was clearly visible in the leaves within 30 min at low VPD, indicating that one hour was more than sufficient for xylem-transported CO_2 to reach the leaves under both VPD treatments.

3.2.4 Leaf gas exchange measurements

Leaf net photosynthesis (A_{net}, µmol CO_2 m^{-2} s^{-1}), stomatal conductance (g_s, mol H_2O m^{-2} s^{-1}), and transpiration (E, mmol H_2O m^{-2} s^{-1}) were measured on a fully expanded lower leaf of all treatment and control branches with a portable photosynthesis system (model Li-6400, Li-Cor, Inc., Lincoln, Nebraska, USA). Measurements were repeated four times over an eight hour period at prevailing growth chamber temperature, light, and humidity conditions and a set atmospheric [CO_2] of 400 ppm. At each measurement time, the average of five measurements recorded at 10 s intervals was used for analysis. Following the last gas exchange measurements, the branches were allowed to transpire for another hour before the lights were switched off and woody and leaf tissues were sampled.

3.2.5 Tissue sampling for ^{13}C analysis

At the end of the 9 h uptake period, branches were removed from the bottles and the remaining amount of solution was subtracted from the original amount to determine the quantity of solution taken up by each branch. Uptake of ^{13}C (mg) was calculated as described in **Chapter 2** (**Equation 2.1**).

For every branch, the portion above the foam gasket at the top of each bottle was divided into three equal length sections (lower, mid, and upper) and all woody and leaf tissues were collected from each section separately. Samples were immediately frozen in liquid nitrogen and transferred to an ultralow freezer at -25°C to stop all metabolic activity. Tissues were later transferred to a walk-in freezer and stored at -9°C.

Each sample was thawed individually before further processing. The leaf area (LA) of each branch section was measured with a LA meter (Model Li-3100, Li-Cor Inc., Lincoln, Nebraska, USA). Mean total LA per branch (±SE) was 1109.1 ± 56.7 cm^2. Non-living bark was removed from woody tissue samples and discarded. The remaining tissue was separated into inner bark and xylem tissue component subsamples. A sample of three mature leaves was removed from each of the three branch sections and divided into subsamples of petiole, primary vein, secondary veins, and mesophyll. The remaining mature leaves of each branch were processed as whole leaves. Baseline samples were processed in the same manner. All xylem, inner bark and leaf samples were dried to constant weight in an oven at 65°C for at least 72 h. The dry mass of all tissues was recorded for scaling the data from the stable isotope analysis to branch level. Finally, subsamples were ground to powder in a ball mill (8000-D Mixer Mill, SPEX SamplePrep, Metuchen, New Jersey, USA) for carbon isotope analysis.

3.2.6 Isotopic analysis of samples

Ground tissue samples of four leaves per treatment were weighed to µg precision in tin capsules and analyzed by Element Analyzer (model 1500 CHN, Carlo-Erba, Italy) coupled to an Isotope Ratio Mass Spectrometry (Delta V, Thermo-Finnigan, Bremen, Germany) (EA-IRMS) at the Stable Isotope and Soil Biology Laboratory (SISBL), Odum School of Ecology, University of Georgia, Athens, Georgia, USA. Bovine with a $\delta^{13}C$ value

of -21.24 ‰ (certified by the National Institute of Standards and Technology, USA) was used as a laboratory reference and all $\delta^{13}C$ are expressed relative to VPDB.

Enrichment of the labeled branch tissues ($\delta^{13}C_t$, ‰) and A of the labeled tissues (A_t, %) was calculated as described in **Chapter 2 (Equations 2.2 and 2.3)**.

3.2.7 Scaling isotope measurements of tissue component samples to branch level

Dry mass of the tissue component subsamples was used to determine the mass proportions of living bark and xylem of the woody tissue and of the different leaf components for each individual branch. These mass proportions were used to separate the total biomass of woody and leaf tissue into component parts by branch section.

Based on A_t, the amount of ^{13}C assimilated in each tissue component ($^{13}C_t$, mg) was calculated for each branch as:

$$\mathbf{^{13}C_t = A_t\, DM\; C} \qquad (3.1)$$

where DM is the dry mass of the tissue per section (mg) and C is the carbon content of the tissue component (%). Mean $^{13}C_t$ was calculated for each label × VPD treatment combination.

3.2.8 Ratio of ^{13}C assimilation to atmospheric CO_2 assimilation

To obtain the total amount of atmospheric carbon assimilated via photosynthesis (A_{atm}, g) during the period of label uptake, A_{net} (µmol CO_2 m^{-2} s^{-1}) averaged for the entire measurement period was scaled to the branch level:

$$\mathbf{A_{atm} = A_{net}\; LA\; 10^{-6}\; A(C)\, t} \qquad (3.2)$$

where LA is the total leaf area of all branch sections (m^2), A(C) is the atomic weight of carbon (12 g mol^{-1}) and t is the time of CO_2-enriched solution uptake (s).

To determine the ratio of total amount of ^{13}C assimilated in a branch ($^{13}C_{assim}$, g) to A_{atm} ($^{13}C_{assim}$ /A_{atm}, %), $^{13}C_t$ was summed for all the sections and tissues and divided by A_{atm}:

$$\mathbf{Ratio} = \left(\mathbf{^{13}C_{assim}}\right) \Big/ \mathbf{A_{atm}} \qquad (3.3)$$

3.2.9 Data processing and statistical analysis

We analyzed $\delta^{13}C_t$ of the woody and leaf tissue components of the treatment branches, as well as $^{13}C_t$, using multi-factorial analysis of variance (ANOVA). For the woody tissues, ^{13}C label concentration (n=2), branch section (n=3), VPD treatment (n=2), and tissue component (n=2, inner bark and xylem) were treated as fixed factors and individual branch (n=5 per label × VPD treatment combination) was treated as a random factor. A similar ANOVA model was used for leaf components (n=4; petiole, primary vein, secondary veins, and mesophyll). We also used a similar ANOVA model to compare $\delta^{13}C_t$ in the treatment versus control branches with branch type (n=3; control, HL, and LL), ^{13}C label concentration (n=2), branch section (n=3), VPD treatment (n=2), and tissue component (n=6) treated as fixed factors and individual branch (n=5) treated as random factor. Ratios of $^{13}C_{assim}$ to A_{atm} were analyzed using an ANOVA model similar to that used for $\delta^{13}C_t$, but with ^{13}C label concentration (n=2) and VPD treatment (n=2) used as fixed factors and individual branch (n=5) treated as random factor. Solution uptake was analyzed using a similar ANOVA model with only branch type (n=3) and VPD treatment (n=2) considered as fixed factors. Average A_{net}, g_s and E were analyzed using a repeated measures ANOVA model with ^{13}C label concentration (n=2), VPD (n=2), and time (n=4) treated as fixed factors and individual branch (n=5) treated as a random factor. Akaike Information Criterion corrected for small sample sizes (AIC_C) was used to determine the covariance structure that best estimated the correlation among individual branches over time. Treatment means were compared using Fisher's Least Significance Difference test. ANOVA analyses were performed using the mixed model procedure (PROC MIXED) of SAS (Version 9.1.3, SAS inc., Cary, NC, USA) with α=0.05.

3.3 Results

3.3.1 Uptake of CO_2 enriched solution

Solution uptake was influenced by VPD (P<0.0001), but not by label treatment (P=0.179). Mean uptake of the $^{13}CO_2$ enriched solution for all treatment branches at high VPD was 144.0 ± 11.0 ml which was significantly higher than the uptake at low VPD (61.5 ± 5.2 ml). Similar results were observed for the amount of solution taken up by

the control branches (148.8 ± 11.8 ml and 82.5 ± 6.3 ml under high and low VPD treatment, respectively).

3.3.2 Carbon isotope composition of woody and leaf tissue components

The ^{13}C enrichment of woody tissues ($\delta^{13}C_t$) was influenced by label concentration, VPD treatment, branch section, and tissue component; however, these individual effects were not independent of each other (i.e., VPD treatment × branch section × tissue component interaction, $P<0.0001$, and a label concentration × VPD treatment × branch section interaction, $P<0.0001$). Averaged across both label treatments, the $\delta^{13}C_t$ of xylem and inner bark was higher at high VPD than at low VPD with the exception of xylem in the lower branch (Fig. 3.1). The $\delta^{13}C_t$ of the inner bark was higher in the lower branch section than in the mid- and upper-branch section, irrespective of VPD treatment, whereas no such variation among branch sections was observed for the xylem (Fig. 3.1). Averaged across xylem and inner bark tissues, mean $\delta^{13}C_t$ of the woody tissue was higher under the high label (HL) treatment than under the low label (LL) treatment at the mid- (305.22 ± 24.23‰ vs. 122.18 ± 22.93‰) and upper-branch section (223.88 ± 14.89‰ vs. 21.50 ± 10.15‰), but there was no difference between label treatments at the lower branch. The $\delta^{13}C_t$ of the woody tissue components of the control branches varied between -0.92 ± 0.07‰ and 2.72 ± 0.84‰ and was substantially lower than the $\delta^{13}C_t$ observed for the woody tissue components of the treatment branches ($P<0.0001$).

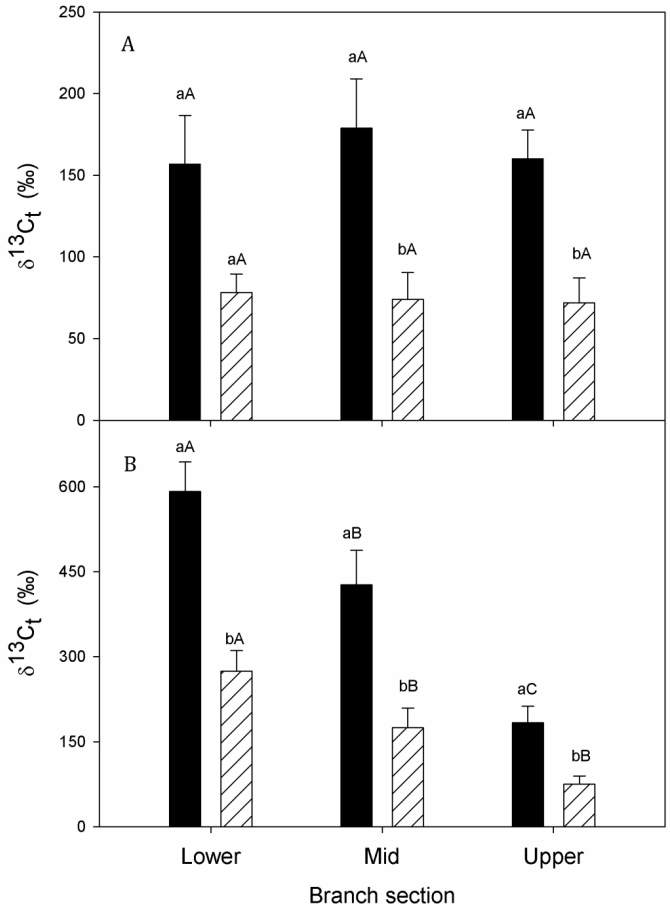

Fig. 3.1 Mean tissue enrichment ($\delta^{13}C_t$, ‰) of xylem (A) and inner bark (B) of three equal-length sections of five branches under high (black) or low (hatched) atmospheric vapor pressure deficit (VPD) averaged for high and low $^{13}CO_2$ concentration solution. $\delta^{13}C_t$ was calculated by subtracting the $\delta^{13}C_t$ value of baseline samples of non-labeled tissue from the $\delta^{13}C_t$ value of the enriched sample of the same tissue. Different lower case letters indicate significant differences ($P<0.05$) in $\delta^{13}C_t$ in inner bark and xylem between VPD treatments within each branch section. Different upper case letters indicate significant differences among different branch sections within tissue component and VPD treatment. Bars indicate standard error of the mean.

For leaf tissue, enrichment of all components was observed under the HL treatment, whereas under the LL treatment, only $\delta^{13}C_t$ of the petioles was elevated. Similar to the $\delta^{13}C_t$ of the woody tissue, $\delta^{13}C_t$ of the leaf tissue was influenced by the same individual effects, which were not independent of each other (i.e., there was a significant VPD treatment × tissue component × branch section × label concentration interaction, P=0.0166). For example, under the HL treatment, the average $\delta^{13}C_t$ of petiole (Fig. 3.2A),

primary vein (Fig. 3.2B), secondary veins (Fig. 3.2C), and leaf mesophyll (Fig. 3.2D) was higher under the high VPD than under the low VPD treatment, regardless of branch section, whereas under the LL treatment higher $\delta^{13}C_t$ at high VPD was observed only for the petioles (Fig. 3.2A). Under the high VPD treatment, the $\delta^{13}C_t$ of all leaf tissue components was higher under the HL treatment than under the LL treatment in all branch sections (Fig. 3.2). Under the low VPD treatment, the $\delta^{13}C_t$ of the petiole (Fig. 3.2A) was higher under the HL treatment than under the LL treatment regardless of branch section, but the other leaf tissue components were not influenced by the label treatment (Fig. 3.2B,C,D). The $\delta^{13}C_t$ of the petioles decreased with increasing branch section (lower to upper), regardless of VPD treatment or label concentration, whereas $\delta^{13}C_t$ of the other leaf tissue components decreased with increasing section only under the HL treatment at high VPD. For the samples processed as whole leaves, the effect of VPD and label treatment on $\delta^{13}C_t$ was similar as observed for the leaf blade tissue components (primary and secondary veins and leaf mesophyll). The $\delta^{13}C_t$ of the leaf tissue components of the control branches varied between -0.99 ± 0.07‰ and 3.39 ± 0.32‰. This was lower than the $\delta^{13}C_t$ of the leaf tissue components under the HL treatment (P<0.0001), regardless of branch section, and the $\delta^{13}C_t$ of the petioles of the branches under the LL treatment (P<0.0001).

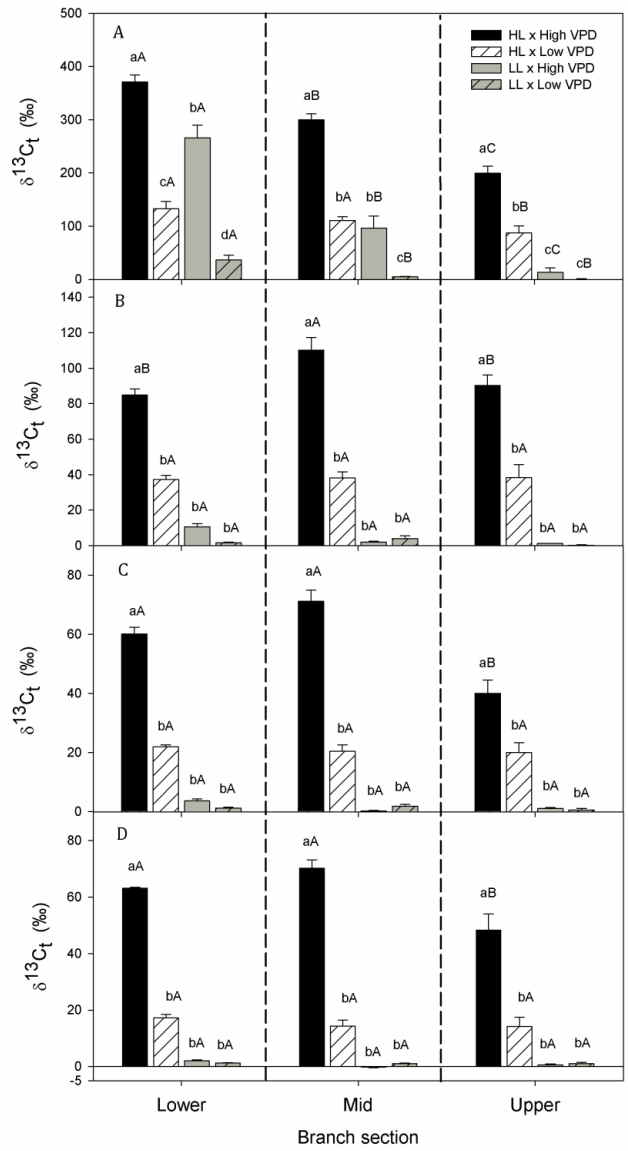

Fig. 3.2 Mean tissue enrichment ($\delta^{13}C_t$, ‰) of petiole (A), primary vein (B), secondary vein (C), and mesophyll (D) of leaves of three equal length sections of five branches allowed to transpire either high $^{13}CO_2$ concentration solution (high label, HL) under the high (black) or low (white hatched) atmospheric vapor pressure deficit (VPD) treatment, or low $^{13}CO_2$ concentration solution (low label, LL) under the high (grey) or low (grey hatched) VPD treatment. $\delta^{13}C_t$ was calculated by subtracting the $\delta^{13}C$ value of baseline samples of non-labeled tissue from the $\delta^{13}C$ value of the enriched sample of the same tissue. Different lower case letters indicate significant differences (P<0.05) in $\delta^{13}C_t$ of tissues among the four label x VPD treatment combinations within each branch section. Different upper case letters indicate significant differences in $\delta^{13}C_t$ among different branch sections within tissue component and label and VPD treatment combinations. Bars indicate standard error of the mean.

3.3.3 ^{13}C assimilation

Generally, more ^{13}C was assimilated ($^{13}C_t$) in leaf tissue than in woody tissue under the HL treatment, whereas the opposite pattern was observed under the LL treatment (Table 3.1). The $^{13}C_t$ of the woody and leaf tissue components was influenced by label concentration, VPD treatment, branch section, and tissue component and these individual effects were not independent of each other (i.e., a VPD treatment × tissue component × branch section × label concentration interaction, P=0.0137). Under the HL treatment, $^{13}C_t$ of the inner bark, petiole, and mesophyll was higher under the high VPD treatment than under the low VPD treatment, whereas $^{13}C_t$ of both woody tissue components and the petiole was higher under the high VPD treatment than under the low VPD treatment in the LL treatment (Table 3.1). Averaged across VPD and label concentration treatments most assimilation of ^{13}C in woody tissue occurred in the inner bark (65.07 ± 4.57%). Averaged across VPD and label concentration treatments, most ^{13}C assimilation in leaves occurred in the mesophyll compared to the petiole, primary vein and secondary vein (Table 3.1). Under the HL treatment, $^{13}C_t$ of the petioles and mesophyll was higher at high VPD than at low VPD in all branch sections, whereas a VPD effect on $^{13}C_t$ under the LL treatment was observed only in the petioles of the lower branch section. In total, between 62.71% and 80.36% of the applied label was assimilated, while it is assumed that the remainder diffused to the atmosphere. Regardless of VPD and label treatment, $^{13}C_t$ of the woody and leaf tissue of the control branches was lower than $^{13}C_t$ of woody and leaf tissue of the treatment branches (P<0.0001).

Table 3.1 Mean ^{13}C assimilation ($^{13}C_t$, mg) (SE) in woody and leaf tissue components of five branches allowed to transpire solutions with dissolved $^{13}CO_2$ at high (high label: HL) or low (low label: LL) concentrations and at high or low atmospheric vapor pressure deficit (VPD). Significant differences between all label × VPD treatment combinations for both woody and leaf tissue components are indicated (P<0.05). $^{13}C_t$ and standard errors displayed as 0.00 (0.00), respectively, were not zero, but have been truncated due to rounding.

Treatment combination	Branch		Leaf				Total
	Xylem branch	Inner bark	Petiole	Primary vein	Secondary vein	Mesophyll	
LL × High VPD	0.39[a] (0.11)	0.93[a] (0.16)	0.75[b] (0.14)	0.01[a] (0.00)	0.00[a] (0.00)	0.82[c] (0.16)	2.9[b] (0.47)
LL × Low VPD	0.11[b] (0.02)	0.22[c] (0.05)	0.01[c] (0.02)	0.00[a] (0.00)	0.00[a] (0.00)	0.14[c] (0.02)	0.48[c] (0.06)
HL × High VPD	0.60[a] (0.12)	1.15[a] (0.14)	1.63[a] (0.20)	0.18[a] (0.03)	0.15[a] (0.01)	5.11[a] (0.59)	8.11[a] (0.64)
HL × Low VPD	0.41[a] (0.08)	0.69[b] (0.13)	0.69[b] (0.10)	0.09[a] (0.01)	0.05[a] (0.00)	1.76[b] (0.28)	3.69[b] (0.33)

3.3.4 Leaf gas exchange

On average, transpiration rate (E) in the high VPD treatment was approximately twice as high as under the low VPD treatment, whereas leaf net photosynthesis (A_{net}) and stomatal conductance (g_S) averaged over all measurements were similar under both VPD treatments (Table 3.2). However, for E, A_{net}, and g_s both treatment responses changed through time (i.e., a VPD treatment × time interaction for E, P<0.0001; a VPD treatment × time interaction for A_{net}, P=0.0363; and a VPD treatment × time interaction for g_s, P<0.0001). Under both the high and the low VPD treatment, E and A_{net} tended to decrease slightly over time. At the last measurement time A_{net} under the low VPD treatment tended to be higher than under the high VPD treatment, which coincided with a difference in g_s observed between the VPD treatments.

Table 3.2 Average (SE) transpiration (E, mmol H_2O m^{-2} s^{-1}), net photosynthesis (A_{net}, µmol CO_2 m^{-2} s^{-1}), and stomatal conductance (g_s, mol H_2O vapor m^{-2} s^{-1}) measured on leaves of branches allowed to transpire solutions with dissolved $^{13}CO_2$ at high (high label: HL) or low (low label: LL) concentrations and at high or low vapor pressure deficit (VPD). Data are averages of four measurements performed at two-hour intervals during an eight hour measurement period on five leaves (one leaf per treatment branch) per label and VPD treatment combination. Lower case letters indicate significant (P<0.05) differences between high and low VPD treatments within ^{13}C label treatments. Standard errors displayed as 0.00 (0.00), respectively, were not zero, but have been truncated due to rounding.

Label treatment	**LL**		**HL**	
VPD	**High**	**Low**	**High**	**Low**
E	2.57[a] (0.02)	1.14[b] (0.03)	2.53[a] (0.03)	1.07[b] (0.03)
A_{net}	8.98[a] (0.15)	7.90[a] (0.22)	8.28[a] (0.13)	7.47[a] (0.25)
g_s	0.15[a] (0.00)	0.13[a] (0.00)	0.15[a] (0.00)	0.11[b] (0.00)

3.3.5 Assimilation of internally transported CO_2 vs. atmospheric CO_2 assimilation

The ratio of total ^{13}C label assimilation to atmospheric CO_2 assimilation ($^{13}C_{assim}/A_{atm}$) was affected by the VPD and label concentration treatments. The ratio was higher under high VPD than under low VPD (Fig. 3.3), independent of label concentration (P<0.0001). However, under the high VPD treatment, the ratio was higher under the HL treatment than under the LL treatment, whereas at low VPD, the ratio was not significantly different between HL and LL treatments (label concentration × VPD treatment interaction, P=0.046, Fig. 3.3).

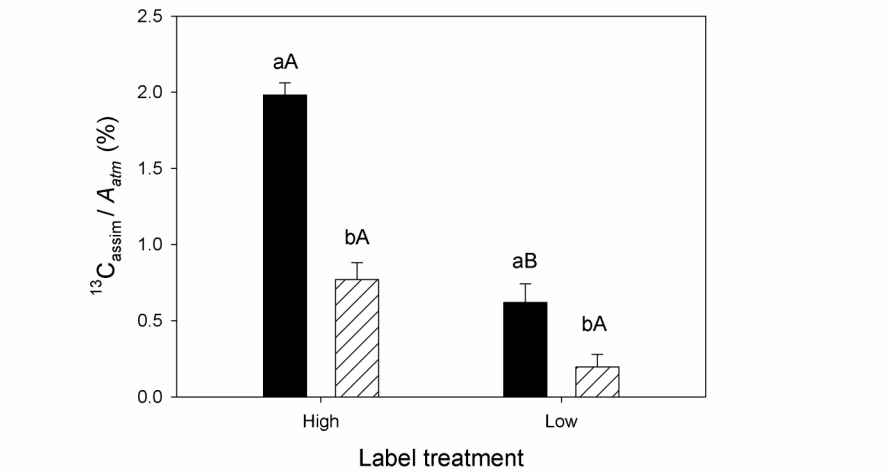

Fig. 3.3 Mean ratio of total assimilation of ^{13}C label in branches (both woody and leaf tissues) to total atmospheric CO_2 assimilation by leaves ($^{13}C_{assim}/A_{atm}$, %), of five branches allowed to transpire solutions with dissolved $^{13}CO_2$ label at high or low concentrations and at high (black or low (hatched) vapor pressure deficit (VPD). Different lower case letters indicate significant differences (P<0.05) in the ratio of ^{13}C assimilation to atmospheric CO_2 assimilation between VPD treatments within $^{13}CO_2$ concentration treatment. Different upper case letters indicate significant differences between $^{13}CO_2$ concentration treatments within VPD treatment. Bars indicate standard error of the mean.

3.4 Discussion

Our results show that transpiration and xylem sap [CO_2] both affect the quantity of xylem-transported CO_2 that is assimilated by woody and leaf tissues. Higher ^{13}C tissue enrichment ($\delta^{13}C_t$) and a larger quantity of assimilated ^{13}C ($^{13}C_t$) were found in branch and leaf tissues of the branches subjected to higher transpiration rate and higher xylem sap CO_2 concentration ([CO_2]). A similar effect of transpiration rate on $\delta^{13}C_t$ and $^{13}C_t$ was observed for leaves as described in **Chapter 2**. The results for the branches were not surprising since the amount of label taken up by the branches was greater under high transpiration rate and high label (25.4 ± 2.4 mg ^{13}C) relative to the other VPD x label treatment combinations (up to 10.7 ± 1.7 mg ^{13}C). A fraction of the label taken up by the branches under high label and high VPD treatment also diffused to the atmosphere (37.3 ± 4.9%), potentially affecting the actual amount of label supplied to the tissues. The low $\delta^{13}C_t$ found in the control branches relative to the treatment branches confirmed that stomatal uptake of ^{13}C label that may have diffused from the bottles or from the

treatment branches was negligible, confirming that tissue enrichment in the treatment branches was solely due to the assimilation of xylem-transported ^{13}C label.

Besides its role in plant water supply, the transpiration stream is also considered as an important sink for internally-transported CO_2 derived from plant respiration below- (Grossiord *et al.,* 2012; Aubrey & Teskey, 2009; Bloemen *et al.*, 2013b) and aboveground (Teskey & McGuire, 2007) (**Chapter 1**). It has been suggested that a substantial fraction of root-respired CO_2 is transported upwards in the xylem where it can either be assimilated by stem, branch, and leaf tissues containing chlorophyll (Saveyn *et al.*, 2008a; McGuire *et al.*, 2009; Saveyn *et al.*, 2010) or diffuse into the atmosphere from stem and branch surfaces (McGuire *et al.*, 2007; Teskey & McGuire, 2007; Saveyn *et al.*, 2008b).

We observed that at higher transpiration, more $^{13}CO_2$ was transported in the branches, thereby increasing the amount of ^{13}C-labeled substrate available for assimilation in woody and leaf tissue. Assimilation occurs both in the xylem and inner bark of woody tissues (Pfanz *et al.*, 2002; Aschan & Pfanz, 2003). While McGuire *et al.* (2009) estimated that CO_2 assimilation in the xylem accounted for 42% of woody tissue photosynthesis; we found an average contribution of 35% in small branches. The highest $\delta^{13}C_t$ was observed in the inner bark of the lower branch sections, likely due to its proximity to the ^{13}C source. However, in contrast to previous observations (McGuire *et al.*, 2009), $\delta^{13}C_t$ of the xylem showed only small variation over the length of the branch. It is possible that our longer period of label application (10 h), compared to the 4.75 h of McGuire *et al.* (2009) induced higher enrichment at mid- and upper-branch sections. McGuire *et al.* (2009) found that most of a ^{13}C label applied to branches was assimilated in the bottom section of the branch xylem, while in our experiment we observed only a small variation in assimilation in the xylem along the branch. The concentration of the ^{13}C label provided at the lowest branch section was very high in our experiment, which suggests that the enzymes which fix the ^{13}C label might have been saturated by the substrate, according to Michaelis Menten kinetics. Therefore, not all the label could be assimilated in the lower branch, and the remaining portion would be transported upward and assimilated higher in the branch. Thus, the longer exposure time in our experiment would result in transfer of more label to the higher branch sections, and explain our

observation of similar enrichment of the xylem in all branch sections. Similar high enrichment of woody tissues more distal from the point of ^{13}C infusion was observed for the same species in a whole-tree experiment in the field (Bloemen *et al.*, 2013b) (**Chapter 4**). However, in whole trees a larger proportion of ^{13}C tracer diffused to the atmosphere (up to 94%, Bloemen *et al.*, 2013b) than in this study (up to 55%), likely due to the longer transport pathway from the point of infusion to these more distal tissues.

In the leaves, the effect of transpiration rate on tissue component enrichment was strongly determined by tissue type. In the petioles, higher $\delta^{13}C_t$ was observed compared to other tissues at both high and low transpiration rate and independent of label concentration. Stringer & Kimmerer (1993) found that 53.7% of a ^{14}C label applied to *P. deltoides* leaves via the xylem was assimilated in the petiole. Hibberd & Quick (2002) noted that photosynthetic cells in the petioles increased plant carbon gain, and related petiole photosynthesis to the possible existence of a C_4-like mechanism in C_3 plants. In our study, transpiration rate determined enrichment in veins and leaf mesophyll only in the HL treatment. At higher transpiration, a larger fraction of the ^{13}C label was fixed in leaf veins and mesophyll tissue. High levels of $^{13}C_t$ were found in branches subjected to the HL treatment under high VPD and in contrast to previous studies (Stringer & Kimmerer, 1993; McGuire *et al.*, 2009), more ^{13}C was assimilated in the leaf mesophyll (5.1 ± 0.6 mg) than in the petioles (1.6 ± 0.2 mg).

Xylem-transported CO_2 has generally been considered as an important potential carbon source only for cells that surround the xylem and phloem in petioles and veins (Stringer & Kimmerer, 1993; McGuire *et al.*, 2009). Our results show that at higher xylem sap [CO_2], internally transported CO_2 can improve carbon substrate availability for the leaf mesophyll as well. Because of their dense vein network and the occurrence of bundle sheath extensions and paraveinal mesophyll tissue, *P. deltoides* leaves are especially well adapted for efficient water transport (Russin & Evert, 1984). Thus, internally transported CO_2 can be delivered very effectively to every part of the leaf which may compensate for the lack of lateral CO_2 diffusion due to compartmentalization of the mesophyll in leaves with heterobaric anatomy (Pieruschka *et al.,* 2005; Leegood, 2008), which is the case for poplar leaves (McClendon, 1992).

Only a few isotope studies on detached leaves (Stringer & Kimmerer, 1993) and branches (McGuire *et al.*, 2009) have reported on the assimilation of internally-transported CO_2 relative to the assimilation of atmospheric CO_2. McGuire *et al.* (2009) estimated that internal CO_2 assimilation averaged 6% of atmospheric uptake in branches, while Stringer and Kimmerer (1993) estimated that in leaves, input of CO_2 via the transpiration stream could account for 2.2% of atmospheric uptake. We observed that both a higher transpiration rate and higher xylem sap [CO_2] increased the contribution of xylem-transported CO_2 to branch carbon gain. There are other factors, not considered in this study, which might increase the ratio of internal compared to atmospheric CO_2 assimilation (McGuire *et al.*, 2009). For example, the branches used in this experiment had a non-leaf mass to leaf mass ratio smaller than one, while a substantially greater non-leaf mass to leaf mass ratio can be expected for branches of other species or for full-grown trees. In addition, there are species with a higher stem chlorophyll content than *P. deltoides* (e.g., *Fraxinus excelsior* and *Quercus robur*, Pfanz *et al.,* 2002), which potentially assimilate more xylem-transported CO_2 than observed in this study. Our ^{13}C based estimates of internal CO_2 assimilation relative to atmospheric uptake do not account for the re-assimilation of locally respired CO_2, which is composed almost entirely of $^{12}CO_2$. Finally, in contrast to our labeling experiment, in the field the amount of dissolved respired CO_2 available for internal CO_2 assimilation will vary, depending on factors affecting respiration and transpiration rate. All these factors could potentially affect the importance of assimilation of internal CO_2 in woody tissue, however our results indicate that the overall amount of xylem-transported CO_2 that is assimilated is small compared to uptake of atmospheric CO_2.

Previous studies have described the potential benefits of internal CO_2 assimilation from a water-use perspective. While leaves open their stomata to assimilate CO_2, thus subjecting plants to the ambient drying power of the atmosphere, CO_2 for internal assimilation is supplied endogenously by respiration, thereby avoiding excessive water loss (Pfanz *et al.*, 2002; Aschan & Pfanz, 2003). Our results showed that at high transpiration rate, the assimilation of xylem-transported CO_2 increased in importance compared to low transpiration rate. Therefore, we suggest that the assimilation of xylem-transported CO_2 in woody and leaf tissues is strongly dependent on transpiration,

which is directly related to stomatal conductance. Beyond a certain threshold, stomatal conductance will exponentially decrease with increasing VPD (Massmann & Kaufmann, 1991; McCaughey & Iacobelli, 1994; Monteith, 1995; Oren *et al.*, 1999) reducing the assimilation of atmospheric CO_2 (Oren *et al.*, 1999). At the same time, transpiration will continue to increase up to some plateau level as VPD increases to a certain level (Jarvis, 1980; Pataki *et al.*, 2000). Therefore, as VPD increases, assimilation of atmospheric CO_2 will reduce, but xylem-transport of respired CO_2 will maximize, suggesting that under these conditions the contribution of internal fixation to the overall carbon budget might become more important. Moreover, during periods of high VPD or low soil water availability, xylem CO_2 assimilation might also have a role in maintaining stem and branch hydraulics due to light-induced repair of embolized xylem vessels (Schmitz *et al.*, 2012) (**Box 1.2**), thereby reducing moisture stress and stomatal closure.

Our results show that assimilation of xylem-transported CO_2 is affected by both the rate of transpiration and xylem [CO_2], which is dependent on respiration. Therefore, the contribution and importance of internal CO_2 assimilation to overall plant carbon gain is likely to change with changes in the factors that control rates of transpiration, respiration, and photosynthesis.

- Chapter 4 -

Xylem transport of belowground respired CO_2 affects aboveground carbon assimilation and CO_2 efflux

After: Bloemen J., McGuire M.A., Aubrey D.P., Teskey R.O., and Steppe K. (2013) Transport of root-respired CO_2 via the transpiration stream affects aboveground carbon assimilation and CO_2 efflux in trees. *New Phytologist* **197**: 555-565.

Abstract

Upward transport of CO_2 via the transpiration stream from below- to aboveground tissues occurs in tree stems. Despite potentially important implications to our understanding of plant physiology, the fate of internally transported CO_2 derived from autotrophic respiratory processes remains unclear. We infused a $^{13}CO_2$-labeled aqueous solution into the base of 7-y-old field-grown eastern cottonwood (*Populus deltoides* Bartr. ex Marsh) trees to investigate the effect of xylem-transported CO_2 derived from the root system on aboveground carbon assimilation and CO_2 efflux. The ^{13}C label was transported internally and detected throughout the tree. Up to 17% of the infused label was assimilated, while the remainder diffused to the atmosphere via stem and branch efflux. The largest amount of assimilated ^{13}C was found in branch woody tissues, while only a small quantity was assimilated in the foliage. Petioles were more highly enriched in ^{13}C than other leaf tissues. Our results confirm a recycling pathway for respired CO_2 and indicate that internal transport of CO_2 from the root system may confound the interpretation of efflux-based estimates of woody tissue respiration and patterns of carbohydrate allocation.

4.1 Introduction

The exchange of carbon between terrestrial ecosystems and the atmosphere has been the subject of many studies (e.g. Baldocchi *et al*., 2005; Luyssaert *et al*., 2007; Luyssaert et *al*., 2010). Carbon dioxide (CO_2) is assimilated in ecosystems by photosynthesis, expressed as gross primary productivity, and is returned to the atmosphere by a variety of metabolic processes both above- and belowground, which comprise total ecosystem respiration (Trumbore, 2006). Belowground, the respiratory processes that contribute to soil CO_2 efflux (E_{soil}) are functionally divided into autotrophic (CO_2 released by roots and associated rhizosphere organisms) and heterotrophic (CO_2 released during decomposition of non-living organic matter) components (Hanson *et al.*, 2000). Different techniques are applied to quantify E_{soil}, but all conventional methodology is based on the assumption that root-respired CO_2 diffuses through the soil and upward to the atmosphere (Kuzyakov, 2006).

A number of studies have investigated the relationship between tree canopy photosynthesis and belowground autotrophic respiration, which are connected through the transport of photosynthates from the leaves to the roots via the phloem (e.g. Högberg *et al.,* 2001; Subke *et al*., 2009; Kuzyakov & Gavrichkova, 2010). In contrast, few studies have focused on the reciprocal relationship: the coupling of autotrophic respiration and carbon assimilation resulting from the internal transport of dissolved CO_2 from belowground. Ford *et al*. (2007) demonstrated in *Pinus* seedlings that small amounts of soil dissolved inorganic carbon (DIC) can be taken up by roots, transported upward in the transpiration stream, and assimilated by foliage (**Chapter 1**). Aubrey & Teskey (2009) observed that a large amount of root-respired CO_2 was transported upward in the transpiration stream to aboveground tissues of *Populus* trees. Therefore, the transport of root-respired CO_2 in the transpiration stream has potentially important implications for measuring belowground respiration and assessing the role of transpiration in forest carbon cycling (Hanson & Gunderson, 2009).

The concentration of CO_2 in the xylem is usually many times greater than that of the atmosphere (Teskey *et al*., 2008) (**Chapter 1**). This internal CO_2 can be transported upward through the plant via the transpiration stream (Teskey & McGuire, 2002; McGuire & Teskey, 2004) where it is released radially into the atmosphere (Teskey &

McGuire, 2005; Steppe *et al.*, 2007) or assimilated within the plant (**Chapter 1**). Small-scale experiments that introduced carbon isotope labeled solutions into detached leaves or branches revealed that CO_2 transported in the transpiration stream can be assimilated in leaf veins, petioles (Stringer & Kimmerer, 1993) (**Chapter 2**), and woody branch tissue (McGuire *et al.*, 2009) (**Chapter 3**). Consequently, xylem-transported root-respired carbon in trees could provide substrate for carbon assimilation which has previously been overlooked. In addition, when large quantities of root-respired CO_2 are transported internally and diffuse into the atmosphere remote from the site of production, efflux-based approaches fail to accurately estimate respiration of both roots and aboveground woody tissues (**Chapter 1**).

Few studies have examined the fate of CO_2 transported internally from belowground. Ford *et al.* (2007) and Ubierna *et al.* (2009) applied ^{13}C-labeled solution to soil around seedlings in pots and around large field-grown trees, respectively, and they found that labeled carbon contributed only 0.8 % to whole seedling carbon gain (Ford *et al.*, 2007) and 1 to 3% to stem CO_2 efflux (Ubierna *et al.*, 2009). However, these studies did not address the transport and fate of CO_2 derived internally from root respiration. Our objective was to label the xylem sap at the base of large trees *in situ* with $^{13}CO_2$ to determine the fate of internally transported carbon. We hypothesized that as the label moved upward in the transpiration stream, a portion would be assimilated by chlorophyll-containing woody and leaf tissues and a portion would diffuse into the atmosphere from stems and branches.

4.2 Materials and methods

4.2.1 Overview

To investigate the role of xylem-transported root-respired CO_2 as a potential carbon substrate for photosynthesis, we infused ^{13}C labeled solution into the xylem at the base of four intact eastern cottonwood (*Populus deltoides* Bartr. ex Marsh) trees and subsequently determined its presence in various tissues throughout the trees. The ^{13}C label served as a proxy for dissolved CO_2 entering the stem from the roots. The experimental trees were part of a 7-y-old plantation in Whitehall Forest, a research

facility of the University of Georgia near Athens, Georgia, USA. Details of the experimental plant material are described in Table 4.1.

Table 4.1 Diameter at breast height (DBH, cm), tree height (m), total amount of $^{13}CO_2$-labeled solution infused (l), amount of ^{13}C infused (g) and cumulative sap flow (l) during the infusion period of four *P. deltoides* trees. Trees 1 and 2 were infused with low label solution; trees 3 and 4 were infused with high label solution.

Tree	DBH	Height	Label solution infused	^{13}C infused	Cumulative sap flow
1	12.7	9.8	41.0	0.71	152.6
2	11.9	7.2	40.0	0.70	157.9
3	13.9	11.1	45.0	6.76	189.5
4	9.7	8.6	45.0	6.76	139.1

4.2.2 Baseline tissue sampling for isotopic analysis

Prior to infusion, on 23 June 2010, samples of woody tissue and leaves were taken from all experimental trees to determine the natural abundance carbon isotopic composition ($\delta^{13}C$) to which $\delta^{13}C$ of labeled tissues would be compared. For this sampling, a mid-canopy branch of each tree was detached and a stem core was taken with an increment borer at approximately the same canopy position. Samples were immediately frozen in liquid nitrogen and then moved to a freezer at -9°C for storage before processing for carbon isotope analysis.

4.2.3 ^{13}C label infusion

$^{13}CO_2$-labeled solutions both at low $^{13}CO_2$ concentrations and high $^{13}CO_2$ concentrations were prepared as described in **Chapter 3.** For this experiment, 20 l containers were filled with solution, of which 1 to 3 l was displaced with ^{13}C-labeled CO_2 (referred to as $^{13}CO_2$ in the text) gas from a cylinder of compressed 100% CO_2 at 99 atom% (A)^{13}C (ICON Services, Summit, NJ, USA) depending on the desired $^{13}CO_2$ concentration. Mean pH, gaseous CO_2 concentration ($[CO_2]$), and dissolved CO_2 concentration ($[^{13}CO_2^*]$) were 5.30 ± 0.05, 3.77 ± 0.20%, and 1.4 ± 0.1 mM for the solutions at low $^{13}CO_2$ concentration (low label treatment, LL) and 6.90 ± 0.02, 6.97 ± 0.05%, and 12.0 ± 0.5 mM for the solutions at high $^{13}CO_2$ concentration (high label treatment, HL), respectively. The pH

and [CO_2] of the enriched solutions were within the range measured previously in *P. deltoides* (Aubrey *et al.,* 2011).

The trees were infused with the labeled solutions in the field. Preliminary experiments showed that infusing solution directly into a lateral root resulted in limited solution uptake, since it was only a small part of the root system, so infusion was performed at the base of the stem instead. A 19 mm diameter hole was drilled 4.5 cm deep into the xylem on two sides of each tree approximately 10 and 15 cm above ground level. A threaded brass hose-barb fitting was inserted 1.5 cm into each hole. The holes were drilled deeper than needed for installation of the fittings to increase the contact surface area of the solution with the sapwood. Both fittings were connected to the 20 l reservoir of labeled solution with 12.8 mm inner-diameter CO_2-impermeable tubing (Bev-a-Line IV, Thermoplastic Processes, Georgetown, Delaware, USA). The solution reservoirs were placed 1.5 m above the holes to provide a small pressure head. Two trees were labeled simultaneously for two days starting at noon (trees 1 and 2 on 25-27 June 2010; trees 3 and 4 on 3-5 July 2010). Trees 1 and 2 were infused with the LL solution and trees 3 and 4 were infused with the HL solution. Based on prior measurements of sap flow, we estimated that it would take *c*. two days for the solution to reach the top of the canopy. Therefore, we waited two additional days after infusion ceased before harvesting the trees for tissue sampling to allow adequate time for assimilation of the ^{13}C label by woody and leaf tissue.

4.2.4 Environmental conditions

Weather during infusion and measurement periods was hot and mostly sunny without precipitation. Mean maximum air temperature and minimum relative humidity (RH) were 30.7°C and 42% and 35.4°C and 45% during the June and July measurement periods, respectively.

4.2.5 Biomass determination and tissue sampling for isotopic analysis

Early on the third morning after the infusion ended, the trees were felled and tissues of the tree organs (stem, branch, and leaf) were sampled for carbon isotope analysis according to Fig. 4.1. Each tree was divided vertically into four strata: one below the canopy and three of equal length within the canopy (lower-, mid-, and upper-canopy).

From each stratum, three 20 cm segments of the main stem were collected, one each from the bottom, middle, and top portion of the stratum (at 10, 50, and 90% of the total stratum length, respectively). Two branches from each canopy stratum were divided into three equal-length sections (A, B, and C, Fig. 4.1). A 20 cm segment of woody tissue and all leaf tissue were collected from each branch section. All samples were placed in plastic bags and immediately transferred to an ultralow freezer at -25°C to stop metabolic activity. Samples were later moved to a walk-in freezer and stored at -9°C. All remaining tissue not sampled for isotopic analysis was collected, separated according to Fig. 4.1, and dried for biomass determination. Length and diameter of every stem and branch was measured and surface area was calculated.

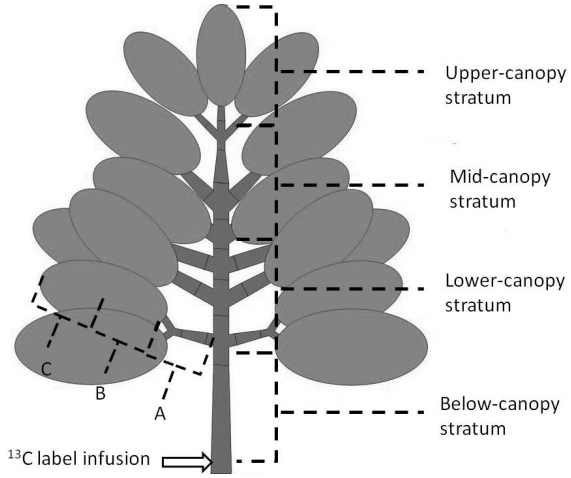

Fig. 4.1 Scheme for biomass harvest and tissue sampling for isotopic analysis of four *P. deltoides* trees infused with $^{13}CO_2$-labeled solutions. Trees were subdivided into four strata: one below-canopy stratum and three canopy strata of equal length (lower-, mid-, and upper-canopy). Two branches from each canopy stratum were sampled. Branches were divided into three sections (A, B, and C) of equal length according to distance from the stem. The arrow indicates the location of infusion of the labeled solution.

4.2.6 Processing of tissue samples

Each tissue sample was thawed individually before subsamples were taken for carbon isotope analysis. Woody tissue was subsampled as follows: for stem sections where diameter was >5 cm, a radial xylem core was taken with an increment borer at the middle of each section (3 per canopy stratum) for analysis. At the same position on the section, a 2 cm ring of outer (non-living) bark was removed. The live inner bark of this

entire ring was then sampled for analysis. For stem sections where diameter was <5 cm, a 2-to-10 cm long (depending on diameter) subsample was taken from the middle of the section. Outer bark was removed and the entire subsample was separated into inner bark and xylem for analysis. Branch samples (2 branches per canopy stratum; 3 sections per branch) were subsampled in the same manner as the stems <5 cm diameter. Leaves were sampled as follows: a subsample of 20 mature leaves was removed from each sample branch section and dissected into petiole, primary (central) vein, secondary veins, and remaining leaf mesophyll. A second subsample of 10 mature leaves was taken and processed as whole leaves. Subsamples of tissues harvested prior to labeling were processed in a similar manner to provide baseline carbon isotope values. All subsamples were dried to constant weight in an oven at 65°C and then ground to powder in a ball mill (8000-D Mixer Mill, SPEX SamplePrep, Metuchen, New Jersey, USA) for ^{13}C analysis.

4.2.7 Isotopic analysis of tissue samples

Ground tissue samples were weighed to µg precision in tin capsules and analyzed by Element Analyzer (model 1500 CHN, Carlo-Erba, Italy) coupled to an Isotope Ratio Mass Spectrometry (Delta V, Thermo-Finnigan, Bremen, Germany) (EA-IRMS) at the Stable Isotope and Soil Biology Laboratory (SISBL), Odum School of Ecology, University of Georgia, Athens, Georgia, USA. Bovine with a $\delta^{13}C$ value of -21.24 ‰ (certified by the National Institute of Standards and Technology, USA) was used as a laboratory reference and all $\delta^{13}C$ are expressed relative to VPDB. Enrichment of the labeled branch tissues ($\delta^{13}C_t$, ‰) and A of the labeled tissues (A_t, %) was calculated as described in **Chapter 2 (Equations 2.2 and 2.3)**.

4.2.8 Scaling isotope measuremens of tissue component samples to organ and whole tree levels

Biomass measurements of the subsamples were used to determine the mass proportions of the woody (inner bark and xylem) and leaf (petiole, primary vein, secondary veins, and mesophyll) tissue components for each organ (stem, branch, leaf) at every canopy stratum and branch section of each tree. These proportions were used to calculate the total biomass of the woody and leaf organs by tissue component for every canopy

stratum and branch section combination (Fig. 4.1) for each tree. Based on A_t, the amount of ^{13}C assimilated in each tissue component ($^{13}C_t$, mg) was calculated as:

$$^{13}C_t = A_t \; DM \; C \quad (4.1)$$

where DM is the dry mass of the tissue component per stratum and section (mg) and C is the carbon content of the tissue component (%).

To determine the amount of ^{13}C assimilated by the three organs (stem, branch, leaf) and the whole tree, the values of $^{13}C_t$ for the individual tissue components of each stratum and section were summed to organ and tree level. The sum of the amount of ^{13}C assimilated by the whole tree ($^{13}C_{assim}$, mg) and the amount of ^{13}C lost to the atmosphere ($^{13}C_{efflux}$, mg) were assumed to be equal to the amount of ^{13}C taken up by the tree ($^{13}C_{uptake}$, mg), based on the following mass balance equation:

$$^{13}C_{uptake} = {}^{13}C_{assim} + {}^{13}C_{efflux} \quad (4.2)$$

Thus, for each tree we estimated $^{13}C_{efflux}$ by subtracting $^{13}C_{assim}$ from $^{13}C_{uptake}$. $^{13}C_{uptake}$ was calculated by multiplying the dissolved $^{13}CO_2$ concentration of the labeled solution by the amount of solution taken up by the tree as described in McGuire *et al.* (2009).

4.2.9 Measurements of sap flow

Sap flow was determined by scaling sap flux density measured with homemade thermal dissipation probes (TDP) (Granier, 1985) with sapwood area. Two TDP sensors were installed in the stem on opposite sides of each tree at a height of 0.45 m. Thermocouple depth was 10 mm and vertical separation of the sensor needles was 50 mm. Zero sap flow conditions were assumed between 03:00 and 05:00 h. Sap flow calibration parameters developed for *P. deltoides* at this site (Sun *et al.,* 2011) were applied to the sap flow measurements as recommended by Steppe *et al.* (2010). Sap flow was recorded with a datalogger (23X, Campbell Scientific, Logan, Utah, USA) at 5 min intervals.

4.2.10 Gas sampling for isotopic analysis

Gas samples were collected from a cylindrical cuvette installed around a section of the stem and a section of a branch of each tree to confirm that ^{13}C label diffused from woody tissues after uptake of the ^{13}C enriched solution. These cuvettes were originally

constructed to measure stem and branch CO_2 efflux, but efflux data will not be presented in this report. Stem cuvettes were installed just below the base of the canopy at an average height of 1.05 m. Branch cuvettes were installed close to the stem in the lower third of the canopy at an average height of 1.70 m. Both stem and branch cuvettes were 15 cm long, constructed of 0.18 mm thick Mylar film (Ridout Plastics, San Diego, California, USA) and sealed to the stem with adhesive closed-cell foam gasket material and non-caustic silicone sealer (RTV162, MG Chemicals, Surrey, British Columbia, Canada). Compressed air at atmospheric composition was supplied from a cylinder to each cuvette at 500 ml min^{-1} with a mass flow controller (FMA5514, Omega Engineering Inc., Kingston, Ontario, Canada). For gas sampling, a needle attached to a 35 ml syringe was inserted through the foam gasket of the cuvette and a sample was withdrawn and injected directly into a 10 ml evacuated vial (Vacutainer, BD, New Jersey, USA) that had been pre-filled with 1 ml distilled deionized water, to limit the diffusion of $^{13}CO_2$ through the septa seal when stored upside down. The septa of the vials were sealed with parafilm and samples were stored upside down to minimize gas diffusion through the septa seal. Starting 24 h after the beginning of label infusion, gas samples were collected every 2 h over a 24 h period and an additional sample was taken at 72 h. This timing was selected to detect changes in the enrichment of the air inside the cuvettes that might be related to the timing of label infusion and/or sap flow rate. Baseline samples of the air inside the cuvettes were taken before the start of infusion to determine natural abundance isotope concentrations.

4.2.11 Isotopic analysis of gas samples

Gas samples were analyzed at the Stable Isotope and Soil Biology Laboratory (SISBL). The enrichment of the air inside the cuvettes due to ^{13}C label diffusion from the stem and branch tissues ($\delta^{13}C_a$, ‰) was calculated by subtracting the $\delta^{13}C$ value of the baseline sample before label infusion ($\delta^{13}C_b$, ‰) from the $\delta^{13}C$ value of the samples during label infusion ($\delta^{13}C_s$, ‰), as performed for calculating $\delta^{13}C_t$ based on **Equation 2.2**.

4.2.12 Data processing and statistical analysis

$\delta^{13}C_t$ of each organ (stem, branch, and leaf) and $^{13}C_t$ were analyzed using multi-factorial analysis of variance (ANOVA). At the stem level, ^{13}C label concentration (n=2), canopy

stratum (*n*=4), and tissue component (xylem and inner bark) were treated as fixed factors, and individual tree (*n*=4) was treated as a random factor. A similar ANOVA model was used at the branch and leaf level with a few differences. At the branch level, the number of canopy strata was reduced by 1 (*n*=3, eliminating the below-canopy stratum), an additional tissue component (leaf) was included, and branch section (*n*=3) was included as a fixed factor. At the leaf level, tissue components consisted only of leaf parts (petiole, primary vein, secondary veins, and mesophyll). A similar ANOVA model was used to compare enrichment of different organs (stem, branch, and leaf). In this case, we confined our measurements to those taken within the canopy and calculated the weighted average of enrichment across tissue components as a function of biomass per canopy stratum. Treatment means were compared using Fisher's Least Significant Difference test. $\delta^{13}C_a$ was analyzed using a repeated measures analysis of variance (ANOVA) with ^{13}C label concentration (*n*=2), tissue (*n*=2), and time (*n*=14) treated as fixed factors and individual tree (*n*=4) treated as the random subject factor. Akaike Information Criterion corrected for small sample sizes (AIC_C) was used to determine the covariance structure that best estimated the correlation among individual trees over time. All analyses were performed using the mixed model procedure (PROC MIXED) of SAS (Version 9.1.3, SAS Inc., Cary, NC, USA) with α=0.05.

4.3 Results

4.3.1 ^{13}C label uptake

Each of the four trees took up between 40 and 45 l of $^{13}CO_2$-labeled solution during the two-day infusion period, which accounted for 23.8 to 32.4% of total sap flow. From visual observation it was clear that most of the solution was taken up during periods of high sap flow during the day while little was taken up at night. Soil moisture was high during the experiment, precluding downward flow into the roots at night. Although solution uptake for all trees was similar, the average amount of dissolved ^{13}C label taken up was nearly 10-fold greater under the high label (HL) treatment (6.76 ± 0.00 g) compared with the low label (LL) treatment (0.71 ± 0.01 g) (Table 4.1).

4.3.2 Carbon isotope composition of woody tissue and leaves

The baseline $\delta^{13}C$ of tissues sampled before labeling ranged from -27.74‰ to -29.71‰. Tissue enrichment results ($\delta^{13}C_t$) showed that the label was transported from the base of the stem and assimilated in all tissues of the tree organs. The $\delta^{13}C_t$ of the organs (calculated by weighted average of the tissue components) was influenced by label concentration, canopy stratum, and organ; however, these factors were not independent of each other (i.e., label concentration × organ interaction, $P<0.0001$ and organ × canopy stratum interaction, $P<0.0001$). The $\delta^{13}C_t$ of the stem and leaves was higher under the HL treatment than under the LL treatment at all canopy strata. In the branches, a significant difference in $\delta^{13}C_t$ between label treatments was observed only at mid- and upper-canopy strata. Under the high-label treatment, $\delta^{13}C_t$ of the branches was higher than that of the stem and leaves at all canopy strata (Fig. 4.2). Mean $\delta^{13}C_t$ of branches was higher at mid-canopy than at upper- and lower-canopy strata, whereas stem and leaf $\delta^{13}C_t$ was similar among canopy strata under the HL treatment (Fig. 4.2).

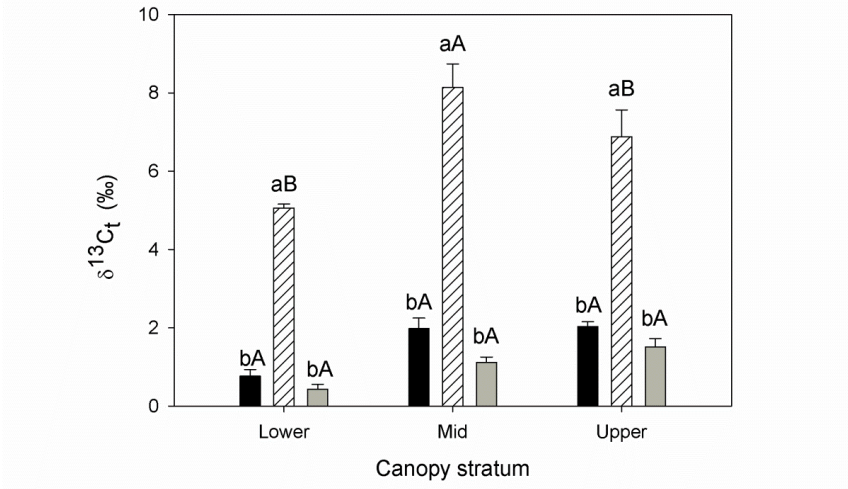

Fig. 4.2 Mean ^{13}C enrichment ($\delta^{13}C_t$, ‰) of stem (black), branch (hatched), and leaf (grey) organs of two *Populus deltoides* trees infused with high label (HL) $^{13}CO_2$ solution showing interaction between organ and canopy stratum. Tissue components of the organs were sampled according to the scheme depicted in Fig. 4.1. $\delta^{13}C_t$ was averaged per organ and canopy stratum. Different lower-case letters indicate significant differences (Fisher's least significant difference test, $P<0.05$) in $\delta^{13}C_t$ among organs within a canopy stratum. Different upper-case letters indicate significant differences in $\delta^{13}C_t$ of the same organ among different canopy strata. Bars indicate standard error of the mean.

In the stems, $\delta^{13}C_t$ was influenced by label concentration, tissue component, and canopy stratum. For example, $\delta^{13}C_t$ of the inner bark was higher under the HL treatment (3.86 ± 0.57‰) than under the LL treatment (0.58 ± 0.21‰) at the upper- and mid-canopy strata, but cortex $\delta^{13}C_t$ was not influenced by label treatment at the lower- or below-canopy strata. Under the HL treatment, $\delta^{13}C_t$ of the inner bark was higher than that of the xylem at the upper- and mid-canopy strata, but not at the lower- or below-canopy strata (i.e., label concentration × tissue component × canopy stratum interaction, P=0.0108) (Fig. 4.3). The $\delta^{13}C_t$ of both the inner bark and xylem under the HL treatment was higher at the upper- and mid-canopy strata than at the lower- and below-canopy strata. (Fig. 4.3).

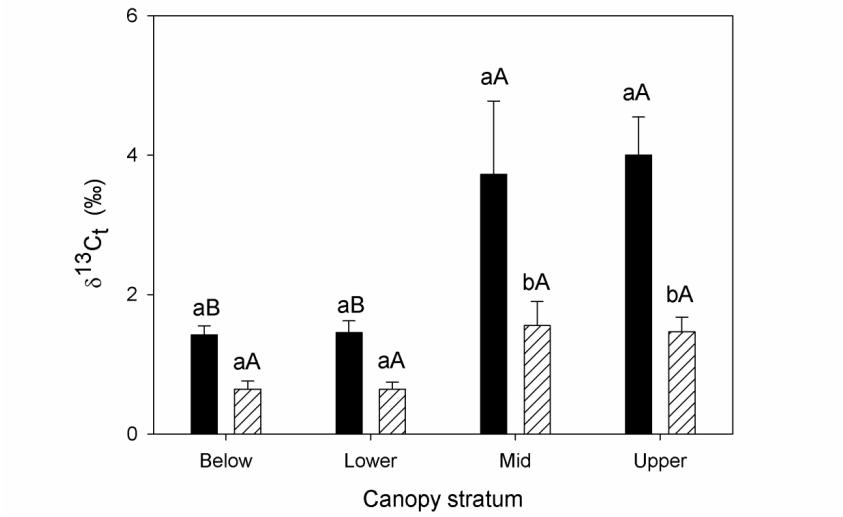

Fig. 4.3 Mean ^{13}C enrichment ($\delta^{13}C_t$, ‰) of inner bark (black) and xylem (hatched) of the stem at four canopy strata of two *Populus deltoides* trees infused with high label (HL) $^{13}CO_2$ solution showing interaction between tissue component and canopy stratum. Tissue components of the stem were sampled according to the scheme depicted in Fig. 4.1. $\delta^{13}C_t$ was averaged for the inner bark and xylem per canopy stratum. Different lower-case letters indicate significant differences (Fisher's least significant difference test, P<0.05) in $\delta^{13}C_t$ between inner bark and xylem within a canopy stratum. Different upper-case letters indicate significant differences in $\delta^{13}C_t$ of the same tissue component among different canopy strata. Bars indicate standard error of the mean.

Overall, in the branches, $\delta^{13}C_t$ was highest in the mid canopy stratum, intermediate in the upper canopy stratum and lowest in the lower canopy stratum (P=0.0013), and was also influenced by label concentration and tissue component; However, the effects of label concentration and tissue component were not independent of each other (i.e., label

concentration × tissue component interaction, P<0.0001). The $\delta^{13}C_t$ of the inner bark was higher under the HL treatment than under the LL treatment. It also differed among the branch tissue components (xylem, inner bark, and leaves) under the HL treatment but not under the LL treatment. Mean $\delta^{13}C_t$ across all canopy strata was highest in the inner bark (10.81 ± 1.13‰), intermediate in the xylem (5.27 ± 0.55‰), and lowest in the leaves (1.04 ± 0.12‰) under the HL treatment.

Mean $\delta^{13}C_t$ of the leaves was higher under the HL treatment than under the LL treatment at the lower-canopy stratum (1.57 ± 0.39‰ vs. -0.67 ± 0.12‰) and at the mid-canopy stratum (2.16 ± 0.34‰ vs. 0.53 ± 0.09‰) (i.e., label concentration × canopy stratum interaction, P=0.0007). Under the HL treatment, petioles were significantly more enriched than the other leaf tissue components regardless of canopy stratum or branch section. However, under the HL treatment, $\delta^{13}C_t$ of the petioles decreased with increasing distance from the stem (i.e., label concentration × tissue component × branch section interaction, P=0.0008) (Fig. 4.4).

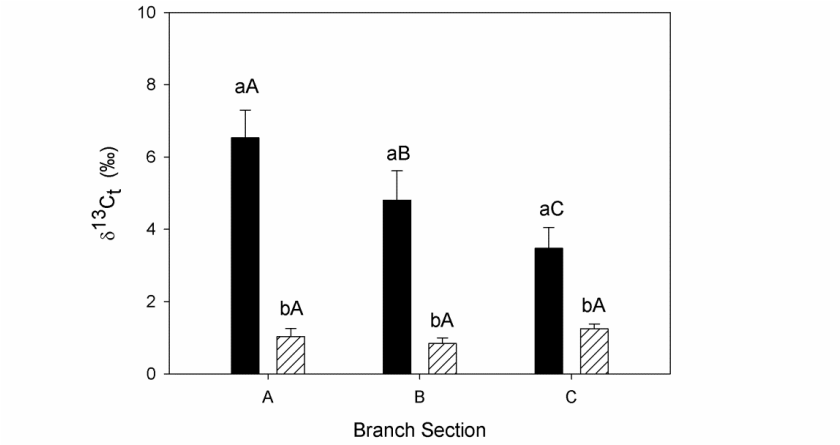

Fig. 4.4 Mean ^{13}C enrichment ($\delta^{13}C_t$, ‰) of petiole (black) and other tissue components (combined primary vein, secondary veins, and mesophyll) (hatched) of the leaves of three equal-length branch sections in the canopy of two *P. deltoides* trees infused with high label (HL) $^{13}CO_2$ solution showing interaction between tissue component and branch section. Tissue components of the leaves were sampled according to the scheme depicted in Fig. 4.1. $\delta^{13}C_t$ was averaged for the petioles and other leaf tissue components per branch section. Different lower-case letters indicate significant differences in $\delta^{13}C_t$ (Fisher's least significant difference test, P<0.05) between petioles and other leaf tissue components within a branch section. Different upper-case letters indicate significant differences in $\delta^{13}C_t$ of either petioles or other leaf tissue components among different branch sections. Bars indicate standard error of the mean.

4.3.3 Amount of ^{13}C assimilated

Generally, the total amount of ^{13}C assimilated ($^{13}C_t$) was higher under the HL treatment than under the LL treatment (Table 4.2), but it also depended on canopy stratum, and organ; however, these individual effects were not independent of each other (i.e., label concentration × organ interaction, P=0.0009 and organ × canopy stratum interaction, P=0.0002). The highest $^{13}C_t$ was observed in the branches compared with stem and leaves under both label treatments (Table 4.2). Mean $^{13}C_t$ of the branches was higher at the lower-canopy stratum than at the mid- and upper-canopy strata (P<0.0001) under the HL treatment.

Within the stem, $^{13}C_t$ was solely dependent on tissue component (P=0.014). Averaged across canopy strata and label treatments, $^{13}C_t$ of the xylem was higher than $^{13}C_t$ of the inner bark (Table 4.2).

Within the branches, $^{13}C_t$ of inner bark and xylem were higher under the HL treatment than the LL treatment, but only in the lower- and mid-canopy strata. Averaged across canopy strata and branch section, $^{13}C_t$ was higher in the xylem than in the inner bark under both label treatments (Table 4.2). Under the HL treatment, $^{13}C_t$ of the xylem decreased with increasing distance from the stem. However, these individual effects were not independent of each other, i.e., $^{13}C_t$ of xylem and inner bark varied with label concentration, tissue component, canopy stratum, and branch section (canopy stratum × label concentration interaction, P<0.0001, canopy stratum × tissue component interaction, P=0.0004, and branch section × tissue component interaction, P=0.0003).

In the leaves, $^{13}C_t$ was affected by label concentration, and varied among tissues and branch sections. Averaged across canopy strata and branch sections, $^{13}C_t$ of the petioles was higher under the HL treatment than under the LL treatment (tissue component × label concentration interaction, P=0.0274) (Table 4.2). Under the HL treatment, $^{13}C_t$ of the petioles was higher than that of the other leaf tissue components at the more distal branch sections B and C, but not at the proximal branch section A, resulting in a branch section × tissue component interaction (P=0.0002).

Table 4.2 Mean (SE) total biomass of tissue components (kg), amount of ^{13}C fixed per tissue ($^{13}C_t$, mg), and amount of ^{13}C assimilated relative to ^{13}C uptake ($^{13}C_t$ /$^{13}C_{uptake}$, %) of *Populus deltoides* trees infused with low label (LL, two trees) and high label (HL, two trees) $^{13}CO_2$ solutions. All data have been scaled to the whole tree level. Standard errors displayed as (0.00) were not zero, but have been truncated due to rounding.

	Stem		Branch		Leaf				Total
	Xylem	Inner bark	Xylem	Inner bark	Petiole	Prim. vein	Sec. vein	Mesophyl	
Low label treatment									
Total biomass (kg)	15.37 (1.73)	2.56 (0.34)	8.54 (3.37)	2.75 (1.19)	0.76 (0.16)	0.25 (0.05)	0.18 (0.01)	5.87 (1.29)	36.28 (2.10)
$^{13}C_t$ (mg)	18.00 (0.01)	4.20 (0.00)	62.00 (0.00)	21.00 (0.00)	8.40 (0.00)	0.24 (0.00)	0.35 (0.00)	10.00 (0.00)	124.19 (0.01)
$^{13}C_t/^{13}C$ uptake (%)	2.52 (0.19)	0.59 (0.04)	8.69 (0.01)	2.94 (0.06)	1.18 (0.01)	0.03 (0.01)	0.05 (0.01)	1.40 (0.06)	17.40 (0.10)
High label treatment									
	Stem		Branch		Leaf				Total
	Xylem	Inner bark	Xylem	Inner bark	Petiole	Prim. vein	Sec. vein	Mesophyl	
Total biomass (kg)	15.34 (6.42)	2.56 (0.85)	7.82 (2.88)	2.48 (0.86)	0.70 (0.27)	0.27 (0.11)	0.16 (0.07)	5.83 (2.05) (1.29)	35.16 (3.72)
$^{13}C_t$ (mg)	64.00 (0.02)	24.00 (0.00)	140.00 (0.01)	120.00 (0.02)	15.00 (0.00)	1.20 (0.04)	0.61 (0.00)	14.00 (0.00)	378.81 (0.02)
$^{13}C_t/^{13}C$ uptake (%)	0.94 (0.04)	0.36 (0.01)	2.10 (0.01)	1.72 (0.03)	0.22 (0.00)	0.01 (0.00)	0.05 (0.00)	0.20 (0.01)	17.40 (0.10)

4.3.4 Carbon isotope composition of air inside stem and branch cuvette

Isotopic signatures of the air inside the stem and branch cuvette confirmed that the ^{13}C label was transported via the transpiration stream and diffused to the atmosphere from aboveground woody tissue. Enrichment of the air inside the cuvettes ($\delta^{13}C_a$) was influenced by label concentration and organ (stem and branch) and changed temporally; however, these individual effects were not independent of each other (i.e., organ × time × label concentration interaction, P=0.0003). Significant temporal variation in $\delta^{13}C_a$ was observed in the stem, but not in the branch under both LL (Fig. 4.5A) and HL (Fig. 4.5B) treatments. The highest $\delta^{13}C_a$ of the stem was observed at 36 h and 24 h from the start of label infusion under LL and HL treatments, respectively. At 72 h from the start of label infusion, $\delta^{13}C_a$ of the branch under both label treatments and $\delta^{13}C_a$ of the stem under the low-label treatment returned to baseline, whereas $\delta^{13}C_a$ of the stem under the HL treatment remained high relative to the baseline. $\delta^{13}C_a$ of the stem, averaged across the observation period (45.40 ± 6.75‰) was significantly higher than that of the branch (3.75 ± 1.92‰) under the low-label treatment. Similarly, $\delta^{13}C_a$ of the stem, averaged across the observation period (41.96 ± 3.75‰) was significantly higher than that of the branch (3.75 ± 1.92‰) under the HL treatment.

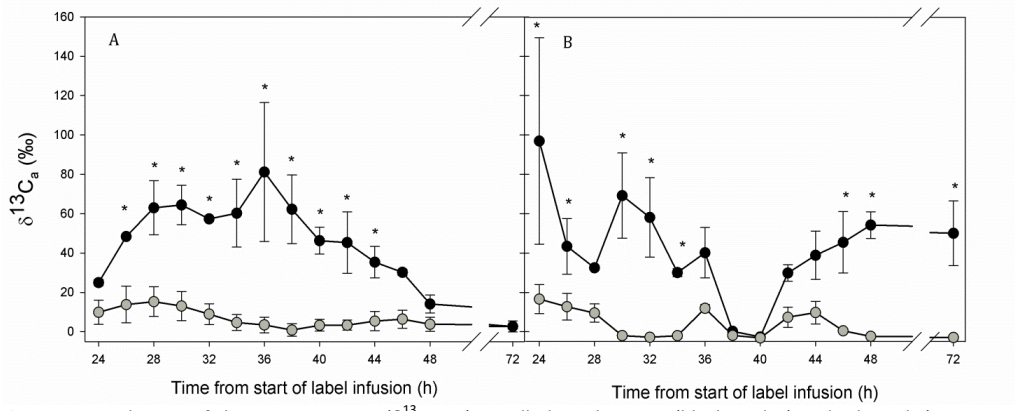

Fig. 4.5 Enrichment of the air in cuvettes ($\delta^{13}C_a$, ‰) installed on the stem (black circles) and a branch (grey circles) of *P. deltoides* trees infused with low label (A, two trees) and high label (B, two trees) $^{13}CO_2$ solutions. Gas samples were taken hourly from 24 h to 48 h and at 72 h after the start of label infusion. Asterisks indicate significant (P<0.05) differences in $\delta^{13}C_a$ between the stem and branch at each observation. Bars indicate standard error of the mean.

4.3.5 Assimilation and efflux of ^{13}C relative to the amount taken up

On average, 17.40 ± 0.10% and 5.60 ± 0.02% of the infused ^{13}C label was assimilated in aboveground tree organs under LL and HL treatments, respectively (Fig. 4.6). ^{13}C assimilation occurred mainly in the branches and, to a lesser extent, in the stem and leaves (Table 4.2, Fig. 4.6). Most of the ^{13}C label was not assimilated and was therefore assumed to have diffused to the atmosphere both via the stem and the branches (82.60 ± 0.10% and 94.40 ± 0.02% under LL and HL treatments, respectively).

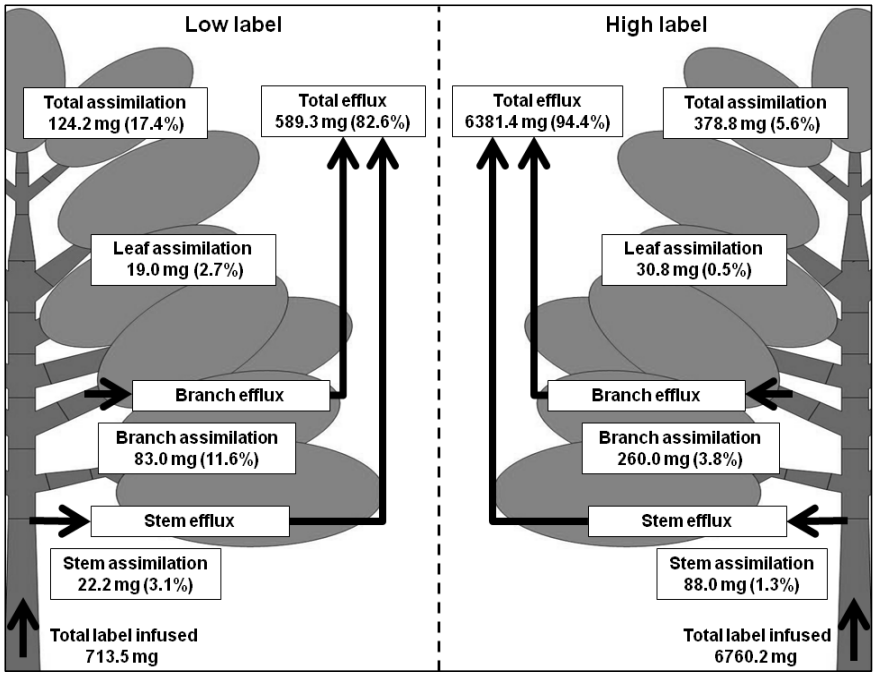

Fig. 4.6 Overview of the fate of a ^{13}C label infused at the base of *Populus deltoides* trees calculated by mass balance. Values are mean assimilation or efflux of the label (percent of total label infused in brackets) for two trees infused with low label solution (left panel) and two trees infused with high label solution (right panel). Total efflux was calculated by subtracting total label assimilated from total label infused.

4.4 Discussion

Our results provide the first experimental evidence that xylem-transported root-respired CO_2 can be assimilated in stems, branches, and leaves of large trees in the field. We found that up to 17% of a ^{13}C label infused at the base of the stem was assimilated in woody and leaf tissues, providing evidence of an internal recycling mechanism for respired CO_2. Moreover, based on mass balance calculations, we estimated that most of the putative root-respired CO_2 diffused to the atmosphere from higher in the stem and branches, suggesting that efflux-based estimates of above- and belowground autotrophic component of respiration (R_a) are inaccurate. Based on the previous observation that a substantial quantity of CO_2 was transported from roots into shoots in xylem sap in this species (Aubrey & Teskey, 2009), the objective of this experiment was to determine the fate of root-respired CO_2 that dissolved in xylem sap. Our infusion of the ^{13}C label at the base of the stem was designed to serve as a proxy for dissolved CO_2 that was transported in xylem sap from the root system into the stem. However, the study also provides insights into the potential fate of xylem-transported dissolved CO_2 that originates from respiring cells in stems and branches (**Chapter 1**).

Recycling of respired CO_2 by woody tissues has been assumed to positively contribute to the overall carbon gain of plants (Aschan & Pfanz, 2003; Teskey *et al.*, 2008). Assimilation of CO_2 in woody tissues has been previously reported in the inner bark of branches and stems (Aschan *et al.*, 2001; Aschan & Pfanz, 2003) where sufficient light for CO_2 assimilation is transmitted to chlorophyll-containing cells (Aschan & Pfanz, 2003). Our results showed that the inner bark of the stem and branches was the most enriched tissue, confirming the potential importance of the inner bark in assimilation of internally transported CO_2. In branches receiving the HL treatment, we found that the average $\delta^{13}C_t$ of the inner bark was twice as high as the xylem, which agrees with results of ^{13}C labeling experiments on detached branches (McGuire *et al.*, 2009) (**Chapter 3**). Notwithstanding the fact that the upper- and mid-canopy strata were more distal from the ^{13}C infusion, the inner bark of woody tissues in these strata was more enriched than in the lower- and below-canopy strata. In the upper canopy, where young tissues are more metabolically active, corticular photosynthesis can be greater than in lower, older canopy sections (Cernusak & Marshall, 2000; Aschan *et al.*, 2001; Pfanz *et al.*, 2002). In

addition to reduced metabolism in lower parts of the canopy, light transmission is substantially lower, which decreases corticular CO_2 assimilation (Aschan & Pfanz, 2003).

The importance of woody tissue CO_2 assimilation to overall carbon gain can only be evaluated when data are scaled to the whole tree. The xylem of stems and branches makes up a large proportion of total tree biomass in comparison to the inner bark (in our study, on average, 65.9% vs. 14.5%, respectively). Scaling $\delta^{13}C_t$ with biomass demonstrated that, despite lower enrichment of xylem compared with inner bark, the greatest quantity of ^{13}C label was assimilated in the xylem, rather than in the inner bark, in both branches and stems. The stems and branches of *P. deltoides* in this study had visibly green xylem. The occurrence of chlorophyll in xylem has been reported for woody species (Rentzou & Psaras, 2008; Saveyn *et al.*, 2010) and chlorophyll-containing pith cells in young *Populus* were found to be capable of fixing $^{14}CO_2$ in the light (Van Cleve *et al.*, 1993). Therefore, from a mechanistic perspective, assimilation of xylem-transported CO_2, which is in essence a carbon recycling process, should be considered when assessing the total quantity of carbon assimilated by trees.

Few studies have described the role of assimilation of xylem-transported CO_2 by leaves in the context of a recycling mechanism. Aubrey & Teskey (2009) estimated that up to 50% of root-respired CO_2 could be transported internally to aboveground tree organs, and based on these results, Hanson & Gunderson (2009) argued that if a large fraction of root-respired CO_2 reached the foliage via the transpiration stream, it could have a substantial impact on the availability of CO_2 for leaf photosynthesis. Powers & Marshall (2011) labeled the xylem of a *Thuja occidentalis* tree in situ and subsequently could not detect any label in the leaves. However, their failure to detect label in the leaves could be partly the result of the small quantity of label solution that was infused and partly due to their strategy of sampling just a small amount of foliage from the top of the canopy. In our study, a portion of the infused label reached the leaves and was assimilated, with the petioles being the most enriched. Previous isotopic labeling experiments on detached branches of *Platanus occidentalis* (McGuire *et al.*, 2009) (**Chapter 3**) and detached leaves of *P. deltoides* (Stringer & Kimmerer, 1993) (**Chapter 2**) reported similar high values of carbon isotope enrichment in petioles compared with more distal leaf components. Apparently, the petioles scrubbed most of the label from

the transpiration stream before it reached the leaf mesophyll. Russin & Evert (1984) reported that in the petioles of *Populus* leaves, chlorophyll-containing cells are in close contact with the vasculature, suggesting that xylem-transported CO_2 may be a carbon source for photosynthetic reactions in adjacent tissues, as was reported by Stringer & Kimmerer (1993) and observed in other species (Hibberd & Quick, 2002; Berveiller *et al.*, 2007b; Leegood, 2008). However, in our study, leaf assimilation of transported ^{13}C label was limited. It appeared that most of the infused label either diffused to the atmosphere or was assimilated by woody tissues before it could reach the foliage.

In total, we found that up to 17% of the infused label was assimilated in woody tissue and leaves. However, our results likely underestimate the actual importance of assimilation of internally transported CO_2, because we could not account for any assimilation of internally sourced ^{12}C, i.e., the ^{13}C label represented only part of the internal carbon available for assimilation. The water taken up by roots and transported upward contained dissolved CO_2 (composed almost entirely of ^{12}C) from root respiration. Based on the proportion of total sap flow that the label solution represented (23.8 to 32.4%), it can be expected that the amount of root-respired CO_2 assimilated was three to five times more than estimated with the label. Finally, CO_2 from aboveground R_a, which is composed almost entirely of $^{12}CO_2$, could be re-assimilated immediately in nearby photosynthetic cells or become part of the internal transport pool. McGuire & Teskey (2004) found that up to 55% of daily stem-respired CO_2 could be transported in the xylem stream, so it is likely that this source contributed substantially to the amount of internal CO_2 available as substrate for assimilation. Moreover, because the xylem was not saturated with $^{13}CO_2$ label after the 2 d infusion period, photosynthetic discrimination against ^{13}C in woody tissue (Cernusak *et al.*, 2001; Saveyn *et al.*, 2010) is another likely source of underestimation. Longer-term labeling would likely have resulted in even greater ^{13}C concentrations in all tissues where the label was assimilated.

Based on our mass balance calculations, we found that the largest fraction of the ^{13}C label (83% and 94% under the LL and HL treatments, respectively) diffused to the atmosphere from the stem and branches. This observation suggests that as root-respired CO_2 is transported from belowground upward through the stem, most of it

diffuses to the atmosphere before reaching the canopy. We assumed that the quantity of ^{13}C label that remained in the xylem in dissolved and gaseous states at the end of the experiment was negligible and that diffusion of the label from the leaves was inconsequential because the direction of CO_2 movement is from the atmosphere into leaves during the day and the amount of CO_2 efflux from leaves at night is only a small fraction of the amount taken up during the day.

As carbon dioxide (CO_2) dissolves in water, pH dependent equilibria are established between the aqueous (CO_2(aq)), bicarbonate (HCO_3^-) and carbonate (CO_3^{2-}) forms of CO_2 (**Chapter 1**). In the xylem, with pH levels reported in the range of 4.7-7.4 (Teskey *et al.*, 2008), CO_2 is present only as CO_2(aq) and HCO_3^- and not in its carbonate form (CO_3^{2-}). Measurements of the pH of the xylem sap in six trees at our site showed the average pH value to be 6.22 ±0.07.

Similarly, the ^{13}C solutions applied in this study, in which the average pH was 5.30 and 6.90 for the low and high-labeled solutions, respectively, contained ^{13}C only in its aqueous ($^{13}CO_2$ (aq)) and bicarbonate ($H^{13}CO_3^-$) forms. Other studies performed with carbon tracers have specifically supplied the bicarbonate or carbonate form of the stable or non-stable isotope to leaves (Stringer & Kimmerer, 1993), herbaceous plants (Hibberd & Quick, 2002), cuttings (Vapaavuori & Pelkonen, 1985) and small trees (Powers & Marshall, 2011) and they all concluded that there was an accumulation of the tracer in various tissues. Moreover, CO_2 and HCO_3^- (^{12}C or ^{13}C) can be assimilated by Ribulose-1,5-biphosphate carboxylase oxygenase (Rubisco) and Phosphoenolpyruvate carboxylase (PEPc)-mediated carboxylation, respectively, and previous studies have reported that Rubisco (e.g. Pfanz *et al.*, 2002; Saveyn *et al.*, 2010) and PEPc (Hibberd & Quick, 2002; Berveiller *et al.*, 2007) in woody and leaf tissues actively contribute to CO_2 refixation. Thus, it is reasonable to believe that the inorganic form of the supplied ^{13}C label was assimilated by biological processes.

Previous experiments demonstrated that CO_2 dissolved in soil water contributed only a small amount to the overall carbon economy of plants (Ford *et al.*, 2007; Jones *et al.*, 2009). Moore *et al.* (2008) found that the isotopic composition of soil CO_2 explained a considerable amount of the variation in the isotopic composition of CO_2 that fluxed from stems, but (Ubierna *et al.*, 2009) observed that neither belowground processes nor CO_2

transported in the transpiration stream had a detectable influence on stem CO_2 efflux. By applying an isotope label to the soil, Ford *et al.* (2007) and Ubierna *et al.* (2009) tested the assumption that CO_2 dissolved in soil water could be taken up by roots and transported in the xylem stream, while our study simulated the transport of CO_2 originating from both root and soil sources by infusing a ^{13}C label at the base of tree stems. The internal [CO_2] measured at the bottom of the stem (Teskey & McGuire, 2007; Aubrey & Teskey, 2009) was substantially higher than the [CO_2] in soil surrounding the roots, indicating that only a small quantity of the CO_2 in the xylem at the base of the stem could have originated from the soil (**Chapter 1**). Therefore, most of the internal CO_2 at the base of the stem must be derived from the root system. Ford *et al.* (2007) and Ubierna *et al.* (2009) were not able to simulate the transport of CO_2 derived internally from root respiration, which has been shown to comprise 92% of the CO_2 transported in xylem from belowground (Aubrey & Teskey, 2009). In addition, Ford *et al.* (2007) and Ubierna *et al.* (2009) were unable to determine the total amount of label that was taken up by the roots, but by infusing the label solution directly into the xylem, we were able to quantify the uptake of ^{13}C, which allowed us to calculate ^{13}C efflux as the difference between uptake and assimilation.

The magnitude of root-respired CO_2 transported in the xylem and subsequently lost to the atmosphere may have important implications for how we assess above- and belowground metabolism (Aubrey & Teskey, 2009; Grossiord *et al.,* 2012) (**Chapter 7**). Given that one-half of root-respired CO_2 may follow an internal flux pathway that cannot be accounted for by soil CO_2 efflux measurements (Aubrey & Teskey, 2009) and that up to 94% of the ^{13}C label infused into trees in this study was lost to the atmosphere, we suggest that up to 47% of root-respired CO_2 could diffuse into the atmosphere from aboveground woody tissues. That a substantial amount of CO_2 diffusing out of the stem and branches actually originates from belowground autotrophic respiration has important implications for how we interpret efflux-based measurements of soil and woody-tissue respiration and patterns of carbohydrate allocation (**Box 1.3**). First, we suggest that the gas-exchange approach for estimating above- and belowground respiration is inaccurate and needs to be adjusted for internal transport of CO_2. Second, our understanding of patterns of allocation of carbohydrates in trees should be

reconsidered because we are routinely under- and over-estimating the carbon needed to sustain below- and aboveground tissues, respectively, when estimates are derived from measurements of CO_2 efflux. In future research, additional measurements of metabolic processes (photosynthesis, root, and stem respiration) conducted simultaneously with measurements of internal CO_2 transport may reveal the implications of this recently recognized carbon flux pathway.

- Chapter 5 -

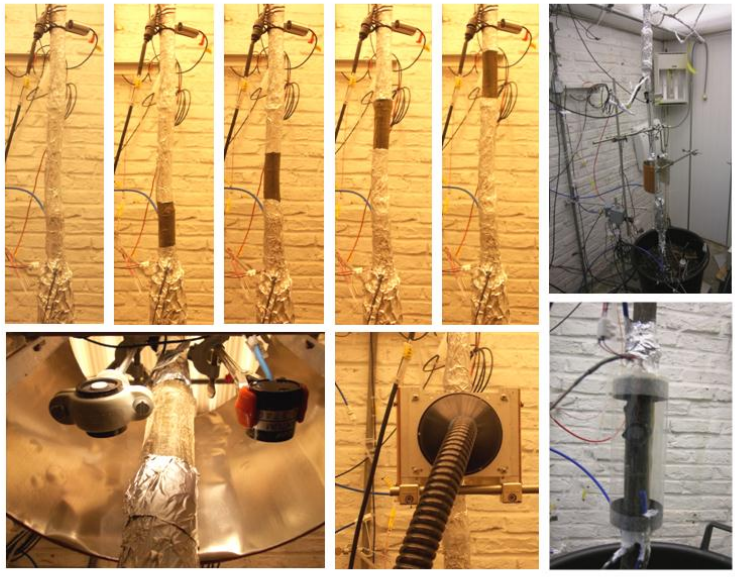

Woody tissue photosynthesis induces axial diffusion of respired CO_2 in dormant oak tree stems

After: Bloemen J., Dupon Y., and Steppe K. (2013) Axial diffusion of respired CO_2 confounds dormant season stem respiration estimates.

Abstract

Previous findings on the transport of respired CO_2 via the transpiration stream led to new insights in how to interpret efflux-based stem respiration measurements. However, no studies have yet addressed whether efflux-based estimates represent actual stem respiration rates at times when no sap flow occurs, for instance during the dormant season. Stem CO_2 efflux (E_{stem}) was measured with a stem cuvette on dormant oak (*Quercus robur* L.) trees in a growth chamber. Different rates of axial CO_2 diffusion were induced by illuminating 10-cm-long stem sections at varying distances from the stem cuvette, while light was excluded from the remainder of the tree. Our results show how axial diffusion of respired CO_2 within dormant tree stems may lead to an underestimation of dormant season stem respiration. Largest non-temperature related reductions in E_{stem} were observed when the stem section closest to the cuvette was exposed to light. Due to axial diffusion of CO_2, E_{stem} decreased by 22% relative to E_{stem} measured when light was excluded from the entire tree. Lower rates of axial diffusion were observed upon illumination of more remote stem sections. While during the growing season, transport of dissolved CO_2 overrules the potential impact of axial diffusion on E_{stem}, our results indicate that dormant season efflux-based estimates of stem respiration might be biased, particularly in 'open' forest stands with sufficient light

penetration. Consequently, this may lead to wrong estimates of dormant season E_{stem} coefficients (Q_{10} and $E_{stem}(ref)$) which are generally used to estimate maintenance respiration throughout the year.

5.1 Introduction

Within forest ecosystems, CO_2 efflux from woody tissues to the atmosphere represents a major component of ecosystem respiration, accounting for about 7 to 50% of gross primary productivity (Ryan *et al.*, 1994; Damesin *et al.*, 2002). The wide range in these estimates partially reflects differences observed between different forest ecosystems (Ryan *et al.*, 1995; Chambers *et al.*, 2004; Yang *et al.*, 2012), but is additionally resulting from our limited ability to accurately measure and model this respiratory flux at the tree level and to scale it to the stand level (Ryan *et al.*, 2009).

However, recent advances have been made on using efflux-based measurements to accurately quantify woody tissue respiration during the growing season. Where past studies mainly highlighted the exponential relationship between stem temperature and stem CO_2 efflux (E_{stem}) (Ryan *et al.*, 1995; Maier *et al.*, 1998; Stockfors, 2000), most recent studies report on non-temperature related factors interfering with E_{stem} (Yang *et al.*, 2012). In particular, CO_2 originating from woody tissue respiration can diffuse into the atmosphere remote from the site of respiration, as dissolved CO_2 is transported internally away from the site of respiration via the transpiration stream (Teskey & McGuire, 2002) (**Chapter 1**). Teskey & McGuire (2007) found that internal transport of respired CO_2 might account for up to 70% of the CO_2 derived from stem respiration, which explains past observations of decreases in stem CO_2 efflux during periods of high transpiration (Negisi, 1974; Martin *et al.*, 1994; McGuire & Teskey, 2004; Bowman *et al.*, 2005; McGuire *et al.*, 2007; Saveyn *et al.*, 2007b). Moreover, Bloemen *et al.* (2013b) recently showed that a considerable fraction of E_{stem} might be derived from belowground respired CO_2 transported with the transpiration stream (**Chapter 4**), indicating the need to measure continuously CO_2 efflux as well as transport of respired CO_2 via the transpiration stream (Trumbore *et al.*, 2013).

When no sap flow occurs, other factors that may influence efflux-based estimates of stem respiration are often neglected. At night-time, lower temperatures and a better

overall tissue water status might lower and increase the overall respiration rate, respectively, as compared to the day-time when temperatures are higher and sap flow depletes the water reserves. Woody tissue photosynthesis in chlorophyll containing bark and xylem tissues can refix a part of the locally respired CO_2 (Pfanz *et al.*, 2002), present in tree stems at CO_2 concentrations ($[CO_2]$) ranging from <1 to over 26% (Teskey *et al.*, 2008). Wittmann *et al.* (2006) observed a reduction in CO_2 diffusion to the atmosphere under illumination because up to 97% of the respired CO_2 was locally assimilated by woody tissue photosynthesis. While an opaque stem cuvette is generally used to measure E_{stem}, preventing local assimilation of respired CO_2, woody tissue photosynthesis in stem or branch sections remote from the site of measurement might account for observed non-temperature related variations in E_{stem} during the dormant season (Saveyn *et al.*, 2008a). Saveyn *et al.* (2008a) hypothesized that woody tissue photosynthesis in the stem sections above or below the stem cuvette might reduce the internal $[CO_2]$ within these sections, inducing an axial diffusion of CO_2 away from the site of respiration. However, we still lack an accurate assessment of the impact of axial diffusion of respired CO_2 on E_{stem} measurements.

Therefore, the aim of this study was to proof the hypothesis of Saveyn *et al.* (2008a) and to illustrate the extent to which axial diffusion of respired CO_2 could have an impact on E_{stem} during dormant season measurements. Although diffusion in the axial direction is higher than in the radial direction, it is still considered insignificant relative to internal transport of CO_2 via the transpiration stream (Hölttä & Kolari, 2009). We measured under controlled conditions E_{stem} with a stem cuvette on dormant oak (*Quercus robur* L.) trees and induced woody tissue photosynthesis at varying heights by illuminating different stem sections, while the remainder of the tree was excluded from light. We hypothesized that a fraction of the respired CO_2 would be transported axially instead of contributing to E_{stem} and that the effect of axial diffusion of CO_2 on E_{stem} would be more pronounced when stem sections closer to the cuvette were illuminated. This hypothesis led us to speculate that previous efflux-based measurements of dormant season stem respiration, generally used to partition respiration in its growth and maintenance component during the growing season may need reconsideration.

5.2 Materials and methods

5.2.1 Plant material and measurement conditions

Experiments were conducted under controlled conditions in a growth chamber (2 m x 1.5 m x 2 m, height x width x length) during the winter of 2011-2012. Measurements were performed on two 4-y-old oak (*Quercus robur* L.) trees, hereafter referred to as QR_1 and QR_2, with both an approximate height of 2 m and a diameter at stem base of 3.22 and 3.19 cm, respectively. Both trees were previously grown outdoors in 50 l containers, containing a potting mixture (LP502D, Peltracom nv, Gent, Belgium) and a fertilizer (Basacot Plus 6M, Compo Benelux nv, Deinze, Belgium). Each tree was moved to the growth chamber one week prior to the measurements, allowing them to adapt to the indoor conditions. To this end we measured stem CO_2 efflux (E_{stem}) before the actual light manipulation started and checked whether E_{stem} remained stable under the controlled constant environmental conditions in the growth chamber. Air temperature (T_{air}) was measured with a Type-T thermocouple (Omega, Amstelveen, The Netherlands), relative humidity (RH) with a capacitive RH-sensor (Model HIH-3605-A, Honeywell, Morristown, NJ, USA) and photosynthetic active radiation (PAR) with a quantum sensor (model Li-190, Li-COR, Lincoln, TE, USA). T_{air} and RH were kept constant during the entire experiment. Light was supplied by densely packed fluorescent lamps (TLD 36 W/85, Philips, Eindhoven, The Netherlands), producing a constant background PAR of 140 µmol m^{-2} s^{-1} at the top of the tree during the entire experiment.

5.2.2 Stem CO_2 efflux measurements

E_{stem} was measured on a stem section at 30 cm above the soil surface, with a stem diameter of 3.06 and 3.02 cm for QR_1 and QR_2, respectively. The cuvette was 13 cm long, constructed of a Polycarbonate film (Roscolab Ltd, London, UK) and sealed to the stem with adhesive closed-cell foam gasket material (Rs components benelux, Anderlecht, Belgium) and non-caustic silicone sealer (Rs components benelux, Anderlecht, Belgium) (**Fig. 1.14A**). Outside air was mixed in a 50 l buffer vessel in order to obtain a stable inlet air [CO_2] and was pumped to the stem cuvette with a membrane pump (model 2-Wisa, Hartmann and Braun, Frankfurt am Main, Germany) at an average flow rate of

1.1 l min^{-1}, as measured with a flow meter (model 5860S, Brooks Instruments, Ede, The Netherlands). The [CO_2] of the air leaving the stem cuvette was measured with an infrared gas analyzer (IRGA, LI-7000, Li-COR, Lincoln, TE, USA) and was compared with the [CO_2] of the air leaving a reference cuvette. This cuvette had the same dimensions as the measurement cuvette but enclosed a PVC tube of 3.2 cm outer diameter, which was approximately similar to the average stem diameter of the sections enclosed for E_{stem} measurements. Every hour a zero measurement was performed to correct for possible drift of the IRGA during the measurements. E_{stem} was calculated according to Long & Hallgren (1985) and was expressed per unit of surface area (**Equation 1.7**). The stem cuvettes were leak tested before the start of the experiment and sealed where needed. Stem temperature (T_{stem}) was measured 2 cm below and 2 cm above the stem cuvette with 1 cm long home-made thermocouple needle (type T, Omega Engineering Omega, Amstelveen, The Netherlands) to verify constant T_{stem} during the experiment.

5.2.3 Axial CO_2 diffusion in tree stems

To account for the potential effect of axial CO_2 diffusion on E_{stem}, we induced a [CO_2] gradient within the tree stem (Fig. 5.1). Where light was excluded from the whole tree and the stem cuvette by loosely wrapping the tree with aluminum foil, a 10 cm long stem section was exposed to a movable fiber optic light source (Model FL-4000, Walz Mess und Regeltechnik, Effeltrich, Germany), producing an average PAR of 850 µmol m^{-2} s^{-1} (**Fig. 1.14B**). A fiber optic light source was selected because it does not emit heat in contrast to other standard light sources while producing a homogenous light distribution. A PVC tube, 10 cm long, cut in half and at the inside covered with reflective foil, was used to illuminate the other side of the stem section at an average PAR of 55 µmol m^{-2} s^{-1}. As a result, woody tissue photosynthesis occurred at this particular stem section, lowering the stem [CO_2] relative to the site of E_{stem} measurements, resulting in an axial diffusion of CO_2 inside the stem (Fig. 5.1). We altered the axial diffusion of CO_2 by illuminating different stem sections along a height gradient: 5-15 cm, 15-25 cm, 25-35 cm, and 35-45 cm above the stem cuvette, hereafter referred to in the text as S_1, S_2, S_3, and S_4, respectively. At every position, the stem section was illuminated for 24 h while background PAR in the growth chamber was fixed at 140 µmol m^{-2} s^{-1} and data from 6 h prior and 12 h after the light exposure was additionally recorded as reference. Between

the periods of illumination of the different stem sections, a reference state was maintained for at least 24 h by loosely wrapping the previously light-exposed stem sections with aluminium foil, until a stable E_{stem} reference reading was obtained.

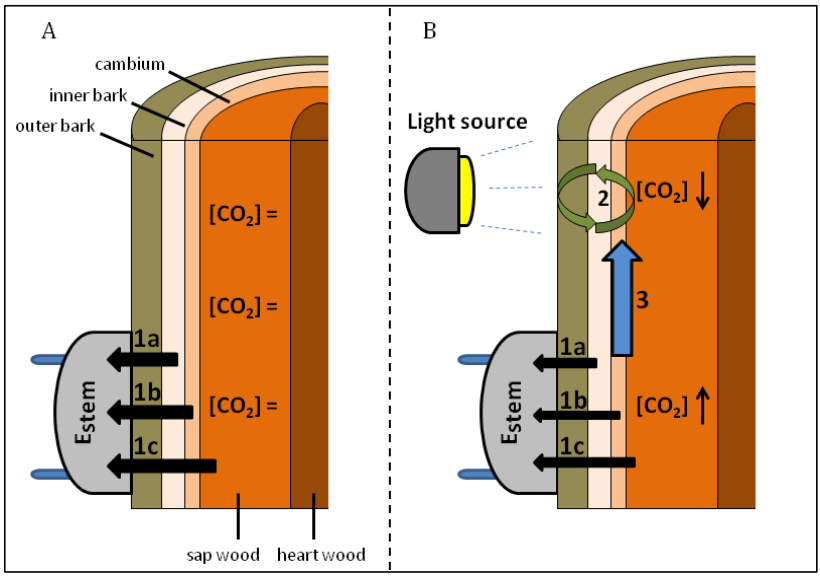

Fig. 5.1 Schematic of radial and axial CO_2 fluxes in a dormant tree stem when measuring stem CO_2 efflux (E_{stem}) with a stem cuvette under different conditions. (A) During tree and stem cuvette light exclusion only outward radial diffusion of respired CO_2 occurs from the inner bark (1a), cambium (1b) and xylem ray cells (1c). (B) A stem section remote from the stem cuvette is illuminated, which triggers woody tissue photosynthesis (2), while light is excluded from the remainder of the stem and the cuvette. Stem CO_2 concentration ($[CO_2]$) decreases within this stem section relative to $[CO_2]$ in the stem section enclosed in the stem cuvette, resulting in an upward axial diffusion of CO_2 (3) and a decreased contribution of radial diffusion of CO_2 to E_{stem} (1a, 1b, and 1c). Adapted from Teskey *et al.* (2008).

5.2.4 Sap flow and stem diameter measurements

Sap flow rate (F_s) and variations in stem diameter (D) were measured to validate whether the trees were dormant. Variations in D were measured using a linear variable displacement transducer (LVDT; model DF 5.0, Solartron Metrology, Leicester, UK). This LVDT was attached to the tree with a custom-made stainless steel holder installed at a height of 0.95 m above the soil. A small circular-shaped hole was made in the aluminium foil to ensure proper contact between the stem and the sensor head of the LVDT. F_s was measured with a heat balance (HB) sensor (model SGB 17-WS, Dynamax Inc., Houston,

USA) at a height of 1.05 m above the soil. Sensor installation and F_s calculation were performed according to the guidelines in the operation manual (van Bavel & van Bavel, 1990).

5.2.5 Measurements of chlorophyll concentration

At the end of each experiment, bark of the stem sections S_1 to S_4 was collected for determination of bark chlorophyll concentration. Per stem section, four samples were randomly collected, immediately frozen in liquid nitrogen and stored at -80°C. Samples were grinded (A11 basic analytic mill, IKA-Werke GmbH & Co. KG, Staufen, Germany) and chlorophyll was extracted by adding 7.5 ml acetone (80%) to 150 mg of sample. After 24 h extraction in the dark, samples were centrifuged and the supernatant was transferred to a glass cuvette and analyzed for chlorophyll concentration with a spectrophotometer (UVIKON XL, Bio-Tek Instruments, Winooski, VT, USA) at wavelengths of 663.6 and 646.6 nm. Chlorophyll concentrations were calculated according to Porra *et al.* (1989) and expressed per unit of bark fresh weight (mg chl g^{-1} FW).

5.2.6 Data and statistical analysis

All data was recorded with a data logger (HP 34970A, Hewlett-Packard, Palo Alto, CA, USA) at a 1 min interval and averaged over 5 min intervals. For statistical analysis, we used a multi-factorial analysis of variance (ANOVA) model to compare the chlorophyll concentration of the different stem sections with stem section (n=4, S_1 to S_4) as fixed factor and individual tree (n=2) as random factor. For statistical analysis of E_{stem}, data was averaged over 1 h intervals and a repeated measures ANOVA was performed with the different experimental stages (n=5, reference and S_1 to S_4) and time (n=42) as fixed factors and individual tree as random factor (n=2). Akaikes information criterion corrected for small sample sizes (AIC_C) was used to determine the covariance structure that best estimated the correlation among individual trees over time. ANOVA analyses were performed using the mixed model procedure (PROC MIXED) of SAS (Version 9.1.3, SAS inc., Cary, NC, USA) with α=0.05.

5.3 Results

5.3.1 Microclimate, sap flow and stem diameter

Both QR_1 and QR_2 were subjected to a constant air temperature (T_{air}) and relative humidity (RH) regime during the entire experiment in the growth room (Table 5.1). Also stem temperature (T_{stem}) was constant, irrespective of the light treatment. For QR_1, averaged T_{stem} below and above the stem cuvette during the reference period was 20.52 ± 0.05°C, which is in the range of the measured average T_{stem} when one of the stem sections was illuminated (20.42 ± 0.18°C to 20.75 ± 0.20°C). Average T_{stem} of QR_2 during reference (20.08 ± 0.02°C) was similar to the average T_{stem} observed during illumination (range from 20.06 ± 0.05°C to 20.16 ± 0.15°C). Therefore changes in E_{stem} measured during stem section illumination are independent of variations in T_{stem}.

Table 5.1 Microclimatological conditions prevailing during the experiments on both oak trees (QR_1 and QR_2). Air temperature (T_{air}, °C), stem temperature (T_{stem}, °C) and relative humidity (RH, %) data are averages (± SD) over the entire measurement period.

	T_{air}	T_{stem}	RH
QR_1	19.86 ± 0.34	20.61 ± 0.22	42.53 ± 5.08
QR_2	20.37 ± 0.08	20.10 ± 0.12	40.81 ± 2.84

Measurements of sap flow rate (F_s) and variation in stem diameter (D) confirmed that both trees were dormant. Heat balance data indicated that there was no heat transfer by convection within the stem, excluding the occurrence of sap flow within the xylem. Variations in D on a diurnal and longer time scale were not observed (data not shown).

5.3.2 Stem CO_2 efflux and axial diffusion of CO_2

Overall, stem CO2 efflux (E_{stem}) was low, with an average reference value of 0.76 ± 0.02 and 1.04 ± 0.02 µmol m^{-2} s^{-1} for tree QR_1 and QR_2, respectively. Illumination of the defined stem segments induced axial diffusion of CO_2 in the stem, which decreased E_{stem} relative to the reference value (Fig. 5.2). The distance between the illuminated stem section and the stem cuvette had a significant effect on the decrease in E_{stem} (P=0.0115). The largest decrease in E_{stem} was observed when S_1 was exposed to light. In QR_1 a reduction of 0.17 µmol m^{-2} s^{-1} was observed 24 h after light exposure (Fig. 5.2) or 22%

relative to the reference E_{stem} (Fig. 5.3). In QR_2 a decrease of 0.14 µmol m^{-2} s^{-1} was detected or 13% relative to the reference (Fig. 5.3). In both trees, the response in E_{stem} on S_1 illumination was fast, with a time lag of 1 h 30 min and 1 h 50 min between light exposure and response for QR_1 and QR_2, respectively. A similar time lag was observed at the end of the S_1 illumination period.

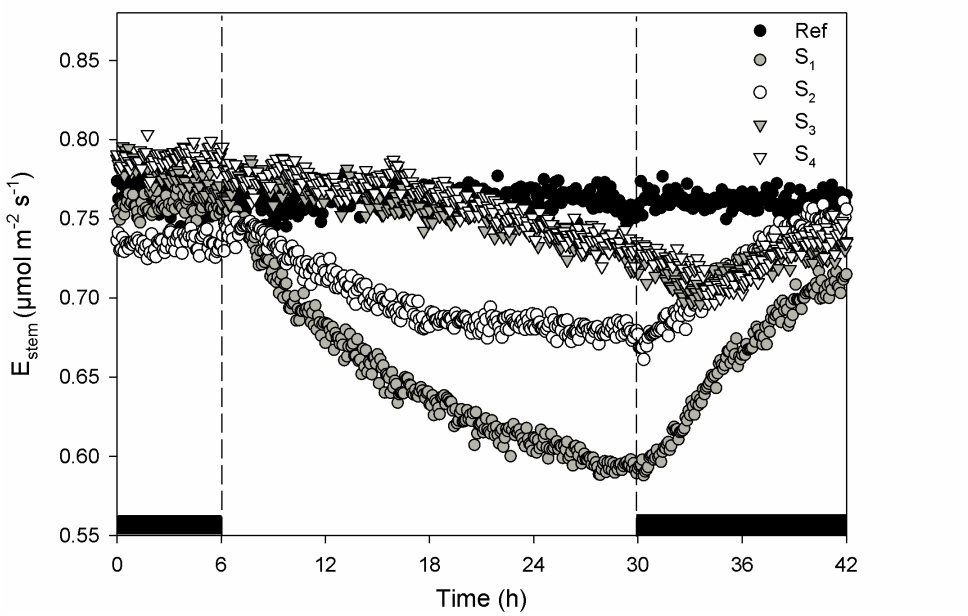

Fig. 5.2 Profiles of stem CO_2 efflux (E_{stem}) measured with a stem cuvette on QR_1 when light was excluded from the entire tree and stem cuvette (Ref, black circles) and when inducing woody tissue photosynthesis in 10-cm-long stem sections remote from the site of E_{stem} measurement by illuminating either S_1 (5-15 cm from the stem cuvette, grey circles), S_2 (15-25 cm from the stem cuvette, open circles), S_3 (25-35 cm from the stem cuvette, grey triangles) or S_4 (35-45 cm from the stem cuvette, open triangles). E_{stem} data are 5 min averages. Beginning and end of stem section illumination are indicated by black boxes and dashed lines.

The more remote the light-exposed stem sections were, the smaller the impact of axial CO_2 diffusion on E_{stem} was. Where illuminating S_2 reduced E_{stem} by 0.10 µmol m^{-2} s^{-1} and 0.12 µmol m^{-2} s^{-1} in QR_1 and QR_2, respectively, a reduction of only 0.06 µmol m^{-2} s^{-1} in E_{stem} was found when exposing S_3 and S_4 in both trees. These findings led us to conclude that the reduction in E_{stem} in these trees due to axial CO_2 diffusion are small and can be ignored when stem sections at a distance of 30 cm or more from the stem cuvette are illuminated (Fig. 5.3). Due to the long distance between stem cuvette and S_3 and S_4, the

transient decrease in E_{stem} due to axial diffusion was slow, with only a slightly lower value in E_{stem} compared to the reference after the end of illumination (Fig. 5.2).

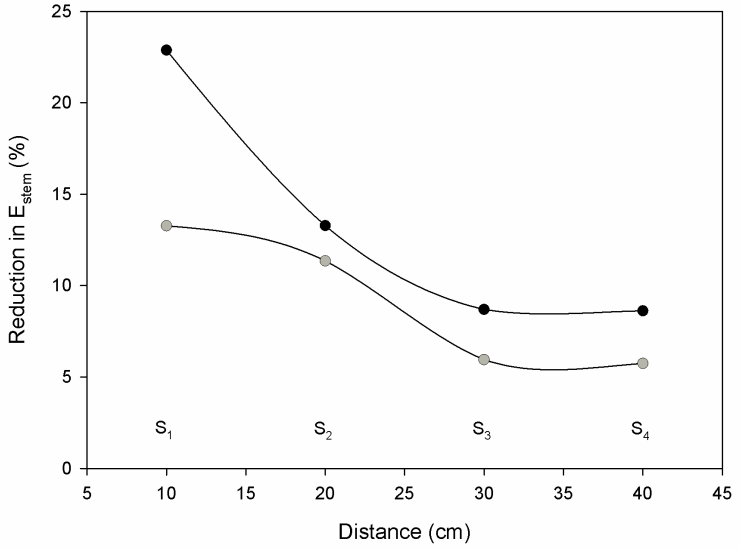

Fig. 5.3 Reduction in stem CO_2 efflux (E_{stem}) measured with a stem cuvette for two dormant *Quercus robur* trees (QR_1, black circles; QR_2, grey circles), when illuminating 10-cm-long stem sections at different distances from the site of E_{stem} measurement, while light is excluded for the remainder of the tree and stem cuvette. Reductions are expressed relative to E_{stem} measurements performed when light was excluded from the entire tree.

5.3.3 Bark chlorophyll concentration

No significant difference in bark chlorophyll concentration among S_1, S_2, S_3, and S_4 was observed (P=0.31) (Table 5.2). Chlorophyll concentrations ranged from 0.37 ± 0.05 to 0.45 ± 0.02 mg chl g FW^{-1} in QR_1 and from 0.35 ± 0.04 to 0.41 ± 0.04 mg chl g FW^{-1} in QR_2. These similar levels in chlorophyll concentration observed in S_1 to S_4 indicate that the capacity for woody tissue photosynthesis can be assumed equal in the different light-exposed stem sections.

Table 5.2 Bark chlorophyll concentrations (mg chl g^{-1} FW) of bark of both oak trees (QR_1 and QR_2), randomly sampled after the experiment for the four different 10-cm-long stem sections (S_1, S_2, S_3, and S_4) exposed to light. Data are averages (±SD) of four samples per stem section per tree.

Stem segment	QR_1	QR_2
S_1	0.45 ± 0.08	0.37 ± 0.08
S_2	0.44 ± 0.04	0.41 ± 0.04
S_3	0.45 ± 0.04	0.35 ± 0.04
S_4	0.37 ± 0.02	0.38 ± 0.02

5.4 Discussion

Recent advances in the field of tree respiration research fostered an important discussion regarding the use of efflux-based measurements to estimate the "actual" stem respiration (Trumbore *et al.*, 2013). Where past studies assumed that stem CO_2 efflux (E_{stem}) equaled stem respiration, it is now acknowledged that CO_2 emitted by stems is derived from a multitude of sources affected by different factors (Yang *et al.*, 2012; Trumbore *et al.*, 2013) (**Chapter 1**). With this study we want to illustrate that axial diffusion of respired CO_2 is an additional factor that should be accounted for when estimating stem respiration. Up till now, this flux was considered insignificant in comparison to xylem transport of respired CO_2 during the growing season (Hölttä & Kolari, 2009), but its importance remained unclear for efflux-based dormant season estimates of stem respiration.

During tree dormancy, it is generally accepted that only maintenance stem respiration contributes to E_{stem} and that its dynamics are mainly driven by temperature (Amthor, 1989; Maier *et al.*, 1998). However, we observed large non-temperature related variations in E_{stem} in dormant oak trees, similar as described by Saveyn *et al.* (2008a). By locally illuminating different stem sections near the stem cuvette, while excluding light from the remainder of the tree and the cuvette, we observed pronounced decreases in E_{stem} rates. More interestingly, we observed the largest reduction in E_{stem} when the stem section closest to the cuvette was exposed to light, with decreases up to 22% due to axial diffusion of respired CO_2 in stems.

Bark chlorophyll concentrations in the dormant oak stems were within the range reported for trees (Pfanz *et al.*, 2002). Assimilation of respired CO_2 within the chlorophyll containing tissues locally reduces the CO_2 concentration ($[CO_2]$) relative to internal $[CO_2]$ at stem sections where woody tissue photosynthesis is excluded, as observed by Saveyn *et al.* (2008a). As a result, a $[CO_2]$ gradient along the stem arose, inducing a spontaneous axial diffusion of respired CO_2 from the site of high to low $[CO_2]$, according to Fick's law of diffusion (Fig. 5.1; Jones, 1992; Saveyn *et al.*, 2008a). As a consequence, a lower fraction of respired CO_2 diffused radially into the stem cuvette, observed as a decrease in E_{stem}. Additionally, Fick's law of diffusion states that the amount of CO_2 diffusing along the concentration pathway is dependent on its length. This explains why the largest decrease in E_{stem} was observed during illumination of the stem section closest to the stem cuvette.

In general, axial diffusion of gases within plants induced by woody tissue photosynthesis has been described to play a role in root aeration in genera of *Alnus*, *Salix* as well as *Betula pubescens* and *Populus tremula* (Grosse *et al.*, 1996; Armstrong & Armstrong, 2005). During illumination of aboveground plant parts, photosynthesis in chlorophyll containing woody tissues increases the internal O_2 concentration, inducing a diffusive transfer of O_2 to the roots (Armstrong & Armstrong, 2005). Moreover, axial diffusion of O_2 is facilitated relative to its radial diffusion due to the anatomy of the tree stem. Sorz & Hietz (2006) reported that for *Quercus robur* diffusion of O_2 in the axial direction was more than 20 times higher than in radial direction, due to the fact that the diffusing gas encounters less cells walls when travelling along the stem axis. For CO_2, a similar high resistance to radial diffusion exerted by the xylem, cambium and bark layers has been described and a radial resistance factor should be included when using efflux-based measurements to model stem respiration (Steppe *et al.*, 2007). The fact that CO_2 might diffuse rapidly in axial direction due to woody tissue photosynthesis was first suggested by Saveyn *et al.* (2008a). Based on the species specific diffusion coefficients for oxygen diffusion for *Quercus robur* (6.9×10^{-8} m^2 s^{-1} at a 15% moisture content, Sorz & Hietz (2006)) we can estimate the time for CO_2 to diffuse axially within stems, as done in Nobel (1999). For a 10 cm distance, oxygen axial diffusion would take around 4.6 h. Axial diffusion of CO_2 will probably take longer, given that molecules with a higher mass

tend to have a lower diffusion coefficient (Nobel, 1999), but the transfer time would be in the same order of hours. This estimate is in contrast with the observation by Gansert (2003), which stated that diffusion of gases in stems is very slow (1 m would take several years), depending on the CO_2 gradient. However Gansert (2003) assumed that movement of gases in stems mainly will occur via the aqueous phase, while an important fraction of the stem consists of gas voids (i.e. 25% gas by volume in stems of *Quercus* sp. (MacDougal *et al.*, 1929; Teskey *et al.*, 2008)), where diffusion occurs much faster than in water (Nobel, 1999).

Our experimental data also allows us to illustrate whether it is justified to neglect axial diffusion of respired CO_2 when estimating E_{stem} during the growing season. Respired CO_2, either derived from below- or aboveground sources, is transported upward via the transpiration stream (Aubrey & Teskey, 2009; Bloemen *et al.*, 2013b) and may confound efflux-based estimates of stem and branch respiration (Teskey & McGuire, 2002; McGuire & Teskey, 2004; McGuire *et al.*, 2007). In a previous study on six 9-y-old field grown *Quercus robur* trees the maximal rate of internal CO_2 transport with the transpiration stream measured at the stem base was about 6 μmol CO_2 s^{-1} through the stem cross section (**Chapter 7**). If we now assume that the maximal observed reduction in E_{stem} in our dormant trees (0.17 μmol CO_2 m^{-2} stem surface area s^{-1}) reflects the potential axial diffusion in these field-grown trees, and we scale this number with the stem surface area of the respective cuvette (0.026 m^2), we obtain an axial diffusion rate of about 0.0045 μmol respired CO_2 s^{-1}. This diffusion rate is approximately three orders of magnitude lower than the internal CO_2 transport rate and therefore it is reasonable to postulate that axial diffusion of respired CO_2 and its impact on E_{stem} is negligible during the growing season when sap flow occurs. On the other hand, the diffusion coefficient of gases in stems is expected to increase with an increase in stem gas volume (Sorz & Hietz, 2006), which occurs concomitant with a decrease in volumetric water content during the change from dormant to growing season (MacDougal *et al.*, 1929; Pausch *et al.*, 2000). Nonetheless, axial diffusion of respired CO_2 remains of lower magnitude during the growing season relative to the internal transport of CO_2 with the transpiration stream.

Accurate efflux-based estimates of stem respiration during dormancy are essential for partitioning respiration in a growth and a maintenance component according to the functional model of respiration (McCree, 1970; Amthor, 1989; Maier, 2001). In field experiments, the most widely used approach to estimate growth and maintenance stem respiration is the mature tissue method (e.g. Maier, 2001; Damesin, 2003; Gaumont-Guay *et al.*, 2006), where temperature-corrected coefficients of dormant season stem respiration, i.e. Q_{10} (coefficient that describes the change in E_{stem} for a 10°C increase in T_{stem}) and $E_{stem}(ref)$ (a regression coefficient that estimates E_{stem} at a reference T_{stem}), are combined with actual T_{stem} data to estimate maintenance stem respiration during the growing season (Lavigne & Ryan, 1997). However, results from an additional experiment on QR_2, in which we determined Q_{10} and $E_{stem}(20)$ under a changing temperature program, showed that the above efflux-based mature tissue method over- and underestimated the first and latter parameter, respectively. When exposing S_1 to light, we found Q_{10} and $E_{stem}(20)$ coefficients of 2.25 and 1.29 µmol CO_2 m^{-2} s^{-1}, respectively compared to the reference Q_{10} (2.05) and $E_{stem}(20)$ (1.40 µmol CO_2 m^{-2} s^{-1}) values. However, we assume that the results obtained during our experiment, where we illuminated stem sections only above the stem cuvette, may underestimate the potential effect of axial CO_2 diffusion on dormant season stem respiration under natural conditions. Larger differences in Q_{10} and $E_{stem}(20)$ were obtained by Saveyn *et al.* (2008) where the entire *Quercus robur* stem surface area above and below a stem cuvette was exposed to low light levels under controlled conditions.

Under natural conditions even larger errors in dormant season Q_{10} and $E_{stem}(ref)$ might arise, because in species that contain higher bark and/or xylem chlorophyll concentrations (Pfanz *et al.*, 2002), a larger axial diffusive flux might build up in the stem and confound dormant season stem respiration estimates. On the other hand larger trees with larger stems will have a thicker dead outer bark than the trees used in our study, thereby reducing the light that reaches the chloroplasts and the potential bias due to axial diffusion of respired CO_2. Moreover, in larger trees the volume of wood relative to the stem surface area would be higher, probably resulting in larger radial contribution to E_{stem} relative to axial diffusion. Nevertheless in larger dormant trees, axial diffusion of respired CO_2 is hypothesized to affect dormant season stem internal

[CO_2], which contributes to E_{stem} (Etzold *et al.*, 2013). Therefore accounting for the effect of axial diffusion of CO_2 when estimating Q_{10} and E_{stem}(ref) respiration coefficients might be crucial to understand and model stem respiration, at least from a mechanistic perspective. However, further validation of the magnitude of axial diffusion of CO_2 in larger trees and in other species is needed.

Our study, hence, illustrates the importance of accurate dormant season stem respiration estimates to generate realistic maintenance respiration data. While in actively transpiring trees during the growing season the impact of internal transport of respired CO_2 on E_{stem} has been established, our results show that axial diffusion of CO_2 induced by woody tissue photosynthesis might affect E_{stem} measurements in dormant trees. Our above findings led us to recommend additional shading in dormant trees of upper and lower stem sections adjacent to the opaque stem cuvette in order to avoid axial diffusion of respired CO_2 away from the site of respiration. This newly proposed methodology will lead to more accurate Q_{10} and E_{stem}(ref) estimates, particularly in 'open' forest stands with sufficient light penetration. These more accurate estimates will enable a more accurate quantification of dormant season stem respiration, which, in turn, is crucial to better understand stand-level respiration dynamics throughout the year.

- Chapter 6 -

Role of woody tissue photosynthesis in tree drought stress resilience

After: Bloemen J., Vergeynst L.L., Overlaet-Michiels L., and Steppe K. (2013). How important is woody tissue photosynthesis in poplar during drought stress?

Abstract

Within trees, a portion of the respired CO_2 is assimilated by woody tissue photosynthesis, but its physiological role in trees remains unclear, in particular under unfavourable conditions like drought stress. We measured leaf gas exchange (maximum leaf net photosynthesis (A_{max}) and transpiration rate (E)) and stem daily growth rate (DG) for *Populus deltoides x nigra* 'Monviso' trees under both well-watered and dry conditions. Half of the trees were subjected to a stem and branch light exclusion treatment to prevent woody tissue photosynthesis, while the others served as controls. We additionally determined bark chlorophyll concentration and measured cavitation in detached control and light-excluded branches to investigate the role of woody tissue photosynthesis in xylem embolism repair. We hypothesized that woody tissue photosynthesis will contribute to overall tree carbon gain both under sufficient water supply and during drought stress and that light-excluded trees will suffer faster and more dramatically from drought stress than (non light-excluded) control trees. Under well-watered conditions, light exclusion resulted in reduced stem DG relative to control trees. In response to drought, stem shrinkage of light-excluded trees was more pronounced as compared to control trees and A_{max} and E decreased more rapidly during drought stress for light-excluded trees compared to control trees. Results from our

acoustic xylem cavitation measurements confirmed the potential role of woody tissue photosynthesis in xylem embolism repair. Therefore, our study indicates that woody tissue photosynthesis may be a key factor in the resilience of trees to drought stress by maintaining both the plant carbon economy and hydraulic function.

6.1 Introduction

Chlorophyll in stem and branch tissues has been found to play a role in carbon acquisition. By assimilating respired CO_2, which is present at high concentrations in trees (**Chapter 1**), these photosynthetically active tissues photo-reduce CO_2 similarly as described for green leaves (Pfanz *et al.*, 2002; Berveiller *et al.*, 2007a). This re-assimilated CO_2 would otherwise be lost to the surrounding atmosphere, which explains why woody tissue photosynthesis is often described within the context of a tree carbon recycling mechanism (Aschan & Pfanz, 2003; Cernusak & Hutley, 2011).

Woody tissue photosynthetic rates are relatively low compared to leaf photosynthetic rates and it rarely results in a positive net CO_2 assimilation rate (Wittmann *et al.*, 2001). Wittmann *et al.* (2006) found that woody tissue photosynthesis was able to assimilate up to 97% of the dark respired CO_2 in young *Betula pendula* Roth. and Coe & McLaughlin (1980) reported a maximum re-assimilation of respired CO_2 of 31% for *Acer rubrum* branches, measured under dormancy. Other studies reported similar maximum re-assimilation values for other trees species (see Table 4 in Pfanz *et al.*, 2002), but overall the impact of woody tissue photosynthesis on plant carbon economy under normal conditions is expected to be limited.

Nevertheless, woody tissue photosynthesis might play an important role during particular events. Different authors consider woody photosynthesis as a potentially important means of bridging the carbon balance between defoliation and re-foliation (Bossard & Rejmanek, 1992; Wittmann *et al.*, 2001; Pfanz, 2008; Eyles *et al.*, 2009) or during bud development (Saveyn *et al.*, 2010). Other studies suggest that woody tissue photosynthesis might improve the stem carbon balance under limited water availability (Wittmann & Pfanz, 2008). In desert and semi-desert habitats, many drought-adapted plants have photosynthetic stems (Gibson, 1983; Nilsen & Sharifi, 1994), which

potentially provide a major fraction of the carbon used to sustain plant metabolism (Comstock & Ehleringer, 1990; Nilsen & Bao, 1990; Aschan & Pfanz, 2003). For temperate plants under moderate drought stress, decreased stomatal conductance can limit the assimilation of atmospheric CO_2 in the leaves (Flexas & Medrano, 2002; Chaves *et al.*, 2003), whereas woody tissue photosynthesis is supplied by endogenously respired CO_2 (Pfanz *et al.*, 2002; Aschan & Pfanz, 2003; Wittmann & Pfanz, 2008). Therefore, the fraction of tree carbon derived from woody tissue photosynthesis might become more important under drought conditions.

However, the exact role of woody tissue photosynthesis during drought stress is not yet well understood. Woody tissue photosynthesis has been shown to be less sensitive to drought stress than leaf photosynthesis (Nilsen, 1992). Moreover, Schmitz *et al.* (2012) hypothesized that woody tissue photosynthesis in xylary chloroplasts might be important for maintaining the hydraulic function of the vasculature, which is crucial during drought stress. Photosynthetic activity in these chloroplasts potentially fulfils local energetic and carbohydrate demands for repair of cavitated vessels (Zwieniecki & Holbrook, 2009; Secchi & Zwieniecki, 2011; Schmitz *et al.*, 2012) (**Box 1.2**). Therefore, by maintaining the carbon balance as well as the plant water status, woody tissue photosynthesis might play a crucial dual role in tree drought stress resilience.

In this study, we investigated the importance of woody tissue photosynthesis in 1-y-old poplar (*Populus deltoides x nigra* 'Monviso') trees under both well-watered and drought stress conditions. We measured photosynthesis and transpiration at leaf level and diameter growth at stem level (both manually and automatically) while manipulating the light availability to stem and branches (control and 100% light-excluded trees). We hypothesized that woody tissue photosynthesis will contribute to overall tree carbon gain both under sufficient water supply and during drought stress. We also hypothesized that light-excluded trees will suffer faster and more dramatically from drought stress than (non light-excluded) control trees. Finally, we tested the hypothesis of Schmitz *et al.* (2012) on the significance of woody tissue photosynthesis in maintaining hydraulic functioning of drought-stressed trees, by acoustically measuring xylem cavitation in branches of light-excluded and control trees (Perks *et al.*, 2004). We

hypothesized that the hydraulic functioning of xylem tissue in light-excluded trees will be less than in control trees.

6.2 Material and methods

6.2.1 Plant material and experimental design

1-y-old cutting-derived trees of *Populus deltoides x nigra* 'Monviso' were used for this study. Twelve cuttings were planted at the end of June 2012 in 50 l containers filled with a potting mixture (LP502D, Peltracom nv, Gent, Belgium) and slow-releasing fertilizer (Basacot Plus 6M, Compo Benelux nv, Deinze, Belgium) and grown in the greenhouse facility at the Faculty of Bioscience Engineering, Ghent University, Ghent, Belgium. Eight plants were selected based on uniform height (approximately 1.6 m) and stem diameter and were randomly assigned to two treatments. Four plants served as control, while the others were used for the light exclusion treatment, which started on 2 August 2012 (day of the year, DOY 214). The stem and woody branches of these light-excluded trees were loosely wrapped with aluminium foil following Saveyn *et al.* (2010), so gaseous diffusion from woody tissues to the atmosphere was not restricted. At this time, all trees were irrigated at least twice a week, ensuring adequate water supply. Subsequently, trees were irrigated for the last time on 30 September 2012 (DOY 273) to impose drought stress. No leaf fall occurred until one week after the start of the drought stress treatment. The fully developed leaf area before drought stress was determined by randomly sampling ten leaves per tree and multiplying this average leaf area with the number of leaves per tree. Leaf area ranged from 3.2 to 4.7 m^2 and from 2.8 to 3.9 m^2 for control and light-excluded trees, respectively, and average leaf area was not different between both treatments (P=0.20*)*.

6.2.2 Microclimate and plant measurements

Relative humidity (RH) in the greenhouse was measured with a capacitive RH sensor (Type hih-3610, Honeywell, Morristown, NJ, USA), air temperature (T_{air}) with a copper constantan thermocouple (Type T, Omega, Amstelveen, USA), and photosynthetic active radiation (PAR) with a quantum sensor (LI-190S, Li-COR, Lincoln, TE, USA). Sensors were installed at a height of approximately 2 m.

Plant measurements were performed from the beginning of July 2012 until mid-October 2012. Stem diameter variations were continuously measured with linear variable displacement transducers (LVDT; model DF5.0, Solartron Metrology, Bognor Regis, UK), installed with custom made stainless steel holders on one control tree and one light-excluded tree. Stem radial daily growth rate (DG) was calculated as the difference between two successive daily maximum values of the stem diameter. On 21 September 2012 (DOY 264), before the start of the drought stress, two additional trees (one control and one light-excluded tree) were instrumented with LVDT sensors. Continuous stem diameter measurements were complemented with weekly calliper-based manual measurements, performed between 10 h and 14 h. Two measurements were made at a height of 30 cm along perpendicular axes. Average DG derived from the manual measurements was calculated as the difference between two successive measurements divided by the elapsed time between both measurements.

At leaf level, maximum net photosynthesis (A_{max}, µmol CO_2 m^{-2} s^{-1}) and transpiration rate (E, mmol H_2O m^{-2} s^{-1}) were measured on all control and light-excluded trees on two fully expanded leaves per tree with a portable photosynthesis system (model Li-6400, Li-Cor, Inc., Lincoln, Nebraska, USA). Measurements were performed at 25°C, prevailing RH conditions, set atmospheric CO_2 concentration of 400 ppm and a PAR level of 1500 µmol m^{-2} s^{-1}. The latter was determined via a preliminary experiment in which light response curves were obtained for one leaf on six trees. Leaf gas exchange measurements were performed biweekly during the period before drought stress between 10 h and 16 h, and at a 2 d interval during the drought stress treatment. At each measurement time, the average of five measurements recorded at 10 s intervals was used for the analysis.

6.2.3 Cavitation measurements

To test the hypothesis of Schmitz *et al.* (2012) on light-dependent repair of cavitated vessels by woody tissue photosynthesis, we performed a dehydration experiment in the lab on cut branches of one non-instrumented control and one light-excluded tree, while acoustically measuring xylem cavitation as described in Lo Gullo & Salleo (1993) and Rosner *et al.* (2006). Measurements were repeated three times: once 9 days before the start of the drought stress treatment (21 September 2012, DOY 265) and twice during

the drought stress treatment (i.e. 5 and 20 days after the start of the drought stress treatment, 5 and 19 October 2012, DOY 279 and 293, respectively). After cutting the branches, the outer end was covered with parafilm to prevent dehydration before the start of the measurement. In the lab, one acoustic emission (AE) sensor (VS150-M sensor and ASCO-P signal conditioner, Vallen systeme, Icking, Germany) was installed per branch. The AE sensors were clamped to the middle of the branches according to Rosner *et al.* (2009). Measurements were performed over a 60 h time span. The maximum peak amplitude per second was recorded using a data acquisition system (Type NI USB 6009, National Instruments, Austin, Texas, USA) and software (Labview 8.2, National Instruments, Austin, Texas, USA). The acoustic signals above a certain threshold were assumed to occur due to cavitation of xylem vessels. The threshold was set at the background noise level (35.5 and 31 dB) and was determined by waving the sensors in the air. The cumulated number of acoustic signals was determined over the 60 h measurement period.

6.2.5 Measurements of bark chlorophyll concentration

We determined the effect of the light exclusion treatment on bark chlorophyll concentration by randomly sampling the bark of stems of two additional control and light-excluded trees on two dates: at the day of light exclusion (2 August 2012, DOY 214) and 53 days after the start of light exclusion (24 September 2012, DOY 267). At the end of the measurement period, 99 days after the start of light exclusion (9 November 2012, DOY 313), bark was sampled from all control and light-excluded trees. Per stem, three samples were randomly collected, immediately frozen in liquid nitrogen and stored at -80°C. Samples were ground (A11 basic analytic mill, IKA-Werke GmbH & Co. KG, Staufen, Germany) and chlorophyll was extracted by adding 7.5 ml aceton (80%) to 150 mg of sample. After 24 h extraction in the dark, samples were centrifuged and the supernatant was transferred to a glass cuvette and analyzed for chlorophyll concentration as described in **Chapter 5**.

6.2.6 Statistical analysis

Data from automated measurements were recorded at 1 min intervals with a datalogger (CR1000, Campbell Scientific, Logan, Utah, USA) and averaged over 30 min intervals. Data were analyzed using Excel 2007 (Microsoft Inc., Redmond, WA, USA).

DG derived from manual and automated measurements, leaf gas exchange data (A_{max} and E) and bark chlorophyll concentration were analyzed using a repeated measures multi-factorial analysis of variance (ANOVA). DG data from manual measurements were confined to those taken during the well-watered conditions with treatment (n=2) and date (n=16) treated as fixed factors and individual tree (n=8) as random factor. A similar model was used to analyze DG data from the automated measurements. In this case our data was derived from a lower number of individual trees (n=4) and confined to the measurements taken one week before and during the drought stress treatment (date, n=16). Similarly, A_{max} and E measurements were confined to those taken during the drought stress treatment (date, n=12) with a higher number of tree replicates (individual tree, n=8). Bark chlorophyll concentration was analyzed with date (n=3), treatment (n=2) and repetition (n=3 per tree) as fixed factors, and tree (n=2 per treatment for the first two dates and n=4 for the last date) as random factor. Treatment means were compared using Fisher's least significant difference test. Akaike Information Criterion corrected for small sample sizes (AICc) was used to determine the covariance structure that best estimated the correlation among individual trees over time. All analyses were performed using the mixed model procedure (PROC MIXED) of SAS (Version 9.1.3, SAS Inc., Cary, NC, USA) with α=0.05.

6.3 Results

6.3.1 Daily growth rate

Light exclusion of the stem and woody branches had an impact DG under both well-watered and drought conditions. Before light exclusion, DG derived from manual stem diameter measurements was similar for both treatments (Fig. 6.1). However, during light exclusion, DG of light-excluded trees was systematically lower than those calculated for the control trees. Significant differences (P<0.05) in DG between both

treatments were observed at specific dates throughout the well-watered period. The average overall stem diameter increment over the period July-September was smaller for the light-excluded trees (4.00 ± 0.12 mm) than for the control trees (5.28 ± 0.57 mm), indicating a 24% impact of light exclusion on stem growth during the period July-September.

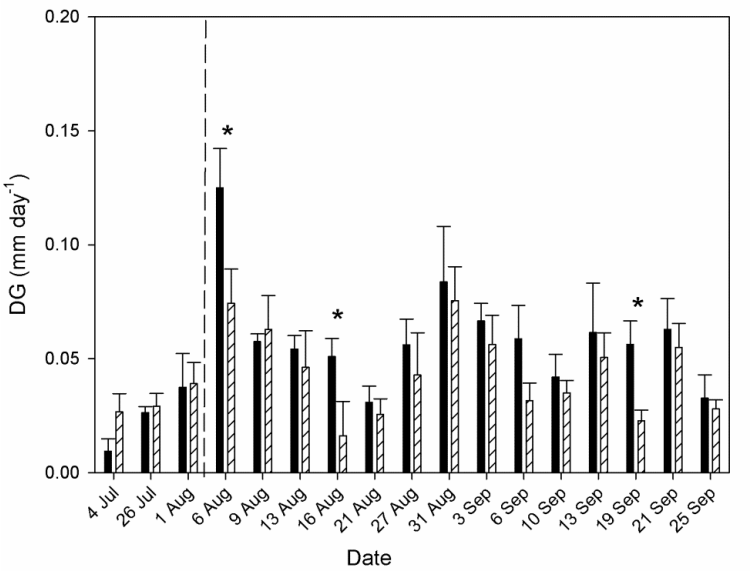

Fig. 6.1 Radial daily stem growth rate (DG) under well-watered conditions derived from manual stem diameter measurements and averaged for control (black) and light-excluded (hatched) trees (n=4 per treatment). DG was calculated as the difference between two successive measurements divided by the elapsed time between both measurements. The dashed line indicates the start of light exclusion of the stem and woody branches. Asterisks indicate significant (P<0.05) differences in DG between both treatments at each observation. Bars indicate standard error of the mean.

During drought stress, LVDT-based measurements indicated that stems of control and light-excluded trees shrank, resulting in a negative DG (Fig. 6.2). Before the onset of drought stress, DG was within the same range as observed for estimates from manual measurements (Fig. 6.1). During drought stress, DG of control trees decreased gradually over time, as expected. However, DG of light-excluded trees first decreased and then slightly increased until five days after the start of the drought stress. Thereafter, DG again decreased to a level lower than observed for the control trees, indicating that at this time light-excluded trees were shrinking faster than control trees (Fig. 6.2).

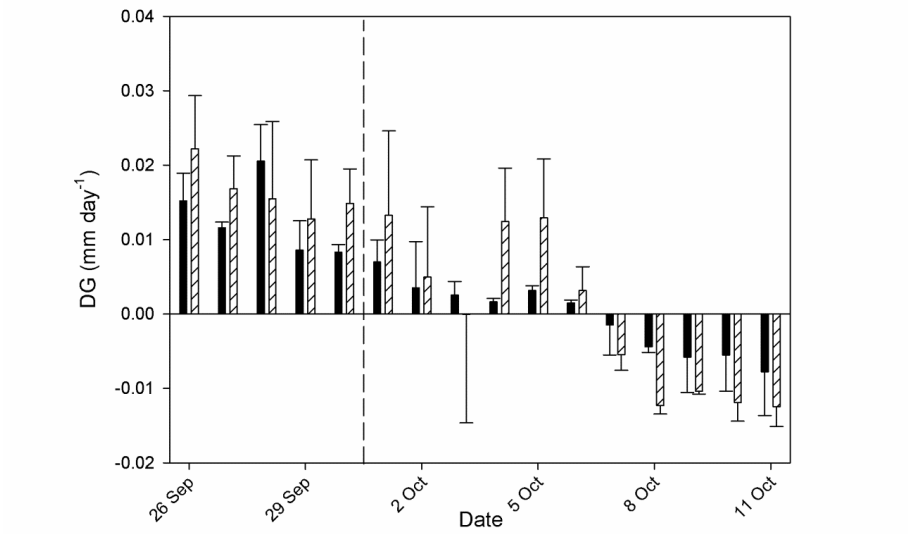

Fig. 6.2 Radial daily stem growth rate (DG) before and during drought stress derived from automated measurements of the stem diameter and averaged for control (black) and light-excluded (hatched) trees (*n*=2 per treatment). DG was calculated as the difference between two successive daily maximum values of the stem diameter. The dashed line indicates the timing of last irrigation before the onset of drought stress. No significant differences ($P<0.05$) in DG between both treatments were observed. Bars indicate standard error of the mean.

6.3.2 Maximum net photosynthesis and transpiration rate

Light exclusion of the stem and woody branches had additionally an impact on leaf gas exchange during drought stress (Fig. 6.3). Before drought stress, similar rates of A_{max} were observed in leaves of control and light-excluded trees. During the drought treatment, A_{max} in light-excluded trees started to decrease about three days earlier than in control trees (4 versus 7 October, Fig. 6.3A) and this was approximately simultaneous to the onset of negative DG during drought stress (Fig. 6.2). A similar difference between control and light-excluded trees was observed in E (Fig 6.3B). Where E of light-excluded trees gradually decreased from 1 October onwards, E of control trees tended to increase to a local maximum at 7 October before finally decreasing to lower rates. Finally, near the end of the drought stress period, similar A_{max} and E rates were observed in both treatments.

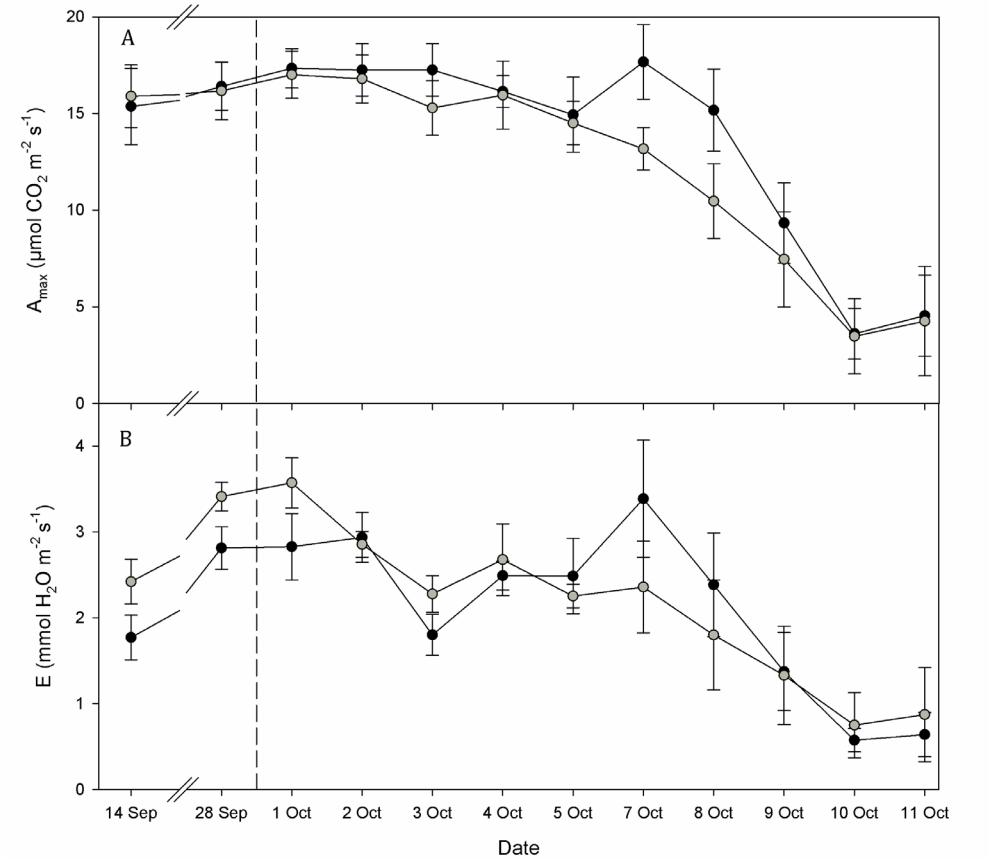

Fig. 6.3 Maximum leaf net photosynthesis (A_{max}) (A) and transpiration rate (E) (B) before and during drought stress, averaged for leaves (*n*=2 per tree) of control (black circles) and light-excluded (grey circles) trees (*n*=4 per treatment). The dashed line indicates the timing of the last irrigation before the onset of drought stress. No significant differences (*P*<0.05) in A_{max} neither E between both treatments were observed. Bars indicate standard error of the mean.

6.3.3 Cavitation

Our results on the AE detection of xylem cavitation in branches of control and light-excluded trees indicate that woody tissue photosynthesis might play an important role in cavitation repair during drought stress. While the cumulative number of acoustic hits was similar in branches of control and light-excluded trees before being subjected to drought stress (Fig. 6.4), we found a larger cumulative number of acoustic hits in the control branches five days after the start of the drought stress treatment (Fig. 6.4). This indicated that more xylem vessels in control branches were hydraulically functional just

before being excised compared to light-excluded ones so that more vessels could still cavitate during the three-day dehydration of the excised branch. Finally, 20 days after the start of the drought stress treatment, a low cumulative number of hits were recorded (Fig. 6.4), regardless of the treatment, implying that the majority of the xylem vessels in the branches were already cavitated before the last branch dehydration experiment started.

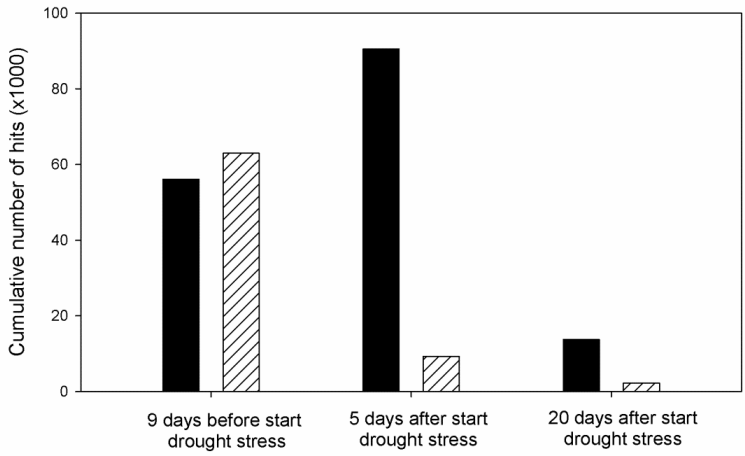

Fig. 6.4 Cavitation in branches of control (black) and light-excluded (hatched) trees measured as the cumulative number of acoustic emissions (AE) over a 60 h dehydration period. Measurements were repeated three times: at 9 d before the start of the drought stress treatment (22-24 September 2012), and 5 and 20 d after the start of the drought stress treatment (5-7 and 19-21 October 2012), respectively. The larger the cumulative number of acoustic hits, the more xylem vessels were hydraulically functional just before being excised and the more vessels could thus still cavitate during dehydration.

6.3.4 Bark chlorophyll concentration

Stem and branch light exclusion clearly affected bark chlorophyll concentration. At the start of the light exclusion treatment, similar bark chlorophyll concentrations were detected in the bark of control and light-excluded trees (Table 6.1).

However, light exclusion resulted in a significant decrease in bark chlorophyll concentration, whereas bark chlorophyll concentration in control trees (no light exclusion) increased over time. In particular, 99 days after the start of the light exclusion treatment, when bark of all control and light-excluded trees was sampled, a large difference was observed in bark chlorophyll concentration between both treatments (Table 6.1).

Table 6.1 Chlorophyll concentration (mg Chl g FW^{-1}) of bark, randomly sampled from *Populus deltoides x nigra* 'Monviso' trees, on different dates (2 August 2012, 24 September 2012, and 9 November 2012) during the light exclusion experiment. On the first two dates, bark was sampled (*n*=3 per tree) from additional trees (*n*=2 per treatment) treated similarly as the measured control and light-excluded trees, while on the last date bark was sampled from all control and light-excluded trees (*n*=4 per treatment). Data are averaged (± SE) per treatment for all samples and all trees. Different letters indicate significant differences in chlorophyll concentration between treatments for a specific date (*P*<0.001).

Treatment	Day of light exclusion	53 days after start light exclusion	99 days after start light exclusion
Control	0.33 ± 0.03[a]	0.41 ± 0.01[a]	0.73 ± 0.02[a]
Light-excluded	0.38 ± 0.02[a]	0.24 ± 0.01[b]	0.28 ± 0.01[b]

6.4 Discussion

Since the first observation of chlorophyll containing woody tissues early 20th century, a large number of studies have been performed on the nature and magnitude of woody tissue photosynthesis in trees (Bossard & Rejmanek, 1992; Nilsen, 1995; Cernusak & Marshall, 2000; Wittmann *et al.*, 2001; Pfanz *et al.*, 2002; Berveiller *et al.*, 2007a) (**Chapter 1**). This photosynthetic tissue uses respired CO_2 as substrate, thereby partially compensating for the loss of carbon by respiration while providing carbon compounds for tissue synthesis or to sustain plant metabolism (Cernusak *et al.*, 2001). The overall supply of carbon by woody tissue photosynthesis as compared to the fraction of carbon derived from leaf level photosynthesis is assumed to be small (Aschan & Pfanz, 2003). However, woody tissue might play an important role as a means to guarantee photosynthate supply when trees are leafless due to environmental (e.g. due to herbivory or fungal disease) or phenological conditions (Pfanz, 2008; Eyles *et al.*, 2009; Saveyn *et al.*, 2010).

In our study, we observed that light exclusion of the stem and the woody branches of foliated *Populus deltoides x nigra* 'Monviso' trees resulted in a decreased DG and bark chlorophyll concentration, implying that even under well-watered growing conditions woody tissue photosynthesis can significantly contribute to the overall plant carbon income. Previously, Saveyn *et al.* (2010) combined a similar light exclusion treatment with stem diameter measurements and observed a reduction in stem diameter and stem

chlorophyll concentration for light-excluded trees of different native Californian species: *Prunus ilicifolia*, *Umbellularia californica* and *Arctostaphylos manzanita*. Based on isotope analysis of wood samples of covered and uncovered branch sections of *Eucalyptus miniata*, Cernusak & Hutley (2011) calculated that 11% of newly formed branch tissue was constructed from stem assimilates. Our estimates of stem increment during the period July-September for control and light-excluded trees indicated that the contribution of woody tissue photosynthesis to radial stem growth was around 24% for *Populus deltoides x nigra* 'Monviso'. Therefore, a large fraction of the sugars derived from stem photosynthesis might rapidly enter pools which are directly or indirectly used in stem growth. Moreover, results from the study of Powers & Marshall (2011) indicated that stem synthesized sugars might be loaded in the phloem and distributed to the other parts of the tree in the order of days. However, lower contributions might be observed for older trees or for species that contain lower concentrations of chlorophyll in their stem and branch tissues (Aschan & Pfanz, 2003). In foliated trees, xylem-transported CO_2 derived from below- and aboveground respiration is available as substrate for woody tissue photosynthesis, besides locally respired CO_2 (McGuire *et al.*, 2009; Bloemen *et al.*, 2013a; 2013b) (**Chapter 1**). During leafless periods, woody tissue photosynthesis solely relies on locally respired CO_2 (**Chapter 5**), which internally concentrates due to the high resistance to radial CO_2 diffusion exerted by woody tissues (Steppe *et al.*, 2007). Therefore, woody tissue photosynthesis in foliated trees may benefit from this additional substrate source and use CO_2 respired in organs remote from the site of assimilation to maintain the local stem and branch carbon status.

More importantly, our study shows that woody tissue photosynthesis might play an important role in tree drought stress resilience. While leaf photosynthesis converts atmospheric CO_2 into carbohydrates, woody tissue photosynthesis relies on endogenously respired CO_2 for sugar synthesis, which makes this process less vulnerable to potentially lethal tissue dehydration under drought conditions (Comstock & Ehleringer, 1988; Nilsen, 1992; Wittmann & Pfanz, 2008). Moreover, the low peridermal water vapour conductance as compared to leaf conductance leads to a high water use efficiency (Wittmann & Pfanz, 2008). In particular in desert and semi-desert environments, where water scarcity is considered as the most important abiotic

constraint for plant growth (Aschan & Pfanz, 2003), plants are assumed to benefit from photosynthesis in green non-leaf tissues. We observed that the stem of light-excluded *Populus deltoides x nigra* 'Monviso' trees tended to shrink more drastically in response to severe drought stress than observed in stems of control trees. Growth processes are known to be very sensitive to drought stress (Hsiao, 1973; Steppe *et al.*, 2006; Saveyn *et al.*, 2007a) and are related to the water status of living stem tissues, of which the cell turgor pressure in the stem tissue is a good measure (Bradford & Hsiao, 1982). In living plant tissues, cell turgor and volume can be maintained by osmotic adjustment (i.e. the accumulation of solutes in the symplast, for instance sugars) (Woodruff *et al.*, 2004; Saveyn *et al.*, 2007a). Sugars synthesized in chlorophyll containing woody tissues are potentially used to maintain cell turgor, which might explain why stems of light-excluded trees tended to shrink more drastically relative to control trees. Stem growth cessation can additionally be explained by a decrease in carbohydrate supply under drought stress (Saveyn *et al.*, 2007b; Steppe *et al.*, 2008; Lavoir *et al.*, 2009; De Schepper & Steppe, 2010; Simpraga *et al.*, 2011). We observed that stem shrinkage under drought stress (i.e. a negative daily growth rate) occurred simultaneously with the pronounced decrease in A_{max}, regardless of the treatment. Leaf photosynthesis measured under drought conditions tended to decline more rapidly when woody tissue photosynthesis was impeded by light exclusion. In contrast to previous assumptions (Wittmann & Pfanz, 2008), we believe that the role of woody tissue photosynthesis in maintaining the carbon status of temperate species under drought stress conditions might extend beyond the stem level.

While past studies mainly described woody tissue photosynthesis from a plant water use efficiency perspective, recent results indicate that stem and branch CO_2 assimilation might directly affect the xylem hydraulic pathway in drought-stressed plants. In these plants, the decrease in hydraulic function due to xylem cavitation has been considered as the main source of productivity loss (Logullo & Salleo, 1993; Hacke *et al.*, 2000; Zwieniecki & Holbrook, 2009). Cavitation of water transporting vessels typically results from the expansion of a vapour/gas void within the liquid phase, when xylem tension exceeds the inward pressure due to the curvature of the void's gas/water interface (Zwieniecki & Holbrook, 2009; Secchi & Zwieniecki, 2011), generating a pressure-wave

induced ultra-sonic emission which can be detected acoustically (Milburn & Johnson, 1966; Tyree & Dixon, 1983; Rosner *et al.*, 2006). Recovery from cavitation may occur under suitable conditions (McCully *et al.*, 1998; Perks *et al.*, 2004; Zufferey *et al.*, 2011) but the actual mechanisms that allow plants to refill embolized xylem conduits and thereby maintain the hydraulic function is still under debate (Clearwater & Goldstein, 2005; Zwieniecki & Holbrook, 2009). Most recent studies hypothesize that sugars play a crucial role in the creation of an osmotic driving force to refill embolized xylem vessels (Secchi & Zwieniecki, 2011) and in the chemical sensing of cavitation (Zwieniecki & Holbrook, 2009).

In this context, woody tissue photosynthesis in chlorophyll containing xylem parenchyma cells might play a role in the local provision of these sugars, in addition to sugars derived from local phloem unloading (Nardini *et al.*, 2011) (**Box 1.2**). In spite of our limited number of replicates, our acoustics measurements illustrate that woody tissue photosynthesis potentially plays an important role in drought-stressed cavitation repair in poplar, as observed previously for mangrove species (Schmitz *et al.*, 2012). Xylem vessels in branches of control drought-stressed trees were probably hydraulically more functional compared to vessels in light-excluded trees, detected as high number of acoustics events during the dehydration experiment. In addition, we performed a qualitative analysis of the acoustic events, based on amplitude analysis, and clear differences were recorded in amplitude distribution between both branches. In the control branches, a number of events with a lower amplitude occurred near the end of the dehydration period measured five days after drought stress. Wolkerstorfer *et al.* (2012) observed similar late low-amplitude acoustic hits when measuring cavitation acoustically during a dehydration experiment and attributed these events to cell wall deformations in the wood, induced by changes in cell wall structure under dehydration (Jakob *et al.*, 1994; 1995). Additional correction for these low-amplitude acoustic signals for our control branches as suggested by Wolkerstorfer *et al.* (2012) resulted in a reduced number of acoustic hits (i.e. 45675 hits), but the total number was still substantially higher than recorded for our light-excluded branches.

Long-term light exclusion treatment probably hindered refilling of the embolized xylem vessels due to the lack of local leakage of sugars from the parenchyma cells into the

xylem vessels. Similarly, Schmitz *et al.* (2012) observed that hydraulic conductivity of mangrove branches decreased following light exclusion. At leaf level, a similar xylem embolism repair mechanism might exist by chlorophyll containing bundle sheath cells in the petiole (Griffiths *et al.*, 2013), which are potentially supplied with either malate from the roots (Hibberd & Quick, 2002) or dissolved respired CO_2 (Bloemen *et al.*, 2013b) transported via the xylem. Stem hydraulics, which is strongly dependent on cavitation of xylem vessels, directly affects leaf water status because plants supply water to their leaves dependent on the degree of cavitation (Hacke *et al.*, 2000). Therefore, the differences in the extent of cavitation repair observed between both treatments might explain why during our measurements transpiration in leaves of light-excluded and control trees responded differently to drought stress, in particular around five days after the start of the drought stress.

In summary, our results expand on our current knowledge on the role of woody tissue photosynthesis in plant functioning under well-watered and drought conditions. Our study shows that assimilation of respired CO_2 might play a dual role in tree drought stress resilience. The sugars synthesized in chlorophyll containing woody tissues might either be used to meet the metabolic carbon demand of drought-stressed plants or to maintain the hydraulic function of the xylem. In particular, the significance of woody tissue photosynthesis in providing local sugars for maintaining cell turgor or in xylem embolism repair merits further study. Therefore, future studies that aim at a full understanding of plant drought stress resilience should consider including measurements of woody tissue photosynthesis.

- Chapter 7 -

Tree girdling confirms that root-respiration contributes to xylem CO_2 transport

After: Bloemen J., Agneessens L., Van Meulebroek, L., Aubrey D.P., McGuire M.A., Teskey R.O., and Steppe K. (2013) Stem girdling affects the quantity of CO_2 transported in xylem as well as CO_2 efflux from soil. *New Phytologist.* in press (doi: 10.1111/nph.12568).

Abstract

There is recent clear evidence that an important fraction of root-respired CO_2 is transported upward in the transpiration stream in tree stems rather than fluxing to the soil. In this study, we aimed at quantifying the contribution of root-respired CO_2 to both soil CO_2 efflux (E_{soil}) and xylem CO_2 transport by manipulating the autotrophic component of belowground respiration. We compared E_{soil} and the flux of root-respired CO_2 transported in the transpiration stream (F_t) in girdled and non-girdled 9-y-old oak trees (*Quercus robur* L.) to assess the impact of a change in the autotrophic component of belowground respiration on both CO_2 fluxes. Stem girdling decreased xylem CO_2 concentration indicating that belowground respiration contributes to the aboveground transport of internal CO_2. Girdling also decreased E_{soil}. These results confirm that root respiration contributes to xylem CO_2 transport and that failure to account for this flux results in inaccurate estimates of belowground respiration when efflux-based methods are used. This research adds to the growing body of evidence that efflux-based measurements of belowground respiration underestimate autotrophic contributions.

7.1 Introduction

In forests, soil CO_2 efflux (E_{soil}) contributes between 30 and 80% to total ecosystem respiration (Goulden *et al.*, 1996; Davidson *et al.*, 2006b) thereby representing the second largest carbon flux after photosynthesis (Davidson *et al.*, 2002; Bond-Lamberty *et al.*, 2004; Subke *et al.*, 2011). As mentioned in **Chapter 1**, the different sources of belowground respiration contributing to E_{soil} can be divided into those originating from living roots, their mycorrhizal fungal symbionts, and rhizosphere micro-organisms (autotrophic component of belowground respiration, $R_{a,b}$) and those from the decomposition of dead organic matter in the bulk soil (heterotrophic component of belowground respiration, $R_{h,b}$) (Edwards *et al.*, 1970; Bowden *et al.*, 1993). Accurate estimates of both $R_{a,b}$ and $R_{h,b}$ are needed to better understand the dynamics in E_{soil}, which is a crucial component in modeling the carbon cycle in forests (Scott-Denton *et al.*, 2006).

By removing a circumferential band of bark and phloem from a tree stem during girdling, the downward transport of photosynthates to roots and associated rhizomicrobial organisms is interrupted (De Schepper *et al.*, 2010), which reduces $R_{a,b}$ (Kuzyakov & Gavrichkova, 2010) while water and nutrient transport in the upward direction in the xylem can continue (Högberg *et al.*, 2001; Frey *et al.*, 2006). Among various forest ecosystems, E_{soil} was reduced by girdling between 24 and 65% relative to E_{soil} measured in non-girdled control plots (see Table 1 in Högberg *et al.*, 2009), illustrating the importance of $R_{a,b}$ contribution to forest E_{soil}. However, these estimates were potentially biased by root death (Bhupinderpal-Singh *et al.,* 2003*)* or increased use of starch (Högberg *et al.*, 2001; Frey *et al.*, 2006) after girdling.

Previous studies of E_{soil} might also have underestimated $R_{a,b}$ because the upward transport of root-respired CO_2 with the transpiration stream (F_t) was not considered. With simultaneous measurements of sap flow and CO_2 concentration ($[CO_2]$) in stems and E_{soil} in an eastern cottonwood (*Populus deltoides*) stand, Aubrey & Teskey (2009) estimated that twice the amount of CO_2 derived from $R_{a,b}$ was transported internally via the xylem compared with that which diffused into the soil environment (**Chapter 1**). This xylem-transported CO_2 contributes to high internal CO_2 concentrations in tree stems (**Chapter 1**), which affects efflux from stems, and is not accounted for with

conventional efflux-based measurements of belowground respiration. Grossiord *et al.* (2012) observed similar internal transport of CO_2 derived from $R_{a,b}$ in *Eucalyptus*, however in a smaller quantity than observed by Aubrey & Teskey (2009). Nevertheless, xylem transport of root-respired CO_2 raises important questions about our understanding of respiration (Hanson & Gunderson, 2009), which is potentially misestimated in studies that neglect to account for it (Aubrey & Teskey, 2009) (**Chapter 1**).

To account for the contribution of $R_{a,b}$ to both F_t and E_{soil} (**Fig 1.12**), we made measurements of sap flow, internal $[CO_2]$, and E_{soil} at high temporal resolution in girdled and non-girdled oak (*Quercus robur* L.) trees. Stem girdling was used to manipulate the contribution of $R_{a,b}$ to belowground respiration. We addressed the following hypotheses: (1) root-respired CO_2 in *Quercus robur* trees does not solely diffuse into the soil environment, rather, a portion dissolves in xylem sap and is transported upward in the transpiration stream; and (2) estimates of belowground respiration based on conventional E_{soil} measurements underestimate $R_{a,b}$ in particular at high sap flow rates (F_s) during the daytime.

7.2 Material and methods

7.2.1 Study site

Two plots of 90 m^2 were established within the plantation, each containing six trees. In each plot, three trees were randomly selected for measurement. Average diameter at stem base and breast height (DBH) was 11.5 ± 0.9 and 6.7 ± 0.6 cm, respectively, in the first (non-girdled) plot, hereafter referred to as the control treatment, and 11.1 ± 0.3 cm and 6.1 ± 0.7 cm in the second (girdled) plot, hereafter referred to as the girdling treatment (Table 7.1). We focused on one control and one girdling plot, because we had limited equipment for the detailed continuous measurements of soil CO_2 efflux (E_{soil}), internal CO_2 concentration ($[CO_2]$), sap flow, and environmental parameters. These measurements at high temporal resolution were essential to understand short term responses in belowground dynamics after stem girdling. The day before girdling, six undisturbed soil samples (0-30 cm depth) were taken per plot to determine soil bulk

density and an additional eight soil subsamples per plot were taken with a soil corer and mixed to a composite sample to determine pH, organic carbon and soil texture for each plot. Analyses of soil bulk density and other soil properties were performed as described by D'Haene *et al.* (2008). In addition, near the end of September (23 September 2011, day of year (DOY) 266), soil samples were taken at 0-30 cm depth at two locations within 1 m of each tree from which roots were collected and dried to constant weight to determine average root biomass density per plot.

Table 7.1 Stem diameter at base (0.1 m, cm) and breast height (DBH, cm) and distance from the plot center (m) for three *Quercus robur* trees selected for measurement in the control and girdling treatment plots.

Treatment	Tree	Diameter at 0.1m	DBH	Distance from center
Control	**1**	11.0	6.6	5.1
	2	10.9	6.1	4.2
	3	12.6	7.4	3.1
Girdling	**1**	11.1	5.2	3.5
	2	11.2	6.6	4.7
	3	11.1	6.4	4.1

In the centre of each plot, soil temperature and soil moisture were recorded at 7.5 and 22.5 cm with a type-T thermocouple (Omega, Amstelveen, The Netherlands) and soil moisture probe (SM-300, Delta-T, Cambridge, UK), respectively. Air temperature (T_{air} ; type-T thermocouple, Omega, Amstelveen, The Netherlands) and relative humidity (RH; Hygroclip, Rotronic AG, Bassersdorf, Switzerland) were measured on site and used to calculate vapour pressure deficit (VPD). All data were recorded at 1 min interval with a datalogger (CR1000, Campbell Scientific, Logan, Utah, USA). Atmospheric pressure was obtained from a weather station located 7 km from the site.

7.2.2 Girdling treatment

On 5 August 2011 (DOY 217), the girdling treatment was applied to the six trees in the girdled plot by carefully removing a 5.5 cm wide circumferential band of bark and phloem at a height of 50 cm from the stem without damaging the xylem tissue (Fig. 7.1). The exposed xylem was covered with clear plastic film to prevent tissue dehydration and to allow visual inspection for formation of new bark tissue, which was removed

when it occurred. In addition to the trees in the girdled plot, four trees in close proximity to the selected trees but outside the plot were girdled to avoid possible edge effects from ingrowing roots of non-girdled trees. The trees in the control plot were left intact.

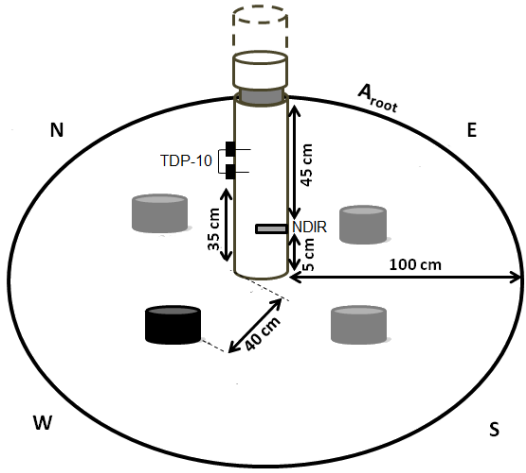

Fig. 7.1 Schematic of the experimental set up, indicating the distances and positions of the tree girdle and equipment installed on the stem and within the soil area occupied by the roots (A_{root}) to measure the flux of root-respired CO_2 transported in the transpiration stream (F_t) and soil CO_2 efflux (E_{soil}). The black and grey chamber(s) represent the measurement of E_{soil} with automated and manual chambers, respectively. Displayed chambers were located at 40 cm from the stem. NDIR, non-dispersive infrared CO_2 sensor; TDP, thermal dissipation probe. The stem thermocouple, installed 3 cm above the NDIR sensor and the manual chambers for E_{soil} measurements performed at 70 cm from the stem are not shown.

7.2.3 Soil CO_2 efflux measurements

For automated measurements of E_{soil}, a PVC chamber (20 cm diameter, 15 cm height, design adapted from Suleau *et al.* (2009)) (**Fig. 1.13A,B**), was inserted 2 cm into the soil 40 cm from the stem base of each tree (Fig. 7.1). A pump (KNF Neuberger GmbH, Freiburg, Germany) was used to circulate air from the chambers to an infrared gas analyzer (GMP 343, Vaisala inc., Helsinki, Finland) via a gas multiplexer system. At the start of a measurement cycle, the collar top of the first chamber was opened in half-open position for 1 min to allow flushing of the tubes before the chamber was closed for 4 min to determine the increase in [CO_2]. Chamber [CO_2] was recorded at a 12 s interval with a datalogger (CR1000x, Campbell Scientific, Logan, Utah, USA). Finally, the collar top was opened. The remaining five chambers were measured sequentially in a similar manner

to complete the measurement cycle. One measurement cycle lasted 30 min and measurements were made alternately in chambers in the control and girdling treatments. Based on the increase in [CO_2] in the chambers over time, E_{soil} was calculated and analyzed as described by Savage *et al.* (2008). The most linear section in increase in [CO_2] over time was identified and the rate of increase (slope) over time was calculated, but only accepted if the coefficient of determination of the linear regression (i.e., R^2) >0.90. Slope estimates were scaled by chamber cross-sectional area and corrected for T_{air} and atmospheric pressure (P) to yield the CO_2 efflux rate, according to Savage *et al.* (2008).

Automated measurements of E_{soil} were complemented with manual measurements (EGM-4 analyzer connected to a SRC-1 chamber, PP systems, Amesbury, Massachusetts, USA) to account for variation in E_{soil} within the rooting area among the different cardinal directions. These measurements were performed on three additional PVC collars (diameter 20 cm, height 12 cm) installed 40 cm from each stem (Fig. 7.1). Later in the growing season (from DOY 231, 19 August 2011 onwards) we performed additional manual measurements with collars installed 70 cm from each stem to account for spatial variation in E_{soil}. Manual data were collected at a three-day interval. Both manual and automated measurements continued for 1.5 months after girdling.

7.2.4 Xylem transport of root-respired CO_2

The six selected trees in the control and girdled plots (three per plot) were instrumented to measure the transport of root-respired CO_2 via the transpiration stream (F_t) simultaneously with E_{soil}. We quantified F_t based on measurements of sap flow rate (F_s) and concentration of dissolved CO_2 in the xylem ([CO_2*]) based on **Equation 1.5.**

Xylem gaseous [CO_2] was measured in situ by inserting non-dispersive infrared (NDIR) CO_2 sensors (model GMM221; Vaisala Inc., Helsinki, Finland) in the base of each stem 5 cm above the soil (Fig. 7.1). Stem temperature (T_{stem}) was recorded in all trees with a type-T thermocouple (Omega, Amstelveen, The Netherlands), installed at 3 cm from the NDIR sensor. We assumed that xylem [CO_2] measured at stem base represented the [CO_2] of xylem sap entering the stem from belowground. Xylem [CO_2] was corrected for T_{stem} and atmospheric pressure based on **Equation 1.2**. Due to technical problems with

the sensors, data for the control trees was limited to the period from 30 July 2011 (DOY 211) till 13 August 2011 (DOY 225). [CO_2*] was calculated using Henry's law coefficients from xylem [CO_2], T_{stem} and biweekly measurements of xylem sap pH (McGuire & Teskey, 2002; Erda *et al.*, 2013), according to **Equation 1.3**. To obtain xylem pH, sap was expressed from excised twigs of nearby non-girdled trees with a pressure chamber (PMS Instruments, Corvallis, Oregon, USA). The expressed sap was transferred with a pipette to a solid-state pH microsensor connected to a pH meter (Hi 9124, Hanna instruments Ltd., Bedfordshire, UK). Mean pH of biweekly samples from five trees during the measurement period was 6.8 ± 0.1. F_s was determined by scaling sap flow density (SFD) with sapwood area. SFD was measured using thermal dissipation probes (model TDP-10, Dynamax Inc., Houston, Texas, USA) installed in each stem at 35 cm height with a vertical needle separation of 40 mm (Fig. 7.1). Zero flow was calculated based on the mean temperature difference (ΔT) between the needles from 03:00 to 05:00 h, assuming no or very limited nocturnal transpiration. Additional trees from the site were used to calibrate the sap flow sensors using a Mariotte-based verification system (Steppe *et al.,* 2010) and generate a site- specific calibration parameter (k) for oak, as recommended by Bush *et al.* (2010), Steppe *et al.* (2010), and Sun *et al.* (2011). Stem [CO_2], temperature, and SFD were recorded with a datalogger (CR1000, Campbell Scientific, Logan, Utah, USA) at 1 min interval.

Because E_{soil} is expressed on a m^2 area basis, F_t was scaled ($F_{t,scaled}$, mg C m^{-2} h^{-1}) with the soil area occupied by the roots (A_{root}, m^2) based on **Equation 1.6**.

To estimate A_{root}, we excavated the entire root system of three additional trees at the same site with similar dimensions as the measured trees. Based on the radii of A_{root} for the three additional trees (0.8, 1.2, and 0.9 m) we estimated average A_{root} as equal to a circular area around the trees with radius 1 m (3.14 m^2), as shown in Fig. 7.1. Manual and automated E_{soil} point measurements performed within this area were assumed to represent average E_{soil} within A_{root}.

7.2.5 Estimation of the autotrophic component of belowground respiration

We estimated $R_{a,b}$ using two methods. The first estimate of $R_{a,b}$ was made according to the approach used in previous girdling studies ($R_{a,b\text{-}conv}$), where $R_{a,b}$ (mg C m^{-2} h^{-1}) is

assumed to be equal to the difference in average E_{soil} between the control ($E_{soil\text{-}c}$) and girdling ($E_{soil\text{-}g}$) treatments, hereafter referred to as the conventional approach:

$$\mathbf{R_{a,b-conv} = (E_{soil-c} - E_{soil-g})} \quad (7.1)$$

The second estimate of $R_{a,b}$ ($R_{a,b\text{-}new}$) additionally accounts for internal transport of root-respired CO_2 by including the difference in average $F_{t,scaled}$ between the control ($F_{t,scaled\text{-}c}$) and girdling ($F_{t,scaled\text{-}g}$) treatments, hereafter referred to as the new approach:

$$\mathbf{R_{a,b-new} = (E_{soil-c} - E_{soil-g}) + (F_{t,scaled-\,c} - F_{t,scaled-g})} \quad (7.2)$$

7.2.6 Soluble sugars and starch concentration of fine roots

We girdled three additional three additional trees at the site for sampling fine roots for sugar and starch analysis. These samples were collected on the girdled trees and three nearby non-girdled trees on the day of girdling and 11 (16 August 2011, DOY 228) and 40 days after girdling (14 September 2011, DOY 237). The sampling dates were selected to obtain data concurrent with the flux measurements and to assess the long-term impact of girdling on fine root soluble sugar and starch content. For sample harvesting, we carefully uncovered part of the root system and excised about 3 mg of fine roots, according to Regier *et al.* (2010). Samples were immediately frozen in liquid nitrogen, transported to the lab and stored in a freezer at -18°C until analyzed for glucose, fructose, sucrose, and starch as described by De Schepper *et al.* (2012). Our intention was to use the soluble sugar and starch data to reveal the relative effect of girdling on fine root sugar content and to identify the potential sources of root-respired CO_2. As for this purpose no absolute fine root soluble sugar and starch concentrations are needed, we normalized concentrations for each tree by dividing the post-treatment concentrations by the concentration on the day of girdling, facilitating inter-treatment comparison and accounting for variation among trees.

7.2.7 Statistical analysis

We compared daily totals of continuously measured F_t and E_{soil} for both treatments using repeated measures multi-factorial analysis of variance (ANOVA). Treatment (n=2, control and girdled) and date (n=14) were treated as fixed factors, while the individual tree (n=3 per treatment) was considered as a random factor. Similarly, automated and

manual measurements performed at 40 cm were compared, but with fewer temporal measurements (n=5). Finally, manual E_{soil} measurements performed at 40 cm and 70 cm were compared, based on the measurements made later in the growing season (date, n=10). Relative sugar and starch concentration were analyzed using a similar ANOVA model, however with fewer temporal measurements (date, n=3) and soluble sugar type (n=4, fructose, glucose, sucrose, and starch) as an additional fixed factor. Akaike's information criterion corrected for small sample sizes (AICc) was used to determine the covariance structure that best estimated the correlation among individual trees over time. All analyses were performed using the mixed model procedure (PROC MIXED) of SAS (Version 9.3, SAS Inc., Cary, NC, USA) with α=0.05.

7.3 Results

7.3.1 Impact of tree girdling on soil CO_2 efflux and xylem CO_2 transport

The soil properties of the control and girdling treatment plots were similar (Table 7.2). Automated measurements showed that soil CO_2 efflux (E_{soil}) prior to girdling was similar in the control and the girdling treatment plots (P=0.95), with an average (± SD) of 162.5 ± 18.4 and 162.6 ± 20.9 mg C m^{-2} h^{-1}, respectively (Fig. 7.2A). Following girdling, automated measurements showed a strong decrease in E_{soil} in the girdling treatment, while E_{soil} in the control treatment remained stable over time. Within 5 d, girdling significantly reduced E_{soil} (P=0.02) by 21.8 ± 3.7% relative to the control treatment (Fig. 7.2A). This pronounced initial decrease of E_{soil} in the girdling treatment was followed by a slower decrease, such that 25 d after girdling, E_{soil} in the girdling treatment was 34.9 ± 4.3% lower than the control treatment. The effect of girdling on E_{soil} was confirmed by manual measurements of E_{soil} 40 cm from the stem base (Fig. 7.2A). For manual measurements, significant differences in E_{soil} between the control and girdling plots were observed for the last two measurement dates (P=0.01). Manual measurements of E_{soil} tended to be slightly higher than automated measurements, but no significant differences were observed between the manual and automated measurements for the control (P=0.92) nor the girdling treatment (P=0.51). In addition, the manual E_{soil} measurements made at 70 cm from the stem base suggested that measurements

performed at 40 cm were representative of E_{soil} in the rooting areas of the trees in the control and girdling treatments.

Table 7.2 Root biomass density (g m^{-2}), pH, Organic carbon (%), and soil bulk density (g cm^{-3}) (± SD) of the control and girdling treatment plots measured to a depth of 30 cm. pH and organic carbon were determined for one composite sample per treatment, while root biomass density (*n*=8) and soil bulk density (*n*=8) were averaged per treatment.

Treatment	Root biomass density	pH	Organic carbon	Soil bulk density
Control	286.7 ± 40.1	5.1	1.8	1.3 ± 0.1
Girdling	287.8 ± 59.6	4.7	2.0	1.2 ± 0.2

Before girdling, xylem CO_2 concentration ($[CO_2]$) measured at the stem base was similar in the control and girdling treatments, averaging 10.7 ± 1.2% and 10.1 ± 1.4%, respectively (Fig. 7.2B). Girdling reduced average xylem $[CO_2]$ by approximately one fifth (i.e by 21.4 ± 1.1%) in the girdling treatment compared with the control treatment within five days after girdling.

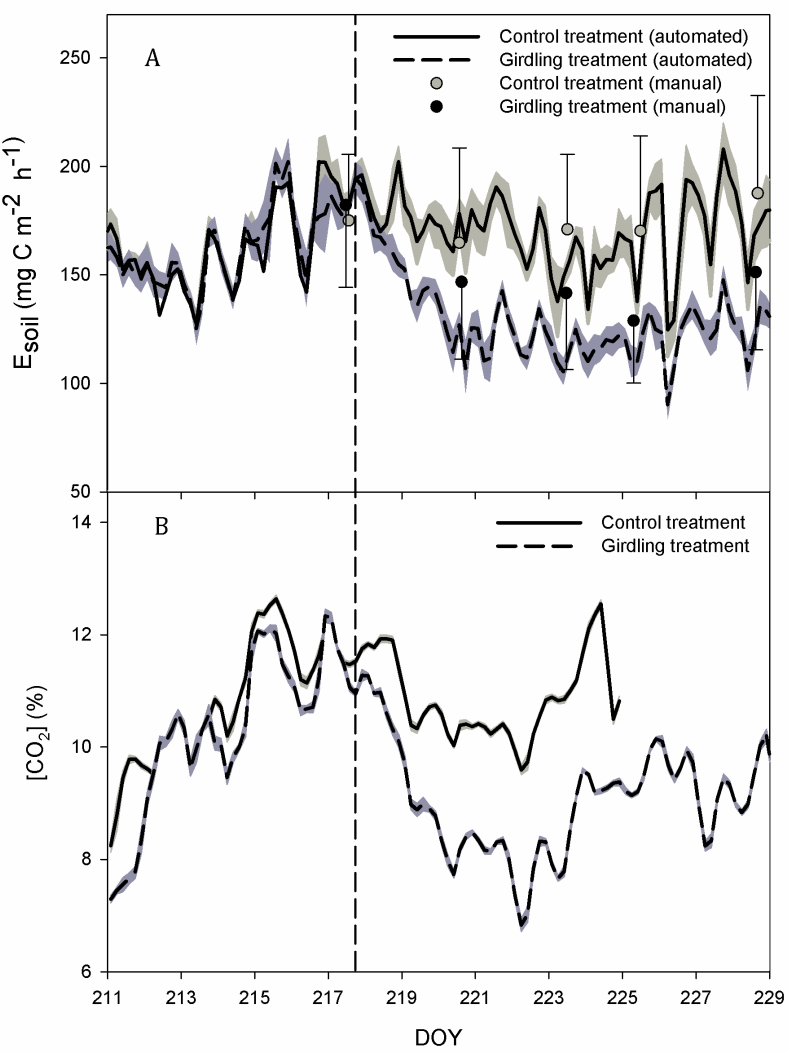

Fig. 7.2 (A) Soil CO_2 efflux (E_{soil}) measured with automated and manual chambers located 40 cm from the base of trees in the control treatment plot (automated: black line, *n*=3; manual: grey circles, *n*=9) and girdling treatment plot (automated: black dashed line, *n*=3; manual: black circles, *n*=9) (see Fig. 7.1). (B) Stem xylem CO_2 concentration ($[CO_2]$) at 5 cm above ground level of trees in the control treatment plot (black line, *n*=3) and girdled treatment plot (black dashed line, *n*=3) (see Fig. 7.1). The vertical dashed line indicates the time of girdling. The shaded areas and bars represent standard deviation. For manual measurements, only upper or lower bars are presented to improve clarity. DOY: day of the year.

7.3.2 Estimation of xylem CO_2 transport in control and girdled trees

Before girdling, sap flow rate (F_s) was slightly lower in the control plot (Fig. 7.3A) relative to the girdled plot (Fig. 7.3B), with 6 d averages of 0.29 ± 0.10 l h^{-1} and 0.36 ±

0.12 l h^{-1}, respectively. After girdling, the three measured trees responded differently to the treatment: a pronounced decrease in F_s was observed in one tree, while F_s remained similar to pre-girdling rates in the other two trees.

The decrease in xylem [CO_2] in response to girdling (Fig. 7.2B) influenced the magnitude of scaled xylem transport of root-respired CO_2 ($F_{t,scaled}$) (Fig. 7.3C). After girdling, $F_{t,scaled}$ was lower compared with the control treatment, particularly on days with the highest sap flow. On these days, average daily total $F_{t,scaled}$ in the control treatment was significantly higher than in the girdling treatment (P=0.03) and at peak sap flow, average maximal $F_{t,scaled}$ in the control treatment (44.7 ± 0.9 mg C m^{-2} h^{-1}) more than doubled the average maximal $F_{t,scaled}$ in the girdling treatment (16.5 ± 2.4 mg C m^{-2} h^{-1}).

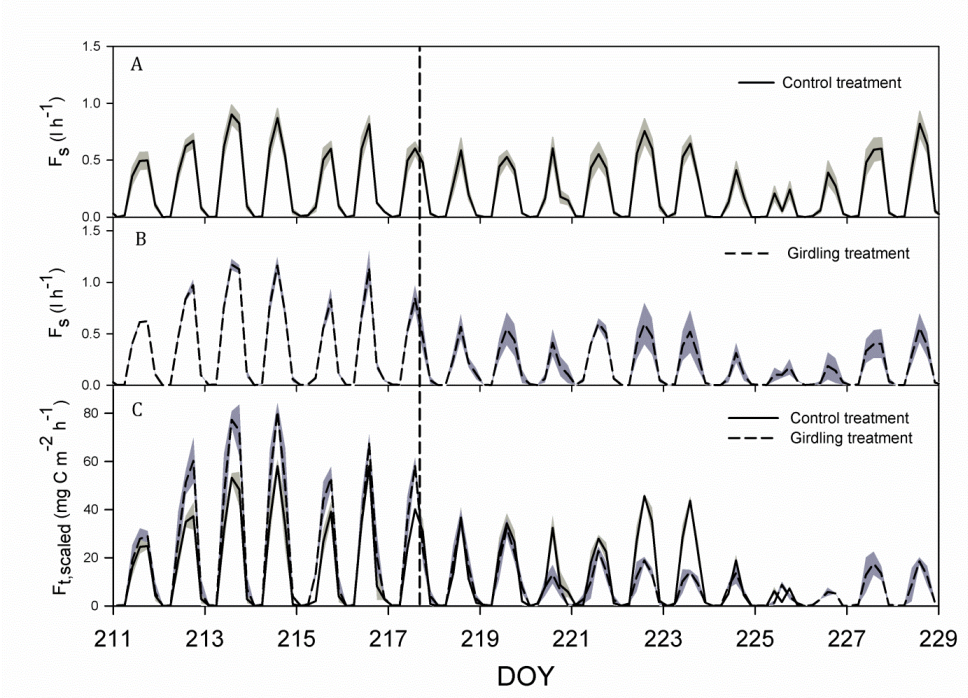

Fig. 7.3 Average sap flow rate (F_s) in (A) control and (B) girdled trees measured with sap flow sensors installed on the tree stem (see Fig. 7.1). (C) Scaled xylem transport of root-respired CO_2 ($F_{t,scaled}$) in control (black line) and girdled (black dashed line) trees. The vertical dashed line indicates the time of girdling. The shaded areas represent standard deviation. DOY: day of the year.

7.3.3 Estimation of the autotrophic component of belowground respiration

For estimating the autotrophic component of belowground respiration ($R_{a,b}$) we used data beginning two days after girdling. Diel variations were less pronounced when $R_{a,b}$ was calculated as in previous girdling studies ($R_{a,b\text{-}conv}$) compared with estimates obtained with the new approach ($R_{a,b\text{-}new}$) (Fig. 7.4A). During the daytime, an important fraction of root-respired CO_2 was transported upward in the xylem, which was not accounted for in $R_{a,b\text{-}conv}$. Especially on the days with highest sap flow (DOY 222-223, Fig. 7.4A), large differences were observed between $R_{a,b\text{-}conv}$ and $R_{a,b\text{-}new}$. $R_{a,b\text{-}conv}$ decreased in the middle of the day, while $R_{a,b\text{-}new}$ peaked during the day, when the highest sap flow occurred (Fig. 7.4A). We expressed $R_{a,b}$ estimates relative to belowground respiration estimated according to the conventional and new approach (Fig. 7.4B). According to the conventional approach, $E_{soil,c}$ is an estimate of total belowground respiration. Averaged over 5 d, we estimated that 27.0 ± 4.5% of belowground respiration was derived from $R_{a,b}$. With the new approach, $E_{soil\text{-}c} + F_{t,scaled\text{-}c}$ was used to estimate belowground respiration and we found that on average 32.8 ± 8.1% of belowground respiration was contributed by the autotrophic component (Fig. 7.4B). Larger differences were observed on the days with highest sap flow (DOY 222-223). On these days, at peak sap flow (from 12h-16h), 25.0 ± 2.7% and 45.4 ± 1.5% of belowground respiration was derived from $R_{a,b}$ calculated by the conventional and new approaches, respectively. During nighttime hours, small differences were observed in $R_{a,b}$ estimates between the two approaches, because low nocturnal sap flow rates (i.e. 1-2% of the 24h flux) had the potential to transport only a small quantity of root-respired CO_2.

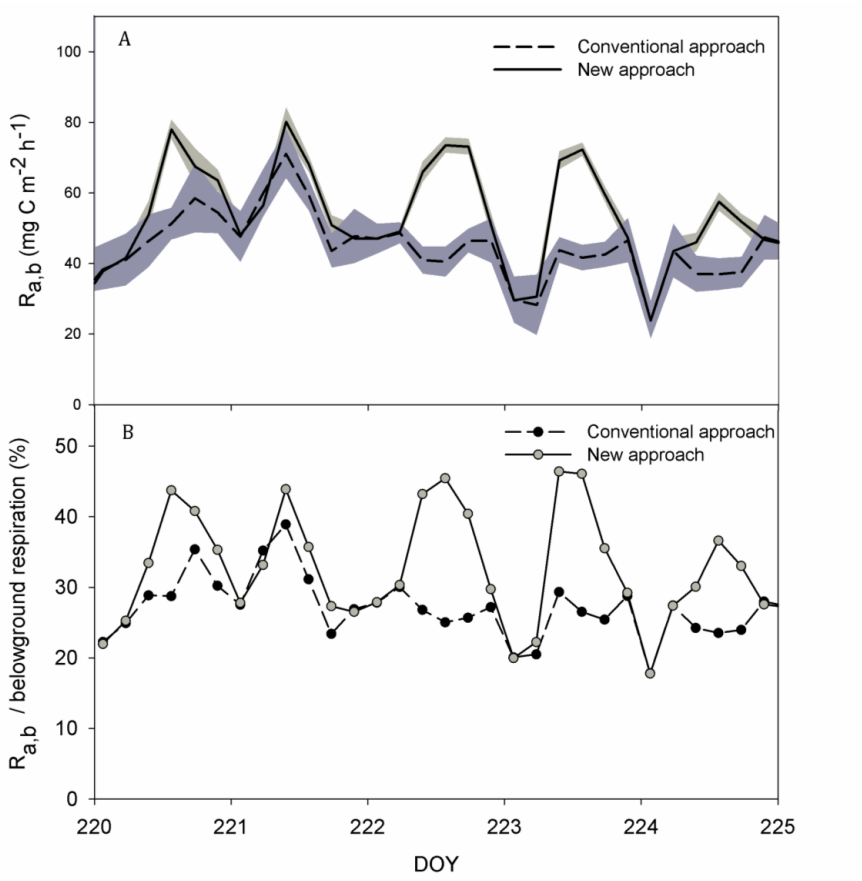

Fig. 7.4 (A) Estimates of the autotrophic component of belowground respiration ($R_{a,b}$) calculated by the conventional approach based solely on measurements of soil CO_2 efflux (E_{soil})(black dashed line), or calculated by the new approach, based on the combination of measurements of E_{soil} and the scaled flux of root-respired CO_2 transported in the transpiration stream ($F_{t,scaled}$) (black line). (B) Contribution of $R_{a,b}$ to belowground respiration, estimated according to the conventional approach (black symbols) and the new approach (grey symbols). Symbols represent four hour averages. DOY: day of the year.

7.3.4 Analysis of fine root samples

Relative to pre-girdling values, the girdling treatment had a significant overall effect on the soluble sugar and starch concentrations of fine roots compared to the control treatment (P=0.002) (Fig. 7.5). At 11 d after girdling, relative starch (Fig. 7.5A), sucrose (Fig. 7.5B) and fructose (Fig. 7.5C) concentrations decreased in fine roots of the girdled trees, while relative soluble sugar and starch concentrations increased in control trees. Relative concentrations between girdled and control trees were significantly different

for glucose (Fig. 7.5D, P=0.02) and sucrose (Fig. 7.5B, P=0.04). At 40 days after girdling, relative sucrose and starch concentrations further decreased in girdled trees, to levels 40.2 ± 2.7% and 14.4 ± 4.8% lower than observed pre-girdling, respectively, while fructose and glucose concentrations returned to the same level and increased relative to the day of girdling, respectively. In the control trees, soluble sugar and starch concentrations were higher relative to the day of girdling, with the largest increases in starch (44.8 ± 2.4%) and sucrose (43.3 ± 11.1%), the latter being significantly higher compared to the girdled trees (P=0.036).

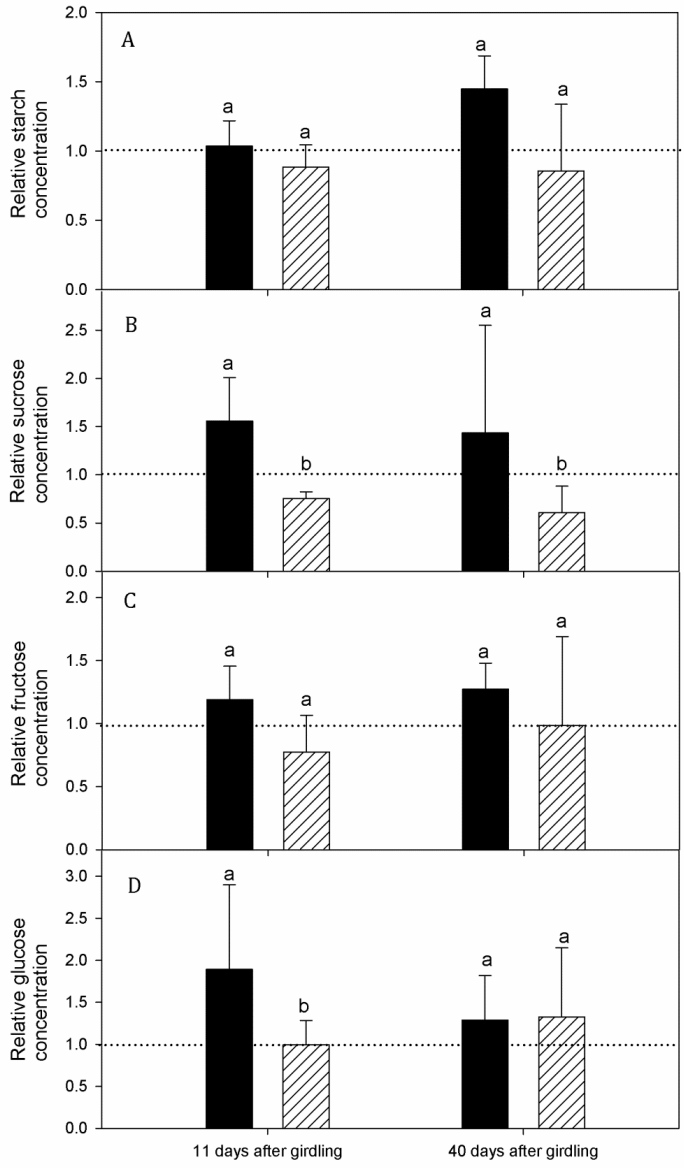

Fig. 7.5 Concentration of (A) starch, (B) sucrose, (C) fructose, and (D) glucose relative to concentration on the day of girdling in the fine roots of control (black) and girdled (hatched) trees at 11 (16 August 2011) and 40 (14 September 2011) days after girdling. Bars represent the mean of three trees per treatment and four samples per tree. Error bars represent standard deviation. The horizontal dotted line represents the relative concentration of fine root soluble sugars and starch on the day of girdling. Significant differences ($P<0.05$) per date between the two treatments are indicated by different letters.

7.4 Discussion

This study provides evidence that autotrophic component of belowground respiration ($R_{a,b}$) contributes to xylem transport of respired CO_2. Root-respired CO_2 either diffuses from the root surface into the soil environment, thereby contributing to soil CO_2 efflux (E_{soil}), or dissolves in xylem sap and is transported upward in the tree with the transpiration stream (F_t). Girdling reduced both E_{soil} and F_t, suggesting that efflux-based methods underestimate the contribution of $R_{a,b}$ to belowground respiration.

The strong reduction in E_{soil} after stem girdling has been described in detail in previous studies (Högberg *et al.*, 2001; Johnsen *et al.*, 2007; Högberg *et al.*, 2009; review by Kuzyakov & Gavrichkova, 2010; Subke *et al.*, 2011). Högberg *et al.* (2001) reported decreases up to 37% in E_{soil} within 5 d after girdling *Pinus sylvestris* trees, while Subke *et al.* (2011) observed a similar decrease (35%) for *Tsuga heterophylla* trees within two weeks after girdling. Data from our high-frequency E_{soil} measurements agree with these previous results. We found that girdling affected E_{soil} after 2 d and reduced E_{soil} after 5 and 25 d by 22% and 35%, respectively, relative to E_{soil} measured in the control treatment.

Previous studies exclusively used the reduction in E_{soil} induced by girdling to quantify the contribution of $R_{a,b}$ to belowground respiration, based on the general belief that all root-respired CO_2 diffuses into the soil and subsequently into the atmosphere. However, recent studies have suggested a large-magnitude upward flux of dissolved CO_2 in xylem of trees derived from $R_{a,b}$ (Aubrey & Teskey, 2009; Grossiord *et al.*, 2012) (**Chapter 1**). Based on measurements of xylem CO_2 concentration ($[CO_2]$) and sap flow near the stem base of *Populus deltoides* trees, Aubrey & Teskey (2009) found that F_t rivaled the flux that contributed to E_{soil}. Additionally, they calculated that only a small fraction of F_t resulted from the uptake of CO_2 dissolved in the soil solution. In our study, we also simultaneously measured the F_t to quantify $R_{a,b}$. Girdling reduced $[CO_2]$ at the stem base by 21% relative to xylem $[CO_2]$ of control trees within 5 d, which was similar to the reduction observed for E_{soil}. This result agrees with previous observations and supports our first hypothesis that a fraction of CO_2 derived from $R_{a,b}$ is transported in the transpiration stream.

Simultaneous high-frequency measurements of F_t and E_{soil} in girdling and control treatment plots allowed us to re-assess our understanding of $R_{a,b}$. When we accounted for F_t, $R_{a,b}$ dynamics were more pronounced during the daytime and indicated a greater contribution of $R_{a,b}$ to belowground respiration than previously reported. In particular, on days with high sap flow, a substantial quantity of root-respired CO_2 was transported upward with the transpiration stream, especially at peak sap flow, resulting in a large underestimation of $R_{a,b}$ when calculated by the conventional efflux-based method (second hypothesis). Similarly, Grossiord *et al.* (2012) reported for *Eucalyptus* that the largest underestimation (24%) of the contribution of autotrophic sources to belowground respiration was observed between 11:00 h and 15:00 h, which was associated with peak sap flow.

Results of girdling studies may be prone to biases related to the interruption of assimilate flow to belowground tissues, which is assumed to reduce $R_{a,b}$. First, girdling leads to an accelerated use of stored carbohydrates in roots (Högberg *et al.*, 2001; Olsson *et al.*, 2005; Högberg *et al.*, 2009), i.e. starch in oak trees (Barbaroux & Breda, 2002; Maunoury-Danger *et al.*, 2010). In this case, $R_{a,b}$ would be underestimated because tree roots would still be respiring after girdling. Girdling also leads to enhanced decomposition of roots and their associated mycorrhizae by soil heterotrophs (Högberg *et al.*, 2001; Bhupinderpal-Singh *et al.*, 2003; Ekberg *et al.*, 2007), resulting in greater fungal abundance and a possible shift in the fungal community from symbiotic to saprophytic fungi in the long term (Subke *et al.*, 2004). These rhizosphere effects could confound the appearance of reduced $R_{a,b}$ in girdled plots (Kuzyakov & Larionova, 2006), leading to underestimation of $R_{a,b}$. However, enhanced decomposition of roots and associated mycorrhizae by heterotrophs and changes in fungal abundance and community structure have been observed to occur at multi-season (Högberg *et al.*, 2001; Subke *et al.*, 2004; Ekberg *et al.*, 2007) and multi-year (Ekberg *et al.*, 2007) scales. Therefore, we assume that these effects were negligible during our relatively short experimental period. Finally, girdling affects the secretion of root exudates into the soil, whose microbial consumption has been found to contribute to $R_{a,b}$ and potentially affect $R_{h,b}$ (negative or positive priming effect). After girdling, we observed a relative decrease in fine root starch concentration of the girdled trees relative to concentrations at the day

of girdling (i.e. by 11% 40 d after girdling). At the same time, starch in fine roots of control trees increased (i.e. by 45% 40 d after girdling), probably due to late-season loading to maintain winter carbon reserves, as has been observed in previous studies (Barbaroux *et al.*, 2003; Regier *et al.*, 2010 and references therein). Increased use of starch in roots in response to girdling was observed in other field studies and has been suggested to lead to conservative estimates of $R_{a,b}$ (Högberg *et al.,* 2001; Frey *et al.*, 2006). In addition, a fraction of the metabolic demand related to starch usage after girdling might be related to starch remobilization (Rodgers *et al.*, 1995; Jordan & Habib, 1996), which suggests that the increased glucose levels we observed after girdling (Fig. 7.5D) could have resulted from hydrolysis of starch (Maunoury-Danger *et al.*, 2010). Therefore, in our study, estimates of $R_{a,b}$ contributions to F_t and E_{soil} in the girdled plot might be lower due to the increased use of stored carbohydrates that potentially fueled $R_{a,b}$ after girdling. There was also potentially an effect of starch mobilization from larger roots to fine roots, as observed by Aubrey *et al.* (2012) in a canopy scorching experiment. All these different processes contribute to the large standard deviations in fine root sugar concentrations observed among trees and might explain why the reduction in starch was not significant in girdled trees as compared to control trees. In spite of increased starch use, both xylem sap [CO_2] and E_{soil} decreased rapidly in response to girdling, presumably due to the interruption of the translocation of photosynthates to the root system. Sucrose is commonly recognized as the main translocated sugar (e.g. Zimmerman, 1957; Rolland *et al.*, 2006) and has a different nature compared to the other sugars. We observed a significant 40% reduction in sucrose concentration in fine roots in response to girdling. This result confirms previous findings that an important fraction of $R_{a,b}$ may be dependent on the rapid turnover of recent photosynthates within roots (Epron *et al.*, 2011; 2012 and references therein). Thus, autotrophic metabolic activity that contributes both to F_t and E_{soil} is likely fueled by a combination of recent photosynthates and stored carbohydrates, as has been observed in other root respiration studies (Lynch *et al.*, 2013). Because root-respired CO_2 both diffuses into the soil and is transported in the transpiration stream (Aubrey & Teskey, 2009) regardless of whether it is derived from recent photosynthates or stored carbohydrates, we expect that the biases due to girdling-related increases in the use of reserves were similar for both fluxes.

Second, girdling may affect whole-tree sap flow (Domec & Pruyn, 2008; De Schepper *et al.*, 2010), inducing different rates of water and nutrient uptake between girdled and non-girdled trees. By removing the bark, the outer xylem tissue is exposed to air and might dry out and become non-functional for water transport. Moreover, a reduction in stomatal conductance of leaves after girdling related to feedback inhibition of photosynthesis (see De Schepper *et al.*, 2010 and references therein) could reduce sap flow. During our study, we tried to avoid desiccation of exposed xylem tissues by wrapping the girdled stem section in plastic film. However, sap flow in girdled trees was reduced by 20% on average relative to control trees, which was similar to the reduction in sap flow observed in a canopy scorching study by Aubrey *et al.* (2012). The decrease in sap flow likely affected both the conventional ($R_{a,b\text{-}conv}$) and new ($R_{a,b\text{-}new}$) estimate of $R_{a,b}$. Due to a reduction in sap flow, a fraction of root-respired CO_2 might have contributed to E_{soil} instead of being transported with the transpiration stream (Aubrey *et al.*, 2012). In addition, previous studies have shown that internal [CO_2] builds up in stems when sap flow decreases, because the transpiration stream is not removing respired CO_2 from the tissues (Teskey & McGuire, 2002; McGuire *et al.*, 2007; Saveyn *et al.*, 2007b); a similar phenomenon may occur in roots, which would also contribute to increased efflux due to the larger concentration gradient.

Because root-respired CO_2 both diffuses into the soil environment and dissolves in the transpiration stream, the two fluxes must be investigated simultaneously to fully understand root metabolism dynamics. For instance, we observed non-temperature related depressions in $R_{a,b\text{-}conv}$ at high F_s when upward transport of root-respired CO_2 with the transpiration stream was large (DOY 222 and 223, Fig. 7.4). Daytime depressions in root CO_2 efflux related to the rate of transpiration have been observed for other species (Bekku *et al.*, 2009; 2011) and Subke *et al.* (2009) observed unexpected decreases in daytime E_{soil} related to depressions in the autotrophic component of E_{soil} (**Box 1.1**). However, these studies lacked measurements of F_t to fully elucidate the observed dynamics in E_{soil} and the tight coupling between the two fluxes. Daytime depressions in root CO_2 efflux could be similar to what has been observed for stems, where daytime depressions in stem CO_2 efflux (E_{stem}) were related to increased internal transport of CO_2 away from the site of respiration due to increased sap flow (Teskey &

McGuire, 2002; Gansert & Burgdorf, 2005; McGuire *et al.*, 2007) or changes in stem turgor pressure (Saveyn *et al.*, 2007a).

We have shown that efflux-based studies may underestimate the actual contribution of $R_{a,b}$ to belowground respiration, as has been suggested previously (Aubrey & Teskey, 2009; Grossiord *et al.*, 2012). Especially at high sap flow rates, a substantial amount of root-respired CO_2 is transported upward with the transpiration stream, resulting in large underestimations in belowground respiration when estimated $R_{a,b}$ is based solely on E_{soil} measurements. Therefore, future studies on the contribution of $R_{a,b}$ to belowground respiration should use approaches for measuring CO_2 fluxes that include the internal transport of respired CO_2 (Bloemen *et al.*, 2013b; Trumbore *et al.*, 2013) and consider potential factors that control the flux of root-respired CO_2 with the transpiration stream, like sap flow. These measurements are crucial for improving the accuracy of estimates of $R_{a,b}$ and our ability to understand belowground respiration dynamics from a mechanistic point of view.

- Chapter 8 -

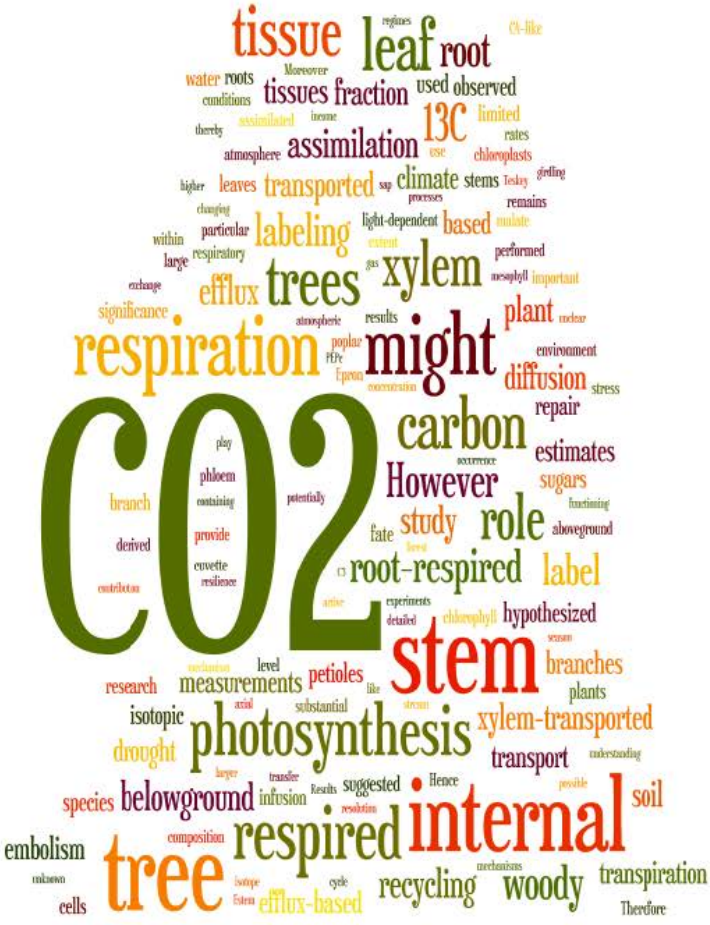
tissue
leaf
root
water
roots
Moreover
tissues
fraction
used
observed
13C
limited
assimilation
rates
chloroplasts
atmosphere
leaves
transported
climate
stems
remains
labeling
based
particular
light-dependent
within
large
respiratory
xylem
performed
trees
efflux
plant
significance
respiration
might
diffusion
environment
repair
carbon
estimates
CO2
However
sugars
branch
role
study
fate
aboveground
derived
root-respired
label
provide
cuvette
hypothesized
stem
branches
research
measurements
petioles
plants
isotopic
photosynthesis
xylem-transported
drought
transport
species
belowground
infusion
suggested
Hence
soil
internal
respired
embolism
tree
composition
recycling
woody
transpiration
cells
efflux-based
Therefore

General conclusions and future perspectives

The main objective of this PhD study was to improve our understanding of internal CO_2 in trees and its role in the tree carbon cycle. In this concluding chapter, the main findings of the performed research are discussed. Subsequently, remaining unanswered questions and suggestions for promising future avenues of research on the role of internal CO_2 in tree functioning are identified and discussed.

8.1 General research outcomes and scientific contributions

Reconsidering efflux-based estimates of above- and belowground woody tissue respiration

One of the most long-standing assumptions in plant research is that CO_2 efflux equals respiration, because of the hypothesized immediate diffusion of tissue respired CO_2 into the atmosphere or soil environment (**Chapter 1**). A corollary is that CO_2 efflux chambers are being used to estimate above- and belowground respiration and their contribution to ecosystem respiration. However, recent observations of the existence of an internal CO_2 transport in trees of large magnitude (Teskey & McGuire, 2002; 2007; Aubrey & Teskey, 2009; Grossiord *et al.,* 2012), which redistributes above- and belowground respired CO_2 by the transpiration stream, questions the use of efflux-based measurements for quantifying tissue respiration.

Results from the girdling study (**Chapter 7**) confirm that a fraction of root-respired CO_2 is not accounted for when using efflux-based measurements of soil respiration. The reduction in internal CO_2 after girdling indicates that a substantial fraction of root-respired CO_2 is transported within the tree, leading to inaccurate efflux-based estimates of belowground respiration. Hence, as proposed in **Chapter 7**, accounting for the internal transport of root-respired CO_2 (F_t) besides its contribution to soil CO_2 efflux (E_{soil}) leads to a more accurate estimate of the autotrophic component of belowground respiration ($R_{a,b}$). In particular during the daytime at peak sap flow, a large fraction of the root-respired CO_2 is transported away from the roots inside the tree, instead of contributing to E_{soil}.

Once aboveground, the largest fraction of F_t is expected to diffuse into the atmosphere, as indicated by the results from the tree labeling study (**Chapter 4**). Aboveground diffusion of root-respired CO_2 implies that efflux-based measurements overestimate the actual metabolic cost of stem and branch respiration, while the amount of carbohydrates needed to sustain root respiration has been underestimated. Moreover, belowground photosynthate allocation in trees is potentially much larger than previously assumed (Aubrey & Teskey, 2009). Therefore, internal transport of respired CO_2 compels us to rethink commonly held assumptions on the tree carbon economy. However, it does not imply that absolute estimates of the ecosystem carbon exchange between forests and the atmosphere need to be revisited.

Carbon isotopes provide us with information on the fate of xylem-transported CO_2 at an unprecedented scale

While above- and belowground sources of xylem-transported CO_2 have been identified (**Chapter 1**), its fate in aboveground tree organs remains largely unknown. Small-scale studies have introduced a carbon isotope label into detached leaves and branches (**Chapter 1**) as performed in **Chapters 2 and 3**, respectively, but few have studied the fate of xylem-transported CO_2 in field-grown trees. To this end, ^{13}C label infusion was used to simulate respired CO_2 entering the stem of poplar trees from belowground while isotope analysis was used to track its fate (**Chapter 4**). During transport, the dissolved ^{13}C label present in inorganic form was assimilated in organic form by Ribulose-1,5-biphosphate carboxylase oxygenase (Rubisco) and phosphoenolpyruvate carboxylase

(PEPc) mediated carboxylation. Between 6-17% of the infused ^{13}C label was assimilated in the tree, mainly in the branches and the stem and in a lesser extent in the leaf petioles. Hence, recycling of respired CO_2 in trees potentially contributes substantially to the tree carbon income. In the branches most of the ^{13}C label was assimilated in the inner bark (**Chapter 4**), where most of the chlorophyll is located, corroborating the results of the detached branch labeling study (**Chapter 3**). At leaf level, assimilation of the ^{13}C label in the petioles underpins the possible existence of a spatially separated C_4-like pathway in temperate trees, as suggested previously for herbaceous species (**Chapter 1**). In the leaf blade, detailed analysis of ^{11}C label distribution showed that near the leaf veins a large fraction of respired CO_2 entering the leaf via the petiole is potentially assimilated in chlorophyll containing cells of the bundle sheath tissue (**Chapter 2**). In contrast to the ^{13}C label, the ^{11}C label was possibly still present in the transpiration stream during label distribution analysis and therefore the data from the ^{11}C labeling gives us different information on internal CO_2 transport relative to the results from ^{13}C labeling. According to Michaelis Menten enzyme kinetics, the more ^{11}C label available as substrate for PEPc and Rubisco mediated carboxylation, the higher the amount of ^{11}C label can be expected to be assimilated in tissues like bundle sheaths. These tissues are positioned in between the phloem and the xylem vasculature, and might directly load synthesized sugars into the phloem sap. In order to reveal these mechanisms, ^{11}C–based labeling in combination with positron emission tomography (PET) (Beer *et al.*, 2010; Kawachi *et al.*, 2011a) might allow a real time *in vivo* detection of sugar transfer from bundle sheaths into the phloem.

Assimilation of xylem-transported CO_2 depends on xylem CO_2 concentration and transpiration rate

The ^{13}C labeling experiments performed under controlled conditions showed that xylem-transported CO_2 assimilation depends on transpiration rate (**Chapters 2 and 3**) and xylem CO_2 concentration ([CO_2] (**Chapter 3**). Therefore, it is important to account for factors controlling transpiration and respiration when estimating the contribution of internal CO_2 recycling to the tree carbon income. For example, under high sap flow rates (F_s) more root-respired CO_2 could be transported upwards, allowing higher assimilation rates by chlorophyll containing tissues in aboveground tree organs. At leaf level, results

from previous studies suggested that a large fraction of the xylem-transported CO_2 reaching the leaves was removed from the transpiration stream by the petioles (Stringer & Kimmerer, 1993; McGuire *et al.*, 2009), which was confirmed by our ^{13}C labeling experiments on leaf (**Chapter 2**), branch (**Chapter 3**), and tree (**Chapter 4**) level. In addition, strong ^{13}C enrichment of the mesophyll was observed under the high ^{13}C label (HL) and high vapor pressure deficit (VPD) treatment (**Chapter 3**), which implies that a substantial amount of internal CO_2 might be transported into the leaf mesophyll under high transpiration and respiration rates. Therefore under specific conditions, xylem CO_2 transport might represent an important pathway for providing carbon substrate to photosynthetically active mesophyll tissues in the leaf blade.

Axial diffusion of respired CO_2 confounds dormant season stem respiration estimates

Under dormancy, assimilation of locally respired CO_2 by woody tissue photosynthesis is hypothesized to confound efflux-based estimates of stem respiration (**Chapter 1**). By lowering internal [CO_2] locally, it is suggested to induce axial diffusion of respired CO_2 away from the site of respiration, hence reducing stem CO_2 efflux (E_{stem}) under temperature stable conditions (Saveyn *et al.*, 2008a). Illuminating stem sections remote from the stem cuvette reduced E_{stem} (**Chapter 5**), with highest reduction in E_{stem} observed when illuminating the stem section closest to the stem cuvette. Therefore, internal movement of respired CO_2 during the dormant season by axial diffusion might have important implications for estimating stem respiration, in particular because dormant season stem respiration estimates are used to quantify maintenance stem respiration throughout the year. Hence, it is advised to exclude woody tissue photosynthesis in neighboring stem sections by shielding stem sections above and below the stem cuvette to obtain accurate efflux-based stem respiration estimates. The shielding height above and below the stem cuvette will depend on the extent of axial diffusion of respired CO_2 in tree stems, which is related to stem (water content, woody density, photosynthetic capacity) and forest stand (open forest vs. closed forest) characteristics, and tree dimensions.

Woody tissue photosynthesis plays a role in tree drought stress resilience

Results from the branch labeling study indicated that internal CO_2 assimilation in woody and leaf tissues is small relative to atmospheric CO_2 fixation via the leaves (**Chapter 3**). However, assimilation of internal CO_2 is hypothesized to play a more pronounced role in sustaining the tree carbon balance when leaf photosynthesis is limited, for instance during drought stress (**Chapter 1**). Under drought stress, stomatal closure is one of the earliest responses affecting leaf photosynthesis, by limiting the uptake of atmospheric CO_2 (Chaves *et al.*, 2002; Flexas & Medrano, 2002; Grassi & Magnani, 2005). Woody tissue photosynthesis is supplied by endogenously respired CO_2, thereby avoiding excessive water loss. The stem and branch light exclusion treatment that prevented woody tissue photosynthesis to occur in poplar trees resulted in reduced growth and altered leaf gas exchange rates (**Chapter 6**), demonstrating the impact of local stem processes like woody tissue photosynthesis on the overall plant status. The observed relationship between woody tissue photosynthesis and leaf level processes is presumably related to its hypothesized possible role in maintaining plant hydraulics under limited water supply (Schmitz *et al.*, 2012). However, the extent to which light-dependent embolism repair might play a role in maintaining the hydraulic function under drought stress remains unclear (**Box 1.2**). Moreover, the ultimate fate of sugars synthesized by woody tissue photosynthesis remains unknown. Nonetheless, based on the results in **Chapter 6**, it can be expected that species that are able to perform woody tissue photosynthesis might have a higher drought stress resilience as compared to non-photosynthesizing species.

8.2 Directions for future research

Detailed analysis of the fate of xylem-transported CO_2: moving towards a laser-based approach

Recent advances in isotopic labeling techniques have made it possible to elucidate patterns and processes in tree carbon cycling at a yet unprecedented resolution (e.g. Marron *et al.*, 2009; Wingate *et al.*, 2010; Bahn *et al.*, 2012; Epron *et al.*, 2012). Of particular interest is the development of Laser Absorption Spectroscopy (LAS), which allows continuous real-time measurements of the concentration and isotopic composition of respiratory CO_2 efflux, based on the absorption of near and mid-infrared

light at selected wavelengths by individual isotopologues (e.g. $^{12}C^{16}O_2$, $^{13}C^{16}O_2$, and $^{18}O^{12}C^{16}O$) (Werner *et al.*, 2012). Within the context of tree carbon cycling, LAS-based measurements of the isotopic composition of CO_2 efflux in combination with cuvettes have been used exclusively to trace the allocation of photosynthates from the leaves to aboveground (Dannoura *et al.*, 2011; Epron *et al.*, 2012) and belowground (Plain *et al.*, 2009; Barthel *et al.*, 2011; Epron *et al.*, 2011) tissues and to assess *in situ* the velocity of downward carbon transfer, after pulse labeling the canopy (Dannoura *et al.*, 2011; Epron *et al.*, 2012). In this PhD study (**Chapter 4**) and in the study by Powers & Marshall (2011), respiratory CO_2 efflux samples were taken manually, providing data on the upward transfer of ^{13}C label at low resolution. LAS could provide us continuous data on the upward xylem transport of a ^{13}C label within the tree, based on the sampling of respiratory efflux or internal CO_2, the latter using porous tubing installed in the stem. Moreover, the use of high temporal resolution isotope tracing after canopy pulse labeling could provide us solid evidence whether root-respired CO_2 transported in the xylem is derived mainly from recently assimilated photosynthates or stored carbon reserves, which remained elusive in our girdling study (**Chapter 7**). Hence, the use of LAS-based approaches to trace isotopic proxies of xylem-transported CO_2 within trees will further deepen our understanding of the significance of internal CO_2 in the tree carbon cycle.

Unraveling the significance of xylem transport of CO_2 and malate as part of a C_4-like mechanisms in C_3 plants

Results from tissue enrichment analysis after ^{13}C labeling (**Chapters 2, 3, and 4**) showed that respired CO_2 can be transported to chlorophyll containing tissues in the stem, leaves, and branches. However, an important fraction of the photosynthetic cells might be supplied with carbon transported in organic form (e.g. malate) (Angert *et al.*, 2012; Trumbore *et al.*, 2013), which is derived from phosphoenolpyruvate carboxylase (PEPc) mediated carboxylation of respired CO_2. Following transport, malate is decarboxylated enzymatically and the CO_2 is re-assimilated by photosynthetically active cells adjacent to the xylem vasculature. These characteristics of C_4 photosynthesis have been shown to occur in stems and petioles of tobacco, a typical C_3 plant (Hibberd & Quick, 2002). It is unclear to what extent such a C_4-like mechanism exists in trees.

Berveiller & Damesin (2008) have reported high activities of PEPc and decarboxylation enzymes in mature *Fagus sylvatica* stems. The assimilation of xylem-transported ^{13}C labeled CO_2 in petioles of poplar observed in our study (**Chapter 4**) and by Stringer & Kimmerer (1993) might support the hypothesized role of petioles in a C_4-like mechanism in trees (Hibberd & Quick, 2002). However, an additional labeling experiment, based on the infusion of malate in the transpiration stream of field-grown trees, might shed a new light on the distinction between C_3 and C_4 photosynthesis in plants.

Exploring the role of woody tissue photosynthesis in light-dependent embolism repair

As mentioned in **Box 1.2**, Schmitz *et al.* (2012) suggested that by recycling respired CO_2 in parenchymatous xylem ray cells (**Fig. 1.4**), xylary chloroplasts play a role in the light-dependent repair of embolized xylem vessels in branches of mangrove species. In **Chapter 6**, it is suggested that a similar mechanism might exist in the stems of young poplar trees, based on acoustic cavitation measurements during a drying out experiment of light-excluded and non light-excluded branches. Maintaining plant hydraulics based on xylary chloroplast sugars is consistent with the hypothesized role of sugars in the refilling of embolized vessels (Salleo *et al.*, 2004; Zwieniecki & Holbrook, 2009; Nardini *et al.*, 2011) or in triggering a biological response to embolism (Secchi & Zwieniecki, 2011). These sugars are assumed to be derived from starch depolymerization (Saleo et al., 2004) or from phloem unloading into xylem parenchyma cells (Nardini *et al.*, 2011). The occurence of chloroplasts in the xylem parenchyma, which lie nearby the xylem vessels susceptible to cavitation, suggests that sugars used in embolism repair might be derived locally (Schmitz *et al.*, 2012). However, the significance of light-dependent embolism repair in trees remains unclear. Their role could be limited to small branches and trees, because the levels of light penetrating the inner tree tissues is generally considered as a limiting factor (Pfanz *et al.*, 2002 and references therein). However, PEPc which is uniformly present in adult tree stems (Berveiller *et al.*, 2007b), might mediate CO_2 assimilation resulting in osmotically active compounds under low light or dark conditions. Eventually, understanding the significance of xylary chloroplasts in

embolism repair and sensing might help us to understand these mechanisms and allow us to explain why chloroplasts are present at such deep stem layers like the pith.

The occurrence of high internal CO_2 concentrations in roots

Within the root system, CO_2 concentrations ($[CO_2]$) are assumed to be higher than observed for the soil (**Chapter 1**), indicating that a portion of root-respired CO_2 accumulates within the root system (**Box 1.1**). In particular in larger roots, where suberized root tissues might represent a substantial barrier to radial diffusion of respired CO_2, a substantial fraction of respired CO_2 might accumulate, as observed for roots of aquatic plants. However, combined measurements of root internal CO_2 and soil CO_2 concentrations are not performed yet and it is unknown whether the accumulation of a part of root-respired CO_2 is a phenomenon omnipresent among root classes and tree species. Drilling a hole in a root section next to the measurement site should lead to fluxing out of CO_2 into the soil environment and a reduced internal $[CO_2]$. In addition, stable isotopes might provide us with detailed information on the occurrence of high internal $[CO_2]$ in roots. First, dynamics in the isotopic composition of internal and rhizosphere CO_2 after infusion of $^{13}CO_2$ labeled gas in the root might prove that the root tissues exert a significant resistance to the diffusion of root-respired CO_2 into the soil environment. Moreover, additional tracing of ^{13}C in the root xylem after $^{13}CO_2$ infusion in the root might enable a detailed quantification of the amount of root-respired CO_2 that is transported in the xylem or diffuses radially into the soil environment.

Unraveling the role of CO_2 recycling in tree functioning under changing climate regimes

There is ample evidence that the terrestrial component of the carbon cycle is responding to climate variations and trends on a global scale (Heimann & Reichstein, 2008). Recycling of internal CO_2 in trees could be one of those plant strategies to cope with changing climate regimes (**Chapter 6**). For instance, the frequency and the intensity of extreme events like drought and heat waves are predicted to increase (Reichstein *et al.*, 2013). In response to these extreme events, plants will close their stomates to a larger degree, thereby negatively affecting leaf gas exchange and plant growth (Bauweraerts *et al.*, 2013). Internal CO_2 recycling is less susceptible to the drying power of the atmosphere and water loss via the stem is limited, leading to an increased plant water

use efficiency under climate extremes (**Chapter 1**). On the potential role of internal CO_2 recycling in tree resilience to climate extremes, much can be learned from internal CO_2 recycling in drought-adapted species inhabiting desert environments. These plants have a limited leaf area and stem photosynthesis is considered as an integral component of the plant carbon balance (e.g. Gibson, 1983; Comstock & Ehleringer, 1990; Nilsen & Sharifi, 1997), stressing the significance of internal CO_2 recycling for their carbon income. Therefore, accurate climate change experiments with combined drought, increased atmospheric CO_2, heat wave and stem and branch light manipulation treatments are needed to test the postulated role of CO_2 recycling in tree functioning under changing climate regimes.

The importance of respired CO_2 transport and recycling in large or mature trees

The results from the experiments performed in this PhD study have indicated the potential importance of respired CO_2 transport and recycling in younger trees (1-9 years old). However, the question is what to expect of the importance of these processes in larger or mature trees? First in larger trees, xylem CO_2 transport with the transpiration stream might represent a flux of larger magnitude as the one observed in younger trees (**Chapter 7**) as larger trees posses a larger sap wood area. Within the stem of aging trees, more respired CO_2 will accumulate as more suberized, older tissues in the bark are expected to exert a larger barrier to radial diffusion, which leads to higher dissolved CO_2 concentrations. Moreover, a fraction of the internal CO_2 could be derived from several-year-old storage pools as recently observed for older tropical trees by Muhr *et al.* (2013). Second, larger trees will have a larger root system, allowing a larger import of more root-respired CO_2 with the transpiration stream into the stem. Teskey & McGuire (2007) observed for *Platanus occidentalis* that trees with a larger diameter had a higher internal [CO_2] at stem base. This probably indicates that larger trees with larger root systems might accumulate more CO_2 in their root system. As root systems age, an increasing proportion becomes suberized (Kramer & Kozlowski, 1966). This will increase the amount of respired CO_2 that remains within the root system (**Chapter 1**) rather than fluxing into the soil environment. Finally, light-driven woody tissue photosynthesis will possibly be lower in aging tree tissues. The amount of light penetrating the rhytidome and periderm is an important limiting factor for light-driven

woody tissue photosynthesis. Older bark layers, where lenticels have lost their light conducting function by rhytidomal thickening, are expected to permit less light penetration up to chlorophyll containing cells in the stems (Wittmann *et al.*, 2001). However, additional measurements of light conductance by mature tissues are needed. Nonetheless, a fraction of the respired CO_2 might still be assimilated by non light-driven woody tissue photosynthesis, as high PEPc activity has been reported in stems of aging trees of varying species (Berveiller & Damesin, 2008).

References

Abiko T, Kotula L, Shiono K, Malik AI, Colmer TD, Nakazono M. 2012. Enhanced formation of aerenchyma and induction of a barrier to radial oxygen loss in adventitious roots of *Zea nicaraguensis* contribute to its waterlogging tolerance as compared with maize (*Zea mays* ssp mays). *Plant Cell and Environment* **35**: 1618-1630.

Amiro BD, Ewing LL. 1992. Physiological Conditions and Uptake of Inorganic ^{14}C by Plant-Roots. *Environmental and Experimental Botany* **32**: 203-211.

Amthor JS. 1989. *Respiration and Crop Productivity*. New York: Springer-Verlag.

Angert A, Muhr J, Juarez RN, Munoz WA, Kraemer G, Santillan JR, Barkan E, Mazeh S, Chambers JQ, Trumbore SE. 2012. Internal respiration of Amazon tree stems greatly exceeds external CO_2 efflux. *Biogeosciences* **9**: 4979-4991.

Araki MG, Utsugi H, Kajimoto T, Han QM, Kawasaki T, Chiba Y. 2010. Estimation of whole-stem respiration, incorporating vertical and seasonal variations in stem CO2 efflux rate, of *Chamaecyparis obtusa* trees. *Journal of Forest Research* **15**: 115-122.

Armstrong W. 1979. Aeration in Higher Plants. In: W. H. Woolhouse ed. *Advances in Botanical Research*. London: Academic Press, 226-232.

Armstrong W, Armstrong J. 2005. Stem photosynthesis not pressurized ventilation is responsible for light-enhanced oxygen supply to submerged roots of alder (*Alnus glutinosa*). *Annals of Botany* **96**: 591-612.

Aschan G, Pfanz H. 2003. Non-foliar photosynthesis - a strategy of additional carbon acquisition. *Flora* **198**: 81-97.

Aschan G, Wittmann C, Pfanz H. 2001. Age-dependent bark photosynthesis of aspen twigs. *Trees-Structure and Function* **15**: 431-437.

Atkin O, Millar H, Turnbull M. 2010. Plant respiration in a changing world. *New Phytologist* **187**: 269-272.

Atkin OK. 2011. Introduction to a Virtual Special Issue on plant respiration in variable environments. *New Phytologist* **191**: 1-4.

Atkin OK, Bruhn D, Hurry VM, Tjoelker MG. 2005. The hot and the cold: unravelling the variable response of plant respiration to temperature. *Functional Plant Biology* **32**: 87-105.

Atkin OK, Edwards EJ, Loveys BR. 2000. Response of root respiration to changes in temperature and its relevance to global warming. *New Phytologist* **147**: 141-154.

Atkinson TJ, Miller AN, Huhndorf SM, Orlovich DA. 2007. Unusual new *Chaetosphaeria* species from New Zealand: intrafamilial diversity and elucidations of the *Chaetosphaeriaceae-Lasiosphaeriaceae* relationship (*Sordariomycetes*, *Ascomycotina*). *New Zealand Journal of Botany* **45**: 685-706.

Aubrey DP, Boyles JG, Krysinsky LS, Teskey RO. 2011. Spatial and temporal patterns of xylem sap pH derived from stems and twigs of *Populus deltoides* L. *Environmental and Experimental Botany* **71**: 376-381.

Aubrey DP, Mortazavi B, O'Brien JJ, McGee JD, Hendricks JJ, Kuehn KA, Teskey RO, Mitchell RJ. 2012. Influence of repeated canopy scorching on soil CO_2 efflux. *Forest Ecology and Management* **282**: 142-148.

Aubrey DP, Teskey RO. 2009. Root-derived CO_2 efflux via xylem stream rivals soil CO_2 efflux. *New Phytologist* **184**: 35-40.

Bahn M, Buchmann N, Knohl A. 2012. "Stable Isotopes and Biogeochemical Cycles in Terrestrial Ecosystems" Preface. *Biogeosciences* **9**: 3979-3981.

Bahn M, Knapp M, Garajova Z, Pfahringer N, Cernusca A. 2006. Root respiration in temperate mountain grasslands differing in land use. *Global Change Biology* **12**: 995-1006.

Baker JM, Van Bavel CHM. 1987. Measurement of Mass-Flow of Water in the Stems of Herbaceous Plants. *Plant Cell and Environment* **10**: 777-782.

Baldocchi D. 2008. Breathing of the terrestrial biosphere: lessons learned from a global network of carbon dioxide flux measurement systems. *Australian Journal of Botany* **56**: 1-26.

Barbaroux C, Breda N. 2002. Contrasting distribution and seasonal dynamics of carbohydrate reserves in stem wood of adult ring-porous sessile oak and diffuse-porous beech trees. *Tree Physiology* **22**: 1201-1210.

Barbaroux C, Breda N, Dufrene E. 2003. Distribution of above-ground and below-ground carbohydrate reserves in adult trees of two contrasting broad-leaved species (*Quercus petraea* and *Fagus sylvatica*). *New Phytologist* **157**: 605-615.

Barthel M, Hammerle A, Sturm P, Baur T, Gentsch L, Knohl A. 2011. The diel imprint of leaf metabolism on the $\delta^{13}C$ signal of soil respiration under control and drought conditions. *New Phytologist* **192**: 925-938.

Beer S, Streun M, Hombach T, Buehler J, Jahnke S, Khodaverdi M, Larue H, Minwuyelet S, Parl C, Roeb G, *et al.* 2010. Design and initial performance of PlanTIS: a high-resolution positron emission tomograph for plants. *Physics in Medicine and Biology* **55**: 635-646.

Beis A, Zotos A, Patakas A. 2009. Influence of sampling time and sap extraction methodology on xylem pH values in two grapevine varieties grown under drought conditions. *Environmental and Experimental Botany* **67**: 305-311.

Bekku YS, Sakata T, Nakano T, Koizumi H. 2009. Midday depression in root respiration of *Quercus crispula* and *Chamaecyparis obtusa*: its implication for estimating carbon cycling in forest ecosystems. *Ecological Research* **24**: 865-871.

Bekku YS, Sakata T, Tanaka T, Nakano T. 2011. Midday depression of tree root respiration in relation to leaf transpiration. *Ecological Research* **26**: 791-799.

Benson AA. 2002. Paving the path. *Annual Review of Plant Biology* **53**: 1-25.

Berveiller D, Kierzkowski D, Damesin C. 2007a. Interspecific variability of stem photosynthesis among tree species. *Tree Physiology* **27**: 53-61.

Berveiller D, Vidal J, Degrouard J, Ambard-Bretteville F, Pierre JN, Jaillard D, Damesin C. 2007b. Tree stem phosphoenolpyruvate carboxylase (PEPc): lack of biochemical and localization evidence for a C_4-like photosynthesis system. *New Phytologist* **176**: 775-781.

Bhupinderpal-Singh, Nordgren A, Lofvenius MO, Hogberg MN, Mellander PE, Hogberg P. 2003. Tree root and soil heterotrophic respiration as revealed by girdling of boreal Scots pine forest: extending observations beyond the first year. *Plant Cell and Environment* **26**: 1287-1296.

Bloemen J, McGuire MA, Aubrey DP, Teskey RO, Steppe K. 2013a. Assimilation of xylem-transported CO_2 is dependent on transpiration rate but is small relative to atmospheric fixation. *Journal of Experimental Botany* **64**: 2129-2138.

Bloemen J, McGuire MA, Aubrey DP, Teskey RO, Steppe K. 2013b. Transport of root-respired CO_2 via the transpiration stream affects aboveground carbon assimilation and CO_2 efflux in trees. *New Phytologist* **197**: 555-565.

Bond-Lamberty B, Wang CK, Gower ST. 2004. A global relationship between the heterotrophic and autotrophic components of soil respiration? *Global Change Biology* **10**: 1756-1766.

Boone RD, Nadelhoffer KJ, Canary JD, Kaye JP. 1998. Roots exert a strong influence on the temperature sensitivity of soil respiration. *Nature* **396**: 570-572.

Bossard CC, Rejmanek M. 1992. Why Have Green Stems. *Functional Ecology* **6**: 197-205.

Bouma TJ, Bryla DR. 2000. On the assessment of root and soil respiration for soils of different textures: interactions with soil moisture contents and soil CO_2 concentrations. *Plant and Soil* **227**: 215-221.

Bouma TJ, Nielsen KL, Eissenstat DM, Lynch JP. 1997. Estimating respiration of roots in soil: Interactions with soil CO2, soil temperature and soil water content. *Plant and Soil* **195**: 221-232.

Bowden RD, Nadelhoffer KJ, Boone RD, Melillo JM, Garrison JB. 1993. Contributions of Aboveground Litter, Belowground Litter, and Root Respiration to Total Soil Respiration in a Temperature Mixed Hardwood Forest. *Canadian Journal of Forest Research-Revue Canadienne De Recherche Forestiere* **23**: 1402-1407.

Bowling DR, Pataki DE, Randerson JT. 2008. Carbon isotopes in terrestrial ecosystem pools and CO_2 fluxes. *New Phytologist* **178**: 24-40.

Bowman WP, Barbour MM, Turnbull MH, Tissue DT, Whitehead D, Griffin KL. 2005. Sap flow rates and sapwood density are critical factors in within- and between-tree variation in CO_2 efflux from stems of mature *Dacrydium cupressinum* trees. *New Phytologist* **167**: 815-828.

Boysen-Jensen P. 1933. Respiration I stamme og grene af traer. *Svenska Skogsvardsforeningens Tidskrift* **31**: 239-241.

Bradford KJ, Hsiao TC. 1982. Physiological responses to moderate water stress. In: O. L. Lange, P. S. Nobel, C. B. Osmond, H. Ziegler eds. *Encyclopedia of plant physiology. New series. Physiological plant ecology II: Water relations and carbon assimilation*. Berlin: Springer-Verlag, 263-324.

Brix H. 1990. Uptake and Photosynthetic Utilization of Sediment-Derived Carbon by *Phragmites australis* (Cav) Trin. Ex. Steudel. *Aquatic Botany* **38**: 377-389.

Brodribb TJ, Feild TS, Sack L. 2010. Viewing leaf structure and evolution from a hydraulic perspective. *Functional Plant Biology* **37**: 488-498.

Brüggemann N, Gessler A, Kayler ZE, Keel SG, Badeck F, Barthel M, Boeckx P, Buchmann N, Brugnoli E, Esperschütz J, *et al.* 2011. Carbon allocation and carbon isotope fluxes in the plant-soil-atmosphere continuum: a review. *Biogeosciences* **8**: 3619-3695.

Bryla DR, Bouma TJ, Eissenstat DM. 1997. Root respiration in citrus acclimates to temperature and slows during drought. *Plant Cell and Environment* **20**: 1411-1420.

Burton AJ, Pregitzer KS. 2002. Measurement carbon dioxide concentration does not affect root respiration of nine tree species in the field. *Tree Physiology* **22**: 67-72.

Burton AJ, Pregitzer KS, Zogg GP, Zak DR. 1998. Drought reduces root respiration in sugar maple forests. *Ecological Applications* **8**: 771-778.

Bush SE, Hultine KR, Sperry JS, Ehleringer JR. 2010. Calibration of thermal dissipation sap flow probes for ring- and diffuse-porous trees. *Tree Physiology* **30**: 1545-1554.

Bushong FW. 1907. Composition of gas from cottonwood trees. *Kansas Academy of Science Transactions* **21**: 53.

Butler JN. 1991. *Carbon dioxide equilibria and their applications*. Boca Raton, FL: CRC Press - 272 Pages

Campbell JA, Strother S. 1996. Seasonal variation in pH, carbohydrate and nitrogen of xylem exudate of Vitis vinifera. *Australian Journal of Plant Physiology* **23**: 115-118.

Carbone MS, Czimczik CI, McDuffee KE, Trumbore SE. 2007. Allocation and residence time of photosynthetic products in a boreal forest using a low-level ^{14}C pulse-chase labeling technique. *Global Change Biology* **13**: 466-477.

Cernusak LA, Hutley LB. 2011. Stable Isotopes Reveal the Contribution of Corticular Photosynthesis to Growth in Branches of *Eucalyptus miniata*. *Plant Physiology* **155**: 515-523.

Cernusak LA, Marshall JD. 2000. Photosynthetic refixation in branches of Western White Pine. *Functional Ecology* **14**: 300-311.

Cernusak LA, Marshall JD, Comstock JP, Balster NJ. 2001. Carbon isotope discrimination in photosynthetic bark. *Oecologia* **128**: 24-35.

Ceschia E, Damesin C, Lebaube S, Pontailler JY, Dufrene E. 2002. Spatial and seasonal variations in stem respiration of beech trees (*Fagus sylvatica*). *Annals of Forest Science* **59**: 801-812.

Chambers JQ, Tribuzy ES, Toledo LC, Crispim BF, Higuchi N, dos Santos J, Araujo AC, Kruijt B, Nobre AD, Trumbore SE. 2004. Respiration from a tropical forest ecosystem: Partitioning of sources and low carbon use efficiency. *Ecological Applications* **14**: S72-S88.

Chase WW 1934. The composition, quantity, and physiological significance of gases in tree stems. *Minnesota Agricultural Experiment Station Technical Bulletin 99*. St. Paul, MS, USA: University of Minnesota.

Chaves MM, Maroco JP, Pereira JS. 2003. Understanding plant responses to drought - from genes to the whole plant. *Functional Plant Biology* **30**: 239-264.

Chaves MM, Pereira JS, Maroco J, Rodrigues ML, Ricardo CPP, Osorio ML, Carvalho I, Faria T, Pinheiro C. 2002. How plants cope with water stress in the field. Photosynthesis and growth. *Annals of Botany* **89**: 907-916.

Chen DM, Zhou LX, Rao XQ, Lin YB, Fu SL. 2010. Effects of root diameter and root nitrogen concentration on in situ root respiration among different seasons and tree species. *Ecological Research* **25**: 983-993.

Clearwater M, Goldstein G. 2005. Embolism repair and long distance transport. In: N. M. Holbrook, M. Zwieniecki eds. *Vascular Transport in Plants*. Burlington, MA, USA: Elsevier Academic Press.

Coe JM, McLaughlin SB. 1980. Winter Season Corticular Photosynthesis in *Cornus floride*, *Acer rubrum*, *Quercus alba*, and *Liriodendron tulipifera*. *Forest Science* **26**: 561-566.

Colmer TD. 2003. Long-distance transport of gases in plants: a perspective on internal aeration and radial oxygen loss from roots. *Plant Cell and Environment* **26**: 17-36.

Comas LH, Eissenstat DM. 2004. Linking fine root traits to maximum potential growth rate among 11 mature temperate tree species. *Functional Ecology* **18**: 388-397.

Comstock J, Ehleringer J. 1990. Effect of Variations in Leaf Size on Morphology and Photosynthetic Rate of Twigs. *Functional Ecology* **4**: 209-221.

Comstock JP, Ehleringer JR. 1988. Contrasting Photosynthetic Behavior in Leaves and Twigs of *Hymenoclea salsola*, a Green-Twigged Warm Desert Shrub. *American Journal of Botany* **75**: 1360-1370.

Craig H. 1953. The geochemistry of the stable carbon isotopes. *Geochimica Et Cosmochimica Acta* **3**: 53-92.

Craig H. 1954. ^{13}C in plants and the relationships between ^{13}C and ^{14}C variations in nature. *Journal of Geology* **62**: 115-149.

Cruiziat P, Tyree MT. 1990. The Rise of Sap in Trees. *Recherche* **21**: 406-413.

Curiel Yuste J, Janssens IA, Carrara A, Ceulemans R. 2004. Annual Q_{10} of soil respiration reflects plant phenological patterns as well as temperature sensitivity. *Global Change Biology* **10**: 161-169.

D'Haene K, Van den Bossche A, Vandenbruwane J, De Neve S, Gabriels D, Hofman G. 2008. The effect of reduced tillage on nitrous oxide emissions of silt loam soils. *Biology and Fertility of Soils* **45**: 213-217.

Damesin C. 2003. Respiration and photosynthesis characteristics of current-year stems of *Fagus sylvatica*: from the seasonal pattern to an annual balance. *New Phytologist* **158**: 465-475.

Damesin C, Ceschia E, Le Goff N, Ottorini JM, Dufrene E. 2002. Stem and branch respiration of beech: from tree measurements to estimations at the stand level. *New Phytologist* **153**: 159-172.

Dannoura M, Maillard P, Fresneau C, Plain C, Berveiller D, Gerant D, Chipeaux C, Bosc A, Ngao J, Damesin C*, et al.* 2011. In situ assessment of the velocity of carbon transfer by tracing ^{13}C in trunk CO_2 efflux after pulse labelling: variations among tree species and seasons. *New Phytologist* **190**: 181-192.

Davidson EA, Belk E, Boone RD. 1998. Soil water content and temperature as independent or confounded factors controlling soil respiration in a temperate mixed hardwood forest. *Global Change Biology* **4**: 217-227.

Davidson EA, Janssens IA, Luo YQ. 2006a. On the variability of respiration in terrestrial ecosystems: moving beyond Q_{10}. *Global Change Biology* **12**: 154-164.

Davidson EA, Richardson AD, Savage KE, Hollinger DY. 2006b. A distinct seasonal pattern of the ratio of soil respiration to total ecosystem respiration in a spruce-dominated forest. *Global Change Biology* **12**: 230-239.

Davidson EA, Savage K, Verchot LV, Navarro R. 2002. Minimizing artifacts and biases in chamber-based measurements of soil respiration. *Agricultural and Forest Meteorology* **113**: 21-37.

Dawson TE, Brooks PD. 2001. Fundamentals of Stable Isotope Chemistry and Measurement. In: M. Unkovich, J. Pate, A. MCNeill, J. D. Gibbs eds. *Stable Isotope Techniques in the Study of Biological Processes and Functioning of Ecosystems*. Dordrecht, The Netherlands: Kluwer Academic Publishers, 1-18.

Dawson TE, Mambelli S, Plamboeck AH, Templer PH, Tu KP. 2002. Stable isotopes in plant ecology. *Annual Review of Ecology and Systematics* **33**: 507-559.

De Schepper V, Steppe K. 2010. Development and verification of a water and sugar transport model using measured stem diameter variations. *Journal of Experimental Botany* **61**: 2083-2099.

De Schepper V, Steppe K, Van Labeke MC, Lemeur R. 2010. Detailed analysis of double girdling effects on stem diameter variations and sap flow in young oak trees. *Environmental and Experimental Botany* **68**: 149-156.

De Schepper V, Vanhaecke L, Steppe K. 2012. Localized stem chilling alters carbon processes in the adjacent stem and in source leaves. *Tree Physiology* **31**: 1194-1203.

De Simone O, Haase K, Muller E, Junk WJ, Hartmann K, Schreiber L, Schmidt W. 2003. Apoplasmic barriers and oxygen transport properties of hypodermal cell walls in roots from four Amazonian tree species. *Plant Physiology* **132**: 206-217.

Dirks RC, Singh M, Potter GS, Sobotka LG, Schaefer J. 2012. Carbon partitioning in soybean (*Glycine max*) leaves by combined ^{11}C and ^{13}C labeling. *New Phytologist* **196**: 1109-1121.

Domec JC, Pruyn ML. 2008. Bole girdling affects metabolic properties and root, trunk and branch hydraulics of young ponderosa pine trees. *Tree Physiology* **28**: 1493-1504.

Edwards CA, Reichle DE, Crossley DAJ. 1970. The role of soil invertebrates in turnover of organic matter and nutrients. In: D. E. Reichle ed. *Analysis of Temperate Forest ecosystems*. New York: Springer-Verlag, 12-172.

Edwards NT, Mclaughlin SB. 1978. Temperature-Independent Diel Variations of Respiration Rates in *Quercus alba* and *Liriodendron tulipifera*. *Oikos* **31**: 200-206.

Eissenstat DM, Wells CE, Yanai RD, Whitbeck JL. 2000. Building roots in a changing environment: implications for root longevity. *New Phytologist* **147**: 33-42.

Ekberg A, Buchmann N, Gleixner G. 2007. Rhizospheric influence on soil respiration and decomposition in a temperate Norway spruce stand. *Soil Biology & Biochemistry* **39**: 2103-2110.

Eklund L, Lavigne MB. 1995. Restricted Lateral Gas Movement in *Pinus strobus* Branches. *Trees-Structure and Function* **10**: 83-85.

Enoch HZ, Olesen JM. 1993. Plant-Response to Irrigation with Water Enriched with Carbon-Dioxide. *New Phytologist* **125**: 249-258.

Epron D. 2009. Separating autotrophic and heterotrophic components of soil respiration: lessons learned from trenching and related root-exclusion experiments. In: W. L. Kutsch, M. Bahn, A. Heinemeyer eds. *Soil Carbon Dynamics*. Cambridge: Cambridge University Press, 157-168.

Epron D, Bahn M, Derrien D, Lattanzi FA, Pumpanen J, Gessler A, Hogberg P, Maillard P, Dannoura M, Gerant D*, et al.* 2012. Pulse-labelling trees to study carbon allocation dynamics: a review of methods, current knowledge and future prospects. *Tree Physiology* **32**: 776-798.

Epron D, Farque L, Lucot E, Badot PM. 1999. Soil CO_2 efflux in a beech forest: the contribution of root respiration. *Annals of Forest Science* **56**: 289-295.

Epron D, Ngao J, Dannoura M, Bakker MR, Zeller B, Bazot S, Bosc A, Plain C, Lata JC, Priault P, *et al.* 2011. Seasonal variations of belowground carbon transfer assessed by in situ $^{13}CO_2$ pulse labelling of trees. *Biogeosciences* **8**: 1153-1168.

Erda F, Bloemen J, Steppe K. 2013. Quantifying the impact of daily and seasonal variation in sap pH on xylem dissolved inorganic carbon estimates in plum trees. *Plant Biology: 10.1111/plb.12009 (in press)*.

Etzold S, Zweifel R, Ruehr NK, Eugster W, Buchmann N. 2013. Long-term stem CO_2 concentration measurements in Norway spruce in relation to biotic and abiotic factors. *New Phytologist*: doi: 10.1111/nph.12115.

Eyles A, Pinkard EA, O'Grady AP, Worledge D, Warren CR. 2009. Role of corticular photosynthesis following defoliation in *Eucalyptus globulus*. *Plant Cell and Environment* **32**: 1004-1014.

Farquhar GD, Ehleringer JR, Hubick KT. 1989. Carbon Isotope Discrimination and Photosynthesis. *Annual Review of Plant Physiology and Plant Molecular Biology* **40**: 503-537.

Farrar JF. 1999. Carbohydrate: where does it come from, where does it go? In: J. A. Bryant, M. M. Burrell, N. J. Kruger eds. *¨Plant Carbohydrate Biochemistry*. Oxford: Bios Scientific Publishers, 29-46.

Farrar JF, Williams JHH. 1990. Control of the rate of respiration in roots. In: M. J. Emes ed. *Compartmentation of Plant Metabolism in Non-photosynthetic Tissues*. Cambridge: Cambridge University Press, 167-188.

Flexas J, Medrano H. 2002. Drought-inhibition of photosynthesis in C_3 plants: Stomatal and non-stomatal limitations revisited. *Annals of Botany* **89**: 183-189.

Ford CR, Wurzburger N, Hendrick RL, Teskey RO. 2007. Soil DIC uptake and fixation in *Pinus taeda* seedlings and its C contribution to plant tissues and ectomycorrhizal fungi. *Tree Physiology* **27**: 375-383.

Frey B, Hagedorn F, Giudici F. 2006. Effect of girdling on soil respiration and root composition in a sweet chestnut forest. *Forest Ecology and Management* **225**: 271-277.

Gansert D, Burgdorf M. 2005. Effects of xylem sap flow on carbon dioxide efflux from stems of birch (*Betula pendula* Roth). *Flora* **200**: 444-455.

Gartner BL, Moore JR, Gardiner BA. 2004. Gas in stems: abundance and potential consequences for tree biomechanics. *Tree Physiology* **24**: 1239-1250.

Gaumont-Guay D, Black TA, Griffis TJ, Barr AG, Morgenstern K, Jassal RS, Nesic Z. 2006. Influence of temperature and drought on seasonal and interannual variations of soil, bole and ecosystem respiration in a boreal aspen stand. *Agricultural and Forest Meteorology* **140**: 203-219.

George K, Norby RJ, Hamilton JG, DeLucia EH. 2003. Fine-root respiration in a loblolly pine and sweetgum forest growing in elevated CO_2. *New Phytologist* **160**: 511-522.

Ghashghaie J, Badeck F-W, Lanigan G, Nogués S, Tcherkez G, Deléens E, Cornic G, Griffiths H. 2003. Carbon isotope fractionation during dark respiration and photorespiration in C_3 plants. *Phytochemistry Reviews* **2**: 145-161.

Gibson AC. 1983. Anatomy of Photosynthetic Old Stems of Nonsucculent Dicotyledons from North-American Deserts. *Botanical Gazette* **144**: 347-362.

Gill RA, Jackson RB. 2000. Global patterns of root turnover for terrestrial ecosystems. *New Phytologist* **147**: 13-31.

Glass ADM. 2002. Nutrient Absorption by Plant Roots: Regulation of Uptake to Match Plant Demand. In: Y. Waisel, A. Eshel, U. Kafkafi eds. *Plant Roots The Hidden Half Third Edition Revised and Expanded*. New York: Marcel Dekkers, 571-586.

Goodwin RH, Goddard DR. 1940. The oxygen consumption of isolated woody tissues. *American Journal of Botany* **27**: 234-237.

Goulden ML, Munger JW, Fan SM, Daube BC, Wofsy SC. 1996. Exchange of carbon dioxide by a deciduous forest: Response to interannual climate variability. *Science* **271**: 1576-1578.

Granier A. 1985. A new method of sap flow measurement in tree stems. *Annales Des Sciences Forestieres* **42**: 193-200.

Grassi G, Magnani F. 2005. Stomatal, mesophyll conductance and biochemical limitations to photosynthesis as affected by drought and leaf ontogeny in ash and oak trees. *Plant Cell and Environment* **28**: 834-849.

Griffiths H, Weller G, Toy LFM, Dennis RJ. 2013. You're so vein: bundle sheath physiology, phylogeny and evolution in C_3 and C_4 plants. *Plant Cell and Environment* **36**: 249-261.

Grosse W, Jovy K, Tiebel H. 1996. Influence of plants on redox potential and methane production in water-saturated soil. *Hydrobiologia* **340**: 93-99.

Grossiord C, Mareschal L, Epron D. 2012. Transpiration alters the contribution of autotrophic and heterotrophic components of soil CO_2 efflux. *New Phytologist* **194**: 647-653.

Gruber A, Wieser G, Oberhuber W. 2009. Intra-annual dynamics of stem CO_2 efflux in relation to cambial activity and xylem development in *Pinus cembra*. *Tree Physiology* **29**: 641-649.

Hacke UG, Sperry JS, Pittermann J. 2000. Drought experience and cavitation resistance in six shrubs from the Great Basin, Utah. *Basic and Applied Ecology* **1**: 31-41.

Hanson PJ, Edwards NT, Garten CT, Andrews JA. 2000. Separating root and soil microbial contributions to soil respiration: A review of methods and observations. *Biogeochemistry* **48**: 115-146.

Hanson PJ, Gunderson CA. 2009. Root carbon flux: measurements versus mechanisms. *New Phytologist* **184**: 4-6.

Hari P, Nygren P, Korpilahti E. 1991. Internal Circulation of Carbon within a Tree. *Canadian Journal of Forest Research-Revue Canadienne De Recherche Forestiere* **21**: 514-515.

Heimann M, Reichstein M. 2008. Terrestrial ecosystem carbon dynamics and climate feedbacks. *Nature* **451**: 289-292.

Herrmann KM, Weaver LM. 1999. The shikimate pathway. *Annual Review of Plant Physiology and Plant Molecular Biology* **50**: 473-503.

Hibberd JM, Quick WP. 2002. Characteristics of C_4 photosynthesis in stems and petioles of C_3 flowering plants. *Nature* **415**: 451-454.

Högberg P, Bhupinderpal-Singh, Lofvenius MO, Nordgren A. 2009. Partitioning of soil respiration into its autotrophic and heterotrophic components by means of tree-girdling in old boreal spruce forest. *Forest Ecology and Management* **257**: 1764-1767.

Högberg P, Hogberg MN, Gottlicher SG, Betson NR, Keel SG, Metcalfe DB, Campbell C, Schindlbacher A, Hurry V, Lundmark T*, et al.* 2008. High temporal resolution tracing of photosynthate carbon from the tree canopy to forest soil microorganisms. *New Phytologist* **177**: 220-228.

Högberg P, Nordgren A, Buchmann N, Taylor AFS, Ekblad A, Hogberg MN, Nyberg G, Ottosson-Lofvenius M, Read DJ. 2001. Large-scale forest girdling shows that current photosynthesis drives soil respiration. *Nature* **411**: 789-792.

Hölttä T, Kolari P. 2009. Interpretation of stem CO_2 efflux measurements. *Tree Physiology* **29**: 1447-1456.

Hook DD, Brown CL. 1972. Permeability of Cambium to Air in Trees Adapted to Wet Habitats. *Botanical Gazette* **133**: 304-310.

Hook DD, Brown CL, Wetmore RH. 1972. Aeration in Trees. *Botanical Gazette* **133**: 443-454.

Houghton RA. 2007. Balancing the global carbon budget. *Annual Review of Earth and Planetary Sciences* **35**: 313-347.

Hsiao TC. 1973. Plant Responses to Water Stress. *Annual Review of Plant Physiology and Plant Molecular Biology* **24**: 519-570.

Jahnke S, Menzel MI, van Dusschoten D, Roeb GW, Buhler J, Minwuyelet S, Blumler P, Temperton VM, Hombach T, Streun M*, et al.* 2009. Combined MRI-PET dissects dynamic changes in plant structures and functions. *Plant Journal* **59**: 634-644.

Jakob HF, Fengel D, Tschegg SE, Fratzl P. 1995. The elementary cellulose fibril in Picea abies: Comparison of transmission electron microscopy, small-angle X-ray scattering, and wide-angle X-ray scattering results. *Macromolecules* **28**: 8782-8787.

Jakob HF, Fratzl P, Tschegg SE. 1994. Size and Arrangement of Elementary Cellulose Fibrils in Wood Cells - a Small-Angle X-Ray-Scattering Study of *Picea abies*. *Journal of Structural Biology* **113**: 13-22.

Janacek SH, Trenkamp S, Palmer B, Brown NJ, Parsley K, Stanley S, Astley HM, Rolfe SA, Quick WP, Fernie AR*, et al.* 2009. Photosynthesis in cells around veins of the C_3 plant *Arabidopsis thaliana* is important for both the shikimate pathway and leaf senescence as well as contributing to plant fitness. *Plant Journal* **59**: 329-343.

Janssens IA, Lankreijer H, Matteucci G, Kowalski AS, Buchmann N, Epron D, Pilegaard K, Kutsch W, Longdoz B, Grunwald T*, et al.* 2001. Productivity overshadows temperature in determining soil and ecosystem respiration across European forests. *Global Change Biology* **7**: 269-278.

Jensen KH, Liesche J, Bohr T, Schulz A. 2012. Universality of phloem transport in seed plants. *Plant Cell and Environment* **35**: 1065-1076.

Johansson N. 1933. Sambandet mellan vedstammens andning och dess tillvaxt. *Svenska Skogsvardsforeningens Tidskrift* **31**: 57-134.

Johnsen K, Maier C, Sanchez F, Anderson P, Butnor J, Waring R, Linder S. 2007. Physiological girdling of pine trees via phloem chilling: proof of concept. *Plant Cell and Environment* **30**: 128-134.

Jones D, Nguyen C, Finlay R. 2009. Carbon flow in the rhizosphere: carbon trading at the soil–root interface. *Plant and Soil* **321**: 5-33.

Jones HG. 1992. *Plants and microclimate: a quantitative approach to plant physiology*. Cambridge, UK: Cambridge University Press.

Jordan MO, Habib R. 1996. Mobilizable carbon reserves in young peach trees as evidenced by trunk girdling experiments. *Journal of Experimental Botany* **47**: 79-87.

Jungk AO. 2002. Dynamics of Nutrient Movement at the Soil-Root Interface. In: Y. Waisel, A. Eshel, U. Kafkafi eds. *Plant Roots The Hidden Half, Third Edition Revised and Expanded*. New York: Marcel Dekker, 587-616.

Kaipiainen LK, Sofronova GI, Hari P, Yalynskaya EE. 1998. The role of xylem in CO_2 exchange in *Pinus sylvestris* woody stems. *Russian Journal of Plant Physiology* **45**: 500-505.

Katayama A, Kume T, Komatsu H, Ohashi M, Nakagawa M, Yamashita M, Otsuki K, Suzuki M, Kumagai T. 2009. Effect of forest structure on the spatial variation in soil respiration in a Bornean tropical rainforest. *Agricultural and Forest Meteorology* **149**: 1666-1673.

Kawachi N, Kikuchi K, Suzui N, Ishii S, Fujimaki S, Ishioka NS, Watabe H. 2011a. Imaging of Carbon Translocation to Fruit Using ^{11}C-Labeled Carbon Dioxide and Positron Emission Tomography. *Ieee Transactions on Nuclear Science* **58**: 395-399.

Kawachi N, Suzui N, Ishii S, Ito S, Ishioka NS, Yamazaki H, Hatano-Iwasaki A, Ogawa K, Fujimaki S. 2011b. Real-time whole-plant imaging of ^{11}C translocation

using positron-emitting tracer imaging system. *Nuclear Instruments & Methods in Physics Research Section a-Accelerators Spectrometers Detectors and Associated Equipment* **648**: S317-S320.

King AW, Gunderson CA, Post WM, Weston DJ, Wullschleger SD. 2006. Atmosphere - Plant respiration in a warmer world. *Science* **312**: 536-537.

Kramer PJ, Boyer JS. 1995. *Water Relations of Plants and Soils*. San Diego, California, US: Academic Press.

Kramer PJ, Kozlowski TT. 1979. *Physiology of woody plants*. New York: Academic Press.

Kuzyakov Y. 2006. Sources of CO_2 efflux from soil and review of partitioning methods. *Soil Biology & Biochemistry* **38**: 425-448.

Kuzyakov Y, Gavrichkova O. 2010. Review: Time lag between photosynthesis and carbon dioxide efflux from soil: a review of mechanisms and controls. *Global Change Biology* **16**: 3386-3406.

Kuzyakov YV, Larionova AA. 2006. Contribution of rhizomicrobial and root respiration to the CO_2 emission from soil (A review). *Eurasian Soil Science* **39**: 753-764.

Lambers H. 1987. Growth, respiration, exudation and symbiotic association: the fate of carbon translocated to roots. In: P. J. Gregory, J. V. Lake, D. A. Rose eds. *Root development and function*. Cambridge: Cambridge University Press, 245-252.

Lambers H, Atkin OK, Millenaar FF. 2002. Respiratory Patterns in Roots in Relation to Their Functioning. In: Y. Waisel, A. Eshel, U. Kafkafi eds. *Plant Roots: The Hidden Half*. New York: Marcel Dekker Inc., 521-552.

Landais P, Finn R. 1989. Online Preparation of [^{11}C] Carbon Dioxide from [^{11}C] Methane. *Applied Radiation and Isotopes* **40**: 265-266.

Lavigne MB, Ryan MG. 1997. Growth and maintenance respiration rates of aspen, black spruce and jack pine stems at northern and southern BOREAS sites. *Tree Physiology* **17**: 543-551.

Lavoir AV, Staudt M, Schnitzler JP, Landais D, Massol F, Rocheteau A, Rodriguez R, Zimmer I, Rambal S. 2009. Drought reduced monoterpene emissions from the evergreen Mediterranean oak *Quercus ilex*: results from a throughfall displacement experiment. *Biogeosciences* **6**: 1167-1180.

Leegood RC. 2008. Roles of the bundle sheath cells in leaves of C_3 plants. *Journal of Experimental Botany* **59**: 1663-1673.

Lendzian KJ. 2006. Survival strategies of plants during secondary growth: barrier properties of phellems and lenticels towards water, oxygen, and carbon dioxide. *Journal of Experimental Botany* **57**: 2535-2546.

Levy PE, Meir P, Allen SJ, Jarvis PG. 1999. The effect of aqueous transport of CO_2 in xylem sap on gas exchange in woody plants. *Tree Physiology* **19**: 53-58.

Li MR, Jones MB. 1995. CO_2 and O_2 Transport in the Aerenchyma of *Cyperus papyrus* L. *Aquatic Botany* **52**: 93-106.

Litton CM, Raich JW, Ryan MG. 2007. Carbon allocation in forest ecosystems. *Global Change Biology* **13**: 2089-2109.

Logullo MA, Salleo S. 1993. Different Vulnerabilities of *Quercus ilex* L. to Freeze-Induced and Summer Drought-Induced Xylem Embolism - an Ecological Interpretation. *Plant Cell and Environment* **16**: 511-519.

Long SP, Hallgren JE. 1985. Measurement of CO_2 assimilation by plants in the field and the laboratory. In: J. Coombs, D. O. Hall, S. P. Long, J. M. O. Scurlock eds. *Techniques of Bioproductivity and Photosynthesis*. Oxford: Pergamon Press, 62-94.

Luyssaert S, Ciais P, Piao SL, Schulze ED, Jung M, Zaehle S, Schelhaas MJ, Reichstein M, Churkina G, Papale D*, et al.* 2010. The European carbon balance. Part 3: forests. *Global Change Biology* **16**: 1429-1450.

Luyssaert S, Inglima I, Jung M, Richardson AD, Reichsteins M, Papale D, Piao SL, Schulzes ED, Wingate L, Matteucci G, *et al.* 2007. CO2 balance of boreal, temperate, and tropical forests derived from a global database. *Global Change Biology* **13**: 2509-2537.

Lyford WH, Wilson BG. 1964. *Development of the root system of Acer rubrum L.* . Harvard University, Petersham, MA, USA.

Lynch DJ, Matamala R, Iversen CM, Norby RJ, Gonzalez-Meler MA. 2013. Stored carbon partly fuels fine-root respiration but is not used for production of new fine roots. *New Phytologist* **199**: 420-430.

Lynch DJ, McInerney FA, Kouwenberg LLR, Gonzalez-Meler MA. 2012. Plasticity in Bundle Sheath Extensions of Heterobaric Leaves. *American Journal of Botany* **99**: 1197-1206.

MacDougal DT. 1927. Composition of gases in trunks of trees. *Carnegie Institution of Washington DC, USA Year Book* **26**: 162-163.

MacDougal DT, Overton JB, Smith GM. 1929. *The hydrostatic-pneumatic system of certain trees: movements of liquids and gases.* . Washington DC, USA: Carnegie Institution of Washington Publication 397.

MacDougal DT, Working EB. 1933. *The pneumatic system of plants especially trees*. Washington DC: Carnegie Institution of Washington Publication 411.

Maier CA. 2001. Stem growth and respiration in loblolly pine plantations differing in soil resource availability. *Tree Physiology* **21**: 1183-1193.

Maier CA, Clinton BD. 2006. Relationship between stem CO2 efflux, stem sap velocity and xylem CO2 concentration in young loblolly pine trees. *Plant Cell and Environment* **29**: 1471-1483.

Maier CA, Zarnoch SJ, Dougherty PM. 1998. Effects of temperature and tissue nitrogen on dormant season stem and branch maintenance respiration in a young loblolly pine (*Pinus taeda*) plantation. *Tree Physiology* **18**: 11-20.

Makita N, Yaku R, Ohashi M, Fukuda K, Ikeno H, Hirano Y. 2012. Effects of excising and washing treatments on the root respiration rates of Japanese cedar (*Cryptomeria japonica*) seedlings. *Journal of Forest Research*: 1-5.

Marron N, Plain C, Longdoz B, Epron D. 2009. Seasonal and daily time course of the ^{13}C composition in soil CO_2 efflux recorded with a tunable diode laser spectrophotometer (TDLS). *Plant and Soil* **318**: 137-151.

Marsden C, Nouvellon Y, Epron D. 2008. Relating coarse root respiration to root diameter in clonal Eucalyptus stands in the Republic of the Congo. *Tree Physiology* **28**: 1245-1254.

Martin TA, Teskey RO, Dougherty PM. 1994. movement of respiratory CO_2 in stems of loblolly pine (*Pinus taeda* L.) seedlings. *Tree Physiology* **14**: 481-495.

Massman WJ, Kaufmann MR. 1991. Stomatal Response to Certain Environmental-Factors - a Comparison of Models for Sub-Alpine Trees in the Rocky-Mountains. *Agricultural and Forest Meteorology* **54**: 155-167.

Matsuhashi S, Fujimaki S, Uchida H, Ishioka NS, Kume T. 2006. A new visualization technique for the study of the accumulation of photoassimilates in wheat grains using $^{11}CO2$. *Applied Radiation and Isotopes* **64**: 435-440.

Maunoury-Danger F, Fresneau C, Eglin T, Berveiller D, Francois C, Lelarge-Trouverie C, Damesin C. 2010. Impact of carbohydrate supply on stem growth, wood and respired CO_2 $\delta^{13}C$: assessment by experimental girdling. *Tree Physiology* **30**: 818-830.

Mccaughey JH, Iacobelli A. 1994. Modeling Stomatal Conductance in a Northern Deciduous Forest, Chalk-River, Ontario. *Canadian Journal of Forest Research-Revue Canadienne De Recherche Forestiere* **24**: 904-910.

McClendon JH. 1992. Photographic Survey of the Occurence of Bundle-sheath Extensions in Deciduous Dicots. *Plant Physiology* **99**: 1677-1679.

McCree KJ. 1970. An equation for the rate of dark respiration of white clover plants grown under controlled conditions. In: I. Setlik ed. *Prediction and Measurement of Photosynthetic Productivity*. Wageningen: Centre for Agric. Publ. and Doc., 221-229.

McCully ME, Huang CX, Ling LEC. 1998. Daily embolism and refilling of xylem vessels in the roots of field-grown maize. *New Phytologist* **138**: 327-342.

McDowell NG, Marshall JD, Qi JG, Mattson K. 1999. Direct inhibition of maintenance respiration in western hemlock roots exposed to ambient soil carbon dioxide concentrations. *Tree Physiology* **19**: 599-605.

McGuire MA, Cerasoli S, Teskey RO. 2007. CO_2 fluxes and respiration of branch segments (*Platanus occidentalis* L.) examined at different velocities, branch diameters, and temperatures. *Journal of Experimental Botany* **58**: 2159-2168.

McGuire MA, Marshall JD, Teskey RO. 2009. Assimilation of xylem-transported ^{13}C-labelled CO_2 in leaves and branches of sycamore (*Platanus occidentalis* L.). *Journal of Experimental Botany* **60**: 3809-3817.

McGuire MA, Teskey RO. 2002. Microelectrode technique for in situ measurement of carbon dioxide concentrations in xylem sap of trees. *Tree Physiology* **22**: 807-811.

McGuire MA, Teskey RO. 2004. Estimating stem respiration in trees by a mass balance approach that accounts for internal and external fluxes of CO_2. *Tree Physiology* **24**: 571-578.

Milburn JA, Johnson RPC. 1966. Conduction of Sap. II. Detection of Vibrations Produced by Sap Cavitation in *Ricinus* Xylem. *Planta* **69**: 43-62.

Minchin PEH, Thorpe MR. 2003. Using the short-lived isotope ^{11}C in mechanistic studies of photosynthate transport. *Functional Plant Biology* **30**: 831-841.

Monteith JL. 1995. A Reinterpretation of Stomatal Responses to Humidity. *Plant Cell and Environment* **18**: 357-364.

Moore DJP, Gonzalez-Meler MA, Taneva L, Pippen JS, Kim HS, DeLucia EH. 2008. The effect of carbon dioxide enrichment on apparent stem respiration from *Pinus taeda* L. is confounded by high levels of soil carbon dioxide. *Oecologia* **158**: 1-10.

Moyano FE, Atkin OK, Bahn M, Bruhn D, Burton AJ, Heinemeyer A, Kutsch WL, Wieser G. 2009. Respiration from roots and the mycorrhizosphere. In: W. L. Kutsch, M. Bahn, A. Heinemeyer eds. *Soil Carbon Dynamics: An Integrated Methodology*. Cambridge: Cambride University Press, 127-156.

Moyano FE, Kutsch WL, Rebmann C. 2008. Soil respiration fluxes in relation to photosynthetic activity in broad-leaf and needle-leaf forest stands. *Agricultural and Forest Meteorology* **148**: 135-143.

Muhr J, Angert A, Negron-Juarez RI, Munoz WA, Kraemer G, Chambers JQ, Trumbore SE. 2013. Carbon dioxide emitted from live stems of tropical trees is several years old. *Tree Physiology* **33**: 743-752.

Nadelhoffer KJ, Fry B. 1994. Nitrogen isotope studies in forest ecosystems. In: K. Lajtha, R. H. Michener eds. *Stable Isotopes in Ecology and Environmental Science*. Oxford: Blackwell Scientific Publications, 22-44.

Nardini A, Lo Gullo MA, Salleo S. 2011. Refilling embolized xylem conduits: Is it a matter of phloem unloading? *Plant Science* **180**: 604-611.

Negisi K. 1974. Respiration rates in relation to diameter and age in stem or branch sections of young *Pinus densiflora* trees. *Bulletin Tokyo University Forests* **66**: 211-222.

Negisi K. 1979. Bark respiration rate in stem segments detached from young *Pinus densiflora* trees in relation to velocity of artifical sap flow *Journal of Japanese Forest Society* **61**: 88-93.

Nilsen ET. 1992. The Influence of Water-Stress on Leaf and Stem Photosynthesis in *Spartium junceum* L. *Plant Cell and Environment* **15**: 455-461.

Nilsen ET. 1995. Stem photosynthesis: Extent, Patterns and Role in Plant Carbon Economy. In: B. Gartner ed. *Plant Stems: Physiology and Functional Morphology*. San Diego, CA: Academic Press.

Nilsen ET, Bao Y. 1990. The Influence of Water-Stress on Stem and Leaf Photosynthesis in *Glycine max* and *Sparteum junceum* (Leguminosae). *American Journal of Botany* **77**: 1007-1015.

Nilsen ET, Sharifi MR. 1994. Seasonal Acclimation of Stem Photosynthesis in Woody Legume Species from the Mojave and Sonoran Deserts of California. *Plant Physiology* **105**: 1385-1391.

Nilsen ET, Sharifi MR. 1997. Carbon isotopic composition of legumes with photosynthetic stems from Mediterranean and desert habitats. *American Journal of Botany* **84**: 1707-1713.

Nobel PS, ed. 1999. *Physicochemical and environmental plant physiology*: Academic Press, San Diego, US.

Norby RJ. 2009. Introduction to a Virtual Special Issue: probing the carbon cycle with ^{13}C. *New Phytologist* **184**: 1-3.

Olsson P, Linder S, Giesler R, Hogberg P. 2005. Fertilization of boreal forest reduces both autotrophic and heterotrophic soil respiration. *Global Change Biology* **11**: 1745-1753.

Oren R, Sperry JS, Katul GG, Pataki DE, Ewers BE, Phillips N, Schafer KVR. 1999. Survey and synthesis of intra- and interspecific variation in stomatal sensitivity to vapour pressure deficit. *Plant Cell and Environment* **22**: 1515-1526.

Pausch RC, Grote EE, Dawson TE. 2000. Estimating water use by sugar maple trees: considerations when using heat-pulse methods in trees with deep functional sapwood. *Tree Physiology* **20**: 217-227.

Perks MP, Irvine J, Grace J. 2004. Xylem acoustic signals from mature *Pinus sylvestris* during an extended drought. *Annals of Forest Science* **61**: 1-8.

Perry TO. 1982. The ecology of tree roots and the practical significance thereof. *Journal of Arboriculture* **8**: 197-211.

Pfanz H. 2008. Bark photosynthesis. *Trees-Structure and Function* **22**: 137-138.

Pfanz H, Aschan G. 2001. The existence of bark and stem photosynthesis and its significance for the overall carbon gain: an eco-physiological and ecological approach. *Progress in Botany* **62**: 477-510.

Pfanz H, Aschan G, Langenfeld-Heyser R, Wittmann C, Loose M. 2002. Ecology and ecophysiology of tree stems: corticular and wood photosynthesis. *Naturwissenschaften* **89**: 147-162.

Pieruschka R, Schurr U, Jahnke S. 2005. Lateral gas diffusion inside leaves. *Journal of Experimental Botany* **56**: 857-864.

Plain C, Gerant D, Maillard P, Dannoura M, Dong YW, Zeller B, Priault P, Parent F, Epron D. 2009. Tracing of recently assimilated carbon in respiration at high temporal resolution in the field with a tuneable diode laser absorption spectrometer after in situ $^{13}CO_2$ pulse labelling of 20-year-old beech trees. *Tree Physiology* **29**: 1433-1445.

Porra RJ, Thompson WA, Kriedemann PE. 1989. Determination of accurate extincion coefficients and simultaneous-equations for assayong chlorophyll-a and chlorophyll-b extracted with 4 different solvents - verification of the concentration of chlorophyll standards by atomic-absorption spectroscopy. *Biochimica et Biophysica Acta* **975**: 384-394.

Powers EM, Marshall JD. 2011. Pulse labeling of dissolved ^{13}C-carbonate into tree xylem: developing a new method to determine the fate of recently fixed photosynthate. *Rapid Communications in Mass Spectrometry* **25**: 33-40.

Pregitzer KS, Laskowski MJ, Burton AJ, Lessard VC, Zak DR. 1998. Variation in sugar maple root respiration with root diameter and soil depth. *Tree Physiology* **18**: 665-670.

Prentice IC, Farquhar GD, Fasham MJR, Goulden ML, Heimann M, Jaramillo VJ, Khesghi HS, Le Querec C, Scholes RJ, Wallace DWR. 2001. The carbon cycle and atmospheric carbon dioxide. In: J. T. Houghton, Y. Ding, D. J. Griggs, M. Noguer, P. J. van der Linden, X. Dai, K. Maskell, C. A. Johnson eds. *Climate change 2001: the scientific basis: contribution of working group I to the Third Assessment Report of the Intengovernmental Panel on Climate Change*. Cambridge, UK: Cambridge University Press, 183-239.

Pruyn ML, Gartner BL, Harmon ME. 2002a. Respiratory potential in sapwood of old versus young ponderosa pine trees in the Pacific Northwest. *Tree Physiology* **22**: 105-116.

Pruyn ML, Gartner BL, Harmon ME. 2002b. Within-stem variation of respiration in *Pseudotsuga menziesii* (Douglas-fir) trees. *New Phytologist* **154**: 359-372.

Pruyn ML, Harmon ME, Gartner BL. 2003. Stem respiratory potential in six softwood and four hardwood tree species in the central cascades of Oregon. *Oecologia* **137**: 10-21.

Pumpanen J, Ilvesniemi H, Peramaki M, Hari P. 2003. Seasonal patterns of soil CO_2 efflux and soil air CO_2 concentration in a Scots pine forest: comparison of two chamber techniques. *Global Change Biology* **9**: 371-382.

Pumpanen J, Longdoz B, Kutsch WL. 2009. Field measurements of soil respiration: principles and constraints, potentials and limitations of different methods. In: W. L. Kutsch, M. Bahn, A. Heinemeyer eds. *Soil Carbon Dynamics: An Integrated Methodoloy*. Cambridge: Cambridge University Press, 17-33.

Qi JE, Marshall JD, Mattson KG. 1994. High Soil Carbon-Dioxide Concentrations Inhibit Root Respiration of Douglas Fir. *New Phytologist* **128**: 435-442.

Rakonczay Z, Seiler JR, Kelting DL. 1997. Carbon efflux rates of fine roots of three tree species decline shortly after excision. *Environmental and Experimental Botany* **38**: 243-249.

Regier N, Streb S, Zeeman SC, Frey B. 2010. Seasonal changes in starch and sugar content of poplar (*Populus deltoides* x nigra cv. Dorskamp) and the impact of stem girdling on carbohydrate allocation to roots. *Tree Physiology* **30**: 979-987.

Reich PB, Tjoelker MG, Pregitzer KS, Wright IJ, Oleksyn J, Machado JL. 2008. Scaling of respiration to nitrogen in leaves, stems and roots of higher land plants. *Ecology Letters* **11**: 793-801.

Reichstein M, Bahn M, Ciais P, Frank D, Mahecha MD, Seneviratne SI, Zscheischler J, Beer C, Buchmann N, Frank DC*, et al.* 2013. Climate extremes and the carbon cycle. *Nature* **500**: 287-295.

Rentzou A, Psaras GK. 2008. Green plastids, maximal PSH photochemical efficiency and starch content of inner stem tissues of three Mediterranean woody species during the year. *Flora* **203**: 350-357.

Rodgers HL, Brakke MP, Ewel JJ. 1995. Shoot Damage Effects on Starch Reserves of *Cedrela odorata*. *Biotropica* **27**: 71-77.

Rogner H-H, Zhou D, Bradley R, Crabbé P, Edenhofer O, Hare B, Kuijpers L, Yamaguchi M, R. Bradley. P. Crabbé OE, B.Hare (Australia), L. Kuijpers, M. Yamaguchi, 2007: Introduction. In Climate, Climate CMCoWGIttFARotIPo*, et al.* 2007. Introduction. In: B. Metz, A. R. Davidson, P. R. Bosch, R. Dave, L. A. Mayer eds. *Climate Change 2007: Mitigation. Contribution of Working Group III to the Fourth Assessment Report of the Intergovernmental Panel on Climate Change*. Cambridge, United Kingdom and New York, NY, USA: Cambridge University Press, 96-116.

Rolland F, Baena-Gonzalez E, Sheen J. 2006. Sugar sensing and signaling in plants: Conserved and novel mechanisms. *Annual Review of Plant Biology* **57**: 675-709.

Rosner S, Karlsson B, Konnerth J, Hansmann C. 2009. Shrinkage processes in standard size Norway spruce wood specimens with different vulnerability to cavitation. *Tree Physiology* **29**: 1419-1431.

Rosner S, Klein A, Wimmer R, Karlsson B. 2006. Extraction of features from ultrasound acoustic emissions: a tool to assess the hydraulic vulnerability of Norway spruce trunkwood? *New Phytologist* **171**: 105-116.

Roth-Nebelsick A, Uhl D, Mosbrugger V, Kerp H. 2001. Evolution and function of leaf venation architecture: A review. *Annals of Botany* **87**: 553-566.

Russin WA, Evert RF. 1984. Studies on the leaf of *Populus deltoides* (Salicaceae) - Morphology and anatomy. *American Journal of Botany* **71**: 1398-1415.

Ryan MG. 1990. Growth and Maintenance Respiration in Stems of *Pinus contorta* and *Picea Engelmannii*. *Canadian Journal of Forest Research-Revue Canadienne De Recherche Forestiere* **20**: 48-57.

Ryan MG, Cavaleri MA, Almeida AC, Penchel R, Senock RS, Stape JL. 2009. Wood CO_2 efflux and foliar respiration for *Eucalyptus* in Hawaii and Brazil. *Tree Physiology* **29**: 1213-1222.

Ryan MG, Gower ST, Hubbard RM, Waring RH, Gholz HL, Cropper WP, Running SW. 1995. woody tissue maintenance respiration of 4 conifers in contrasting climates. *Oecologia* **101**: 133-140.

Ryan MG, Hubbard RM, Clark DA, Sanford RL. 1994. Woody tissue respiration for *Simarouba amara* and *Minquartia guianensis*, two tropic wet forest trees with different growth habits. *Oecologia* **100**: 213-220.

Ryan MG, Hubbard RM, Pongracic S, Raison RJ, McMurtrie RE. 1996. Foliage, fine-root, woody-tissue and stand respiration in *Pinus radiata* in relation to nitrogen status. *Tree Physiology* **16**: 333-343.

Sack L, Holbrook NM. 2006. Leaf hydraulics. *Annual Review of Plant Biology* **57**: 361-381.

Sakuratani T, Abe J. 1985. A Heat-Balance Method for Measuring Water-Flow Rate in Stems of Intact Plants and Its Application to Sugarcane Plants. *Jarq-Japan Agricultural Research Quarterly* **19**: 92-97.

Salleo S, Lo Gullo MA, Trifilo P, Nardini A. 2004. New evidence for a role of vessel-associated cells and phloem in the rapid xylem refilling of cavitated stems of Laurus nobilis L. *Plant Cell and Environment* **27**: 1065-1076.

Sands R, Nugroho PB, Leung DWM, Sun OJ, Clinton PW. 2000. Changes in soil CO_2 and O_2 concentrations when radiata pine is grown in competition with pasture or weeds and possible feedbacks with radiata pine root growth and respiration. *Plant and Soil* **225**: 213-225.

Savage K, Davidson EA, Richardson AD. 2008. A conceptual and practical approach to data quality and analysis procedures for high-frequency soil respiration measurements. *Functional Ecology* **22**: 1000-1007.

Saveyn A. 2007. *Dynamic interactions between CO_2 efflux, sap flow and internal CO_2 concentration in tree stems: implications towards the assessment of actual stem respiration.* PhD Thesis, Ghent University, Gent, Belgium.

Saveyn A, Steppe K, Lemeur R. 2007a. Daytime depression in tree stem CO_2 efflux rates: Is it caused by low stem turgor pressure? *Annals of Botany* **99**: 477-485.

Saveyn A, Steppe K, Lemeur R. 2007b. Drought and the diurnal patterns of stem CO_2 efflux and xylem CO_2 concentration in young oak (*Quercus robur*). *Tree Physiology* **27**: 365-374.

Saveyn A, Steppe K, Lemeur R. 2008a. Report on non-temperature related variations in CO_2 efflux rates from young tree stems in the dormant season. *Trees-Structure and Function* **22**: 165-174.

Saveyn A, Steppe K, McGuire MA, Lemeur R, Teskey RO. 2008b. Stem respiration and carbon dioxide efflux of young Populus deltoides trees in relation to temperature and xylem carbon dioxide concentration. *Oecologia* **154**: 637-649.

Saveyn A, Steppe K, Ubierna N, Dawson TE. 2010. Woody tissue photosynthesis and its contribution to trunk growth and bud development in young plants. *Plant, Cell & Environment* **33**: 1949-1958.

Schmitz N, Egerton JJG, Lovelock CE, Ball MC. 2012. Light-dependent maintenance of hydraulic function in mangrove branches: do xylary chloroplasts play a role in embolism repair? *New Phytologist* **195**: 40-46.

Schneider H, Wistuba N, Miller B, Gessner P, Thurmer F, Melcher P, Meinzer F, Zimmermann U. 1997. Diurnal variation in the radial reflection coefficient of intact maize roots determined with the xylem pressure probe. *Journal of Experimental Botany* **48**: 2045-2053.

Schulze ED, Ciais P, Luyssaert S, Schrumpf M, Janssens IA, Thiruchittampalam B, Theloke J, Saurat M, Bringezu S, Lelieveld J, *et al.* 2010. The European carbon balance. Part 4: integration of carbon and other trace-gas fluxes. *Global Change Biology* **16**: 1451-1469.

Schurr U. 1998. Xylem sap sampling - new approaches to an old topic. *Trends in Plant Science* **3**: 293-298.

Scott-Denton LE, Rosenstiel TN, Monson RK. 2006. Differential controls by climate and substrate over the heterotrophic and rhizospheric components of soil respiration. *Global Change Biology* **12**: 205-216.

Secchi F, Zwieniecki MA. 2011. Sensing embolism in xylem vessels: the role of sucrose as a trigger for refilling. *Plant Cell and Environment* **34**: 514-524.

Shirley VS, Lederer CM. 1980. Table of nuclides. In: G. Friedlander, J. W. Kennedy, E. S. Macias, J. Malcom Miller eds. *Nuclear and Radiochemistry (third edition)*. New York: John Wiley and Sons Inc., 606-650.

Simpraga M, Verbeeck H, Demarcke M, Joo E, Pokorska O, Amelynck C, Schoon N, Dewulf J, Van Langenhove H, Heinesch B, *et al.* 2011. Clear link between drought stress, photosynthesis and biogenic volatile organic compounds in *Fagus sylvatica* L. *Atmospheric Environment* **45**: 5254-5259.

Smith DM, Allen SJ. 1996. Measurement of sap flow in plant stems. *Journal of Experimental Botany* **47**: 1833-1844.

Soe ARB, Buchmann N. 2005. Spatial and temporal variations in soil respiration in relation to stand structure and soil parameters in an unmanaged beech forest. *Tree Physiology* **25**: 1427-1436.

Sorz J, Hietz P. 2006. Gas diffusion through wood: implications for oxygen supply. *Trees - Structure and Function* **20**: 34-41.

Steppe K, De Pauw DJW, Doody TM, Teskey RO. 2010. A comparison of sap flux density using thermal dissipation, heat pulse velocity and heat field deformation methods. *Agricultural and Forest Meteorology* **150**: 1046-1056.

Steppe K, De Pauw DJW, Lemeur R. 2008. Validation of a dynamic stem diameter variation model and the resulting seasonal changes in calibrated parameter values. *Ecological Modelling* **218**: 247-259.

Steppe K, De Pauw DJW, Lemeur R, Vanrolleghem PA. 2006. A mathematical model linking tree sap flow dynamics to daily stem diameter fluctuations and radial stem growth. *Tree Physiology* **26**: 257-273.

Steppe K, Saveyn A, McGuire MA, Lemeur R, Teskey RO. 2007. Resistance to radial CO2 diffusion contributes to between-tree variation in CO2 efflux of Populus deltoides stems. *Functional Plant Biology* **34**: 785-792.

Stockfors J. 2000. Temperature variations and distribution of living cells within tree stems: implications for stem respiration modeling and scale-up. *Tree Physiology* **20**: 1057-1062.

Stoll M, Loveys B, Dry P. 2000. Hormonal changes induced by partial rootzone drying of irrigated grapevine. *Journal of Experimental Botany* **51**: 1627-1634.

Stringer JW, Kimmerer TW. 1993. Refixation of Xylem Sap CO_2 in *Populus deltoides*. *Physiologia Plantarum* **89**: 243-251.

Stumm W, Morgan JJ. 1996. *Aquatic chemistry: chemical equilibria and rates in natural waters. Third Edition*. New York, USA: John Wiley & Sons.

Subke J-A, Vallack HW, Magnusson T, Keel SG, Metcalfe DB, Högberg P, Ineson P. 2009. Short-term dynamics of abiotic and biotic soil $^{13}CO_2$ effluxes after in situ $^{13}CO_2$ pulse labelling of a boreal pine forest. *New Phytologist* **183**: 349-357.

Subke JA, Hahn V, Battipaglia G, Linder S, Buchmann N, Cotrufo MF. 2004. Feedback interactions between needle litter decomposition and rhizosphere activity. *Oecologia* **139**: 551-559.

Subke JA, Inglima I, Cotrufo MF. 2006. Trends and methodological impacts in soil CO_2 efflux partitioning: a meta-analytical review *Global Change Biology* **12**: 1813-1813.

Subke JA, Vallack HW, Magnusson T, Keel SG, Metcalfe DB, Hogberg P, Ineson P. 2009. Short-term dynamics of abiotic and biotic soil $^{13}CO_2$ effluxes after in situ $^{13}CO_2$ pulse labelling of a boreal pine forest. *New Phytologist* **183**: 349-357.

Subke JA, Voke NR, Leronni V, Garnett MH, Ineson P. 2011. Dynamics and pathways of autotrophic and heterotrophic soil CO_2 efflux revealed by forest girdling. *Journal of Ecology* **99**: 186-193.

Suleau M, Debacq A, Dehaes V, Aubinet M. 2009. Wind velocity perturbation of soil respiration measurements using closed dynamic chambers. *European Journal of Soil Science* **60**: 515-524.

Sun H, Aubrey D, Teskey R. 2011. A simple calibration improved the accuracy of the thermal dissipation technique for sap flow measurements in juvenile trees of six species. *Trees - Structure and Function*: 1-10.

Taiz L, Zeiger E. 2006. *Plant Physiology: Fourth Edition*. Sunderland, MA, US: Sinauer Associates, Inc. .

Tang JW, Baldocchi DD, Qi Y, Xu LK. 2003. Assessing soil CO_2 efflux using continuous measurements of CO_2 profiles in soils with small solid-state sensors. *Agricultural and Forest Meteorology* **118**: 207-220.

Terashima I. 1992. Anatomy of Nonuniform Leaf Photosynthesis. *Photosynthesis Research* **31**: 195-212.

Teskey RO, McGuire MA. 2002. Carbon dioxide transport in xylem causes errors in estimation of rates of respiration in stems and branches of trees. *Plant Cell and Environment* **25**: 1571-1577.

Teskey RO, McGuire MA. 2005. CO_2 transported in xylem sap affects CO_2 efflux from *Liquidambar styraciflua* and *Platanus occidentalis* stems, and contributes to observed wound respiration phenomena. *Trees-Structure and Function* **19**: 357-362.

Teskey RO, McGuire MA. 2007. Measurement of stem respiration of sycamore (*Platanus occidentalis* L.) trees involves internal and external fluxes of CO_2 and possible transport of CO_2 from roots. *Plant Cell and Environment* **30**: 570-579.

Teskey RO, Saveyn A, Steppe K, McGuire MA. 2008. Origin, fate and significance of CO_2 in tree stems. *New Phytologist* **177**: 17-32.

Thompson MV, Holbrook NM. 2004. Scaling phloem transport: information transmission. *Plant Cell and Environment* **27**: 509-519.

Thorpe MR, Ferrieri AP, Herth MM, Ferrieri RA. 2007. ^{11}C-imaging: methyl jasmonate moves in both phloem and xylem, promotes transport of jasmonate, and of photoassimilate even after proton transport is decoupled. *Planta* **226**: 541-551.

Trumbore S. 2006. Carbon respired by terrestrial ecosystems - recent progress and challenges. *Global Change Biology* **12**: 141-153.

Trumbore SE, Angert A, Kunert N, Muhr J, Chambers JQ. 2013. What's the flux? Unraveling how CO_2 fluxes from trees reflect underlying physiological processes. *New Phytologist* **197**: 353-355.

Tyree MT, Dixon MA. 1983. Cavitation Events in *Thuja occidentalis* L. - Utrasonic Acoustic Emissions from the Sapwood Can Be Measured. *Plant Physiology* **72**: 1094-1099.

Ubierna N, Kumar AS, Cernusak LA, Pangle RE, Gag PJ, Marshall JD. 2009. Storage and transpiration have negligible effects on $\delta^{13}C$ of stem CO_2 efflux in large conifer trees. *Tree Physiology* **29**: 1563-1574.

van Bavel MG, van Bavel CHM. 1990. Dynagage installation and operation manual. *Dynamax Inc., Texas*.

Van Cleve B, Forreiter C, Sauter JJ, Apel K. 1993. Pith cells of Poplar contain photosynthetically active chloroplasts. *Planta* **189**: 70-73.

Vandegehuchte MW, Steppe K. 2013. Sap-flux denity measurement methods: working principles and applicability. *Functional Plant Biology: 10.1071/FP12233 (in press)*.

Vapaavuori EM, Pelkonen P. 1985. HCO_3^- Uptake through the Roots and Its Effect on the Productivity of Willow Cuttings. *Plant Cell and Environment* **8**: 531-534.

Volder A, Smart DR, Bloom AJ, Eissenstat DM. 2005. Rapid decline in nitrate uptake and respiration with age in fine lateral roots of grape: implications for root efficiency and competitive effectiveness. *New Phytologist* **165**: 493-501.

Vuorinen AH, Vapaavuori EM, Lapinjoki S. 1989. Time-Course of Uptake of Dissolved Inorganic Carbon through Willow Roots in Light and in Darkness. *Physiologia Plantarum* **77**: 33-38.

Wang W, Peng SS, Fang JY. 2010. Root respiration and its relation to nutrient contents in soil and root and EVI among 8 ecosystems, northern China. *Plant and Soil* **333**: 391-401.

Werner C, Schnyder H, Cuntz M, Keitel C, Zeeman MJ, Dawson TE, Badeck FW, Brugnoli E, Ghashghaie J, Grams TEE*, et al.* 2012. Progress and challenges in using stable isotopes to trace plant carbon and water relations across scales. *Biogeosciences* **9**: 3083-3111.

Wetzel RG, Grace JB. 1983. Aquatic plant communities. In: E. R. Lemon ed. *CO_2 and plants- the response of plants to rising levels of atmospheric carbon dioxide*. Boulder, CO, USA: Westview Press, 223-280.

Wilkinson S. 1999. pH as a stress signal. *Plant Growth Regulation* **29**: 87-99.

Wingate L, Ogee J, Burlett R, Bosc A, Devaux M, Grace J, Loustau D, Gessler A. 2010. Photosynthetic carbon isotope discrimination and its relationship to the carbon isotope signals of stem, soil and ecosystem respiration. *New Phytologist* **188**: 576-589.

Wittmann C, Aschan G, Pfanz H. 2001. Leaf and twig photosynthesis of young beech (*Fagus sylvatica*) and aspen (*Populus tremula*) trees grown under different light regime. *Basic and Applied Ecology* **2**: 145-154.

Wittmann C, Pfanz H. 2008. Antitranspirant functions of stem periderms and their influence on corticular photosynthesis under drought stress. *Trees-Structure and Function* **22**: 187-196.

Wittmann C, Pfanz H, Loreto F, Centritto M, Pietrini F, Alessio G. 2006. Stem CO_2 release under illumination: corticular photosynthesis, photorespiration or inhibition of mitochondrial respiration? *Plant Cell and Environment* **29**: 1149-1158.

Wolkerstorfer SV, Rosner S, Hietz P. 2012. An improved method and data analysis for ultrasound acoustic emissions and xylem vulnerability in conifer wood. *Physiologia Plantarum* **146**: 184-191.

Woodruff DR, Bond BJ, Meinzer FC. 2004. Does turgor limit growth in tall trees? *Plant Cell and Environment* **27**: 229-236.

Yang JY, Teskey RO, Wang CK. 2012. Stem CO_2 efflux of ten species in temperate forests in Northeastern China. *Trees-Structure and Function* **26**: 1225-1235.

Zelawski W, Riech FP, Stanley RG. 1970. Assimilation and Release of Internal Carbon Dioxide by Woody Plant Shoots. *Canadian Journal of Botany* **48**: 1351-&.

Ziegler H. 1957. Über den Gaswechsel verholzter Achsen. *Flora* **144**: 229-250.

Zimmerman MH. 1957. Translocation of Organic Substances in Trees. I. The Nature of the Sugars in the Sieve Tube Exudate of Trees. *Plant Physiology* **32**: 288-291.

Zufferey V, Cochard H, Ameglio T, Spring JL, Viret O. 2011. Diurnal cycles of embolism formation and repair in petioles of grapevine (*Vitis vinifera* cv. Chasselas). *Journal of Experimental Botany* **62**: 3885-3894.

Zwieniecki MA, Holbrook NM. 2009. Confronting Maxwell's demon: biophysics of xylem embolism repair. *Trends in Plant Science* **14**: 530-534.

Zwieniecki MA, Melcher PJ, Holbrook NM. 2001. Hydrogel control of xylem hydraulic resistance in plants. *Science* **291**: 1059-1062.

Zwieniecki MA, Thompson MV, Holbrook NM. 2002. Understanding the hydraulics of porous pipes: Tradeoffs between water uptake and root length utilization. *Journal of Plant Growth Regulation* **21**: 315-323.

Summary

Since our childhood we are learned that trees are "The green lungs of our planet" because they take up CO_2 and emit O_2 during photosynthesis. However, respiration is a second vital plant process, during which CO_2 is emitted into the atmosphere. At the global scale, both fluxes of CO_2 uptake and release are several orders of magnitude larger than the anthropogenic one and approximately balance. In contrast to our understanding of photosynthesis, we (i.e. the scientific community) lack the ability to accurately quantify and model the contribution of the different above- and belowground sources to the respiratory flux from forest ecosystems into the atmosphere. In our attempts to quantify the respiratory fluxes from a single source, efflux-based methods are being used, based on the general believe that all locally respired CO_2 is released immediately into the atmosphere at the site of respiration thereby contributing to the local CO_2 efflux.

However, recent literature has shown that a fraction of the respired CO_2 remains within the tree instead of diffusing into the atmosphere. As a result internal CO_2 concentrations ($[CO_2]$) in different trees species are reported in a range (<1 to over 26%) significantly higher than the atmospheric one (c. 0.04% at 2013). While aboveground respired CO_2 has previously been recognized as an important source of internal CO_2, most recent reports suggest that also a fraction of root-respired CO_2 is transported within the tree, instead of diffusing into the soil environment. Nevertheless, internal CO_2 in trees remains a missing link in our understanding of the tree carbon cycle. Therefore, this PhD study aimed at increasing our knowledge on the fate and importance of respired CO_2 in the tree carbon economy based on results obtained during experimental studies.

In particular, the fate of xylem-transported CO_2 remains poorly understood. In this PhD study, a ^{13}C-labeled CO_2 (referred to as $^{13}CO_2$) tracer experiment was performed to study the fate of xylem-transported CO_2 in full size field-grown trees. Dissolved $^{13}CO_2$ was

infused at the stem base of *Populus deltoides* Bartr. ex Marsh trees and isotope analysis was used to reveal whether the isotopic proxy was assimilated in the tree or diffused to the atmosphere. Results from the isotopic analysis from the gas and tissue samples demonstrate not only the upward transport of the label, but also the assimilation of the $^{13}CO_2$ in the stem, canopy and leaf tissues. The largest fraction of the $^{13}CO_2$ label diffused to the atmosphere. Therefore, a substantial amount of belowground respired CO_2 might diffuse from stem and branch surface into the atmosphere, leading to misestimates of above- and belowground respiration. Additional experiments, based on the introduction of $^{13}CO_2$ in the xylem of poplar branches from the same species and leaves (*Populus x canadensis* Moench 'Robusta'), were performed under controlled conditions. Xylem CO_2 transport was manipulated either by altering the uptake rate or the xylem $^{13}CO_2$ concentration of the infused solution. For the woody and leaf tissues of the branches allowed to take up the ^{13}C label, inner bark and petioles, respectively, were most enriched, regardless of the uptake rate of xylem $^{13}CO_2$. However, the total assimilation of $^{13}CO_2$ relative to the uptake of atmospheric CO_2 was small (up to 1.9%). In leaves, detailed distribution of xylem-transported CO_2 was obtained using positron autoradiographic detection of ^{11}C. This high-resolution data indicated that assimilation of xylem-transported CO_2 mainly occurred near the leaf veins, which is presumably related to the occurrence of bundle sheath cells surrounding the leaf veins.

Assimilation of internal CO_2 has been considered as an important means for improving the tree carbon balance under reduced atmospheric CO_2 uptake, like under drought stress. To this end, it was tested to which extent woody tissue photosynthesis contributed to the overall tree carbon gain of *Populus deltoides x nigra* 'Monviso' trees under well-watered and drought-stressed conditions. Light exclusion was used to prevent woody tissue photosynthesis to occur and stem growth rate and leaf gas exchange were assessed both for control and light-excluded trees. Moreover, the hypothesis that woody tissue photosynthesis might play a role in light-dependent embolism repair was tested. Under well-watered conditions, reduced stem growth was observed for light-excluded trees. Under drought-stressed conditions, trees lacking woody tissue photosynthesis shrank more pronounced and showed a faster reduction in leaf gas exchange. Moreover, acoustic measurements confirmed that woody tissue

photosynthesis could play a role in embolism repair in trees by synthesizing sugars used for embolism sensing and refilling. Therefore, assimilation of internal CO_2 might be one of the overlooked strategies of plants to cope with drought.

Similarly, woody tissue photosynthesis might have an important role in leafless dormant trees. When sap flow is absent, reduction of the local stem internal [CO_2] by woody tissue photosynthesis can induce axial diffusion of respired CO_2 away from the site of respiration, hence confounding dormant season efflux-based stem respiration estimates. In this PhD study, the significance of the axial diffusion of respired CO_2 induced by woody tissue photosynthesis for estimating dormant season stem respiration was evaluated. Stem CO_2 efflux (E_{stem}) was measured under temperature-controlled conditions with a light-excluded stem cuvette, while axial CO_2 diffusion was induced by illuminating remote stem sections at varying distances from the stem cuvette. Due to axial diffusion by woody tissue photosynthesis, E_{stem} measured with the stem cuvette was reduced by 22% relative to control conditions when no woody tissue photosynthesis occurred. Highest reductions were observed when woody tissue photosynthesis was induced in the stem section closest to the stem cuvette, while the effect was negligible when stem sections were illuminated at 30 cm and more from the stem cuvette. Temperature-corrected dormant-season stem respiration estimates are used for partitioning growing season stem respiration into a growth and maintenance component. Therefore, failure to account for the effect of woody tissue photosynthesis on dormant season E_{stem} might bias component respiration estimates throughout the year.

The recent discovery that a fraction of root-respired CO_2 contributes to internal CO_2 rather than fluxing into the soil environment cast doubt on common efflux-based approaches for quantifying the autotrophic component of belowground respiration. Therefore, a re-estimation of the autotrophic component of belowground respiration at ecosystem level is necessary. In this PhD study, the contribution of root-respired CO_2 to both soil CO_2 efflux (E_{stem}) and xylem CO_2 transport (F_t) from root respiration was estimated in an oak tree (*Quercus robur* L.) plantation based on the manipulation of the autotrophic component of belowground respiration ($R_{a,b}$) by removing a circumferential band of bark during tree girdling. Next to E_{soil}, xylem [CO_2] at stem base decreased in

response to girdling, corroborating the previous observations on F_t in trees. Accounting for both the reduction in E_{soil} and scaled F_t led to more accurate estimates of $R_{a,b}$. In particular, large differences with the previous efflux-based estimates of the autotrophic component of belowground respiration were observed during the day, when root-respired CO_2 is transported away from the site of respiration with the transpiration stream.

In conclusion, results from this PhD study demonstrate that internal CO_2 plays an important role in the tree carbon cycle, regardless whether it is transported with the transpiration stream, assimilated in chlorophyll containing tissues or diffused to the atmosphere. Hence, measurements of internal CO_2 and related ecophysiological parameters should be more widely applied to improve our ability to understand and model the flow of carbon within trees.

Samenvatting

Sinds onze kindertijd wordt ons verteld dat bomen “De groene longen van onze planeet” zijn, aangezien ze CO_2 opnemen en O_2 terug afgeven tijdens fotosynthese. Echter, respiratie is een tweede vitaal plant proces, waarbij CO_2 wordt afgegeven aan de atmosfeer. Globaal gezien is de opname en afgifte van CO_2 door planten vele malen groter dan de antropogene CO_2 flux en beide zijn ongeveer in balans. In tegenstelling tot onze kennis over fotosynthese ontbreekt het ons (met name de wetenschappers) aan kennis om zeer accuraat de bijdrage te kwantificeren en te modelleren van de verschillende boven- en ondergrondse bronnen tot de gerespireerde CO_2 flux van bos ecosystemen tot de atmosfeer. In onze pogingen om deze bijdragen te kwantificeren gebruiken we efflux-gebaseerde methodes, volgens het algemeen aanvaard geloof dat al het lokaal gerespireerd CO_2 direct diffundeert naar de atmosfeer en bijgevolg bijdraagt aan CO_2 efflux.

Echter, recent gepubliceerde resultaten geven aan dat een deel van het gerespireerd CO_2 in de boom blijft in tegenstelling tot directe diffusie naar de atmosfeer. Bijgevolg, worden voor verschillende boomsoorten intern CO_2 concentraties ($[CO_2]$ gerapporteerd in een grootteorde (<1 to over 26%) significant hoger dan de atmosferische $[CO_2]$ concentratie (c. 0.04% in het jaar 2013). Waar voorheen bovengronds gerespireerd CO_2 werd erkend als een belangrijke bron van intern CO_2, suggereren de meest recente resultaten dat zelfs een deel van het ondergronds gerespireerd CO_2, afgeleid van de wortels, kan getransporteerd worden in de boom en zo bijdragen aan intern CO_2. Niettegenstaande, intern CO_2 in bomen blijft een ontbrekende schakel in onze kennis over de koolstof cyclus van bomen. Daarom had dit doctoraatsonderzoek als doel onze kennis te verbeteren over de rol van intern CO_2 in de koolstof economie van bomen, gebaseerd op de resultaten van experimentele studies.

Het ontbreekt ons vooral aan kennis over de bestemming van xyleem getransporteerd CO_2. In dit doctoraatsonderzoek werd een ^{13}C-gelabeld CO_2 (verder vernoemd als $^{13}CO_2$)

tracer experiment uitgevoerd met als doel het bestuderen van de bestemming van xyleem getransporteerd CO_2 in grote bomen onder veld omstandigheden. Een infusie van een $^{13}CO_2$ label in de basis van de stam van *Populus deltoides* Bartr. Ex Marsh bomen werd gebruikt om te bestuderen of xyleem getransporteerd CO_2 wordt geassimileerd in de boom of diffundeert naar de atmosfeer. Resultaten van de isotopen analyses van gas-, blad- en houtstalen gaven aan dat het label werd getransporteerd in de boom en dat assimilatie van $^{13}CO_2$ optrad in de stam en de kruin. De grootste fractie van de $^{13}CO_2$ label diffundeerde naar de atmosfeer. Dit geeft aan dat een substantieel deel van het ondergronds gerespireerd CO_2 mogelijks diffundeert van stam en tak oppervlakken naar de atmosfeer, wat aangeeft dat methodes gebaseerd op het meten van CO_2 efflux de hoeveelheid boven- en ondergrondse respiratie verkeerd inschatten. Extra labeling experimenten werden uitgevoerd op takken van dezelfde populierensoort en op bladeren (*Populus x canadensis* Moench 'Robusta') onder gecontroleerde condities. Het transport van xyleem CO_2 werd gemanipuleerd door het veranderen van de opnamesnelheid of door het wijzigen van xyleem $^{13}CO_2$ concentratie van de oplossing. Voor de blad - en houtige weefsels waren het binnenste van de bast en de bladpetiolen het meest aangerijkt in ^{13}C, respectievelijk, ongeacht de hoeveelheid opgenomen oplossing of de $^{13}CO_2$ concentratie. Relatief ten opzichte van de opname van atmosferische CO_2 door de bladeren was de totale assimilatie van $^{13}CO_2$ klein (maximaal 1.9%). De autoradiografische detectie van ^{11}C in bladeren zorgde voor een gedetailleerde analyse van distributie van xyleem getransporteerd CO_2. Deze hoge resolutie data geeft aan dat de assimilatie van xyleem getransporteerd CO_2 ter hoogte van de bladeren en de bladnerven hoogstwaarschijnlijk gerelateerd is aan het voorkomen van bundel schede cellen langsheen de bladnerven.

Assimilatie van intern CO_2 in bomen wordt over het algemeen beschouwd als een mogelijke strategie ter verbetering van de koolstof balans van bomen wanneer opname van atmosferisch CO_2 beperkt is, zoals onder droogtestress. In dit doctoraatsonderzoek werd daarvoor nagegaan wat de bijdrage was van stam en tak fotosynthese tot de koolstof opname door *Populus deltoides x nigra* 'Monviso' bomen, onder goed bewaterde en droogte stress condities. Beschaduwen van de stam werd gebruikt voor het uitsluiten van stam en tak fotosynthese. Stamgroei en gasuitwisseling ter hoogte van de bladeren

werden opgemeten voor controle en beschaduwde bomen. Daarenboven werd de hypothese over de lichtafhankelijke rol van stam en tak fotosynthese in het herstel van gecaviteerde xyleem vaten getest. Onder goed bewaterde condities werd een beperktere stamgroei geobserveed voor de beschaduwde bomen relatief ten opzichte van de stam groei bij de controle bomen. Onder droogtestresscondities kromp de stam van beschaduwde bomen meer uitgesproken en daalde gasuitwisseling op bladniveau sterker. Daarenboven bevestigden akoestische metingen dat stam en tak fotosynthese mogelijks een rol speelt in het herstel van gecaviteerde xyleem vaten, door de synthese van suikers gebruikt voor het hervullen en het opsporen van gecaviteerde vaten in de boom. Mogelijks is assimilatie van intern CO_2 dus één van de over het hoofd geziene processen waarmee planten met droogte omgaan.

Op een gelijkaardige manier zou stam en tak fotosynthese een belangrijke rol kunnen spelen in bladloze dormante bomen. Wanneer sap stroom afwezig is, kan een daling in lokale stam intern CO_2 concentratie door stam en tak fotosynthese een axiale diffusie van gerespireerd CO_2 teweeg brengen weg van de plaats van respiratie. Bijgevolg heeft dit een sterk effect op de efflux gebaseerde schattingen van stam respiratie tijdens het dormante seizoen. In dit doctoraatsonderzoek werd nagegaan wat het belang is van de axiale diffusie van gerespireerd transport door stam en tak fotosynthese voor de schatting van stam respiratie. Stam CO_2 efflux werd gemeten onder temperatuur gecontroleerde condities met een beschaduwde stam cuvette terwijl een verschillende mate van axiale diffusie van gerespireerd CO_2 in de stam werd geïnduceerd door het belichten van naburige stam segmenten op een verschillende afstand van de stam cuvette. Relatief ten opzichte van controle omstandigheden waarbij geen tak of stam fotosynthese optrad werd een daling in stam CO_2 efflux waargenomen tot 22%. De grootste daling trad op wanneer stam fotosynthese plaats vond in het stam segment het dichtst bij de stam cuvette, terwijl het effect van stam fotosynthese op stam CO_2 efflux verwaarloosbaar was op afstand van 30 cm en meer, gemeten vanaf de stam cuvette. Temperatuur gecorrigeerde schattingen van stam respiratie gedurende het dormante seizoen worden gebruikt om respiratie tijdens het groei seizoen onder te verdelen in een groei en een onderhouds component. Bijgevolg, metingen van stam respiratie die

het effect van stam fotosynthese niet in acht nemen zullen mogelijks leiden tot verkeerde inschattingen van de respiratie componenten gedurende de rest van het jaar.

De recente ontdekking dat een deel van het wortel gerespireerd CO_2 bijdraagt tot intern CO_2 in plaats van te diffunderen in de bodem trekt de conventionele efflux gebaseerde methodes voor het schatten van de autotrofe component van ondergrondse respiratie in twijfel. Bijgevolg, een hernieuwde schatting van de autotrofe component van ondergrondse respiratie op ecosysteem niveau is noodzakelijk. In dit doctoraatsonderzoek werd de bijdrage van wortel gerespireerd CO_2 aan zowel bodem CO_2 efflux als xyleem CO_2 transport geschat voor eiken (*Quercus robur* L.) plantage. Deze schatting werd uitgevoerd op basis van de manipulatie van de autotrofe component van ondergronds respiratie door het ringen van de stam (het verwijderen van een strook de bast). Door het ringen van de stam daalde naast bodem CO_2 ook de xyleem [CO_2] ter hoogte van de basis van de stam, wat de vorige waarnemingen van xyleem transport van ondergronds gerespireerd CO_2 in bomen onderbouwt. Bijgevolg zal het in rekening brengen van zowel de daling in bodem CO_2 efflux als de daling in de geschaalde flux van intern CO_2 transport na ringen leiden tot betere schattingen van de autotrofe component van ondergrondse respiratie. Een verschil tussen de nieuwe en oude schattingen van de autotrofe component van ondergrondse respiratie zal voornamelijk gedurende de dag waargenomen worden, wanneer een deel van het wortel gerespireerd CO_2 getransporteerd wordt weg van de plaats van respiratie via de sapstroom in de boom in plaats van bij te dragen aan bodem CO_2 efflux.

In conclusie, de resultaten van dit doctoraatsonderzoek geven aan dat intern CO_2 een belangrijke rol speelt in de koolstofcyclus van bomen, ongeacht of het nu getransporteerd wordt met de sapstroom, geassimileerd wordt in chlorofyl houdende weefsels of diffundeert naar de atmosfeer. Bijgevolg moeten metingen van intern CO_2 en gerelateerde ecofysiologische parameters meer uitgevoerd worden wat onze capaciteit om de stroom van koolstof in bomen te begrijpen en te modelleren zal verbeteren.

Curriculum vitae

Personal details

Name:	Jasper Toon Tine Bloemen
Date of birth:	05 may 1986
Place of birth:	Roeselare (Belgium)
Nationality:	Belgian
Civil State:	Married (to Katrien Haeck)
Adress:	Koersenstraat 22, 9000 Gent, Belgium
Mobile:	+32(0)494662613
E-mail:	Jasper.Bloemen@ugent.be

Education/work experience

1998-2004	Secondary school, Science-Mathematics, Koninklijk Atheneum I Brugge centrum, Brugge, Belgium
2004-2007	Bachelor degree in Bioscience Engineering (Environmental technol.), Faculty of Bioscience Engineering, Ghent University, Ghent, Belgium (distinction)
2007- 2009	Masters degree in Bioscience Engineering (Environmental technol.), Faculty of Bioscience Engineering, Ghent University, Ghent, Belgium (Great distinction) Master thesis: Performed at the Department of Applied Ecology and Environmental Biology, Laboratory of Plant Ecology, Ghent University, Ghent, Belgium Dutch title: "Dynamische interactie tussen fotosynthese, transpiratie en BVOS emissie in bosecosystemen" Promotor: Prof. dr ir. Kathy Steppe

2010-present	PhD training program in Applied Biological Sciences, Faculty of Bioscience Engineering, Ghent University, Ghent, Belgium
	Courses followed in the framework of this program:
	Ecophysiology
	Bio-imaging
	ANOVA: analysis of variance
	Advanced Academic English
	Introduction to SAS
	Applying for a post doctoral job

Professional experience

2009 - 2013	Research assistant at the Department of Applied Ecology and Environmental Biology, Laboratory of Plant Ecology Ghent University, Gent, Belgium

Other Scientific activities

Jan - June 2008	Université Laval, Québec, Canada, Study exchange within the framework of a bilateral agreement framework (Atlantis program)
Nov - Jan 2009	Research visit at the laboratory of prof. Andrew D. Richardson Harvard University, Boston, MA, US. Data analysis of soil and ecosystem respiration measurements. Introduction to the use of webcams to monitor phenology
June - July 2010	University of Georgia, Daniel B. Warnell school of Forestry and Natural Resources, Athens, Georgia, USA. Growth chamber and field experiments with ^{13}C isotopes
Sept 2012	INRA Research center, Champenoux, France. Training school Stable Isotopes in ecosystem research in the framework of the SIBAE COST action (ES0806)

June 2013	Member of the Editorial Board of the 9th International Workshop on Sap Flow, Ghent, Belgium, 4-7 June 2013
July –Aug 2013	Universität Innsbruck, Institute of Ecology (lab of Prof. Michael Bahn) Innsbruck, Austria. Introduction to the use of a quantum cascade laser system to trace stable isotopes in tree CO_2 efflux . Short Term Scientific Mission (STSM) within the framework of the SIBAE COST action (ES0806)
2009-2013	Review tasks for Tree Physiology, Flora, and Annals of Botany

Grants and prizes

June 2010	Grant from the Scientific Research Committee (CWO) for the research visit at the University of Georgia, Athens, Georgia, USA
April 2012	Grant from the Fund for Scientific Research (FWO) for attending the EGU general assembly conference, Vienna, Austria
April 2012	Grant from the Scientific Research Committee (CWO) for attending the EGU general assembly conference, Vienna, Austria
Sept 2012	COST Travel grant for attending the course on stable isotopes in the framework of the SIBAE COST action (ES0806), Nancy, France
Dec 2012	Grant from the Scientifc Research Committee (CWO) for attending the AGU Fall meeting, San Francisco, California, USA
May 2013	Grant from the Fund for Scientific Research (FWO) for attending the SIBAE COST (ES0806) meeting, Wroclaw, Poland
July-August 2013	COST STSM grant for the research visit at Universität Innsbruck Innsbruck, Austria

Educational activities

2010 - present	Guest lecturer practial part courses “Plant water relations”, “Ecology”, and “Terrestrial ecology”.
2010 - 2011	Tutor of the Master thesis of Sim Minnaert Dutch title: “Invloed van licht en warmte op BVOC emissie bij schaduwbladeren van beuk (*Fagus sylvatica* L.)”
2011 - 2012	Tutor of the Master thesis of Laura Agneessens Dutch title: “Autotrofe bodemrespiratie in bosecosystemen: hoe belangrijk is intern CO_2 transport via sapstroom?”
2011 - 2012	Tutor of the Master thesis of Yentl Dupon Dutch title: “Temperatuursonafhanjelijk variatie in stam CO_2 efflux bij eiken (*Quercus robur* L.) tijdens dormantie”
2011 - 2012	Tutor Bachelor project Dutch title: “CO_2 in bomen: even verder denken dan fotosynthese”

Scientific output

International publications with peer review

Pokorska O., Dewulf J., Amelynck C.,Schoon N.,Joó E., Šimpraga M., Bloemen J., Steppe K., and Van Langenhove H. (2012) Emissions of biogenic volatile organic compounds from Fraxinus excelsior and Quercus robur under ambient conditions in Flanders (Belgium). *International Journal of Environmental Analytical Chemistry* **92 (15):** 1729-1741

Bloemen J., McGuire M.A., Aubrey D.P., Teskey R.O., and Steppe K. (2013) Transport of root-respired CO_2 via the transpiration stream affects aboveground carbon assimilation and CO_2 efflux in trees. *New Phytologist* **197**: 555-565.

Erda F., Bloemen J., and Steppe K. (2013) Quantifying the impact of daily and seasonal variation in sap pH on xylem dissolved inorganic carbon estimates in plum trees. *Plant Biology* , in press (doi:10.1111/plb.12009)

Bloemen J., McGuire M.A., Aubrey D.P., Teskey R.O., and Steppe K. (2013) Assimilation of xylem-transported CO_2 is dependent on transpiration rate, but small relative to atmospheric fixation. *Journal of Experimental Botany* **64:** 2129-2138

Šimpraga M., Verbeeck H*., Bloemen J.*, Vanhaecke L., Demarcke M., Joó E., Pokorska O., Amelynck C., Schoon N., Dewulf J., Van Langenhove H., Heinesch B., Aubinet M., and Steppe K. (2013) Vertical canopy gradient in photosynthesis and monoterpenoid emissions: An insight into the chemistry and physiology behind. *Atmospheric Environment* **80**: 85-95
*equal contributions

Bloemen J., Agneessens L., Lieven Van Meulebroek, Aubrey D.P. , McGuire M.A., Teskey R.O., and Steppe K. (2013) Stem girdling affects the quantity of CO_2 transported in xylem as well as CO_2 efflux from soil. *New Phytologist*, in press (doi: 10.1111/nph.12568)

Bloemen J., Bauweraerts I., De Vos F., Vanhove C., Vandenberghe S., Boeckx P., and Steppe K. (2013) Fate of xylem-transported ^{11}C- and ^{13}C- labeled CO_2 in leaves of poplar. *Physiologia Plantarum* (submitted)

Bloemen J., McGuire M.A., Aubrey D.P., Teskey R.O., and Steppe K. (2013) Internal recycling of respired CO_2 may be important for plant functioning under changing climate regimes. *Plant Signaling and behavior* (revision)

Proceedings
Bloemen J., Overlaet-Michiels L. and Steppe K. (2013) Understanding Plant Responses to Drought: How Important Is Woody Tissue Photosynthesis? Acta Horticulturae **991**: 149-157

Scientific Reports

Steppe K., Šimpraga M., Verbeeck H., Bloemen J., Joó E., Pokorska O., Dewulf J., Van Langenhove H., Demarcke M., Amelynck C., Schoon N., Müller J-F., Laffineur Q., Aubinet M., Heinesch B. and Lemeur R. (2009) IMPECVOC: Impact of Phenology and Environmental Conditions on BVOC Emissions from Forest Ecosystems. Final Report Phase 1. Brussels: Belgian Science Policy, 49 p. (Research Programme Science for a Sustainable Development)

Dewulf J., Joó É., Steppe K., Šimpraga M., Verbeeck H., Bloemen J., Pokorska O., Demarcke M., Amelynck C., Schoon N., Müller J-F., Laffineur Q., Aubinet M., Heinesch B., Van Langenhove H. (2009) IMPECVOC: Impact of Phenology and Environmental Conditions on BVOC Emissions from Forest Ecosystems. Annual report phase II. Brussels: Belgian Science Policy, 41 p. (Research Programme Science for a Sustainable Development)

Participation in conferences, symposia or workshops

Bloemen J., Šimpraga M, Verbeeck H, Amelynck C and Steppe K (2009) Dynamical interaction between photosynthesis and BVOC emissions in forest ecosystems. Study Day for Starters in Forest Research, Brussels, Belgium, 19 March 2009 (poster presentation)

Bloemen J., Steppe K., Davidson E., Munger J.W., O'Keefe J., Savage K., Verbeeck H., Richardson A.D. (2010) Influence of springtime phenology on the ratio of soil respiration to total ecosystem respiration in a mixed temperate forest. 24th New Phytologist symposium: Plant respiration and climate change: scaling from mitochondria to the globe, Oxford, UK, 11-14 April 2010 (poster presentation)

Bloemen J. (2011) Quantification of Belowground respiration and fate of root-derived CO2 in trees. Workshop Importance of phenology, carbon partitioning and allocation for tree and forest function, Class of Excellence prof. John S. King , 19 May 2011 (oral presentation)

McGuire M.A., Bloemen J., Aubrey D.P., Steppe K., Teskey R.O. (2011) Fixation of xylem transported CO_2 in branches and leaves of populous trees in the field: a preliminary analysis, 96th ESA annual meeting, Austin, Texas, USA, 7-12 August 2011 (poster presentation)

Bloemen J., McGuire M.A., Aubrey D.P., Teskey R.O. and Steppe K. (2012) Transport of root-derived CO_2 via the transpiration stream affects aboveground tree physiology. EGU general assembly, Vienna, Austria, 22-27 April 2012 (oral presentation)

McGuire M.A., Bloemen J., Aubrey D.P., Steppe K., Teskey R.O. 2012. Xylem-transported respiratory CO_2 as a substrate for carbon assimilation in trees. 97th ESA annual meeting, Portland, Oregon, USA, 5-10 August 2012 (oral presentation)

Bloemen J., Agneessens L., Aubrey D.P., McGuire M.A., Vanhaecke L., Teskey R.O., Steppe K. (2012) How important is root-derived CO_2 transport via the transpiration stream when assessing belowground carbon allocation? AGU Fall meeting 2012, San Francisco, California, USA, 3-7 December 2012 (oral presentation)

Bloemen J. and Steppe K. (2013) ^{13}C as a tracer for respired CO_2 transport in the xylem at leaf, branch and tree level. COST-SIBAE meeting, Wroclaw, Poland, 14-17 May 2013 (oral presentation)

Bloemen J., Overlaet-Michiels L. and Steppe K. (2013) Understanding Plant Responses to Drought: How Important Is Woody Tissue Photosynthesis? 9th International Workshop on Sap Flow, Gent, Belgium, 4-7 June 2013 (poster presentation)

McGuire M.A., Bloemen J., Aubrey D.P., Steppe K., Teskey R.O. 2013. Assimilation of xylem-transported CO_2: Effects of xylem CO_2 concentration and transpiration rate. 98th ESA annual meeting, Minneapolis, Minnesota, USA, 4-9 August 2013 (poster presentation)

Now everyone dreams of a love lasting and true
But you and I know what the world can do
So let's make our stripes less than the other way
And I'll wait for you
It's deceit fall behind
Wait for me